

# Fire Behavior of Pressure-Sensitive Adhesive Tapes and Their Influence in Bonds

Inaugural-Dissertation  
to obtain the academic degree  
Doctor rerum naturalium (Dr. rer. nat.)

submitted to the Department of Biology, Chemistry, Pharmacy  
of Freie Universität Berlin

by  
Vitus Hupp

Berlin, 2024

This doctoral dissertation was prepared from January 2020 until September 2024 at the Bundesanstalt für Materialforschung und -prüfung (BAM) in 12205 Berlin, Germany under the supervision of Prof. Dr. Bernhard Schartel.

1<sup>st</sup> reviewer: Prof. Dr. rer. nat. habil. Bernhard Schartel, Bundesanstalt für Materialforschung und -prüfung (BAM) (Berlin).

2<sup>nd</sup> reviewer: Prof. Dr. rer. nat. habil. Rainer Haag, Freie Universität Berlin.

Date of defense: 25.11.2024

I hereby declare that I alone am responsible for the content of my doctoral dissertation and that I have only used the sources or references cited in the dissertation.

## Acknowledgements

I would like to thank Prof. Dr. Bernhard Schartel for his constant support throughout the whole dissertation process. Your academic advice, constructive critique, and motivational speeches were unparalleled and essential to the completion of this challenging milestone of my career. Thank you for your honest and direct way of communication and last, for believing in me.

I thank Prof. Dr. Rainer Haag for the possibility to write this dissertation in his working group at FU Berlin, for letting me communicate my findings in his circle of scientists and for reviewing this doctoral thesis.

During my doctoral work I had the privilege of working with extraordinary people in academic and industrial institutions. My thanks go to Prof. Dr. Andreas Hartwig who played a crucial role in concepting and managing the projects which results depict a substantial part of this dissertation. His exceptional scientific knowledge and simple way of communicating led to a harmonic cooperation between our research institutes. I would like to thank Dipl. Ing. Kerstin Flothmeier who is a working group member of Prof. Dr. Andreas Hartwig and directly contributed to the published articles and the dissertation in word and action.

I wish to thank Fernanda Romero and Dr. Yin Yam Chan for their support in UL 94, OI and fire resistance measurements and Dr. Alexander Battig for his support and measurements with the Py-GC/MS, fruitful discussions, and pep talks. Special thanks to Michael Schneider, Tobias Lauterbach, and Detlev Rättsch for the preparation of hundreds of samples and measurement equipment. Thank you, Dr. Volker Wachtendorf and Yannik Wägner for your expertise and measurements at the hot-stage FTIR. I would like to say thank you to my colleagues in department 7.5: Daniel Rockel, Sebastian Goller, Jose Pablo Chacon Castro, Dr. Mateusz Dudziak, Dr. Sven Brehme, Dr. Analice Turski-Silva Deniz, Maria Jauregui, Dr. Lars Daus, Sandra Falkenhagen, Weronika Tabaka, Karla Itzel Garfias González, Patrick Klack, Dr. Tanja Gnutzmann, Benjamin Klaffke, Tina Raspe, and Dr. Simone Krüger. Thank you for the countless fruitful discussions, laughter, critique, the conferences and, of course, the coffee.

My most sincere thank you to my closest friends who gave me the strength and motivation to persevere and not give up during the whole time of my doctoral work. I would like to thank my mother, Hedwig Hupp, my brother Falko Hupp who gave me the power to overcome personal crisis and gave me strength to continue my academic career. Further, I would like to thank my recently passed away father, Paul Hupp, whose perseverance served as an example and helped me to overcome crisis and motivation valleys during this journey.

## Abbreviations

|                 |   |
|-----------------|---|
| ATH             | Aluminum (tri)hydroxide                                     |
| CO <sub>2</sub> | Carbon dioxide  |
| CO              | Carbon monoxide   |
| CAGR            | Compound annual growth rate                                 |
| CLT             | Cross laminated timber                                      |
| DIY             | Do it yourself  |
| DOPO            | 6H-dibenzo[c,e][1,2]oxaphosphinine 6-oxide                  |
| DSC             | Differential scanning calorimetry                           |
| EVA             | Ethylene-vinyl acetate                                      |
| FGC             | Fire growth capacity  |
| FIGRA           | Fire growth rate index                                      |
| FTIR            | Fourier-transform infrared spectroscopy                     |
| HRC             | Heat release capacity                                       |
| HRR             | Heat release rate   |
| MARHE           | Maximum average rate of heat emission                       |
| m/z             | Mass per charge number                                      |
| N <sub>2</sub>  | Nitrogen  |
| OI              | Oxygen index  |
| O <sub>2</sub>  | Oxygen  |
| P               | Phosphorus  |
| PC              | Bisphenol-A-polycarbonate                                   |
| PCFC            | Pyrolysis combustion flow calorimeter                       |
| PHRR            | Peak of heat release rate                                   |
| PMMA            | Poly(methyl methacrylate)                                   |
| PSA             | Pressure-sensitive adhesives                                |
| PTFE            | Poly(tetrafluoroethylene)                                   |
| Py-GC/MS        | Pyrolysis gas chromatography coupled with mass spectrometry |
| R               | Rest  |
| RDP             | (3-diphenoxyphosphoryloxyphenyl) diphenyl phosphate         |
| rh              | Relative humidity   |
| SAFT            | Shear adhesion failure temperature                          |
| T <sub>g</sub>  | Glass-transition temperature                                |
| TGA             | Thermogravimetric analysis                                  |
| t <sub>ig</sub> | Time to ignition  |
| UL              | Underwriters Laboratory                                     |
| vol.-%          | Volume percentage   |

|                            |   |
|----------------------------|---|
| wt.-%                      | Weight percentage   |
| $\theta(t)$                | Time dependent protection layer factor                          |
| $\mu$                      | Char yield  |
| $\chi$                     | Combustion efficiency   |
| $h_c$                      | Heat of complete combustion of the volatiles                    |
| $h_g$                      | Enthalpy of gasification of the volatiles                       |
| $\dot{q}''_{\text{ext}}$   | External heat flux  |
| $\dot{q}''_{\text{flame}}$ | Heat flux of the flame  |
| $\dot{q}''_{\text{rerad}}$ | Reradiated heat flux from the sample surface                    |
| $\dot{q}''_{\text{loss}}$  | Heat lost by conduction into the sample and to the environment. |
| 1K PU                      | One component polyurethanes                                     |

## Table of contents

|   |    |
|---|----|
| 1. Introduction .....   | 1  |
| 2. Scientific goals and approach.....   | 3  |
| 3. Scientific background .....  | 4  |
| 3.1. PSA and PSA tapes .....  | 4  |
| 3.1.1. Acrylic PSA.....   | 4  |
| 3.1.2. Adhesive tapes.....  | 5  |
| 3.1.3. Mechanical properties of PSA.....  | 6  |
| 3.2. Fire behavior and flame retardancy.....  | 7  |
| 3.3. Flame retardant modes of action in polymers .....  | 9  |
| 3.4. Flame retardants in PSA .....  | 10 |
| 4. Materials and methods.....   | 13 |
| 4.1. Materials for the preparation of PSA (tapes) and flame retardants.....   | 13 |
| 4.2. Adhesive analysis .....  | 15 |
| 4.3. Pyrolysis analysis .....   | 15 |
| 4.3.1. Thermogravimetric analysis coupled with Fourier-transform infrared spectroscopy (TGA FTIR).....                    | 16 |
| 4.3.2. Hot-stage FTIR .....   | 16 |
| 4.3.3. Pyrolysis gas chromatography coupled with mass spectrometry (Py-GC/MS).....  | 17 |
| 4.3.4. Pyrolysis combustion flow calorimeter .....  | 17 |
| 4.4. Reaction to a small flame simulating the ignition stage of a fire.....   | 19 |
| 4.4.1. UL94.....  | 19 |
| 4.4.2. Oxygen index (OI).....   | 19 |
| 4.4.3. Single-flame source test.....  | 20 |
| 4.5. Fire behavior in the developing fire scenario .....  | 21 |
| 4.6. Fire resistance in the fully developed fire scenario.....  | 22 |
| 5. Publications .....   | 24 |
| 5.1. Fire behavior of pressure-sensitive adhesive tapes and bonded materials ....   | 24 |
| 5.2. Pyrolysis and flammability of phosphorus based flame retardant pressure sensitive adhesives and adhesive tapes ..... | 40 |
| 5.3. Flame Retarded Adhesive Tapes and Their Influence on the Fire Behavior of Bonded Parts.....                          | 73 |

|                                 |     |
|---------------------------------|-----|
| 6. Further investigations ..... | 96  |
| 7. Summary.....                 | 97  |
| 8. Zusammenfassung .....        | 101 |
| 9. References .....             | 105 |



# 1. Introduction

Adhesives are omnipresent in our daily life and indispensable in almost every area. Their market value has increased sharply over the recent years and is expected to grow even further in the coming years [1,2]. Because they are often cheaper, easier to apply, and have favorable properties depending on the application, adhesives have increasingly replaced mechanical fasteners such as screws or rivets. The spectrum in which adhesives are used nowadays is a very wide one and ranges literally from aerospace [3] to the deep sea [4]. In the transportation and construction industries, adhesives are used to manufacture cars, railway vehicles or to construct (residential) housing, where flammability and fire behavior are crucial parameters that can mean the difference between life and death. The fire behavior of adhesives and bonded materials is therefore an important research topic for industry and academia. The fast-growing area of laminated timber products is the most researched area for flame retardant adhesives. Especially, plywood [5,6] and cross laminated timber (CLT) [7,8] contain large amounts of adhesives that are modified with flame retardants. Further, insulation panels that consist of multiple layers bonded by adhesives seem to be reliant on flame retardants [9] to improve the fire behavior of the bonded materials.

In the transportation and construction industries, special types of adhesives, namely pressure-sensitive adhesives (PSA) or PSA tapes, are often used to bond interior parts and claddings of cars and railway vehicles and is used in the roofing of housing, where their fire behavior is exceptionally important. PSA tapes are mostly based on rubber like polymers [10], which are intrinsically flammable and thus need to be flame retardant. They can be applied over a wide temperature range and have a good tack (adhesive strength immediately after application) due to their low glass-transition temperature ( $T_g$ ) [11]. These adhesives adhere to a large variety of surfaces and can “flow” into gaps and cracks due to their viscoelastic state making wetting agents unnecessary. The fire behavior of PSA tapes and their bonds is from great interest to PSA tape manufacturers and applicants and is not yet fully understood. Patents for flame retardant PSA tapes have already been published [12,13], showing the importance of these developments in industrial applications. Literature serves with very few articles to investigate the action and mechanisms of flame retardants on the fire behavior of PSA tapes [14-16], and in contrast to adhesives for plywood and cross laminated timber, very little knowledge is found on the fire behavior of PSA-bonded materials. The current way of producing and developing flame retardant double-sided PSA tapes is to make them pass certain flammability tests and expect them to have a beneficial influence on the bonded material. However, this beneficial influence has

not yet been proven, and the question arises as to how the (flame retardant) adhesive tapes influence the burning characteristics of PSA-bonded materials.

This doctoral thesis brings some light into the darkness by investigating the flame retardancy of PSA (tapes) and their influence on the fire behavior of their bonds. Therefore, the fire behavior of market available products and self-prepared acrylic PSA tapes are investigated and subsequently bonded to a spectrum of materials which represent applications in the transportation and construction industries. Phosphorus flame retardants, more precisely 6H-dibenzo[c,e][1,2]oxaphosphinine 6-oxide (DOPO)-derivates and (3-diphenoxyphosphoryloxyphenyl) diphenyl phosphate (RDP), were used to investigate the individual benefits of different flame retardant modes of action in a PSA matrix. A clear, structured analysis of the interaction between the substrate (material that is to be bonded), the adhesive tape carrier (middle layer of a double-sided adhesive tape), and the adhesive layer is performed in differently scaled methods to examine their individual contributions to the fire behavior of their adhesive joints. The behavior of PSA tapes and bonded materials is not only investigated in different specimen dimensions, but also in different fire scenarios ranging from the ignition phase to the fully developed fire.

The results that are obtained from PSA tapes are expected to be transferable to other adhesives and adhesive joints and should serve as scientific communication basis for further research in flame retardancy of adhesives, adhesive tapes, and bonded materials.

## 2. Scientific goals and approach

Despite their use in the transportation and construction industries, where the fire behavior is an important parameter, the fire behavior of PSA tapes and their bonds is poorly understood. PSA tapes with good flammability characteristics are manufactured without any correlation between the flammability of the tape and the fire behavior of the bonded material being proven.

Three publications examine and describe the fire behavior of double-sided PSA tapes and their bonds in detail, building a solid knowledge foundation for new ways of developing flame retardant PSA and PSA-bonded materials (section 5).

The first publication (section 5.1) deals with the fire behavior of commercially available double-sided acrylic adhesive tapes, with and without flame retardants. The pyrolysis and flammability analysis shows the microscopic and macroscopic effect of flame retardants in a PSA matrix and their benefits in adhesive tapes as objects that are not bonded to any substrate. These acrylic adhesive tapes are subsequently used to bond different substrates and analyze their fire behavior in bonds. Different fire scenarios and bond designs are used to understand the fire behavior of PSA-bonded materials and the interaction between the PSA tape and the individual substrate.

To gain a deeper insight into the mechanism and modes of action of different flame retardants in a PSA matrix, the pyrolysis of four different self-synthesized, double-sided flame retardant acrylic PSA are thoroughly analyzed and a relation between pyrolysis and flammability is deduced (section 5.2). Three phosphorus-based flame retardants with individual modes of action and structures are implemented into the PSA to gain information about the specific benefits of each mode of action and its interaction with a PSA (tape) matrix. Two DOPO-derivates (one blended and one covalently bonded) and RDP are used as flame retardants to represent a predominantly gas phase active, a condensed phase active and a flame retardant that is covalently bonded to the polymer backbone.

These self-made flame retardant acrylic PSA are then coated onto different carriers to obtain different PSA tapes which are subsequently used to bond several substrates (section 5.3). These tapes and bonds are analyzed in several fire scenarios to understand the influence of different carriers in adhesive tape bonds and the individual effect of flame retardant, PSA, carrier, and substrate on the fire behavior of the bonded materials.

To ease the understanding of the findings of doctoral dissertation, a rough introduction on acrylic PSA (tapes), different fire scenarios, fire behavior and flame retardants is provided in the following chapter.

### 3. Scientific background

#### 3.1. PSA and PSA tapes

PSA are permanently sticky adhesives that are applied by slight pressure. Since the development of the first PSA which were based on natural rubber and used in medical plasters [17], a large variety of PSA products have been researched and introduced to the market. Next to the natural rubber-based PSA, synthetic rubber, acrylics, silicones, polyurethanes, polyesters, polyether, and ethylene-vinyl acetate copolymers (EVA) are popular polymers for PSA nowadays [18], with acrylic PSA accounting for the largest share [19].

##### 3.1.1. Acrylic PSA

All acrylic PSA are synthesized by the (co-)polymerization of the following monomer structures (Figure 1) with the goal of yielding tacky adhesives without any tackifier or wetting agent necessary.

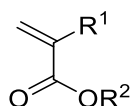


Figure 1: Acrylic monomer structure for PSA.

To ensure good mechanical and wetting properties, which are closely connected to a low  $T_g$  of acrylic PSA,  $R^1$  is either a hydrogen which refers to acrylates or a methyl group, which results in methacrylates. Formers have a lower  $T_g$  and often constitute the main component of PSA. The latter have a higher  $T_g$  [20] due to their reduced chain flexibility but can be beneficial for mechanical properties.  $R^2$  is mostly an alkyl rest that determines  $T_g$ , cohesion and adhesion. Long, unbranched alkyl rests yield in low  $T_g$  polymers [21] due to their inhibiting effect on crystallization and the formation of long van der Waals effected segments that confine the rotational freedom of the polymer backbone. At the same time, the steric hinderance of the side chains is small. Popular monomers for acrylic PSA are n-butyl acrylate and 2-ethylhexyl acrylate due to their good balance between cohesion, adhesion, and tack. Integrating more complex structures into the polymer, such as branched or aromatic side chains, can reduce the  $T_g$ -lowering effect of the side chain and even lead to an increased  $T_g$ . The  $T_g$  of copolymers can be calculated using the Fox equation [22] (equation 1), where  $w_x$  is the wt.-% of the monomer x and  $T_{g,x}$  is the  $T_g$  of a homopolymer of monomer x.

$$\frac{1}{T_g} = \frac{w_1}{T_{g,1}} + \frac{w_2}{T_{g,2}} \quad (1)$$

Acrylic acid and methacrylic acid as well as other polar acrylates are often copolymerized to increase the cohesive strength of the PSA due to their polarity and ability to build hydrogen bonds.

Free radical (co-)polymerization is performed in bulk, solution, emulsion, or suspension, aiming polymers with high molecular weights. Even though solvent polymerization leads to better mechanical properties, waterborne polymerization techniques are often preferred due to their many advantages. Emulsion polymerization yields higher molecular weight of the polymers, avoids the safety and environmental hazards of solvents, and yields aqueous solutions which are well coatable due to their low viscosities. These are the reasons for the strong market growth in water borne adhesives [23]. After synthesis, the adhesives are usually coated onto a carrier to make the adhesive easy applicable, resulting in adhesive tapes or labels that we all know from our daily lives.

### 3.1.2. Adhesive tapes

Depending on the application, adhesive tapes can be either single-sided or double-sided. Figure 2 shows the typical structure of double-sided adhesive tapes which are used in this doctoral dissertation.

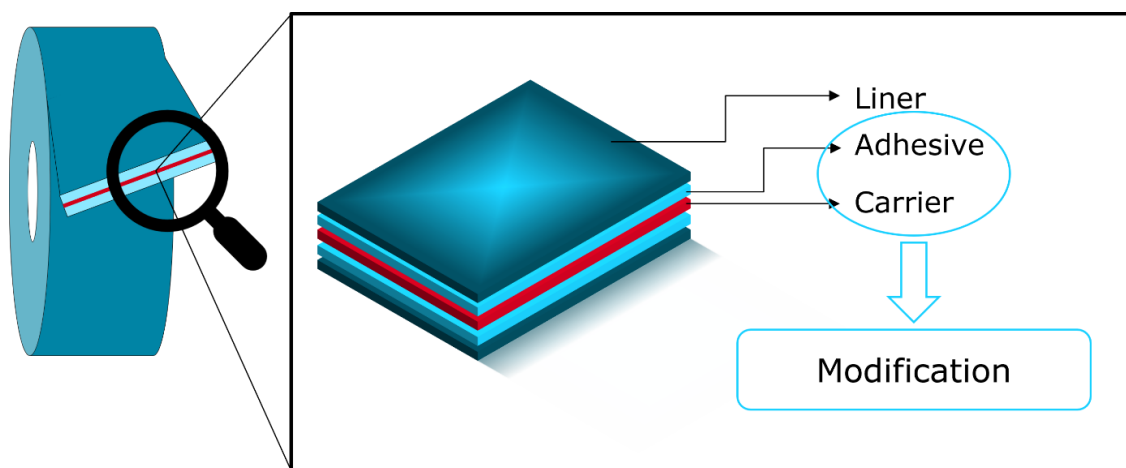


Figure 2: Structure of a double-sided adhesive tape.

The liner protects the adhesive layer from undesired sticking to surfaces and contamination and is removed shortly before application. It is usually made of kraft paper or polymeric films that are coated with silicone or fluoropolymers, both of which have very low surface energy [24] and thus serve as non-stick surfaces.

The adhesive and the carrier are the materials that remain in the bonded material and, together with the substrates, display the adhesive joint. All adhesive (tape) properties such as internal bond strength between carrier and adhesive, cohesive strength of the adhesive, adhesion characteristics, tack, temperature stability of the bond, chemical resistance, and fire behavior are thus determined by the adhesive formulation, the choice of carrier, and the substrate. These properties and how to modify them are briefly introduced in the following chapters.

### **3.1.3. Mechanical properties of PSA**

The most important mechanical properties of PSA are peel adhesion, shear adhesion, and tack, which are all measured by several adhesive specific standardized test methods.

Peel adhesion or peel resistance is defined as the force required to remove an adhesive tape from a surface at a defined angle and is measured on adhesive tapes which are prepared by coating the adhesive onto defined backings such as polyethylene terephthalate (PET) film or aluminum (AL) foil. After conditioning, the tape is adhered to a defined surface of steel or glass at a defined pressure and let dwell for a specified time. The tape is then peeled of the surface in a defined velocity and a specified angle (90 or 180°) [25].

The shear adhesion of adhesive tapes is measured by bonding an adhesive tape to a specified surface. A weight is attached to the adhesive tape, applying a constant shear force onto the bond. The time of failure is recorded [26].

Shear adhesion can also be measured under elevated temperature. The shear force/weight is kept constant as in the normal shear adhesion testing with the difference of the environment temperature being increased by a specific heat ramp (oven). The temperature at which the adhesive fails determines the shear adhesion failure temperature (SAFT) [27].

The tack of a PSA is the adhesion between the adhesive tape and the substrate directly after application and can be measured by different tests. The loop tack test is one of the most common ones, in which a loop of adhesive is brought into contact with a defined surface over a defined, short period of time. Subsequently, the tape is removed and the force which is necessary to remove the tape is measured [28].

This list of tests is, of course, not comprehensive but should display the most common tests and the ones used in this doctoral dissertation. Besides to the mechanical properties of the adhesives there are, depending on the end application, other demands for PSA tapes such as permeability or fire behavior. The use of PSA in railway vehicles, automobiles, aircrafts, and construction demands a good fire behavior of these tapes.

### **3.2. Fire behavior and flame retardancy**

Due to the high fire behavior requirements of materials in the above mentioned applications, flame retardants are often used to help achieve the demanded fire behavior for specific applications and are a key additive in almost every polymer formulation. To understand how flame retardants work and what their effect on different matrices are, one needs to understand how fires develop and where a flame retardant can possibly intervene to prevent the further development of a fire.

Fires can be divided into different stages with variations in temperature, heat flux, and ventilation as shown in Figure 3. In the incipient stage, the ignition takes place at low temperatures and a good ventilation. As the flame sustains and spreads, the developing stage begins. The temperature rises and more and more combustible gases are volatilized by the ongoing pyrolysis of the materials. At some point, the temperature reaches the ignition temperature of the evolved pyrolysis gases and leads to the so called flashover, where these gases are ignited, leading to a rapid increase in temperature. After the flashover took place, the new stage of a fully developed fire begins which is defined by a high temperature that almost remains in a steady state until insufficient fuel or oxygen concentration leads to a decrease in heat release rate (HRR) and temperature. This decrease marks the start of the decaying stage where fuel release and temperature decreases.

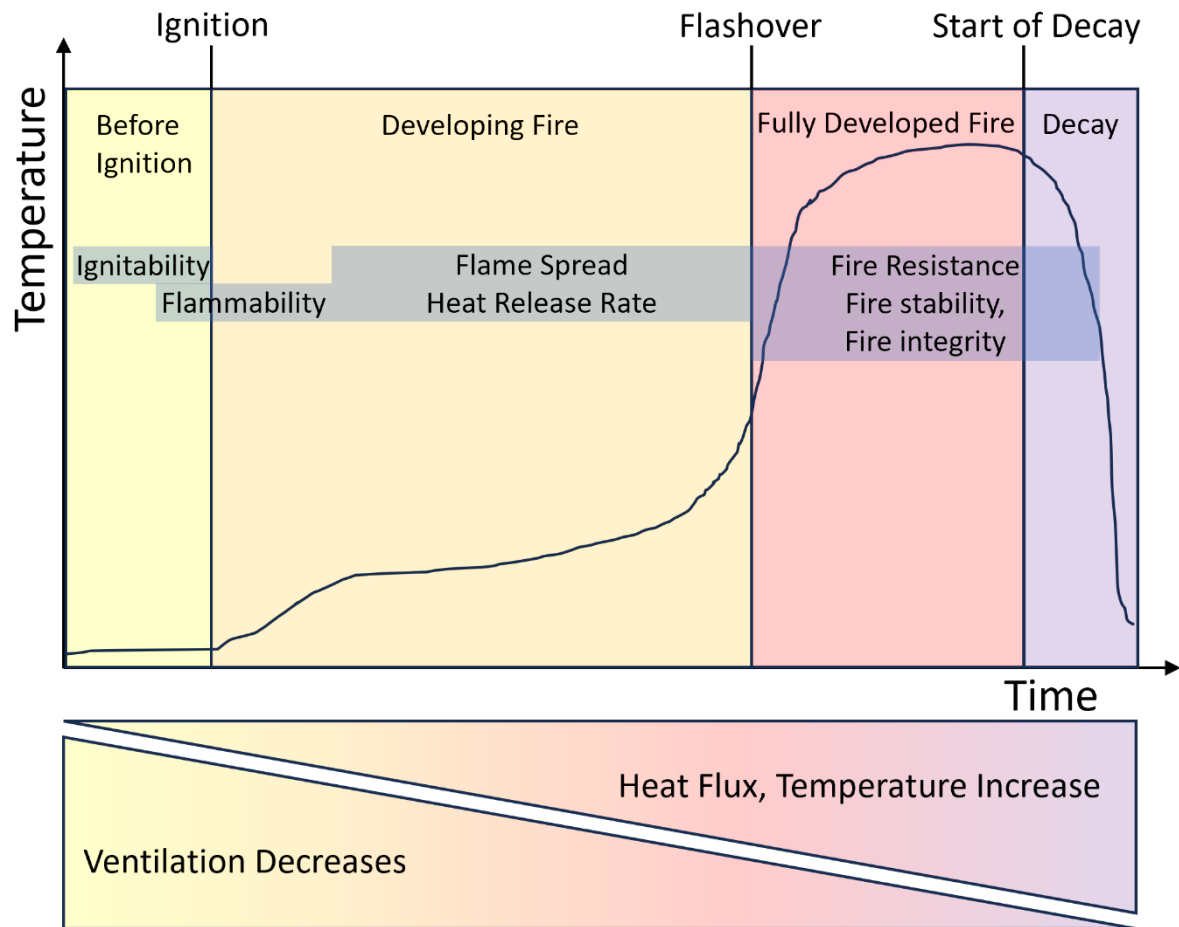


Figure 3: Development of temperature, heat flux, ventilation of a fire and the different stages with their protection goals. Based on [29].

Because the burning behavior of materials is rather a reaction to a specific fire scenario than an inherent material property [30], it is not possible to develop a fire test that comprehensively investigates the fire behavior or the flame retardancy of a material in all scenarios of fire and at all scales. Rather, fire tests are developed that represent a specific stage of a fire and simulate a fire scenario which resembles the hazards of a specific fire. Flame retardants work in the first three stages of a fire, acting in different ways to hinder or delay the burning process. In the ignition phase of a fire, the flammability/ ignitability determines the material's behavior and can be enhanced by several flame retardants. The behavior of a material in the developing stage is characterized by the flame spread, heat release and fire load of the material. In the third stage of a fire, it is important to keep the mechanical integrity of a material, making fire resistance the most important parameter for a material to perform well in this stage. Depending on the fire stage, different flame retardants can act in a variety of modes of action to improve a material's response to different fire scenarios and meet specified protection goals.



### 3.3. Flame retardant modes of action in polymers

The flame retardant modes of action describe how the flame retardant protects the matrix from the impact of a flame or other heat source and are divided into chemical and physical modes. Building a protective layer, cooling of the flame zone and the substrate, and dilution of the fuel gases are physical ways for a flame retardant to improve the fire behavior of polymers. A protective layer with low thermal conductivity slows down the degradation of the protected polymer matrix and lowers the amount of fuel gases that enter the flame zone. Flame retardants with endothermic decomposition, such as aluminum (tri)hydroxide (ATH) cool the substrate surface and slow down the degradation process. Additionally, ATH releases water, which dilutes the fuel gases and thus slows down the combustion process. The chemical action of flame retardants can happen in both, the condensed and the gas phase. In the condensed phase, one of the most important protection modes of flame retardants is to generate or promote a char layer that acts as a barrier with low thermal conductivity. The protective layer can also consist of inorganic glass like material [31]. A special form of generating a protective layer is Intumescence which is based on blowing agents, an acid source and a charring agent and builds up a voluminous, insulating, carbonaceous char layer [32].

Paradoxical to the barrier effect that protects the polymer from pyrolysis, acceleration of the polymer breakdown is another chemical mode of action of flame retardants, which leads to retreat of the polymer from the external heat source combined with the loss of burning/hot material [33].

The individual effects can be explained along the single parameters describing the HRR of a material in a fire scenario (equation 4). The HRR of a material is the most important response to a fire scenario and is determined by the combustion efficiency  $\chi$ , the potentially occurring protection layer effect  $\theta(t)$ , the char yield  $\mu$ , the ratio of heat of complete combustion of the volatiles to the enthalpy of gasification  $\frac{h_c}{h_g}$ , and the net heat flux  $\dot{q}''_{net}$ .  $\dot{q}''_{net}$  is the sum of the heat fluxes to and from the sample surface [34].

$$HRR = \chi * \theta(t) * (1 - \mu) * \frac{h_c}{h_g} * \dot{q}''_{net} \quad (2)$$

$$\dot{q}''_{net} = \dot{q}''_{ext} + \dot{q}''_{flame} - \dot{q}''_{rerad} - \dot{q}''_{loss} \quad (3)$$

$$HRR = \chi * \theta(t) * (1 - \mu) * \frac{h_c}{h_g} * (\dot{q}''_{ext} + \dot{q}''_{flame} - \dot{q}''_{rerad} - \dot{q}''_{loss}) \quad (4)$$

Combustion efficiency  $\chi$ , defined as the ratio of the heat release of combustion in a fire scenario to the heat release of complete combustion of the volatiles, can be lowered by flame poisoning flame retardants. Flame poisoning flame retardants scavenge radicals from the flame zone and lead to incomplete combustion of the evolving gases which reduces the  $\dot{q}''_{\text{flame}}$ . The time-dependent protection layer factor  $\theta(t)$  can be influenced by flame retardants that induce or increase the protection layer of the matrix in a fire. This factor is lowered with an increasing protection effect.  $\mu$  can be increased by charring agents and char inducing flame retardants which increase this value between 0 (no charring) and 1 (pure char). The factor  $\frac{h_c}{h_g}$  can be influenced by flame retardants in two ways.  $h_c$  can either be lowered by flame retardants that release incombustible gases such as  $\text{N}_2$ ,  $\text{H}_2\text{O}$ , or  $\text{CO}_2$ , or  $h_g$  can be increased by the gasification of these inert gases.  $\dot{q}''_{\text{ext}}$  as an external source is the only factor in the HRR equation which cannot be changed by any flame retardant.  $\dot{q}''_{\text{flame}}$  is sensitive to fuel dilution which then reduces the combustion rate in the flame zone and thus the temperature of the flame. The  $\dot{q}''_{\text{rerad}}$  can be increased by a protection layer that heats up and reradiates the heat of the external heat source, resulting in a decrease of the HRR. Another option for lowering the outcome of equation 4 is to increase the  $\dot{q}''_{\text{loss}}$  by increasing the thermal conductivity of the polymer in fires or by coating the polymer with an IR mirror that increases the IR reflectance [35].

Describing all these effects individually does not mean that they occur in isolation. On the contrary, they often occur simultaneously, and synergistic effects of different flame retardants are used to obtain polymers with good fire behavior and little flame retardant concentrations at the same time.

These modes of action give an overview of the possibility of flame retardants to protect a polymer matrix from fire. For the very specific matrix of PSA tapes discussed in this dissertation, flame retardants must meet certain requirements in order to enhance the fire behavior.

### 3.4. Flame retardants in PSA

Protecting PSA from the impact of a flame is not as simple as blending in some commercially available flame retardants. Adhesive properties such as adhesion, cohesion and tack suffer from blending in inorganic flame retardants [36,37] such as ATH (the quantitatively most important mineral flame retardant throughout the world), talc, or graphene [38]. This reduction of the mechanical properties is also known for other additives [39,40]. The fact that a PSA stays in a viscoelastic form even after application is an additional problem, leading to easier migration of additives and

reduced adhesion [41]. To overcome these challenges, flame retardants are needed that can be chemically modified to be well compatible with the polymer and meet the demands that a PSA matrix postulates. A good example is phosphorus-based flame retardants, which are a very versatile class of flame retardants that can be adjusted to the specific demands of the of the polymer matrix and application. Since halogenated flame retardants are under critique due to toxicity and environmental concerns [42], phosphorus flame retardants have been widely used as an alternative and become more and more popular. Due to the multitude of phosphorus flame retardants [43], it is useful to divide their mode of action into gas and condensed phase. The general flame retardant mechanism of phosphorus species in the gas phase is to scavenge radicals and poison the flame (Figure 4). The OH and H radical concentration and  $\chi$  are lowered which leads, according to equation 4, to a reduced HRR and can even lead to extinguishing of a fire. PO [44] and PO<sub>2</sub> [45] radicals play major roles in the scavenging of radicals in the gas phase and are released by many phosphorus-based flame retardants [46-49].

The condensed phase mechanism of phosphorus is based on phosphorus species building phosphoric acid or in a further dehydration step polyphosphoric acid [50]. These acids force the elimination of OH groups from the polymer and thus boost the formation of double bonds in the condensed phase resulting in enhanced char formation. Phosphorus flame retardants can also build an inorganic glassy protection layer [51]. It should be considered that the condensed effect is strongly dependent not only on the chemical environment of phosphorus, but also on the polymer matrix. To act in the condensed phase, the polymer matrix must react with the decomposing flame retardant which requires the flame retardant to stay in the condensed phase until the polymer matrix decomposes. If this prerequisite is fulfilled, phosphorus species with a higher oxidation state, such as phosphates, have a higher tendency to act in the condensed phase than flame retardants with lower oxidation states of phosphorus [52]. To yield a good condensed phase effect, it is best for the flame retardant to decompose at a similar temperature to that of the polymer matrix [53].

Especially in (pressure-sensitive) adhesives, the many-sided ways for modification of phosphorus flame retardants results in well compatible flame retardants for various applications. The 1972 patented (Sanko Chemical Co. Ltd.) DOPO (Figure 5) serves as a perfect example for the versatility of phosphorus-based flame retardants. It can be derivatized in multiple ways [54] to act as a flame retardant in applications such as textiles [55], epoxy resins [56], polyesters [57], polyamides [58], adhesives [16], and many more. The commonly known problem of the segregation of flame retardants

can be overcome by covalently bonding the flame retardant to the polymer backbone [59]. Thereby, the flame retardant is entirely immobilized and cannot migrate.

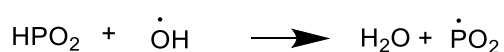
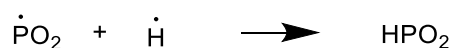
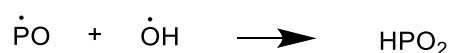
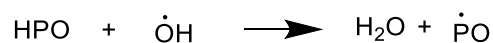
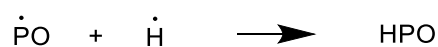


Figure 4: Gas phase flame retardant mechanism of phosphorus. Modified from [60].

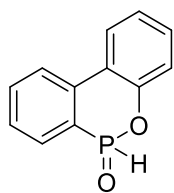


Figure 5: DOPO flame retardant.

The versatility of phosphorus-based flame retardants is demonstrated in this dissertation by implementing phosphorus flame retardants with different modes of action into PSA and PSA tapes. The effect of these modes of action is subsequently analyzed in different bond designs and fire scenarios to examine the interaction between substrates, PSA, carrier, and flame retardants.

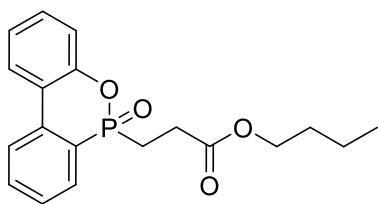
## 4. Materials and methods

### 4.1. Materials for the preparation of PSA (tapes) and flame retardants

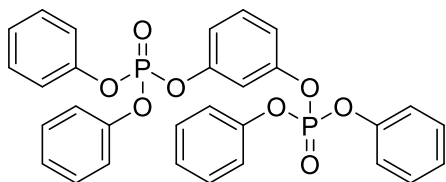
Double-sided adhesive tapes are a very special form of adhesives and thus not only need special preparation techniques but also special test methods to investigate their mechanical properties and fire behavior. These specific preparation and investigation techniques are therefore described in the following section.

Commercially available PSA tapes, self-synthesized flame retardant PSA and self-made PSA tapes were used as samples for a thorough investigation of the flame retardant mechanism and mode of action in PSA (tapes) and bonded materials. Several poly(n-butyl acrylate)-based PSA were prepared with the flame retardants that are shown in Figure 6. DOPO-pentyl-methacrylate, PSA and PSA tapes were prepared at IFAM Bremen by Kerstin Flothmeier under the supervision of Prof. Dr. Andreas Hartwig. DOPO-pentyl-methacrylate was synthesized according to Bier et. al. [61]. The synthesis is described in detail in the second publication (5.2).

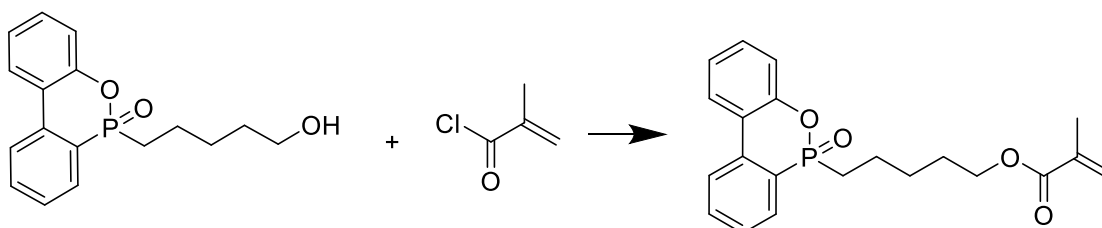
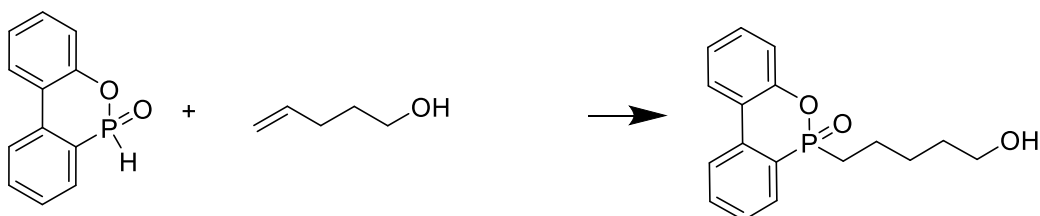
The flame retardants were chosen to represent phosphorus-based flame retardants that differ in the chemical environment of phosphorus, their potential mode of action, and the way they are incorporated into the polymer matrix. DOB 11, as a DOPO-derivate (phosphinate) can, depending on the matrix, act in the condensed or gas phase. RDP as a phosphate is a precursor of phosphoric/polyphosphoric acid and reported to be a condensed phase active flame retardant that improves charring. DOPO-pentyl-methacrylate as an innovative reactive flame retardant is copolymerized with n-butyl acrylate and on this way covalently bonded to the polymer backbone. All PSA were coated onto PET and AL tapes, yielding four different PSA tapes and two commercially available tapes. To connect the pyrolysis and flame retardant mode of action of the flame retardants with the flammability of the adhesive tapes and their effects in the bonded materials, the tapes were used to bond several substrates in different bond designs (Figure 7).



DOB 11



RDP



DOPO-pentyl-methacrylate

Figure 6: Structure of the PSA flame retardants (adopted from 5.2).

To connect the burning behavior of the tape as free-standing object, coating and in an adhesive joint, Beech wood, poly(methyl methacrylate) (PMMA), bisphenol-A-polycarbonate (PC), steel, and mineral wool were chosen as substrates due to their vast spectrum of burning behavior. (Beech) wood, as a unique natural material, builds up a char layer which cracks open within the burning process [62]. PMMA, as a thermoplastic material, melts, does not char and burns without leaving residue. PC first melts and subsequently creates a voluminous char structure similar to an intumescent behavior. Steel, as a metal, does not decompose and has, in contrast to all other organic materials, a high heat conductivity. Mineral wool was used as the second inherently flame retardant substrate, but in unlike steel, it is a porous medium with low heat conductivity.

To point out the influence of the adhesive tapes in the bonded materials, the burning behavior of the substrate as a monolithic (consisting of one material) material was compared to the burning behavior of the same substrate bonded by PSA tapes.

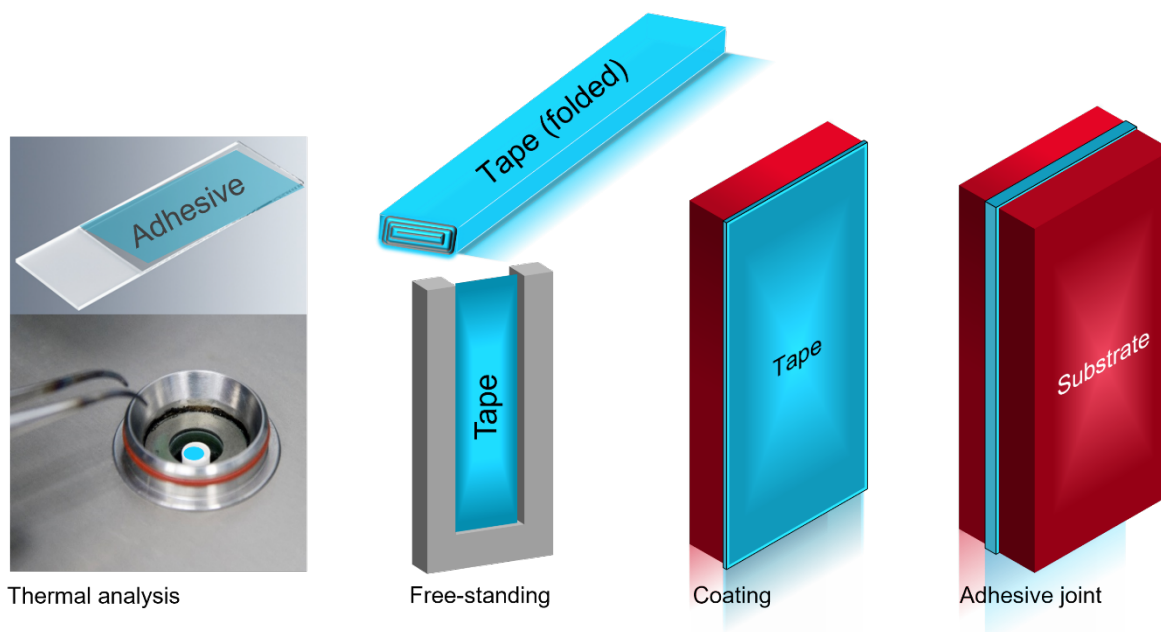


Figure 7: Sample designs for the pyrolysis and fire behavior analysis.

#### 4.2. Adhesive analysis

To ensure a good sample preparation and a possible application as PSA tapes, the mechanical properties of the tapes were analyzed, even though the focus of this doctoral thesis is on the fire behavior. To guarantee a good tack and permanent stickiness, the  $T_g$  of the self-synthesized PSA was determined by differential scanning calorimetry (DSC).

The SAFT test and a peel test were used to investigate the adhesion and cohesion properties at room and elevated temperatures.

#### 4.3. Pyrolysis analysis

One of the goals of this work is to connect the pyrolysis characteristics with the fire behavior of PSA tapes. Therefore, the pyrolysis of the adhesive, the flame retardant, and the polymer matrix were investigated separately, providing information on the interaction between the flame retardant and the matrix and elaborating the mode of protection. Different methods were used to investigate the decomposition temperature, the decomposition steps and mechanisms, the combustibility of the evolved gases, and to identify the gasified species evolved during pyrolysis. Additionally,

the pyrolysis process of the condensed phase was analyzed at macroscopic and molecular scale. Pyrolysis analysis was performed in the absence of oxygen, which represents the anaerobe conditions at a material surface in a fire (diffusion flame) [63].

#### 4.3.1. Thermogravimetric analysis coupled with Fourier-transform infrared spectroscopy (TGA FTIR)

The TGA FTIR investigates the thermal decomposition of a material by measuring the mass loss under a defined heating ramp. Decomposition temperatures and decomposition steps at certain temperatures lead to an understanding of how the material decomposes. The evolving gases and substances in the gas phase are then led to a FTIR detector by a transfer line to gain information on the chemical properties of the decomposition products and deduce a decomposition mechanism.

#### 4.3.2. Hot-stage FTIR

While TGA FTIR gives information about the gas phase products, the hot-stage FTIR analyzes the surface of the pyrolyzing material, yielding information about the functional groups of the material surface. The sample is heated at a defined heat ramp in a nitrogen atmosphere while an FTIR microscope is directed onto the surface, recording spectra at different temperatures and positions. This way, chemical processes at the surface can be observed and condensed phase mechanism can be analyzed. The microscope can also take digital images of the adhesive surface for macroscopic observation. A scheme of the hot-stage FTIR is shown in Figure 8. Both methods, TGA FTIR and hot-stage FTIR, only require milligrams of sample. This method is particularly suitable for PSA tapes and PSA because the viscosity of the adhesive films decreases, the film spreads and the thickness decreases allowing transmission and absorption FTIR measurements.

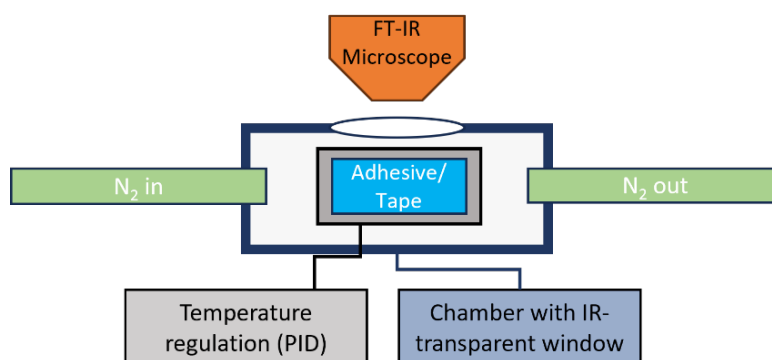


Figure 8: Systematic scheme of the hot-stage FTIR.



### 4.3.3. Pyrolysis gas chromatography coupled with mass spectrometry (Py-GC/MS)

To obtain detailed information about the decomposition products of the PSA matrix, the flame retardant and their interaction, the samples were analyzed by Py-GC/MS. The sample is pyrolyzed in a preheated pyrolyzer at 500 °C and the gasified pyrolysis products are led through a heated capillary column where the products are separated according to their physical and chemical characteristics. Subsequently, the volatiles are led to an MS where the pyrolysis products are fragmented, ionized, and separated by mass per charge number ( $m/z$ ). The MS spectra of the pyrolysis products are finally compared to a library for identification. A systematic sketch of a Py-GC/MS is shown in Figure 9.

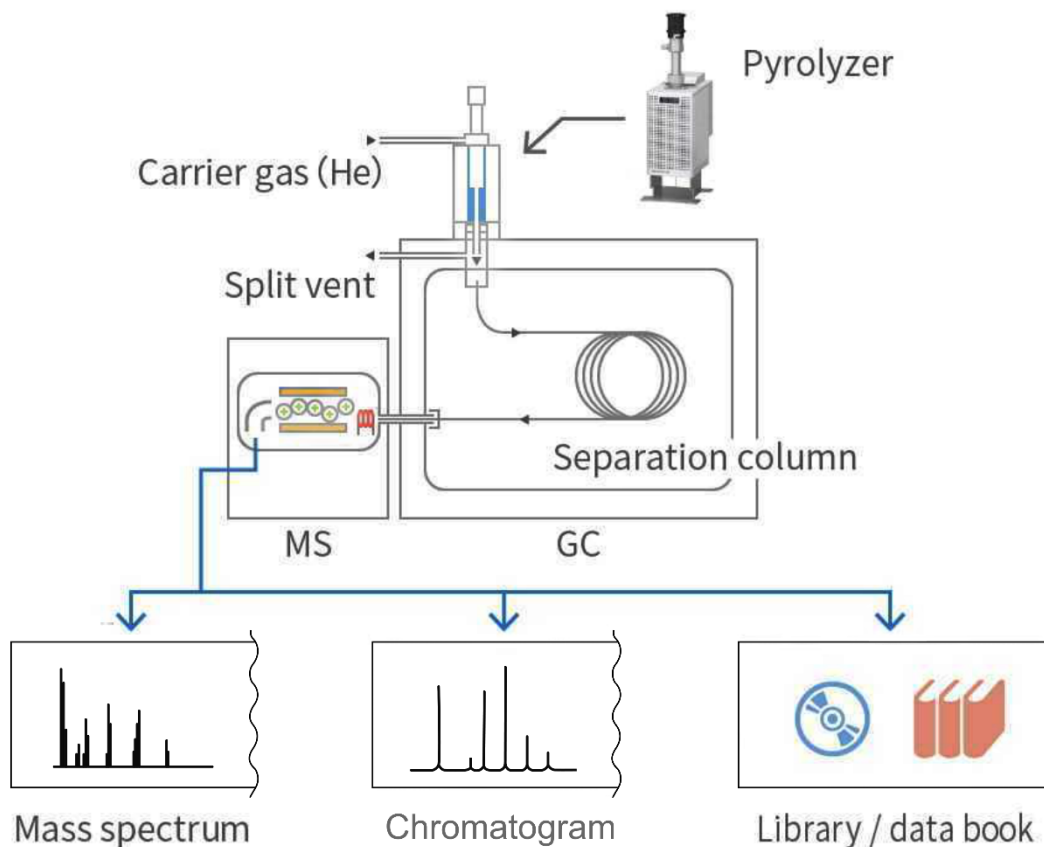


Figure 9: Systematic scheme of a Py-GC/MS. Modified from [64].

### 4.3.4. Pyrolysis combustion flow calorimeter

The pyrolysis combustion flow calorimeter (PCFC) imitates the burning process of a material in a flame and thus gives information on the combustion process of the PSA

and flame retardants. It pyrolyzes the material (milligram scale) in a pyrolizer under a nitrogen atmosphere with a heating ramp of  $1 \text{ K s}^{-1}$  and leads the gasified decomposition products into a gas stream where the nitrogen/fuel gas stream is mixed with 20 vol.% oxygen. In the heated combustor the volatile pyrolysis products are oxidized, leading to complete combustion of the volatiles. Heat release data are measured indirectly via the oxygen consumption (each organic material produces 13.1 MJ per kg  $\text{O}_2$  consumed [65]). Peak of heat release rate (PHRR), heat release capacity (HRC), fire growth capacity (FGC) and residue define the PCFC results and give insight into the combustion process and indicate fire hazards of the material. Particularly for the detection of the production of incombustible gases, which dilute the fuel gases, it is a suitable analysis method due to the lower oxygen consumption compared to pure organic fuel gases. Due to the forced complete combustion of the volatiles and the milligram scale, the PCFC is blind for flame poisoning and macroscopic effects such as melt dripping or intumescence [66]. The structure and the parallels between the PCFC and the flaming combustion of a burning material are shown in Figure 10 (red box). On the right hand side, the actual apparatus (FAA Micro Calorimeter, Fire testing technology, UK) is shown.

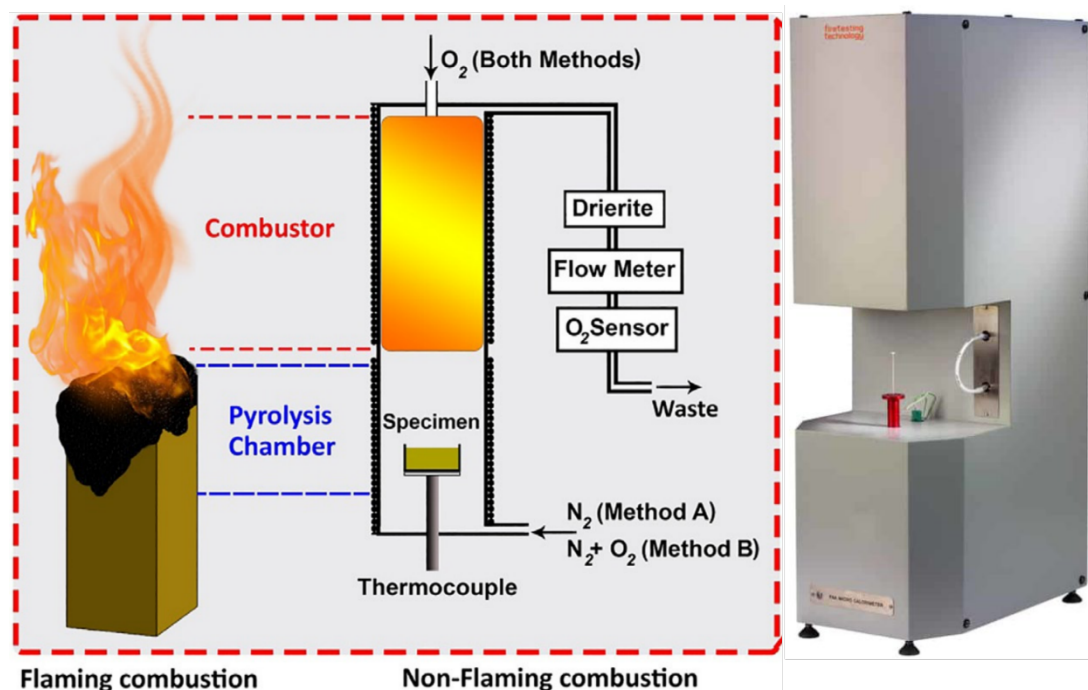


Figure 10: Systematic scheme of a pyrolysis combustion flow calorimeter as a combination of [67] and [68].

## 4.4. Reaction to a small flame simulating the ignition stage of a fire

### 4.4.1. UL94

In order to correlate the aforementioned pyrolysis with the flammability of the PSA tapes and bonds, UL 94 and OI measurements were performed. In the UL 94 test which is the state-of-the-art assessment for electronic applications, specimens of 125x13 mm are held over a Bunsen burner by a clamp and are ignited at the bottom edge. The specimen thickness depends on the application. Time and distance traveled by the upward moving flame are recorded and used to divide the samples into classes. Due to the flexibility and the thinness of the adhesive tapes, these samples had to be stacked to 1 mm thickness to obtain repeatable and comparable measurements (Figure 11 a)). The thin samples would otherwise distort and avoid the burner flame. Substrates and bonded samples were measured at a thickness of 4-8 mm.

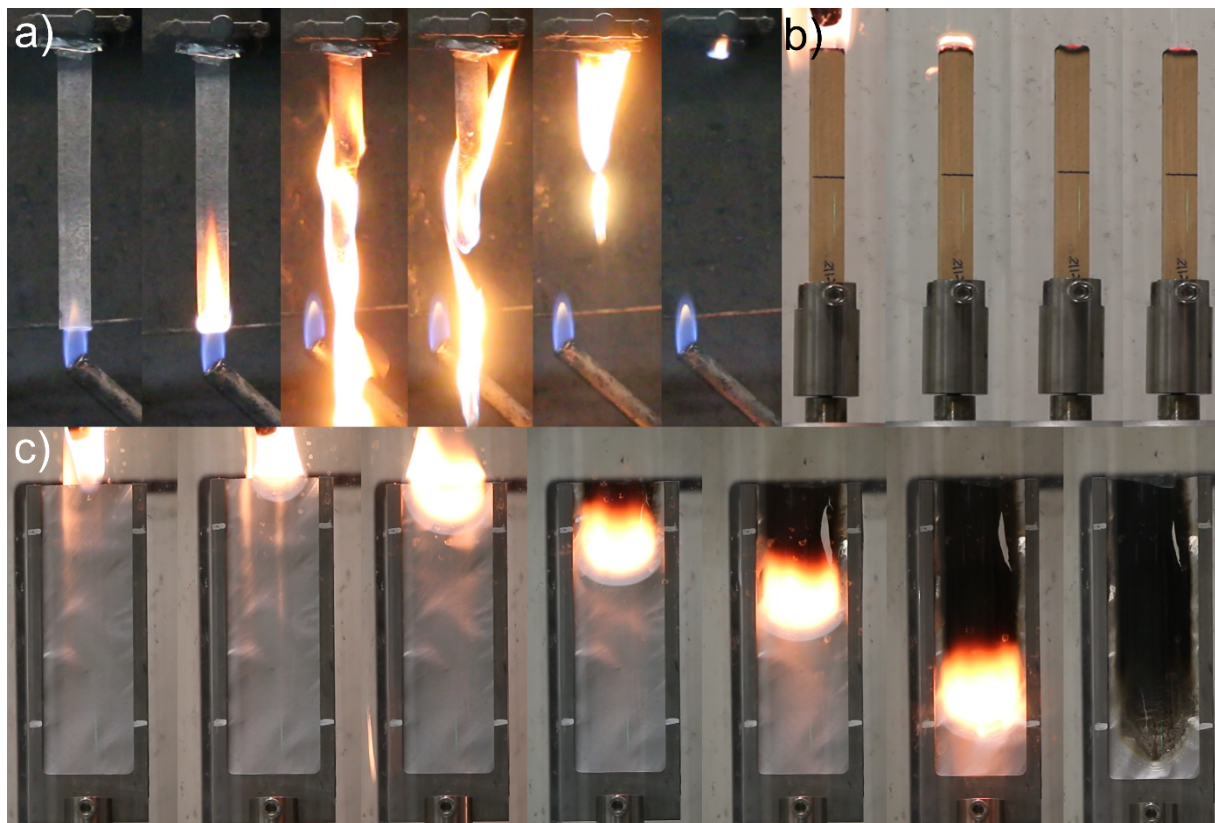


Figure 11: Flammability tests for adhesive tapes, bonded materials, and substrates.

### 4.4.2. Oxygen index (OI)

The OI, according to ISO 4689-2, is a method for determining the fire behavior of materials in an ignition fire scenario in which the material is ignited from the top and the distance and time of the flame propagation are recorded. The sample is placed

in a chimney to ensure a homogenous and defined nitrogen/oxygen atmosphere. After reaching a traveled distance of 50 mm for method 1 and (80 mm for method 2), the sample fails the test. The OI is finally defined as the minimal vol.% of oxygen in the controlled atmosphere to sustain the flame. The OI was measured using two different specimen designs due to the missing bending stiffness of the adhesive and the distorting under flame exposure. For the first method, the tapes are folded and formed into a rod with the dimensions 70x7x1.5 mm which is then tested by method one. All substrates and bonded materials were also tested in method one (Figure 11 b)). The second method, used for AL carrier tapes, takes place in the modified specimen holder for thin foils (Figure 11 c)). Measuring in this frame resulted in repeatable and comparable measurements for all AL PSA tapes.

#### 4.4.3. Single-flame source test

The EN 11925-2 single-flame source test continued the structured fire behavior investigations from the freestanding tape, through the one-side coated substrate, to the bonded material (Figure 7), pointing out the influence of substrate, bond design and flame retardant. A burner is aimed at the specimen at a defined angle and ignites either at the bottom edge or at the lateral sample surface area. Materials are classified according to ignition and flame spread over time.

The test is used to identify the interaction between the substrate, the adhesive tape, and the influence of flame retardant. The strong influence of the substrate and the flame retardant on the burning behavior of the adhesive tapes in the single-flame source test is shown in Figure 12.

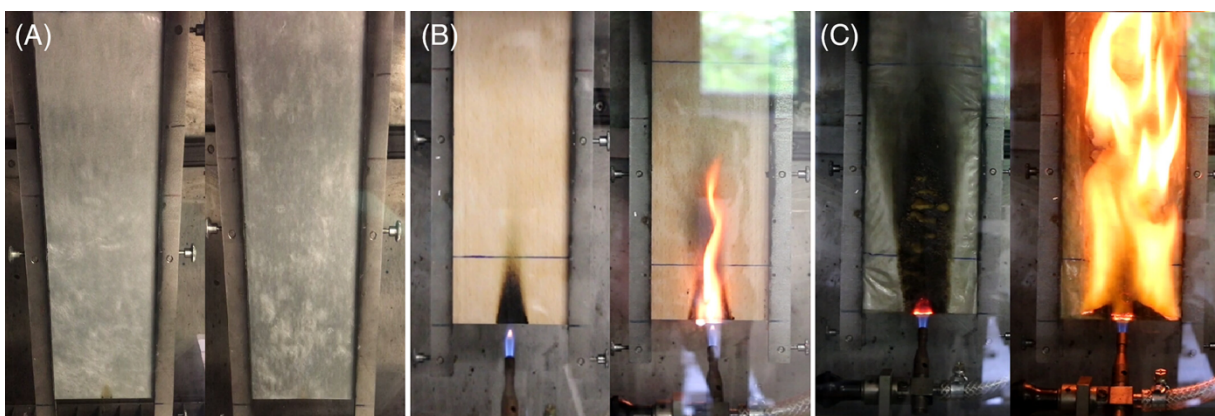


Figure 12: ISO 11925-2 single-flame source test of different adhesive tapes coated on different materials. Flame retardant (left) and not flame retardant (right) tape on A: zinc-plated steel, B: Beech wood and C: Mineral wool. Figure used from 5.1.

#### 4.5. Fire behavior in the developing fire scenario

The fire behavior of substrates and bonded materials in a developing fire scenario was investigated using the cone calorimeter, which was constructed and published by V. Babrauskas in 1982 [69]. After its development, the cone calorimeter rapidly became the most common and most important bench scale test for the fire behavior of polymeric materials and is well defined in ISO 5660 and ASTM E1354.

Figure 13 shows a sketch of the cone calorimeter and the sample setup where the sample is heated up by the conical heater and the evolving gases are ignited by the ignition source (optional). The gases are led through the exhaust system where the gas sampling takes place, and the oxygen consumption is measured. The HRR is then calculated using the oxygen consumption theory (section 4.3.4) and describes the fire behavior of a material. In addition to the time to ignition ( $t_{ig}$ ) and the HRR, CO and CO<sub>2</sub> concentrations are analyzed in the exhaust gas stream and smoke production is monitored. Because the complete HRR curve requires expertise to interpret, key indices such as the fire growth rate index (FIGRA) and maximum average of heat emission (MARHE) have been established over the last decades to indicate different fire hazards. The cone calorimeter can quantify flame retardant modes of action (section 3.3) in the form of flame poisoning, protection layers, fuel dilution, cooling, intumescence, etc. by comparing the non-flame retardant with the flame retardant material.

The effect of adhesives and adhesive tapes on the burning behavior of bonded materials was investigated in the same way, comparing the monolithic material to the bonded material. The cone calorimeter was used to precisely find out about the influence of adhesive tape, flame retardant and adhesive tape carrier in an adhesive joint and how the substrate changes this influence. Furthermore, various substrate-specific fire risks were pointed out, resulting in a better understanding of how to develop adhesive tapes and how to select the right adhesive tape for certain substrate classes. All measurements were performed without a retainer frame and at 50 kW m<sup>-2</sup>, which refers to the release relevant cone calorimeter measurements for railway vehicle interiors (EN 45545-2). The distance between cone heater and sample is increased from 25 mm (standard) to 35 mm due to potential inherent intumescent behavior of the PC samples. ScharTEL et. al. prove that up to 40 mm between the cone heater and the sample is acceptable and yields in a homogenous irradiance over the sample surface in compliance with the ISO 5660 standard [70]. In addition to the sample holder, wooden samples were held in position by four wires wrapped around the sample and the AL tray. This prevented the wood layers from distorting and wood pieces from

falling off the sample holder. All Samples were ignited using a spark igniter according to the standard.

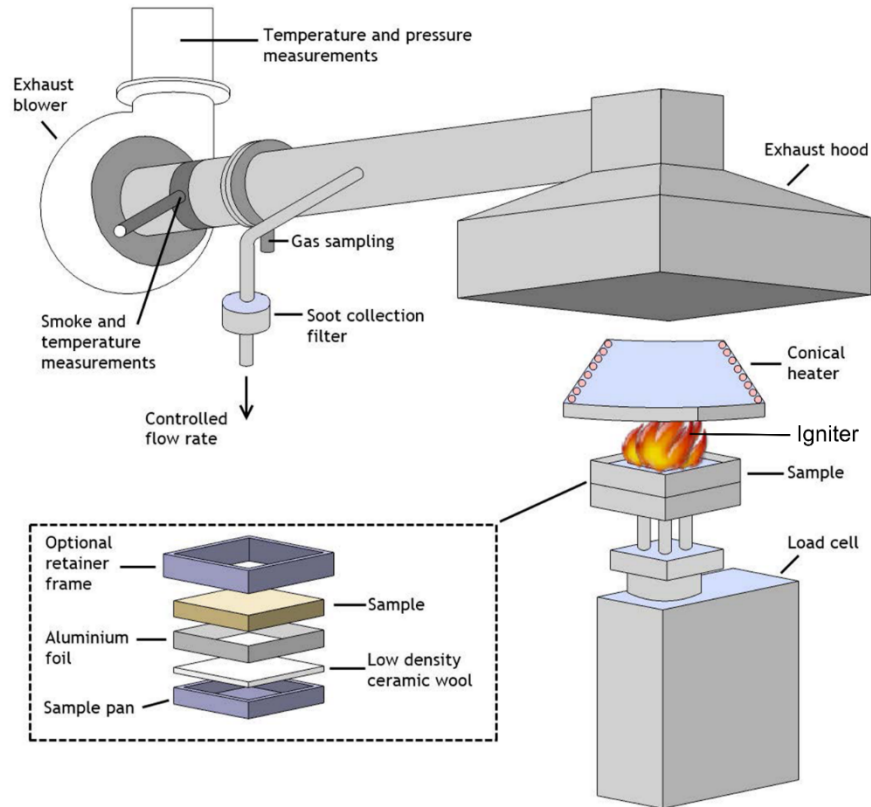


Figure 13: Cone calorimeter sketch from [71] with addition of the ignition source.

#### 4.6. Fire resistance in the fully developed fire scenario

The fire resistance test investigates the adhesive tape bonds in a fully developed fire scenario and examines the relationship between the mechanical properties, pyrolysis, and flammability of the PSA tapes and their performance in the last stage of a fire before decay. Fire resistance tests are usually very costly and time consuming. This was the reason for developing a self-designed bench scale test to compare the fire resistance of the different adhesive tapes and the adhesive bonds. The fire resistance test consists of a sample holder in which the bonded materials can be clamped in a fixed position, loaded with a defined weight, and exposed to a burner flame that simulates a fully developed fire. To ensure a constant heat flux, a Nextgen® burner was calibrated to  $75 \text{ kW m}^{-2}$  using a dummy specimen in the same dimensions as the real specimen. The dummy was equipped with a heat flux meter which was positioned

in a recess and exposed to the burner flame in the same way as the samples in the test. For the test procedure, the distance, position, and gas flow of the burner flame were kept constant so that the heat flux and the impact zone of the burner stayed constant. With the setup shown in in Figure 14, the fire resistance of the adhesive tape bonds was determined measuring the failure time and the backside temperature of the first substrate layer.

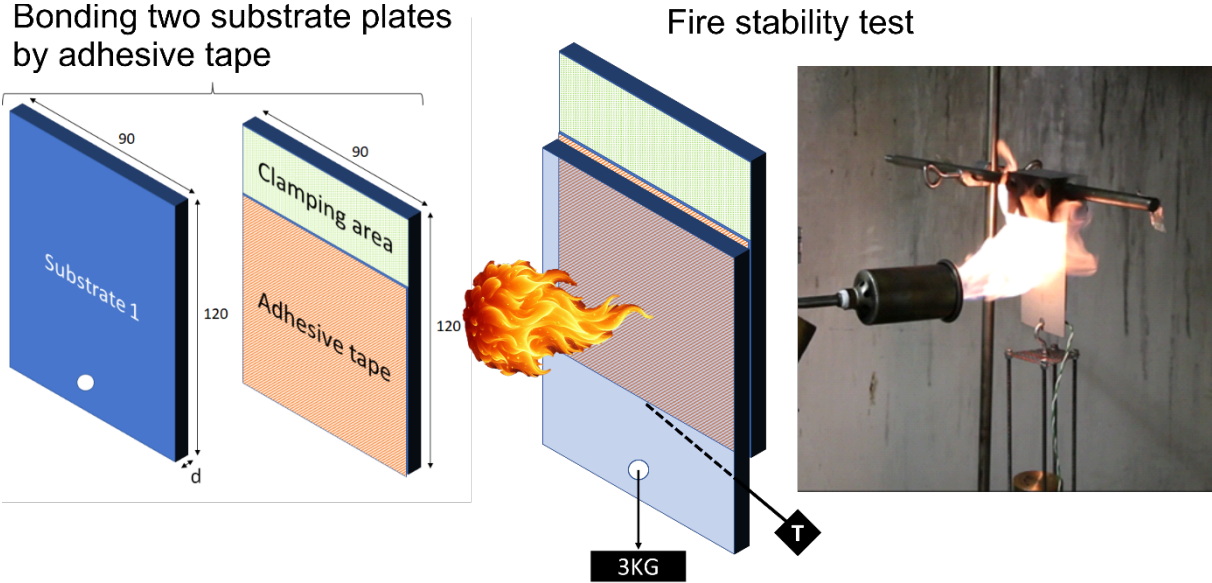


Figure 14: Fire resistance test (adopted from 5.3).

The fire resistance test completes the structured analysis of the fire behavior of adhesive tapes and their bonds, covering all fire scenarios before decay.

## 5. Publications

### 5.1. Fire behavior of pressure-sensitive adhesive tapes and bonded materials

Vitus Hupp, Bernhard Schartel, Kerstin Flothmeier, Andreas Hartwig  
Fire and Materials, **2024**; 48, 114-127.  
<https://doi.org/10.1002/fam.3171>

Published under a Creative Commons license:  
<https://creativecommons.org/licenses/by/4.0/>

This article was accepted and published.

Author contribution:

- Conceptual work for the paper and experiments
- Sample preparation
- Developing test methods to examine the fire behavior of tapes and bonded materials
- Pyrolytic investigations of the PSA and PSA tapes
  - TGA FTIR
  - ATR FTIR
  - Hot-stage FTIR evaluation
  - PCFC
  - Py-GC/MS evaluation
- Fire testing of adhesive tapes and adhesive tape-bonded specimens
  - UL 94
  - OI
  - Cone Calorimetry
  - Single-flame source test (ISO 11925-2)
- Data evaluation
- Figure ideas and design throughout the article
- Scientific discussion and writing the article
- Correction, spell-checking all versions



## **Abstract**

Pressure-sensitive adhesive tapes are used in several industrial applications such as construction, railway vehicles and the automotive sector, where the burning behavior is of crucial importance. Flame retarded adhesive tapes are developed and provided, however, often without considering the interaction of adhesive tapes and the bonded materials during burning nor the contribution of the tapes to fire protection goal of the bonded components in distinct fire tests. This publication delivers an empirical comprehensive knowledge how adhesive tapes and their flame retardancy effect the burning behavior of bonded materials. With a special focus on the interaction between the single components, one flame retarded tape and one tape without flame retardant are examined in scenarios of emerging and developing fires, along with their bonds with the common materials wood, zinc-plated steel, mineral wool, polycarbonate, and polymethylmethacrylate. The flame retardant significantly improved the flame retardancy of the tape as a free-standing object and yielded a V-2 rating in UL 94 vertical test and raised the Oxygen Index by 5 vol.%. In bonds, or rather laminates, the investigations prove that the choice of carrier and substrates are the factors with the greatest impact on the fire properties and can change the peak of heat release rate and the maximum average rate of heat emission up to 25%. This research yielded a good empirical overall understanding of the fire behavior of adhesive tapes and bonded materials. Thus, it serves as a guide for tape manufacturers and applicants to develop tapes and bonds more substrate specific.

## RESEARCH ARTICLE

WILEY

# Fire behavior of pressure-sensitive adhesive tapes and bonded materials

Vitus Hupp<sup>1</sup> | Bernhard Schartel<sup>1</sup> | Kerstin Flothmeier<sup>2</sup> | Andreas Hartwig<sup>2,3</sup>

<sup>1</sup>Bundesanstalt für Materialforschung und -prüfung (BAM), Berlin, Germany

<sup>2</sup>Fraunhofer Institute for Manufacturing Technology and Advanced Materials, Bremen, Germany

<sup>3</sup>Department 2 Biology/Chemistry, University of Bremen, Bremen, Germany

## Correspondence

Bernhard Schartel, Bundesanstalt für Materialforschung und -prüfung (BAM), Unter den Eichen 87, 12205 Berlin, Germany.  
Email: [bernhard.schartel@bam.de](mailto:bernhard.schartel@bam.de)

## Funding information

Allianz Industrie Forschung, Grant/Award Number: 20762 N

## Abstract

Pressure-sensitive adhesive tapes are used in several industrial applications such as construction, railway vehicles and the automotive sector, where the burning behavior is of crucial importance. Flame retarded adhesive tapes are developed and provided, however, often without considering the interaction of adhesive tapes and the bonded materials during burning nor the contribution of the tapes to fire protection goal of the bonded components in distinct fire tests. This publication delivers an empirical comprehensive knowledge how adhesive tapes and their flame retardancy effect the burning behavior of bonded materials. With a special focus on the interaction between the single components, one flame retarded tape and one tape without flame retardant are examined in scenarios of emerging and developing fires, along with their bonds with the common materials wood, zinc-plated steel, mineral wool, polycarbonate, and polymethylmethacrylate. The flame retardant significantly improved the flame retardancy of the tape as a free-standing object and yielded a V-2 rating in UL 94 vertical test and raised the Oxygen Index by 5 vol.%. In bonds, or rather laminates, the investigations prove that the choice of carrier and substrates are the factors with the greatest impact on the fire properties and can change the peak of heat release rate and the maximum average rate of heat emission up to 25%. This research yielded a good empirical overall understanding of the fire behavior of adhesive tapes and bonded materials. Thus, it serves as a guide for tape manufacturers and applicants to develop tapes and bonds more substrate specific.

## KEYWORDS

adhesives, cone calorimeter, flame retardancy, laminates, phosphorus flame retardants, pressure-sensitive adhesive, tapes

## 1 | INTRODUCTION

Pressure-sensitive adhesives (PSA) are permanent tacky polymers that can adhere to a variety of surfaces by applying light pressure. The permanent tack is achieved using polymers, copolymers, or blends with a low glass transition temperature ( $T_g$ ). PSA tapes became very popular in the construction, transport, and automotive industries in recent decades due to their advantages over mechanical fasteners and liquid

adhesives. To mention just a few of their properties: they can absorb noise and vibrations, have good gap-filling properties, are easy to apply and cause no weak spots at bounded surfaces.<sup>1</sup> Despite all these advantages, there is one major disadvantage, namely poor behavior under high temperature and fire conditions. Most PSA consist of rubber-like polymers and are intrinsically flammable.<sup>2</sup> The improvement achieved by using halogen-free flame retardants such as phosphorus-based ones has been investigated in very few papers,<sup>3</sup> so

This is an open access article under the terms of the [Creative Commons Attribution](https://creativecommons.org/licenses/by/4.0/) License, which permits use, distribution and reproduction in any medium, provided the original work is properly cited.

© 2023 The Authors. *Fire and Materials* published by John Wiley & Sons Ltd.

that the general burning behavior of tape-bonded materials is not yet understood. Previous research has shown that combinations of polymeric materials behave differently in fires than the sum of the single components,<sup>4</sup> which indicates that the multi-layer arrangement of bonded substrates has its own specific fire properties. It is well known that thin materials such as films and coatings can change the burning behavior drastically and exhibit special burning characteristics,<sup>5-7</sup> and that the adhesive formulation can have an influence on the burning behavior of bonded construction elements,<sup>8-10</sup> which leads to the assumption that double-sided PSA tapes as thin films will impact the burning behavior of bonded materials. Since the literature shows that non-flammable interlayers in materials can improve the flame retardancy of laminates,<sup>11</sup> it is supposed that varying the carrier (the middle layer in double-sided adhesive tapes) has a strong impact on the burning behavior of bonded materials. All these clues lead to the question as to whether and in which way PSA tapes influence the burning behavior of bonded construction and passenger transport materials. How do PSA tapes impact flammability and flame spread? Are there any direct links between the flame retardancy of the free-standing adhesive tape and the burning behavior of the distinct bonded substrates? Do different tape-substrate configurations and different fire scenarios highlight different phenomena? These are the main issues of this research paper and are investigated to avoid human and economic damage and health hazards. Acrylate based tapes as the most common class of PSA for durable product is intrinsically flammable due to their polyacrylate backbone with hydrocarbon chains. The pyrolysis and the fire properties of a flame-retardant tape and a non-protected tape are investigated, and subsequently these tapes are used to manufacture sandwich-like bonds between common construction and passenger transport materials. The interactions between different material combinations and the effect of flame retardants in the adhesive formulation on different setups are then determined in a variety of materials. To address different carriers, aluminum as a non-flammable material and polyethylene terephthalate (PET) as a flammable polymer were compared in the developing fire scenario. This comprehensive empirical approach delivers a valuable insight in the fire behavior in different fire scenarios of the freestanding tapes, tapes in contact with substrates, and the bonded components. Differing properties are identified as key to understand the distinct fire properties, the conclusions may serve as guideline for future tailored development.

## 2 | MATERIALS AND METHODS

### 2.1 | Materials

Two double-sided tapes with acrylic adhesives coated on a nonwoven PET were provided by Lohmann GmbH & Co. KG (Germany). The tapes differed in their adhesive formulation. The commercially available flame retarded DuploColl® 94 100 FR, referred here as Tape FR, and a tape with the same basis formulation without flame retardant, referred here as Tape RE, were investigated. In addition, transfer

tapes (adhesives without a carrier) were provided for the pyrolysis investigations of the different adhesives. The double-sided adhesive tapes were used in combination with five different substrates, namely beechwood, zinc plated steel, mineral wool, polymethylmethacrylate (PMMA), bisphenol-A polycarbonate (PC) and acrylonitrile butadiene styrene copolymer (ABS). The beechwood specimens were cut from untreated beechwood planks. The wooden samples were all cut in the same fiber orientation since this influences fire testing results.<sup>12</sup> The zinc plated steel was used in a thickness of 1 mm and prepared via guillotine cutting. Rockwool Termarock 50 was purchased and used as an insulating wool with a defined raw density of 50 kg/m.<sup>3</sup> Extruded colorless PMMA (Plexiglas® XT) from Evonik Industries AG (Germany) served as the thermoplastic, non-charring substrate and was cut with a buzz saw to the demanded sizes. PC from Covestro AG (Germany) (Makrolon® GP) was used as a second plastic substrate and cut with a buzz saw. PC and PMMA were purchased from Thyssenkrupp Plastics GmbH (Germany) in the dimensions 1000 × 2000 × 2 mm<sup>3</sup>. ABS plates were purchased from S-Polytec GmbH (Germany) and cut with a buzz saw from a 1000 × 1000 × 1 mm<sup>3</sup> plate. For the investigation of different carriers, an aluminum foil was purchased from VWR International GmbH, Germany in a thickness of 30 μm.

The substrates were chosen due to the large variation in their burning characteristics and their industrial applications. Sandwich-like samples were manufactured by combining them with the acrylic adhesive tapes as intermediate layers (substrate/tape/substrate). The fire behavior of these samples was compared to the homogenous substrates to determine the effect of the tapes. A wide range of sample dimensions was used and varied depending on the material and test scenario. To manufacture coated samples, the adhesive tapes were adhered to the substrates; then air bubbles and inhomogeneities in the surface were eliminated via hand-pressure-roll. The sandwich elements were manufactured by releasing the liner paper of the acrylic adhesive tapes and bonding the second substrate layer on top of the tape surface. Again, the pressure roll was applied to optimize the homogenous contact between tape and substrate. Additionally, sandwich elements with an intermediate aluminum layer were manufactured (PMMA/adhesive tape/aluminum foil/adhesive tape/PMMA). In this case, the aluminum foil was coated with the double-sided tapes on each side and subsequently incorporated into the laminates in the same manner as described above.

### 2.2 | Methods

#### 2.2.1 | Mechanical tests

The mechanical properties of the bonds prepared with the double-sided tapes were analyzed in peel and SAFT tests to investigate the influence of the flame retardant on the adhesive strength and temperature resistance. The peel test was carried out according to DIN EN ISO 29862 (1939) and measured the peel strength at an 180° angle. In order to test them as single-sided tapes, the double-sided tapes were laminated on

either PET or aluminum foil. Specimens  $24 \times 300$  mm in size were laminated onto stainless steel ( $50 \times 200$  mm) according to Afera 5013 and stored for 24 h in a climate chamber at  $23^\circ\text{C}$  and a relative humidity of 50%. The test was performed using an Instron universal testing machine with a peel rate of 300 mm/min. The SAFT test was carried out according to Afera 5013 and measured the thermal stability of the bond. Single-sided tapes were prepared as described for the peel test. PSA tapes/laminates were bonded to a standard steel ( $50 \times 100$  mm<sup>2</sup>) with a contact area of  $24 \times 24$  mm<sup>2</sup> and placed in the test rack. A heating rate of  $0.5 \text{ K min}^{-1}$ , a maximum temperature of  $160^\circ\text{C}$  and a weight of 500 g were applied. For both mechanical tests, five specimens were tested for each tape.

## 2.2.2 | Pyrolysis analysis

To analyze the thermal decomposition of the adhesive, a transfer film was investigated by TGA in a Netzsch TG 209 F1 Iris (Germany) under nitrogen atmosphere (flow:  $30 \text{ mL min}^{-1}$ ). 10 mg of adhesives were cut out of a representative transfer film sheet and subsequently adhered to the bottom of the crucible. The sample was heated from  $30^\circ\text{C}$  to  $900^\circ\text{C}$  at a heating rate of  $10 \text{ K min}^{-1}$ . The emerging gases were transferred to a Bruker Optics Tensor27 infrared spectrometer, where the IR analysis took place. The transfer line was heated up to  $270^\circ\text{C}$ .

The transfer films were investigated in Py-GC/MS to investigate the emerging gases during pyrolysis. 30  $\mu\text{g}$  adhesive samples were pyrolyzed in a micro-furnace double-shot pyrolyzer (PY3030iD, Frontier Laboratories, Japan) at  $500^\circ\text{C}$  and subsequently led via split-/splitless inlet port to a gas chromatograph (7890B, Agilent Technologies, USA). The following column parameters were used: Ultra Alloy  $+5$  capillary column ( $l = 30$  m,  $iD = 0.25$  mm, film thickness =  $0.25$   $\mu\text{m}$ ), helium flow:  $1 \text{ mL min}^{-1}$ . Column temperature:  $40^\circ\text{C}$  for 2 min. Then a heating ramp of  $10^\circ\text{C min}^{-1}$  to  $300^\circ\text{C}$  followed. This temperature was kept constant for 10 min. The mass spectrometer used was a mass selective detector (5977B, Agilent Technologies, USA) using 70 eV ionization energy and a scan range of 15–550 amu. The split was adjusted to 1:30 and the GC injector was used at  $300^\circ\text{C}$ . The peaks were referenced with the NIST14 MS library.

Hot stage FTIR can give useful insights into the chemical processes taking place in the condensed phase during pyrolysis.<sup>13,14</sup> Halogen-free flame retardants, based on phosphorus, can act in different modes in the condensed and gas phases. The adhesives of Tape RE and Tape FR were measured horizontally as transfer films in a THMS600 cell from Linkam, UK. The IR transmission spectra were recorded by a Lumos 2 IR microscope from Bruker, USA. Representative pieces ( $3 \times 3 \times 0.1$  mm<sup>3</sup>) of the films were cut out of DIN A4 sheets and placed on a plain KBr window. The samples were heated from room temperature to  $600^\circ\text{C}$  at a heating rate of  $25^\circ\text{C min}^{-1}$ . The first spectra were recorded at  $100^\circ\text{C}$  followed by measurement intervals of  $50^\circ\text{C}$ . After  $350^\circ\text{C}$  was reached, the interval was decreased to  $10^\circ\text{C}$  until a temperature of  $600^\circ\text{C}$  was reached.

PCFC measures the heat release rate of pyrolysis gases of materials on a small scale and can give information about the combustion

of the gases released from a material during pyrolysis.<sup>15,16</sup> Representative 5 mg adhesive samples were cut out of transfer films of adhesives and subsequently stuck to the bottom of the crucible. The measurements were performed in a FAA Micro Calorimeter (Fire Testing Technology Ltd., UK) according to ASTM D7309-21b. At a heating rate of  $1 \text{ K s}^{-1}$ , the samples were heated from 100 to  $750^\circ\text{C}$  in a nitrogen atmosphere with a flow of  $80 \text{ mL min}^{-1}$ . Subsequently the gases were led to the combustor, where the oxidation process took place at  $900^\circ\text{C}$  under an additional oxygen flow of  $20 \text{ mL min}^{-1}$ . The heat capacity was determined by analyzing the oxygen depletion and subsequently applying the Huggett's relation.<sup>17</sup>

## 2.2.3 | Flammability tests

The vertical UL 94 test is one of the most widely applied flammability assessment tests for polymeric materials.<sup>18</sup> It was performed in an UL 94 chamber from Fire Testing Technology (UK). The thickness of the tapes was increased, and an eight-layer specimen was manufactured to avoid the evasion of the 20 mm flame. The samples were  $13 \pm 0.5$  mm wide,  $125 \pm 1$  mm long and  $0.9 \pm 0.1$  mm thick.

The OI was determined according to ISO 4589 in a standardized apparatus from Fire Testing Technology (UK) and is a common small burner test to investigate the flammability of materials in the scenario of an emerging fire. A representative piece of tape was cut and subsequently folded to ensure that the bending stiffness of the tape was sufficient. The emerging sample was then able to stand free without support in the clamp of the test apparatus. The dimensions of the resulting specimen were  $70 \times 65 \times 3$  mm<sup>3</sup>. The specimen size was chosen to minimize the amount of sample needed and to achieve sufficient bending stiffness for the free-standing material in the clamp.

The fire behavior of the tapes that were glued on one side of a substrate plate was determined in the single flame source test according to ISO 11925-2 to systematically investigate the interaction between tape and substrate. Edge application of the flame was chosen and a burning chamber from Fire Testing Technology was used. The 20 mm flame was applied for 30 s.

## 2.2.4 | Fire behavior in the cone calorimeter

The cone calorimeter (Fire Testing Technology, UK) was used to investigate the fire behavior in developing fires under forced flaming conditions according to ISO 5660. A distance of 35 mm between the sample and cone heater and an irradiation of  $50 \text{ kW m}^{-2}$  were chosen to avoid contact of the samples with the cone heater and provide for homogenous heat and irradiance distribution over the specimen surface.<sup>6</sup> A distance longer than the standard (25 mm) was used due to the charring and expansion of PC in the cone calorimeter test. The high irradiation level is the same for a standard cone calorimeter test used to assess railway vehicle components according to EN 45545. Specimens of  $100 \times 100$  mm<sup>2</sup> were prepared with a thickness of 4 mm for PMMA and PC and 8 mm for wood. Each material was

**TABLE 1** Peel and SAFT test of Tape RE and Tape FR with the use of different carriers.

| Tape    | Carrier | Peel test                |       | SAFT test |       |
|---------|---------|--------------------------|-------|-----------|-------|
|         |         | $F_{\text{mean}}$ (N/mm) |       | $T$ (°C)  |       |
| Tape RE | Al      | 1.22                     | ±0.17 | 119.3     | ±1.0  |
|         | PET     | 0.82                     | ±0.03 | 71.6      | ±5.7  |
| Tape FR | Al      | 0.65                     | ±0.12 | 116.6     | ±2.7  |
|         | PET     | 0.66                     | ±0.05 | 104.6     | ±11.4 |

measured as a monolithic substrate plate and the burning behavior was compared to that of two tape-bonded substrates. The thickness of the substrates was 2/4 mm. The samples were measured in an aluminum tray without a retainer frame, resulting in an irradiated surface area of 100 cm<sup>2</sup>. For wooden samples, four metal wires were mounted as a grid to avoid distortion or bending of the flat sample. Both acrylic double-sided tapes and the silicon-based tape were measured as a coating on beechwood, zinc plated steel and mineral wool. Sandwich elements of beechwood, PC and PMMA were measured under the same conditions. Time to ignition ( $t_{\text{ig}}$ ), heat release rate (HRR), peak of heat release rate (PHRR), maximum average rate of heat emission (MARHE), fire growth rate (FIGRA) and the total heat evolved (THE) were emphasized as the most important result values.

### 2.2.5 | Flammability of bonded substrates

The flammability of bonded materials was determined via OI and UL 94. For UL 94 tests, sandwich samples in the dimensions of 125 × 13 × 4 mm<sup>3</sup> were manufactured. Samples of ABS and zinc plated steel (2 mm) were prepared to investigate the behavior of thinner materials bonded by tapes. For OI measurements, samples 100 × 10 × 4 mm<sup>3</sup> in size were manufactured corresponding to the standard.

## 3 | RESULTS AND DISCUSSION

### 3.1 | Tape analysis

The peel test in Table 1 shows that the Tape FR has less peel strength compared to Tape RE. This behavior is often to be found in adhesives where additives are added, as part of the adhesive formulation that is responsible for the cohesive and adhesive strength is exchanged for the flame retardant. The peel strength is still sufficient for a non-structural bond. The SAFT test in contrast, shows that the heat resistance of Tape FR is similar and with the PET carrier even higher than the heat resistance of Tape RE.

The pyrolysis and fire behavior of both tape adhesives were analyzed to obtain information about the decomposition of the basic formulation of the tape and the efficiency of the flame retardants. The TGA curve of the tapes (Figure 1a) shows a shift in the temperature at

the beginning of decomposition. Tape RE starts to decompose later and loses 5% of its mass at 333°C, whereas Tape FR loses 5% mass at 292°C (Table 2). The main decomposition temperatures of both tapes are around 400°C, which leads to the assumption that the flame retardant decomposes and is mainly released earlier. The residue of Tape FR is higher by 2.3 wt.%, which proves that there is a slight condensed phase action of the flame retardant.

The PCFC measurements of the adhesives in Table 3 show distinct behaviors for Tape RE and Tape FR (Figure 1b). Tape FR has a shoulder at 350°C, which can be attributed to the flame retardant that volatilizes earlier. Thus, the HRC, which is defined as the PHRR/heating rate, decreases by 15.7%. The fire growth capacity, which is an indicator for the fire hazard of materials,<sup>19</sup> decreases by 7.1% compared to Tape RE, because Tape FR has improved charring behavior and some fire load was replaced by flame retardant. The residue of Tape FR (2.2 wt.%) is higher than the residue of Tape RE (1.4 wt.%). All these results agree with those of the TGA and confirm the slight condensed phase action of the flame retardant.

To analyze the condensed phase during pyrolysis, the sample was heated under nitrogen atmosphere while recording the IR transmission spectrum. Figure 2 shows the hot stage FTIR transmission spectra of Tape RE and Tape FR at different temperatures. The spectra were normalized based on the maximum of the CO peak at 1735 cm<sup>-1</sup>. Figure 2a shows the spectra of Tape RE and Tape FR at 100°C for comparison. Both adhesives show the typical peaks for acrylates, with maximum absorption at 1740 cm<sup>-1</sup> due to the strong CO vibration. The C—O—C stretching of the ester group can be found between 1300 and 1100 cm<sup>-1</sup>.<sup>20</sup> In this area, the absorbance of the films is too high for the differentiation of the peaks and yields in a cut-off peak. The C—H bending vibrations of the alkyl rest takes place at 1454 and 1376 cm<sup>-1</sup>.

The peaks at 832, 894, 1072, and 1315 cm<sup>-1</sup> exist only for the Tape FR, which leads to the conclusion that these peaks are specific to the flame retardant, as this was the only difference between the two adhesive formulations. Some of their bands are also found in many phosphorus flame retardants that have been investigated in the literature.<sup>21,22</sup> For instance, the 1315 cm<sup>-1</sup> peak is typical for PO vibrations and 1070 can be referred to a P—O—C vibration. Figure 2b shows a decrease in the flame retardant peaks already at a low temperature (250°C), which shows that the flame retardant or its decomposition products are volatilized and can act in the gas phase. Figure 3 shows both tapes after heating them to 600°C. Tape RE decomposes and has a smooth surface with bubble-like charred spots on its surface, while Tape FR builds a char network at around that temperature. The char network is the effect of the flame retardant acting with the nonwoven PET used as carrier for the flame retarded adhesive, increasing the residue and potentially acting as a barrier.

The Py-GC/MS was used to identify the volatile pyrolysis products of the tape adhesives. Figure 4 depicts the chromatogram of the Tape FR adhesive and chemical information of the pyrolysis products. The decomposition of the acrylate is proven to be a typical depolymerization as shown in the literature.<sup>23,24</sup> The volatile products can be identified as shown in Table 4.

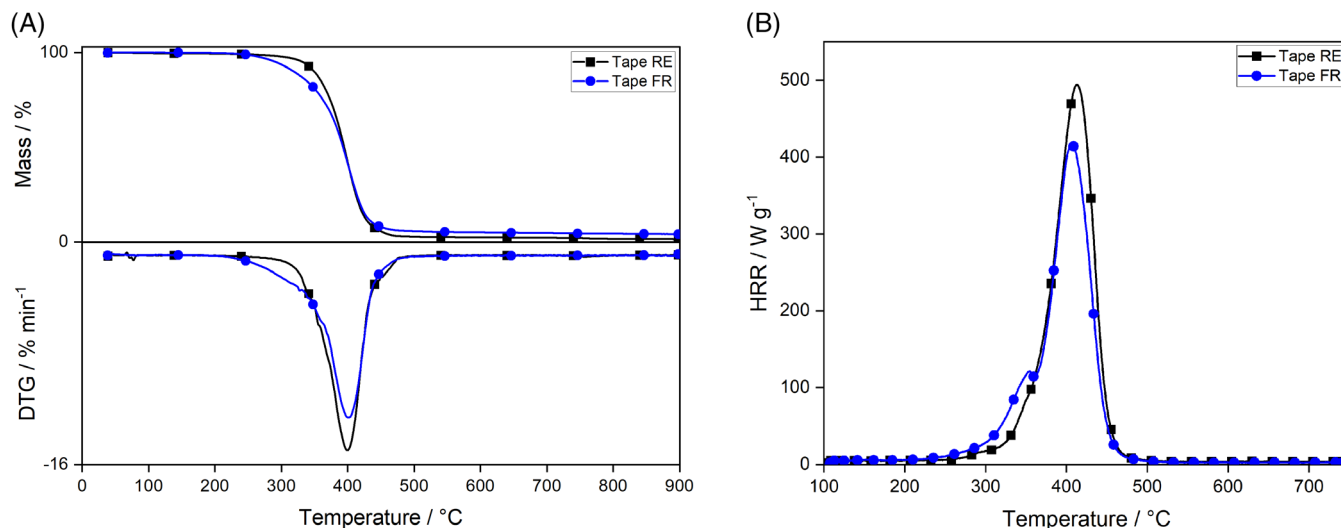


**FIGURE 1** (A) TGA mass loss and DTG comparison between Tape RE and Tape FR adhesives. (B) Pyrolysis combustion flow calorimeter measurements of Tape RE and Tape FR.

**TABLE 2** 5% mass loss,  $T_{\max}$ , and residue comparison of Tape RE and Tape FR adhesives in TGA.

| Sample  | $T(m = 95\%)$ (°C) | $T_{\max}$  | Residue (wt.%) |
|---------|--------------------|-------------|----------------|
| Tape RE | $333 \pm 2$        | $398 \pm 1$ | $1.4 \pm 0.2$  |
| Tape FR | $292 \pm 2$        | $399 \pm 1$ | $3.7 \pm 0.5$  |

**TABLE 3** PCFC results for Tape RE and Tape FR.

| Sample  | Residue (wt.%) | HRC ( $W g^{-1}$ ) | FGC ( $W g^{-1} s^{-1}$ ) |
|---------|----------------|--------------------|---------------------------|
| Tape RE | $1.4 \pm 0.3$  | $497 \pm 6$        | $402 \pm 2$               |
| Tape FR | $2.2 \pm 0.1$  | $419 \pm 5$        | $326 \pm 7$               |

The decomposition products are either educt-acrylates that emerged during the depolymerization, copolymer educts, flame retardant or inhibitor. The good volatilization of the flame retardant corresponds to the behavior of flame retardants with a gas phase mode of action and is coherent with the information from TGA and PCFC. It is very common and effective to protect films like adhesive tapes by gas phase active flame retardants but not yet understood, how these tapes and flame retardants work in bonds.

### 3.2 | Flammability tests

The vertical UL 94 test of both tapes measured as a single layer film did not achieve a vertical rating, because it either escaped the burner flame or ignited and burned to the clamp within a few seconds. The multilayer samples of Tape RE no longer shrank away from the flame, instead igniting and burning up to the clamp within 30 s, which results in no UL 94 V rating. Tape FR, by contrast, ignited and self-extinguished by dripping. The drops ignited the cotton wool, leading

to a V-2 rating for the tape. Folded tapes were used to avoid shrinking of the tapes and in order to obtain consistent results. Tape RE burned self-sufficiently at an oxygen concentration of 17.5 vol.%. Tape FR needed an oxygen concentration of 22.8 vol.% to burn continuously. The large difference of 5.3 vol.% confirms the good protective effect of the flame retardant. UL 94 Test and OI Values are to be found in Table 5.

### 3.3 | Tapes as coatings

To investigate the interaction between tape and substrate, the above-mentioned tapes were investigated as free-standing films and coatings in the single flame source test (according to ISO 11925-2) as illustrated in Figure 5. All free-standing films dodged the burner flame by shrinking away from the burner flame so that the films were self-extinguishing. As coatings, the burning characteristics varied strongly on different substrates. On the zinc plated steel substrate (Figure 5a), neither tape ignited within 30 s and almost no harm to the tape was recognized. After ignition on wood (Figure 5b), both tapes burned differently. Tape FR extinguished after the burner flame was removed, whereas Tape RE kept burning self-sufficiently until the whole tape and large parts of the substrate were consumed by the flame. On mineral wool (Figure 5c), both tapes ignited after approximately 2 s. All of Tape RE was consumed after 23 s, whereas Tape FR was self-extinguishing and only consumed in the area surrounding the burner flame. In contrast to the free-standing tape, the substrates served as mechanical support, so that shrinking away from the burner flame and dripping were prevented.

The different burning characteristics of the adhesive tape on the varying substrates can be easily explained by the different thermal conductivity, specific heat capacity, and the density of the substrates, or better, by the different square root of the product of these

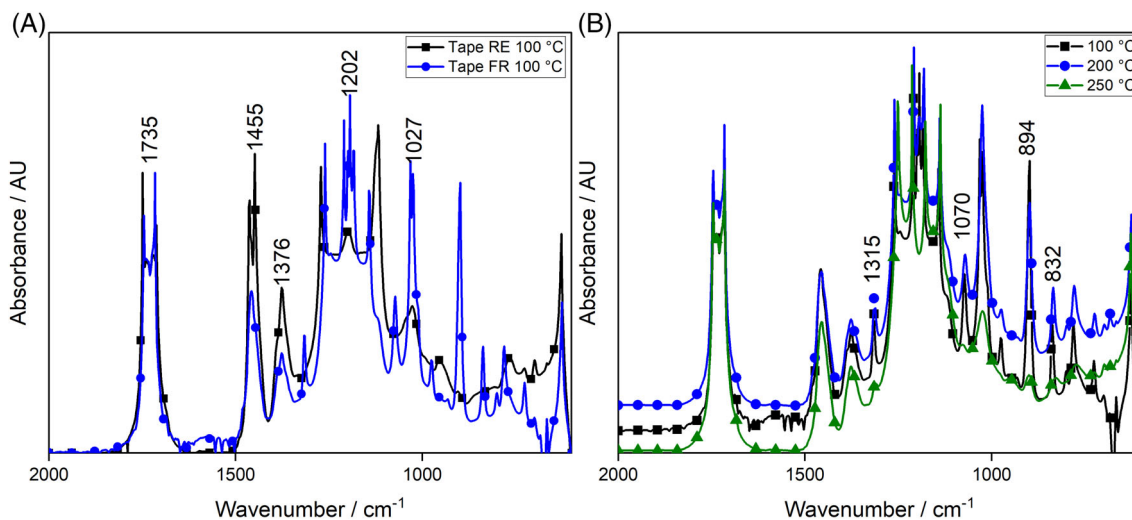


**FIGURE 2** Hot stage measurements of Tape RE and Tape FR adhesives: (A) comparison of IR spectrum at 100°C; (B) Tape FR at 100, 200, 250°C.

**FIGURE 3** Hot stage images of Tape RE and Tape FR after pyrolysis at 600°C.

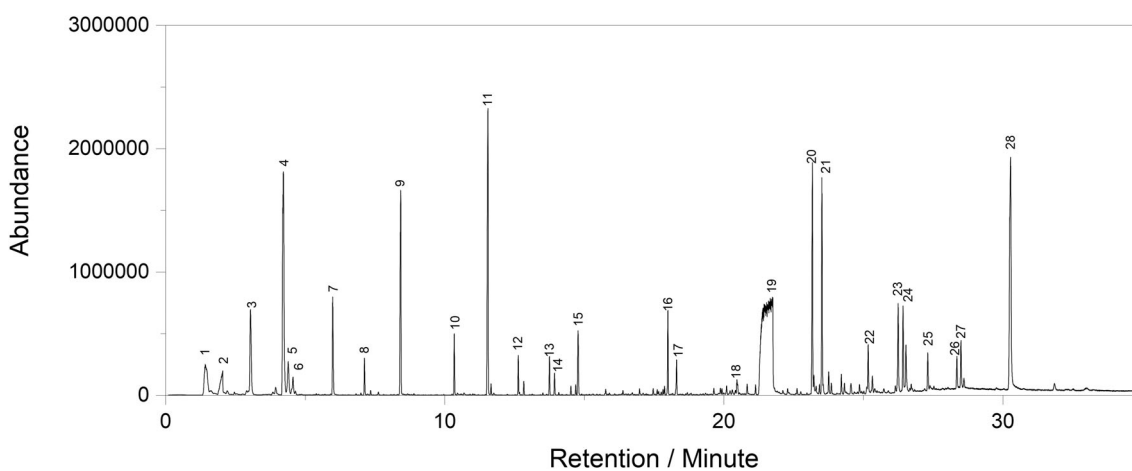
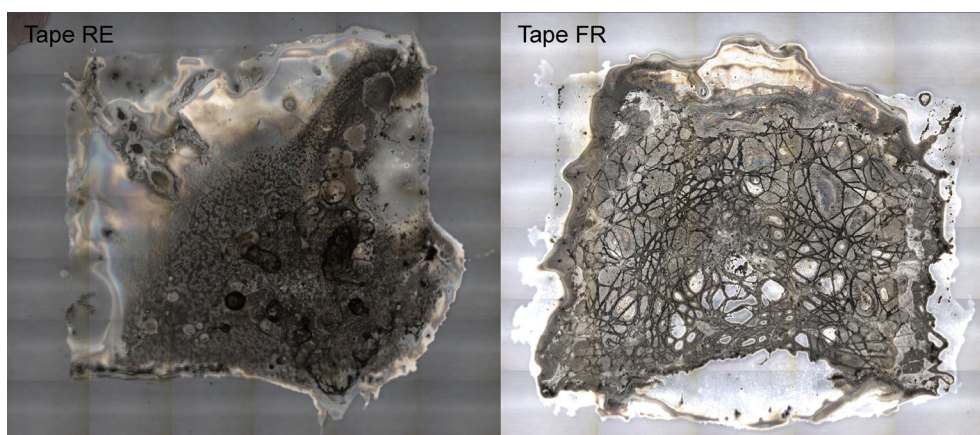


**FIGURE 4** Pyrolysis gas chromatogram of Tape FR.

properties, their heat effusivity (Table 6). The values were taken from the literature and shall only depict the magnitude<sup>25–27</sup> of the materials' ability to discharge thermal energy from the tapes.

The condition for ignition in this test is that the fuel gases emerging from thermal decomposition of the tapes or samples produce an ignitable mixture with the surrounding air.<sup>12</sup> For zinc plated steel, this

**TABLE 4** Decomposition products of Tape FR in Py-GC/MS.

| Peak number | Time (min)  | Decomposition product                      |
|-------------|-------------|--|
| 1           | 1.409       | CO <sub>2</sub>                            |
| 2           | 2.04        | Acetic acid                                |
| 3–6         | 3.036–4.638 | Aliphatic copolymer                        |
| 7           | 5.99        | Aromatic copolymer                         |
| 8 + 9       | 7.12–8.42   | Alkanol rest from acrylates                |
| 10–15       | 10.3–15.0   | Educt-acrylates and decomposition products |
| 16 + 17     | 17.9–18.4   | Dimers of acrylate decomposition products  |
| 18 + 19     | 20–22       | Phosphorus based flame retardant           |
| 20–21       | 23–25       | Dimers and trimers of acrylates            |
| 22–28       | 26–30       | Inhibitor and decomposition products       |

**TABLE 5** UL 94 test and Oxygen Index of both adhesive tapes as layered specimens.

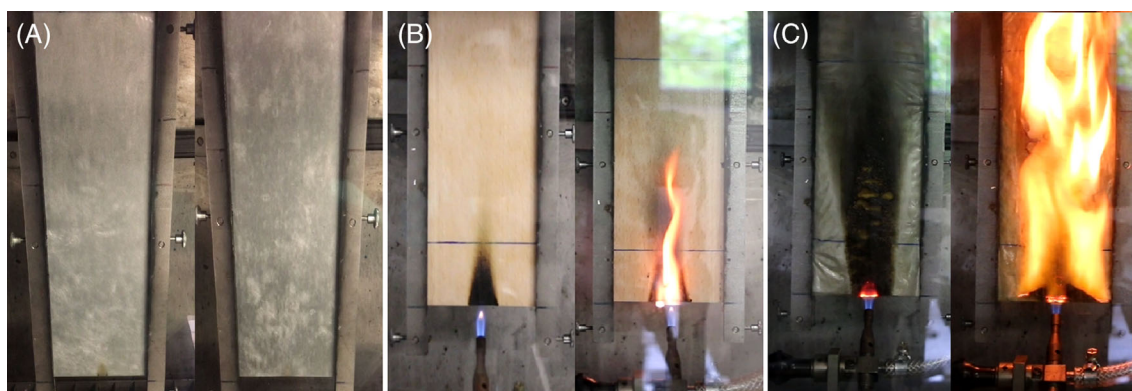
| Adhesive tape | UL 94 V rating | Oxygen index (vol.%) |
|---------------|----------------|----------------------|
| Tape RE       | N.R.           | 17.5 ± 0.2           |
| Tape FR       | V-2            | 22.8 ± 0.2           |

condition is not fulfilled due to the low temperatures at the application point of the flame. Metals are very good heat conductors, and thus the heat of the applied flame was distributed too quickly to reach the temperatures required for decomposition. The maximum temperature is 210°C at 60 s (end of test) (Figure 6a). The maximum surface temperature of mineral wool in contrast, exceeds 500°C (510°C), which is quite sufficient for decomposition and ignition (Figure 6b).

The flammability ranking of the tapes as coatings on substrates corresponds with the flammability ratings in UL 94 and OI. Comparing the substrates yields that heat dissipation is the main factor for the flammability of the coated sample. For materials with a high heat conductivity such as steel, the heat loss  $q''_{\text{loss}}$  via conduction is so high that ignition cannot take place. For insulating wool and wood,  $q''_{\text{loss}}$  is much smaller so that the tape heats up until there are enough fuel gases for ignition and the exothermic chain reaction of the burning process is started. The results are expected to be transferrable to one-sided tapes.

### 3.4 | Glued laminates

Laminates (substrate/tape/substrate) were investigated in different fire and pyrolysis tests to investigate the influence of an adhesive gap and PSA tapes for different bonded materials. The flammability of the materials was assessed by UL 94 test (Table 7).

**FIGURE 5** Burning behavior of Tape FR (left) and Tape RE (right) on (A) zinc plated steel, (B) beechwood, and (C) mineral wool in the single burning item test according to ISO 11925-2.**TABLE 6** Thermophysical properties of the substrates used in EN ISO 11925-2 test.

|                 | Thermal conductivity (W m <sup>-1</sup> K <sup>-1</sup> ) | Specific heat capacity (J kg <sup>-1</sup> K <sup>-1</sup> ) | Density (kg m <sup>-3</sup> ) | Heat effusivity (J m <sup>-2</sup> K <sup>-1</sup> s <sup>½</sup> ) |
|-----------------|---|--|-------------------------------|---|
| Beechwood       | 0.2   | 1400   | 700                           | 443   |
| Zinc            | 115   | 380  | 7000                          | 17 490  |
| Insulating wool | 0.004   | 840  | 50                            | 13  |
| Steel           | 45  | 480  | 7840                          | 13 013  |



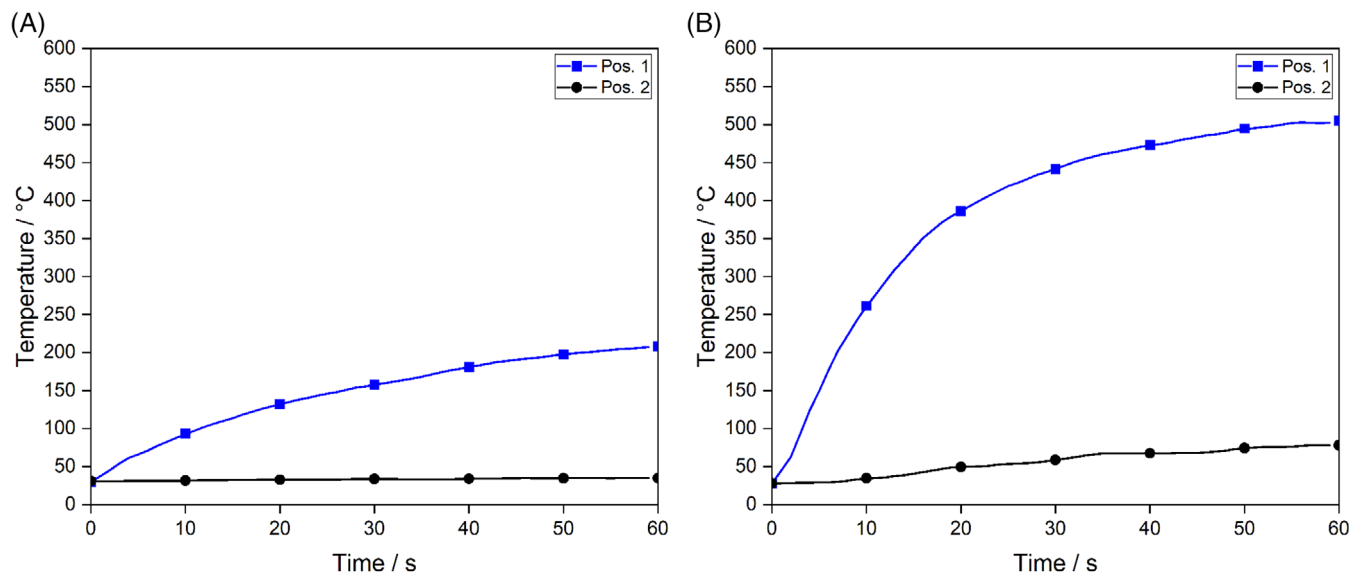


**FIGURE 6** Surface temperature development during EN ISO 11925-2. (A) Zinc plated steel and (B) insulating wool by comparison. Pos.1 = surface temperature in the burner flame application area. Pos. 2 = surface temperature 200 mm above the burner flame application zone.

**TABLE 7** Vertical UL 94 test of the sandwich-like specimen. Substrate thickness: Wood: 4 mm, steel: 1 mm, PMMA: 2 mm, polycarbonate: 2 mm.

| Tape       | Wood | Steel | PMMA | Polycarbonate |
|------------|------|-------|------|---------------|
| Tape RE    | N.R. | V-0   | N.R. | V-2           |
| Tape FR    | N.R. | V-0   | N.R. | V-2           |
| Monolithic | N.R. | V-0   | N.R. | V-2           |

**TABLE 8** Burning velocity of monolithic PMMA compared with Tape RE and Tape FR bonded to PMMA in the same thickness.

| Adhesive joint  | Burning velocity (mm/min) |
|-----------------|---------------------------|
| PMMA monolithic | 32.5 ± 0.2                |
| PMMA + Tape RE  | 36.7 ± 0.4                |
| PMMA + Tape FR  | 32.4 ± 0.6                |

The wood samples ignited and burned up to the clamp within 30 s and did not pass the vertical test. The adhesive gap widened when the flame was applied, but no delamination and dripping took place. The bonded steel element did not ignite within 10 s and achieved a V-0 rating with no dripping. There was no visible change in the adhesive gap. The PMMA sample burned up to the clamp, with burning drops falling off the sample and igniting the cotton wool. The sample did not achieve a rating in the vertical test. Polycarbonate samples were ignited, and the sample burned up to 40 mm. At the bottom of the sample where the flame was applied, a char layer built up on the surface. After the burner flame was removed, the sample extinguished by dripping. Part of the sample fell off and ignited the underlying cotton wool. A V-2 rating was achieved. The substrates dominated the flammability of the glued materials which had the same



**FIGURE 7** UL 94 vertical test of (A) polycarbonate 4.1 mm, (B) wood 8.1 mm, (C) ABS 2.1 mm.

UL 94 ratings. In the horizontal test, the PMMA samples differed in their burning velocity (Table 8). The PMMA sandwich element with Tape RE and the monolithic PMMA burned faster than the Tape FR PMMA sample.

**TABLE 9** Oxygen index of adhesive joints in vol.%

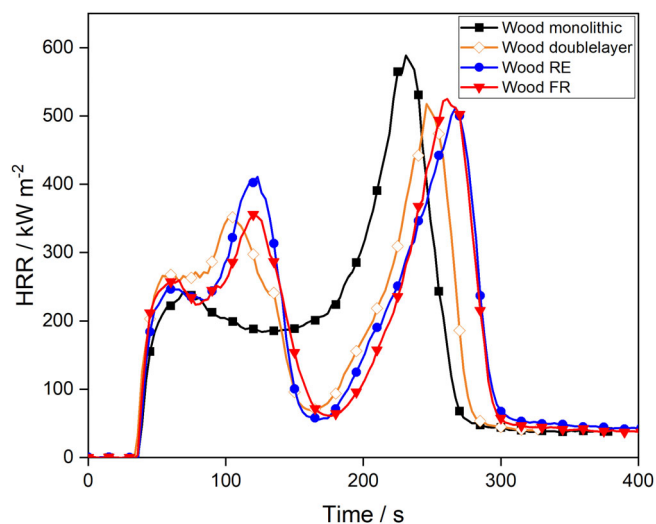
| Adhesive joint | PMMA $\pm$ 0.2 | PC $\pm$ 0.3 | Wood $\pm$ 0.2 | Steel |
|----------------|----------------|--------------|----------------|-------|
| Monolithic     | 17.7           | 27.1         | 27.7           | NR    |
| Tape RE        | 17.6           | 26.1         | 27.9           | NR    |
| Tape FR        | 18.0           | 27.0         | 27.9           | NR    |

If samples with a reduced thickness (2.1 mm) are tested in UL 94 vertical test, the single layers of the substrates wrap themselves up and expose more material, and especially tape, to the flame. This can lead to a faster burning process and was observed for 1 mm thick ABS plates that were taped with Tape RE and Tape FR resulting in a 2.1 mm specimen (Figure 7c).

A popular test for assessing burning behavior in an emerging fire scenario is the oxygen index (OI). The results are concluded in Table 9. Monolithic PMMA and taped PMMA with Tape RE burned self-sufficiently at an oxygen concentration of 17.6 vol.%. This value corresponds with the manufacturer information (17.5 vol.%). The taped sample with Tape FR tended toward a higher OI. As a charring polymer, PC had a higher OI. Monolithic and Tape FR samples had a similar OI of 27 vol.%, which corresponds with the manufacturer statement of 28 vol.%. Tape RE lowered the OI slightly, to 26.1%. All wood samples had a very similar OI, which corresponds with the literature values for different kinds of wood.<sup>28–30</sup> The char layer builds up on taped samples as well and there is no delamination. For PC, the taped samples started to delaminate during the burning process. The area of the tape exposed to the propagating flame increased accordingly, thus increasing the impact of the tape on the OI value, which explains the lower OI value for the Tape RE sample of bonded PC.

The sandwich elements were investigated in the single flame source test according to ISO 11925-2. Wood, steel and insulating wool were all self-extinguishing as monolithic material and as taped material. In zinc plated steel and insulating wool, no ignition of the sample was possible. The temperature in the adhesive gap was measured via thermocouple and did not exceed 130°C, which is not sufficient to form sufficient fuel gases for ignition. The adhesive tape did not drip or act as a wick in steel or insulating wool as suspected. Monolithic and bonded wood were both self-extinguishing, whereas the adhesive gap in the latter widened. Since there are no relevant wick effects or delamination in this thickness, the ratio between the exposed surface areas of tape and substrate (1:40) can explain that the burning behavior is dominated by the substrate material.

The cone calorimeter was used to determine the behavior in a forced flaming condition depicting a developing fire. Figure 8 shows the HRR curve of a monolithic beechwood sample of 8 mm thickness compared with layered wood (two layers of wood, each 4 mm) and two taped (via Tape RE and Tape FR) samples of the same thickness. The monolithic sample had two PHRRs, which is typical for wood.<sup>31–33</sup> The first peak occurred immediately after ignition of the volatile products emitted from the surface. Then a char layer built up and the HRR decreased due to the heat and fuel barrier effect. After around 180 s the protective layer cracked, fuel gases were emitted

**FIGURE 8** Cone calorimeter HRR curves of monolithic, layered, and taped wood samples. Sample thickness: 8 mm. Irradiation: 50 kW m<sup>-2</sup>. Distance: 35 mm.

more freely into the flame zone and the sample started to burn intensely, causing the second peak (main peak) in HRR. After 240 s the sample reached the PHRR and extinguished immediately afterwards. The layered and taped samples (double layer, RE, FR) behaved differently. After the slightly earlier ignition at 34 s, a first PHRR emerged which tended to be more pronounced for the layered samples. Then a char layer built up and the first local minimum of HRR was observed. Subsequently the char layer cracked, volatiles passed the char layer, the first layer of the sample delaminated and the tape in the bonded samples was consumed, all of which resulted in the second PHRR. The second PHRR was the main difference between the monolithic and the layered samples and the “additional” peak. This peak led to a higher ARHE at this time and a higher MARHE<sub>1</sub> (200  $\pm$  14 kW m<sup>-2</sup>) for the first two peaks (PHRR<sub>1+2</sub>) compared with the MARHE<sub>1</sub> (153  $\pm$  10 kW m<sup>-2</sup>) for the first PHRR of the monolithic wood. After the first wood layer was consumed by the flame, a char residue was left on top of the second wood layer on all laminates. The thick char residue of the first wood layer and the thin char layer of the second wood layer worked as a strong heat and volatile barrier, resulting in the all-time minimum of HRR, which is around 60% lower than in the monolithic sample. This minimum is characteristic for layered wood materials which delaminate in fires, such as plywood.<sup>34</sup> After the layer cracked, volatiles passed through the char layers again and PHRR<sub>3</sub> was observed. PHRR<sub>3</sub> was lower and shifted to a later time for all laminates compared to the PHRR<sub>2</sub> of monolithic wood. After the consumption of the second layer, the sample extinguished quickly and exhibited a wood-typical afterglow. Table 10 shows the most important parameters to evaluate and assess the burning properties of the wood specimen. The layer-wise burning of the laminates shows some characteristics that lead to improved fire properties, such as a stronger insulating layer and a very low HRR at around 180 s, shifting the last PHRR by around 30 s and lowering it by around 10%. But the separate burning of the layers leads to an additional PHRR

**TABLE 10** Cone calorimeter data for monolithic, layered, and taped wood samples. Sample thickness: 8 mm. Irradiation: 50 kW m<sup>-2</sup>. Distance: 35 mm.

| Sample            | $t_{ig}$ (s)<br>± 2 | PHRR <sub>1</sub><br>(kW m <sup>-2</sup> )<br>± 10 | PHRR <sub>2</sub><br>(kW m <sup>-2</sup> )<br>± 30 | PHRR <sub>3</sub><br>(kW m <sup>-2</sup> )<br>± 50 | FIGRA<br>(kW m <sup>-2</sup> s <sup>-1</sup> )<br>± 0.5 | MARHE <sub>1</sub><br>(kW m <sup>-2</sup> )<br>± 10 | MARHE <sub>2</sub><br>(kW m <sup>-2</sup> )<br>± 10 | THE<br>(MJ m <sup>-2</sup> )<br>± 3 | Residue<br>(%) ± 1 |
|-------------------|---------------------|--|--|--|---|---|---|-------------------------------------|--------------------|
| Wood monolithic   | 37                  | 245  | 589  | -  | 4.0   | 153   | 229   | 66                                  | 15.8               |
| Wood double layer | 34                  | 271  | 363  | 547  | 5.3   | 204   | 220   | 64                                  | 15.8               |
| Wood RE           | 33                  | 249  | 392  | 499  | 4.6   | 202   | 218   | 69                                  | 14.6               |
| Wood FR           | 34                  | 258  | 366  | 521  | 4.7   | 197   | 219   | 67                                  | 14.7               |

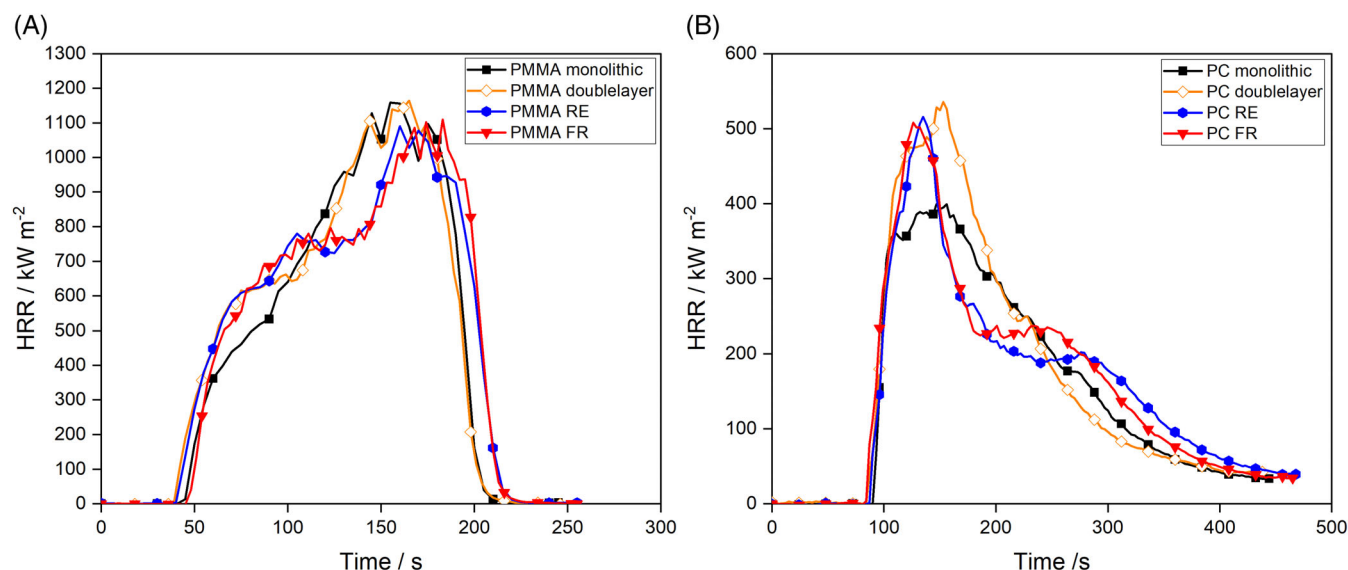


**FIGURE 9** (A) Cone calorimeter comparison between monolithic PMMA, layered PMMA without adhesive tape, sandwich-like PMMA bonded with Tape RE, and sandwich-like PMMA bonded with Tape FR. (B) Cone calorimeter data of monolithic, layered, and taped polycarbonate samples. Sample thickness: 4 mm.

which emerges at around 110 s, leading to a MARHE<sub>2</sub> that is 33% higher than the MARHE<sub>1</sub> of monolithic wood. This additional PHRR presents a fire risk that needs to be addressed and can determine the potential for certifications for the material based on MARHE, such as the EN 45545. Also, the FIGRA, which is defined as the max (HRR(t)/t) and is an indicator for the fire hazard of a material, is 15% higher for bonded wood due to that first PHRR<sub>1</sub>.

In Figure 9a, the HRR curves of monolithic, layered, and taped PMMA are shown. The first step in the burning process is the ignition of the volatiles, which resulted in an immediate increase in the HRR. This built up the shoulder in the diagrams of all four samples. The HRR within this shoulder was higher for the taped and layered materials due to the air gap or tape that is located between the plates. This leads to a reduced thermal thickness and thus a higher HRR and fire risk at the beginning of pyrolysis.<sup>35</sup> After the first shoulder, the thermal thickness and heat dissipation within all samples decreased, which results in faster heating of the sample, a larger pyrolysis zone, more volatiles and a higher HRR until the PHRR was reached. Then the

sample extinguished rapidly, and no afterglow occurred. This HRR curve is typical for PMMA under these conditions and is comprehensively discussed in the literature.<sup>36–38</sup> For both bonded samples, the HRR stagnated after 120 s and built a small plateau which is caused by the tape that has PET as a carrier. The carrier disturbs the melt flow in the pyrolysis zone and has a higher melting range (270°C) than PMMA (160°C). After finishing the plateau, the PHRR was reached at a temperature around 10°C lower than the PHRR of monolithic PMMA, and subsequently the samples extinguished quickly without any afterglow and complete consumption of the material. Due to the lower PHRR and MARHE, and the shift of the PHRR to a later time, the MARHE indicates a slightly lower fire risk for the bonded materials compared to the layered and monolithic PMMA. In the layered PMMA plates, the air gap is eliminated quickly due to the melt zone, where there happens to be much convection, and which even increases with a reduced sample thickness.<sup>39</sup> Thus, the sample behaves similar to monolithic PMMA. The FIGRA for the bonded samples, determined by the first shoulder in the HRR curve, is the same

**TABLE 11** Cone calorimeter data of monolithic, layered, and taped PMMA samples.

| Sample            | $t_{ig}$ (s) $\pm$ 4 | FIGRA<br>( $\text{kW m}^{-2} \text{s}^{-1}$ ) $\pm$ 0.4 | PHRR<br>( $\text{kW m}^{-2}$ ) $\pm$ 16 | MARHE<br>( $\text{kW m}^{-2}$ ) $\pm$ 5 | THE<br>( $\text{MJ m}^{-2}$ ) $\pm$ 2 |
|-------------------|----------------------|---|---|---|---------------------------------------|
| PMMA monolithic   | 38                   | 8.1   | 1181                                    | 587                                     | 118                                   |
| PMMA double layer | 35                   | 8.5   | 1155                                    | 601                                     | 118                                   |
| PMMA RE           | 44                   | 8.2   | 1029                                    | 565                                     | 118                                   |
| PMMA FR           | 37                   | 7.9   | 1059                                    | 575                                     | 121                                   |
| PC monolithic     | 85                   | 3.4   | 411                                     | 199                                     | 66                                    |
| PC double layer   | 79                   | 4.0   | 529                                     | 232                                     | 71                                    |
| PC RE             | 79                   | 4.0   | 519                                     | 198                                     | 72                                    |
| PC FR             | 81                   | 4.1   | 512                                     | 197                                     | 71                                    |

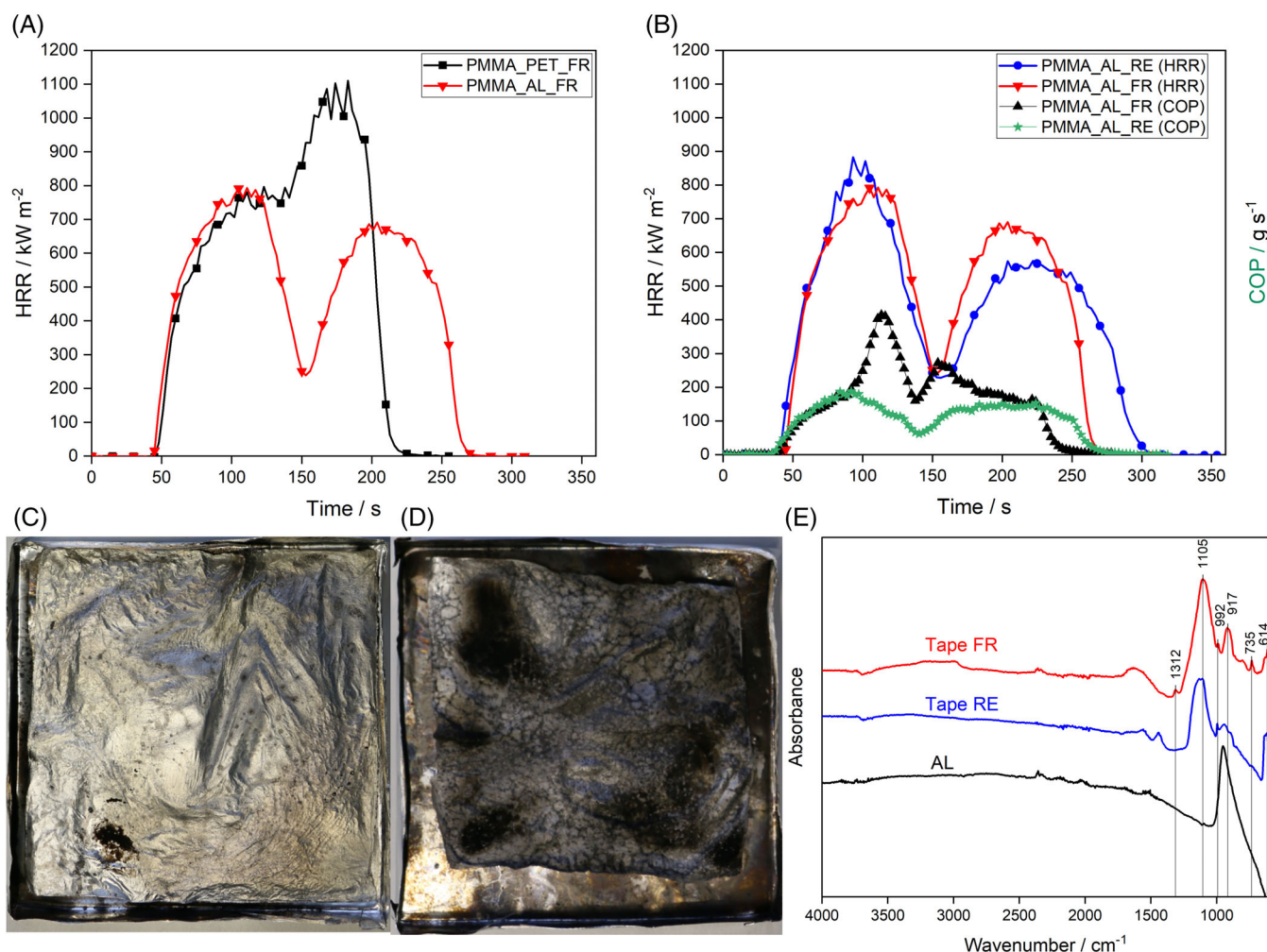


**FIGURE 10** (A) Comparison between bonded PMMA (with Tape FR) with and without an aluminum middle layer. (B) Cone calorimeter HRR and CO formation (COP) of taped PMMA samples with Tape RE and Tape FR with an aluminum middle layer (AL). Sample thickness: 4 mm. (C) Cone calorimeter residues of Tape RE and (D) Tape FR with an aluminum middle layer used to connect two PMMA plates. (E) ATR-FTIR spectrum of cone calorimeter residues of Tape RE and Tape FR with an aluminum middle layer used to connect two PMMA plates. Comparison to the untreated aluminum foil that was used as a middle layer.

for monolithic samples where it is determined by the PHRR. Table 11 contains the most important parameters of the PMMA cone calorimeter measurements.

Figure 9b shows the HRR curves of the different PC samples. The monolithic PC showed typical behavior for a charring material.<sup>40</sup> After ignition and the rise of the HRR, a char layer built up and the HRR

decreased until fuel depletion and transition to a strong afterglow. The same effects occurred for the layered and taped samples, but the HRR had a higher peak after ignition. Due to the separation of layers by tape or air, the heat transfer within the sample is disturbed, so that the first layer heats up faster and shows a higher PHRR.<sup>6</sup> After the first pronounced PHRR, the HRR dropped fast to a plateau, where the char, mainly formed by the first layer, protected the underlying material. This manner of protection by a first layer is known for laminates,<sup>41</sup> and the plateau is characteristic for a strong protective char layer.<sup>42</sup> The double layer PC showed a slightly higher and wider PHRR and a MARHE 15% higher, and developed no char plateau. The missing connection between the first and second layers leads to faster growth of the sample into the cone heater, which exposes the surface to higher irradiation and thus results in a higher HRR (Table 11). After the second PC layer started to form less fuel gases, since more and more char was building up and less fire load was available, the HRR decreased to the same amount of afterglow as the monolithic PC.

To investigate the influence of different carriers within the PSA tapes, an aluminum foil layer was placed between two layers of double-sided PSA tape. Figure 10a shows the HRR curve of bonded PMMA samples. The black curve shows the laminates of PMMA bonded with the PET carrier tape, and the red curve shows the laminate with an aluminum layer as a middle layer (AL), simulating a different carrier. The aluminum layer acts as a non-flammable interlayer and protects the second layer of PMMA. The positive effect of metal foils or flame retardant interlayers is known from the literature<sup>11</sup> and is in this case responsible for the minimum of HRR at 150 s and the lower, shifted PHRR of the PMMA laminate.

Figure 10b shows the HRR and the COP curve of the Tape RE and Tape FR-bonded samples with the aluminum middle layer. Because phosphorus flame retardants can increase CO production in cone calorimeter measurements,<sup>9,43</sup> the COP was used to determine the time when the pyrolysis front reached the tapes. The HRR curves show that there is a minor impact of the flame retardant on the PHRR<sub>1</sub> and the time of the first peak. The action of Tape FR, which was active in the gas phase, was shown by the increased COP at around 100 s. After the aluminum layer was reached and the all-time minimum of HRR took place at about 150 s, the second layer of PMMA started to burn and led to a second peak of HRR. Again, the flame retardant on the backside of Tape FR showed its effect on the COP. The shape of the PHRR<sub>2</sub> depended on whether Tape RE or Tape FR was used. Tape RE exhibited a lower second peak of HRR and a longer burning time. In contrast, the second peak of HRR was higher for Tape FR and the second PMMA layer was consumed faster. This can be explained by Figure 10c–e where the residues of both samples are depicted. For Tape RE (c), the area of the remaining aluminum foil is much larger than for Tape FR (d). This explains the better barrier effect of the aluminum carrier with Tape RE and the associated later, lower PHRR<sub>2</sub>. The reduced area of the aluminum Tape FR sample can be explained by the ATR-FTIR results in Figure 10e, which shows the ATR-FTIR spectra of the residue surfaces from the cone calorimeter tests compared with the untreated aluminum foil used to

manufacture the cone calorimeter samples. The aluminum foil shows an uncluttered spectrum that shows mainly the 950 cm<sup>-1</sup> Al–O vibration. Tape RE shows a dominant peak around 1100 cm<sup>-1</sup> which is attributed to C–H vibrations, which are also present in the spectrum of Tape FR. The Tape FR spectrum also shows peaks at 1312 and 735 cm<sup>-1</sup>, which are attributed to P–O vibrations and suggest that the phosphorus flame retardant reacted with the aluminum surface.

## 4 | CONCLUSIONS

Phosphorus-based flame retardants have a major impact on the flame retardancy of PSA tapes as free-standing films and drastically improve flammability ratings in UL 94 vertical test and OI.

Bonded to substrates on one side, the flame retardancy of the tapes is no longer the only factor that determines the fire characteristics of this connection. The thermal effusivity of the substrate plays a significant role and determines the flame spread over the material. The fire behavior of PSA-bonded laminates (substrate/tape/laminate) depends on how the tape works as an insulation layer between the bonded layers, the flammability of the tape itself becomes a minor factor. The burning behavior then depends on the substrates and the tape used in the gap, and on how these materials interact with each other. The interfaces determine the burning behavior in different ways depending on the substrate and the carrier properties. In wood and PMMA there are positive as well as negative aspects influencing the fire behavior of monolithic and bonded materials. In wood, there is an additional PHRR at the beginning, but a strong insulating effect of the tapes. In PMMA the separation of the layers by tape leads to a faster heating up of the first layer in cone calorimeter testing, but a barrier effect that shifts and lowers the PHRR. In PC, there is a significant increase in the fire risk when bonded materials are used. The PHRR at the start is much higher than in monolithic PC, which leads to a higher MARHE and FIGRA. Also, the carrier has a major impact on the fire behavior: for example, when PET and ALU carriers are compared in PMMA, the aluminum improves the fire properties crucially, lowering PHRR and working as a barrier for the second layer. All these complex interactions yielded fundamental knowledge about how tape-bonded materials behave in fires and how the modification of these tapes can improve the fire behavior of bonded substrates. This paper may feed the communication between tape developers and applicants and serve as guide to develop flame retarded tapes tailored to achieve the distinct protection goals of the bonded components.

## ACKNOWLEDGMENTS

The research was based on an IGF Project. The IGF Project (20762 N) of the Research Association DECHEMA (Deutsche Gesellschaft für Chemische Technik und Biotechnologie e. V., 60486 Frankfurt am Main, Germany) was supported by the AiF within the framework of the program “Förderung der Industriellen Gemeinschaftsforschung (IGF)” of the German Federal Ministry for Economic Affairs and

Climate Action, based on a decision of the Deutschen Bundestag. I would like to thank Fernanda Romero who supported the UL 94 and OI measurements, Yannik Wägner and Volker Wachtendorf for their expertise in hot stage FTIR measurements, Alexander Battig for his support in measuring and evaluating Py-GC/MS and finally Michael Schneider and Detlev Rättsch for the sample manufacturing. Open Access funding enabled and organized by Projekt DEAL.

### CONFLICT OF INTEREST STATEMENT

The authors declare no conflict of interest.

### DATA AVAILABILITY STATEMENT

The data that support the findings of this study are available on request from the corresponding author. The data are not publicly available due to privacy or ethical restrictions.

### ORCID

Vitus Hupp  <https://orcid.org/0009-0003-1338-551X>

Bernhard Schartel  <https://orcid.org/0000-0001-5726-9754>

Andreas Hartwig  <https://orcid.org/0000-0002-3320-6414>

### REFERENCES

- Brockmann W, Geiß PL, Klingen J, Schröder KB. *Adhesive Bonding: Materials, Applications and Technology*. Mikhail B Wiley; 2009:432.
- Feldstein MM, Moscalets AP. *Innovations in Pressure-sensitive Adhesive Products*. Smithers Rapra; 2016:148.
- Wang X-L, Chen L, Wu J-N, Fu T, Wang Y-Z. Flame-retardant pressure-sensitive adhesives derived from epoxidized soybean oil and phosphorus-containing dicarboxylic acids. *ACS Sustain Chem Eng*. 2017;5(4):3353-3361.
- Sonnier R, Viretto A, Dumazert L, Gallard B. A method to study the two-step decomposition of binary blends in cone calorimeter. *Combust Flame*. 2016;169:1-10.
- Liang S, Neisius NM, Gaan S. Recent developments in flame retardant polymeric coatings. *Prog Org Coat*. 2013;76(11):1642-1665.
- Schartel B, Bartholmai M, Knoll U. Some comments on the use of cone calorimeter data. *Polym Degrad Stab*. 2005;88(3):540-547.
- Schartel B, Beck U, Bahr H, Hertwig A, Knoll U, Weise M. Submicrometre coatings as an infrared mirror: a new route to flame retardancy. *Fire Mater*. 2012;36(8):671-677.
- Frangi A, Fontana M, Hugl E, Jübstl R. Experimental analysis of cross-laminated timber panels in fire. *Fire Saf J*. 2009;44(8):1078-1087.
- Grexa O, Horváthová E, Bešínová O, Lehocký P. Flame retardant treated plywood. *Polym Degrad Stab*. 1999;64(3):529-533.
- Li K, Li Y, Zou Y, Yuan B, Walsh A, Carradine D. Improving the fire performance of structural insulated panel core materials with intumescent flame-retardant epoxy resin adhesive. *Fire Technol*. 2023;59(1):29-51.
- Timme S, Trappe V, Korzen M, Schartel B. Fire stability of carbon fiber reinforced polymer shells on the intermediate-scale. *Compos Struct*. 2017;178:320-329.
- Quintiere JG. *Fundamentals of Fire Phenomena*. 1st ed. Wiley; 2006:456.
- Battig A, Markwart JC, Wurm FR, Schartel B. Matrix matters: hyperbranched flame retardants in aliphatic and aromatic epoxy resins. *Polym Degrad Stab*. 2019;170:108986.
- Perret B, Schartel B, Stößl K, et al. A new halogen-free flame retardant based on 9,10-dihydro-9-oxa-10-phosphaphenanthrene-10-oxide for epoxy resins and their carbon fiber composites for the automotive and aviation industries. *Macromol Mater Eng*. 2011;296(1):14-30.
- Lyon RE, Walters RN. Pyrolysis combustion flow calorimetry. *J Anal Appl Pyrolysis*. 2004;71(1):27-46.
- Schartel B, Pawlowski KH, Lyon RE. Pyrolysis combustion flow calorimeter: a tool to assess flame retarded PC/ABS materials? *Thermochim Acta*. 2007;462(1):1-14.
- Huggett C. Estimation of rate of heat release by means of oxygen consumption measurements. *Fire Mater*. 1980;4(2):61-65.
- Schartel B, Kebelmann K. Fire testing for the development of flame retardant polymeric materials. In: Yuan Hu XW, ed. *Flame Retardant Polymeric Materials*. CRC Press; 2019:35-55.
- Lyon RE, Safronava N, Crowley S, Walters RN. A molecular-level fire growth parameter. *Polym Degrad Stab*. 2021;186:109478.
- Kawasaki A, Furukawa J, Tsuruta T, Wasai G, Makimoto T. Infrared spectra of poly(butyl acrylates). *Die Makromol Chem*. 1961;49(1):76-111.
- Chen L, Luo Y, Hu Z, Lin G-P, Zhao B, Wang Y-Z. An efficient halogen-free flame retardant for glass-fibre-reinforced poly(butylene terephthalate). *Polym Degrad Stab*. 2012;97(2):158-165.
- Wang C, Wu Y, Li Y, et al. Flame-retardant rigid polyurethane foam with a phosphorus-nitrogen single intumescent flame retardant. *Polym Adv Technol*. 2018;29(1):668-676.
- Özlem S, Hacıoğlu J. Thermal degradation of poly(n-butyl methacrylate), poly(n-butyl acrylate) and poly(t-butyl acrylate). *J Anal Appl Pyrolysis*. 2013;104:161-169.
- Straus S, Madorsky SL. Pyrolysis of styrene, acrylate, and isoprene polymers in a vacuum. *J Res Natl Bur Stand*. 1953;50(3):165-176.
- Kurzweil P, Frenzel B, Gebhard F. *Physik-Formelsammlung: für Ingenieure und Naturwissenschaftler/Peter Kurzweil; Bernhard Frenzel; Florian Gebhard*. 1. Aufl. ed. Studium Technik. Vieweg; 2008.
- Czajkowski Ł, Olek W, Weres J. Effects of heat treatment on thermal properties of European beech wood. *Eur J Wood Wood Prod*. 2020;78(3):425-431.
- Watts A. *Modern Construction Handbook*. 4th ed. Birkhäuser; 2016:504.
- Donmez CA. Effect of various wood preservatives on limiting oxygen index levels of fire wood. *Measurement*. 2014;50:279-284.
- Tomak ED, Cavdar AD. Limited oxygen index levels of impregnated scots pine wood. *Thermochim Acta*. 2013;573:181-185.
- Yu LP, Luo ZY, Li LF, Xi XD, Wu ZG, Zhang BG. Study of burning behaviors and fire risk of flame retardant plywood with cone calorimeter and TG test. *J Renew Mater*. 2021;9(12):2143-2157.
- Rabe S, Klack P, Bahr H, Schartel B. Assessing the fire behavior of woods modified by N-methylol crosslinking, thermal treatment, and acetylation. *Fire Mater*. 2020;44(4):530-539.
- Spearpoint MJ, Quintiere JG. Predicting the burning of wood using an integral model. *Combust Flame*. 2000;123(3):308-325.
- Grexa O, Lübke H. Flammability parameters of wood tested on a cone calorimeter. *Polym Degrad Stab*. 2001;74(3):427-432.
- Wang W, Zammarano M, Shields JR, et al. A novel application of silicone-based flame-retardant adhesive in plywood. *Constr Build Mater*. 2018;189:448-459.
- Schartel B, Hull TR. Development of fire-retarded materials—interpretation of cone calorimeter data. *Fire Mater*. 2007;31(5):327-354.
- Luche J, Rogaume T, Richard F, Guillaume E. Characterization of thermal properties and analysis of combustion behavior of PMMA in a cone calorimeter. *Fire Saf J*. 2011;46(7):451-461.
- Rhodes BT, Quintiere JG. Burning rate and flame heat flux for PMMA in a cone calorimeter. *Fire Saf J*. 1996;26(3):221-240.
- Babrauskas V. Development of the cone calorimeter—a bench-scale heat release rate apparatus based on oxygen consumption. *Fire Mater*. 1984;8(2):81-95.

39. Schartel B, Weiß A. Temperature inside burning polymer specimens: pyrolysis zone and shielding. *Fire Mater.* 2010;34(5): 217-235.
40. Schartel B, Braun U, Knoll U, et al. Mechanical, thermal, and fire behavior of bisphenol a polycarbonate/multiwall carbon nanotube nanocomposites. *Polym Eng Sci.* 2008;48(1):149-158.
41. Lee JH, Marroquin J, Rhee KY, Park SJ, Hui D. Cryomilling application of graphene to improve material properties of graphene/chitosan nanocomposites. *Compos Part B Eng.* 2013;45(1):682-687.
42. Kempel F, Schartel B, Linteris GT, et al. Prediction of the mass loss rate of polymer materials: impact of residue formation. *Combust Flame.* 2012;159(9):2974-2984.
43. Braun U, Schartel B. Flame retardant mechanisms of red phosphorus and magnesium hydroxide in high impact polystyrene. *Macromol Chem Phys.* 2004;205(16):2185-2196.

**How to cite this article:** Hupp V, Schartel B, Flothmeier K, Hartwig A. Fire behavior of pressure-sensitive adhesive tapes and bonded materials. *Fire and Materials.* 2024;48(1):114-127. doi:[10.1002/fam.3171](https://doi.org/10.1002/fam.3171)

## **5.2. Pyrolysis and flammability of phosphorus based flame retardant pressure sensitive adhesives and adhesive tapes**

Vitus Hupp, Bernhard Schartel, Kerstin Flothmeier, Andreas Hartwig

Journal of Analytical and Applied Pyrolysis, **2024**; 181, 106658.

<https://doi.org/10.1016/j.jaap.2024.106658>

Published under a Creative Commons license:

<https://creativecommons.org/licenses/by/4.0/>

This article was accepted and published.

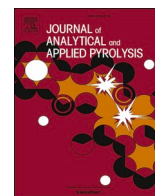
Author contribution:

- Conceptual work for paper and experiments
- Sample preparation and cooperation with IFAM Bremen
- Choice of flame retardant in cooperation with IFAM and industry
- Pyrolytic investigations of the PSA and PSA tapes
  - TGA FTIR
  - ATR FTIR
  - Hot-stage FTIR evaluation
  - PCFC
  - Py-GC/MS evaluation
- Fire testing of adhesive tapes and adhesive tape-bonded materials
  - UL 94
  - OI
- Data evaluation
- Figure ideas and design throughout the article
- Scientific discussion and writing the article
- Correction, spell-checking all versions



## **Abstract**

Pressure-sensitive adhesive tapes are used in a variety of applications such as construction, aircrafts, railway vehicles, and ships, where flame retardancy is essential. Especially in these applications, phosphorus-based flame retardants are often chosen over halogenated ones due to their advantages in terms of toxicity. Although there are pressure-sensitive adhesives with phosphorus flame retardants available on the market, their flame-retardant modes of action and mechanisms are not entirely understood. This research article provides fundamental pyrolysis research of three phosphorus-based flame retardants that exhibit different mechanisms in a pressure-sensitive adhesive matrix. The flame-retardants modes of action and mechanisms of a 9,10-dihydro-9-oxa-10-phosphaphenanthrene-10-oxide (DOPO) derivate, an aryl phosphate, and a self-synthesized, covalently bonded DOPO derivate (copolymerized) are investigated. The blended DOPO derivate is volatilized at rather low temperatures while the covalently bonded DOPO derivate decomposes together with the polymer matrix at the same temperature. Both DOPO derivates release PO radicals which are known for their flame inhibition. The aryl phosphate decomposes at higher temperatures, releases small amounts of aryl phosphates into the gas phase, and acts predominantly the condensed phase. The aryl phosphate acts as precursor for phosphoric acid and improves the charring of the pressure sensitive adhesive matrix. All flame retardants enhance the flammability of the adhesives depending on their individual mode of action while the covalently bonded flame retardant additionally improves the mechanical properties at elevated temperatures making it a promising future technology for pressure-sensitive adhesives.



# Pyrolysis and flammability of phosphorus based flame retardant pressure sensitive adhesives and adhesive tapes

Vitus Hupp<sup>a</sup>, Bernhard Schartel<sup>a,\*</sup>, Kerstin Flothmeier<sup>b</sup>, Andreas Hartwig<sup>b,c</sup>

<sup>a</sup> Bundesanstalt für Materialforschung und -prüfung (BAM), Unter den Eichen 87, Berlin 12205, Germany

<sup>b</sup> Fraunhofer Institute for Manufacturing Technology and Advanced Materials, Wiener Straße 12, Bremen 28359, Germany

<sup>c</sup> University of Bremen, Department 2 Biology/Chemistry, Leobener Straße 3, Bremen 28359, Germany

## ARTICLE INFO

### Keywords:

Pyrolysis of flame retardant  
Pyrolysis gas chromatography  
Mass spectrometry  
Phosphorus flame retardant  
Decomposition mechanism  
Flame retardant pressure sensitive adhesives  
Flame retardancy

## ABSTRACT

Pressure-sensitive adhesive tapes are used in a variety of applications such as construction, aircrafts, railway vehicles, and ships, where flame retardancy is essential. Especially in these applications, phosphorus-based flame retardants are often chosen over halogenated ones due to their advantages in terms of toxicity. Although there are pressure-sensitive adhesives with phosphorus flame retardants available on the market, their flame-retardant modes of action and mechanisms are not entirely understood. This research article provides fundamental pyrolysis research of three phosphorus-based flame retardants that exhibit different mechanisms in a pressure-sensitive adhesive matrix. The flame-retardants modes of action and mechanisms of a 9,10-dihydro-9-oxa-10-phosphaphenanthrene-10-oxide (DOPO) derivate, an aryl phosphate, and a self-synthesized, covalently bonded DOPO derivate (copolymerized) are investigated. The blended DOPO derivate is volatilized at rather low temperatures while the covalently bonded DOPO derivate decomposes together with the polymer matrix at the same temperature. Both DOPO derivatives release PO radicals which are known for their flame inhibition. The aryl phosphate decomposes at higher temperatures, releases small amounts of aryl phosphates into the gas phase, and acts predominantly the condensed phase. The aryl phosphate acts as precursor for phosphoric acid and improves the charring of the pressure sensitive adhesive matrix. All flame retardants enhance the flammability of the adhesives depending on their individual mode of action while the covalently bonded flame retardant additionally improves the mechanical properties at elevated temperatures making it a promising future technology for pressure-sensitive adhesives.

## 1. Introduction

Pressure-sensitive adhesive (PSA) tapes are permanent tacky adhesive tapes that are applied by slight pressure. The viscoelasticity of the adhesives allows the adhesive to “flow” like a fluid so that surfaces can be wetted, and cavities can be filled. The low glass transition temperature ( $T_g$ ) provides for permanent tackiness and easy application [1]. Because most PSAs consist of natural rubber or acrylic polymers, they are intrinsically flammable and considered to be a fire hazard. In many PSA applications such as construction, railway vehicles, airplanes and ships, the fire behavior and pyrolysis of these tapes and of materials bonded by them is of distinguished significance. These applications demand comprehensive investigation into the fire hazards that emerge from PSA tapes and how to develop flame-retarded pressure-sensitive adhesive tapes. In the above mentioned applications, phosphorus flame

retardants are often chosen over halogenated ones due to their lower toxicity and persistence [2,3]. The literature shows a few approaches with different flame retardants for flame-retardant PSAs [4,5] but there is a lack of understanding how different phosphorus-based flame retardants act in these materials and how the pyrolysis mechanism of these flame retardants works. There is especially little knowledge about the development and the fire behavior of PSAs that are used for double-sided tape applications [6,7]. Studies address rather fire behavior and mechanical properties of PSAs and bonds than the mechanisms and flame-retardant modes of actions. Most flame-retardant PSA tapes are used in single-sided tape applications and are based on silicone-based PSAs [8]. For acrylic tapes, the most frequently used class of PSA tapes, there have been investigations and new developments in flame retardancy [9,10] but a deep understanding of the flame retardancy mechanism has yet to be acquired. Often, flame retardants in

\* Corresponding author.

E-mail address: [bernhard.schartel@bam.de](mailto:bernhard.schartel@bam.de) (B. Schartel).

<https://doi.org/10.1016/j.jaap.2024.106658>

Received 25 April 2024; Received in revised form 15 July 2024; Accepted 25 July 2024

Available online 26 July 2024

0165-2370/© 2024 The Author(s). Published by Elsevier B.V. This is an open access article under the CC BY license (<http://creativecommons.org/licenses/by/4.0/>).

**Table 1**  
Composition of prepared PSA emulsions and their phosphorus content.

| Name            | Flame retardant          | P content [wt%] | FR content [wt%] | FR content [g] |
|-----------------|--------------------------|-----------------|------------------|----------------|
| But_Ac          | */*                      | 0               | 0                | 0              |
| But_DOB11_0.5 P | DOB11                    | 0.5             | 4.8              | 8.3            |
| But_DOB11_1.5 P | DOB11                    | 1.5             | 14.3             | 25.0           |
| But_RDP_0.5 P   | RDP                      | 0.5             | 4.0              | 7.0            |
| But_DOPO_0.8 P  | DOPO-pentyl-methacrylate | 0.8             | 8.0              | 13.6           |

adhesives can bloom out or migrate easily [11–13] which reduces or eliminates flame retardancy. To prevent these effects, the flame retardants mixed in physically can be substituted by covalently bonded flame retardants leading to reduced migration [14]. Using covalently bonded flame retardants can improve the mechanical properties of the adhesive compared to blended flame retardants [15–17]. The mechanisms and the effect of both blended and covalently bonded flame retardants on PSA tapes are relevant for research and industry and need to be investigated to deliver the basis for future development.

The investigations presented here show the mode of action and the pyrolysis analysis of three different phosphorus-based flame retardants in PSAs and their effect on the flammability of the corresponding PSA tape. One flame retardant is a non-reactive additive that should act predominantly in the gas phase, the second additive tends to stay in the condensed phase, and the third is covalently bonded to the acrylic polymer backbone. The two commercially available, additive flame retardants are a 9,10-Dihydro-9-oxa-10-phosphaphenanthren-10-oxid (DOPO) -derivate and resorcinol bis(diphenyl phosphate) (RDP) as two different phosphorus species with good flame retardancy results in different materials. The covalently bonded flame retardant, 3-(6-oxido-6 H-dibenzo[c,e][1,2]oxaphosphinin-6-yl) pentyl methacrylate (DOPO-pentyl-methacrylate) is synthesized and subsequently copolymerized with butyl methacrylate to prepare an intrinsically flame-retarded adhesive. It has already been shown that a copolymerization of styrene with a DOPO-acrylate is possible [18] and that copolymerization with a DOPO-derivate can lead to improved flammability and fire behavior [19].

All flame-retardant PSAs and flame retardants are analyzed in terms of their mechanical properties and their individual advantages are compared for different demands/applications.

## 2. Experimental

### 2.1. Materials

#### 2.1.1. Educts for pressure-sensitive adhesives and adhesive tapes

Dihydro-9-oxa-10-phosphaphenanthrene-10-oxide (DOPO) was obtained from Schill+Seilacher GmbH (Böblingen, Germany) as a fine powder, 6H-dibenz[c,e][1,2]oxaphosphorin-6-propanoic acid-butyles ter-6-oxide (DOB11) from Metadynea (Krems, Austria) and resorcinol bis(diphenyl phosphate) Fyrolflex RDP (phosphate phenol ester CAS 57583–54–7) from ICL Industrial Products (Tel Aviv, Israel) were supplied as liquids. Disponil FES 32 and Disponil A1080 were provided by BASF (Ludwigshafen, Germany) as liquid emulsifiers. Disponil FES 32 is an anionic surfactant and chemically the sodium salt of a fatty alcohol ethersulfate with 4 ethylenoxide units. Disponil A 1080 is a non-ionic surfactant consisting of ethoxylated fatty alcohol with 10 ethylenoxide units. Sodium peroxodisulphate (99 % purity), n-dodecyl mercaptan (purity 98 %), acrylic acid (99 % purity), n-pentanol (99 % purity), methacryloyl chloride (97 % purity) and n-butyl acrylate (99 % purity) were obtained from Merck (Taufkirchen, Germany).

As carriers of the PSA tapes, a 23 µm thick poly(ethylene terephthalate) (PET) foil was provided by TESA (Hamburg, Germany) and aluminum (AL) foil in a thickness of 30 µm was purchased from VWR

International GmbH (Darmstadt, Germany).

#### 2.1.2. Preparation of pressure-sensitive adhesives

Due to its chemical ambivalence, DOPO can be used to synthesize a variety of different flame retardants [20–22]. In this research article, the reactive flame retardant DOPO-pentyl-methacrylate was synthesized according to Bier et al. [23] and subsequently used in the PSA that was synthesized by an emulsion polymerization.

To prepare a homogenous PSA emulsion, it is necessary to previously prepare a pre-emulsion and an initiator solution. All flame retardants were added to the pre-emulsion. The procedure of polymerization is shown with the following example and is similar for every flame retardant/ PSA. The applied amounts of flame retardants and concentrations are listed in Table 1. All adhesive names are described in the form But\_X\_YP where But\_Ac is the pure PSA polymer poly(n-butyl acrylate) (PButAc) without any flame retardant. X displays the type of flame retardant and Y the phosphorus content in wt.-%.

In a first step the pre-emulsion and the initiator solution were prepared. Water (57 g), Disponil FES 32 (4.77 g), Disponil A1080 (0.94 g) and acrylic acid (0.72 g) were placed in a 500 ml beaker and stirred magnetically. Then n-butyl acrylate (149.25 g), the flame retardant, and n-dodecyl mercaptan (0.15 g) were added and stirred continuously. For the initiator solution, sodium peroxodisulfate (0.48 g) was dissolved in water (12.3 g) in a 50 ml beaker.

Water (82 g) and Disponil FES 32 (0.67 g) were placed in a 500 ml reaction vessel and heated to 85 °C while stirring under argon atmosphere. Next, 0.8 g initiator solution was added in a single shot and 4.5 g pre-emulsion was added after 15 minutes. Subsequently, the rest of the initiator solution was poured into the pre-emulsion and this mixture was dropped into the reaction vessel over one hour. The reaction was stirred for two hours at 85 °C. Finally, the dispersion was filtered through a 50 µm sieve.

The phosphorus content was chosen considering the processability and compatibility of flame retardants and adhesives. DOB11 was added in two concentrations, only one DOB11 concentration was picked for Py-GC/MS, since the decomposition mechanism is independent of concentration. Higher amounts of flame retardants in the dispersions resulted in inhomogeneity and polymer flocculation. For better processability, the pH of all dispersions was adjusted to pH 8 with 25 % ammonia solution and Rheovis AS 1125 (1 wt%) was added.

#### 2.1.3. Preparation of double-sided adhesive tapes

The dispersions were coated onto the PET or AL foil with a Zehnter automatic film applicator ZAA 2300 at a speed of 25 mm s<sup>-1</sup>. The wet film thickness was adjusted to 110 µm. After five min drying in air at ambient conditions, the films were heated for ten minutes in an oven at 110 °C. The back was coated in the same way after application of a release paper on the already coated side. Eight different double-sided adhesive tapes were manufactured to obtain products with different flame retardants and carriers. All flame retardants and the synthesis of DOPO-pentyl-methacrylate are shown in Fig. 1.

## 2.2. Methods

### 2.2.1. Analysis of physical properties

**DSC:** Differential scanning calorimetry (DSC) was performed with a Discovery DSC 2500 (TA instruments, New Castle, USA) under air atmosphere. Samples of 10–15 mg in an aluminium pan were cooled down to -90 °C and heated at 10 K per minute to 250 °C.

**Peel Test:** This test measures the peel strength at a 180° angle. Peel tests were carried out according to DIN EN ISO 29862 (2019). To test the adhesives, single-sided tapes with PET and AL carriers were manufactured. PSA tape specimens 24 mm × 300 mm in size were laminated onto stainless steel (50 mm × 200 mm) according to Afera 5013 and stored for 24 h in a climate chamber at 23 °C and a relative humidity of 50 %. The test was carried out with an Instron universal testing machine at a peel

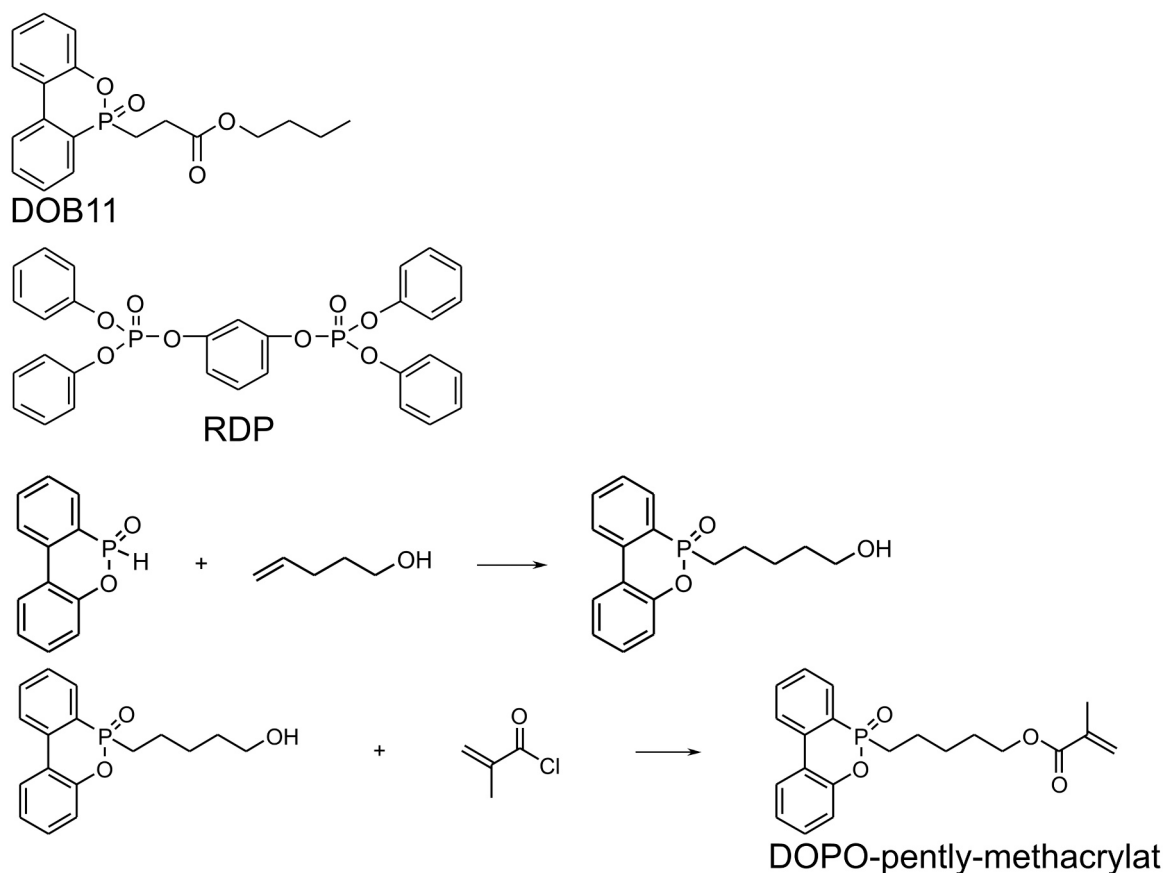


Fig. 1. Structure of the different flame retardants used in the PSA tapes.

**Table 2**

$T_g$  of the compounds and PSA formulations measured by DSC, and  $T_g$  of PSA calculated by the Fox equation.

| Sample                   | $T_g$ exp. [°C] | $T_g$ calc. [°C] |
|--------------------------|-----------------|------------------|
| DOB11                    | $-34 \pm 1$     |                  |
| RDP                      | $-41 \pm 1$     |                  |
| DOPO-pentyl-methacrylate | $-45 \pm 5$     |                  |
| But_Ac                   | $-49 \pm 1$     |                  |
| But_DOB11_1.5 P          | $-49 \pm 1$     | $-47.9$          |
| But_RDP_0.5 P            | $-49 \pm 1$     | $-49.0$          |
| But_DOPO_0.8 P           | $-45 \pm 1$     | $-48.2$          |

**Table 3**

Peel test of the different PSA tapes: SF = substrate failure, AF = adhesive failure on the carrier side, CF = cohesive failure.

| Sample          | Carrier | $F_{mean}$ [N/mm] | Failure |
|-----------------|---------|-------------------|---------|
| But_Ac          | Al      | $0.85 \pm 0.07$   | SF      |
|                 | PET     | $0.29 \pm 0.04$   | AF      |
| But_DOB11_1.5 P | Al      | $0.31 \pm 0.03$   | CF      |
|                 | PET     | $0.31 \pm 0.01$   | CF      |
| But_RDP_0.5 P   | Al      | $0.36 \pm 0.06$   | AF      |
|                 | PET     | $0.71 \pm 0.02$   | CF      |
| But_DOPO_0.8 P  | Al      | $0.23 \pm 0.07$   | AF      |
|                 | PET     | $0.23 \pm 0.08$   | AF      |

rate of  $300 \text{ mm min}^{-1}$ . A fivefold determination was carried out.

**SAFT test:** The shear adhesion failure temperature (SAFT) test measures the thermal stability of a bond. The bond is loaded with a distinct weight, heated, and the temperature at which they peel off the PSA tape is recorded. The test was carried out according to Afera 5013 with a SAFT Tester type SAFT 12/24/36 from Sneepe Industries BV

**Table 4**

SAFT test results of different pressure-sensitive adhesives coated on different carriers.

| Adhesive tape    | Carrier | T [°C]      |
|------------------|---------|-------------|
| But_Ac           | Al      | $67 \pm 7$  |
|                  | PET     | $78 \pm 2$  |
| But_DOB11_1.5 P  | Al      | $40 \pm 1$  |
|                  | PET     | $41 \pm 1$  |
| But_RDP_0.5 P    | Al      | $40 \pm 1$  |
|                  | PET     | $41 \pm 1$  |
| But_DOPO_0.8 P * | Al      | $112 \pm 5$ |
|                  | PET     | $79 \pm 8$  |

(Strijen, The Netherlands). The laminates with the double-sided tapes were prepared with AL and PET foil as a carrier as described for the peel test. PSA tapes were bonded to a standard steel ( $50 \text{ mm} \times 100 \text{ mm}$ ) specimen with a contact area of  $24 \text{ mm} \times 24 \text{ mm}$  and placed in the test rack. A heating rate of  $0.5 \text{ K min}^{-1}$ , a maximum temperature of  $160 \text{ °C}$ , and a weight of  $500 \text{ g}$  were applied. Five test specimens were prepared for each kind of material. The temperature and time at which the weight falls off is recorded. Samples that did not fall off at  $160 \text{ °C}$  were additionally tested with a  $1000 \text{ g}$  weight.

### 2.2.2. Pyrolysis behavior

**Thermogravimetric analysis (TGA):** The TGA was performed in a Netzsch TG 209 F1 Iris (Germany).  $10 \text{ mg}$  adhesive was heated from  $30 \text{ °C}$  to  $900 \text{ °C}$  under a nitrogen atmosphere with a flow of  $30 \text{ ml min}^{-1}$ . The heating ramp was adjusted to  $10 \text{ K min}^{-1}$ . The volatile products were led through a transfer line which was heated to  $270 \text{ °C}$  to a Bruker Optics Tensor27 infrared spectrometer (US), where these products were analyzed in an IR cell.

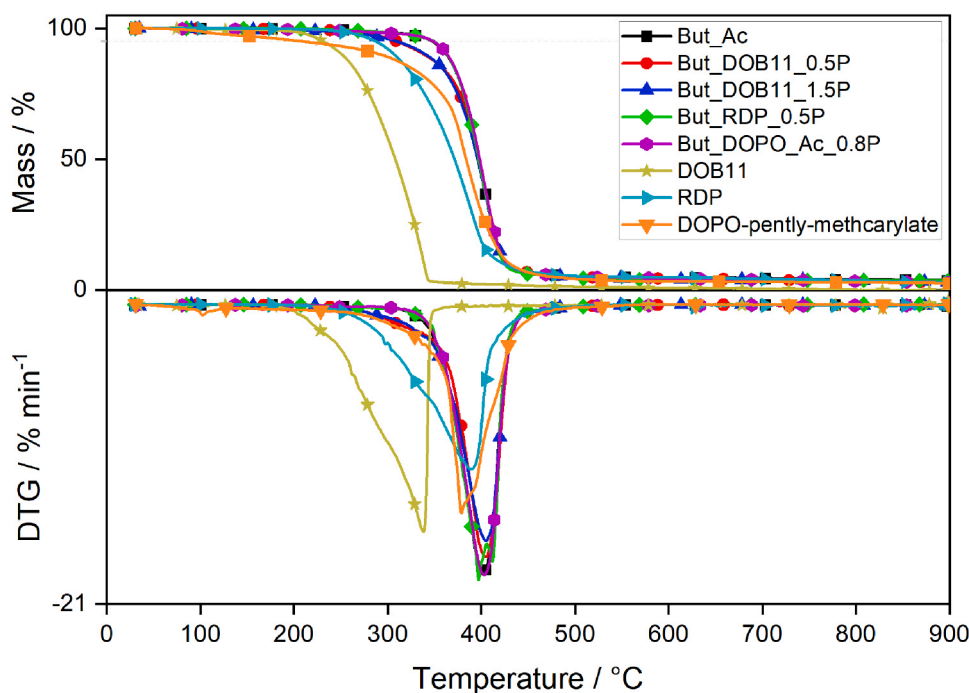


Fig. 2. TGA of all adhesives and the pure flame retardants.

Table 5

TGA of all flame retardants and adhesives.

| Name                     | T(m=95 %) [°C] | T <sub>max</sub> | Residual [wt%] |
|--------------------------|----------------|------------------|----------------|
| But_Ac                   | 344 ± 5        | 399 ± 4          | 3.5 ± 0.1      |
| But_DOB11_0.5 P          | 308 ± 1        | 405 ± 1          | 2.9 ± 0.4      |
| But_DOB11_1.5 P          | 308 ± 1        | 405 ± 1          | 2.9 ± 0.3      |
| But_RDP_0.5 P            | 347 ± 4        | 404 ± 10         | 3.5 ± 0.1      |
| But_DOPO_0.8 P           | 349 ± 1        | 402 ± 1          | 2.9 ± 0.2      |
| DOB11                    | 230 ± 1        | 339 ± 1          | 0.5 ± 0.3      |
| RDP                      | 285 ± 3        | 386 ± 6          | 2.5 ± 0.3      |
| DOPO-pentyl-methacrylate | 207 ± 5        | 379 ± 4          | 2.5 ± 0.4      |

**Pyrolysis combustion flow calorimeter (PCFC):** PCFC measurements were performed in a FAA Micro Calorimeter from Fire Testing Technology Ltd., UK. A 5 mg sample of the adhesive was placed in the bottom of the Al<sub>2</sub>O<sub>3</sub> crucible. Then the sample was heated at a ramp of 1 K s<sup>-1</sup> from 100 to 750 °C under a nitrogen flow of 80 ml min<sup>-1</sup>. The emerging gases were led to a combustion cell where an oxygen flow of 20 ml min<sup>-1</sup> was applied, and the gases were combusted at 900 °C.

**Pyrolysis-gas chromatography-mass spectrometry (Py-GC/MS):** Py-GC/MS is a helpful tool to investigate key products formed by thermal decomposition and the mechanism of phosphorus flame retardants [24,25]. The Py-GC/MS measurements of the adhesives were carried out at 500 °C with a micro furnace double shot pyrolyzer (PY3030iD, Frontier Laboratories, Japan) which was coupled with a gas chromatograph (7890B, Agilent Technologies, US). The pyrolysis products were led into the gas chromatograph via split/splitless inlet port. An Ultra Alloy<sup>+</sup>-5 capillary column (I = 30 m, iD = 0.25 mm, film thickness = 0.25 μm) and a helium flow of 1 ml min<sup>-1</sup> was used. The column

Table 6

Significant results of PCFC measurements.

| Sample          | Residual [%] | T <sub>max</sub> [°C] | PHRR [W g <sup>-1</sup> ] | HRC [kJ g <sup>-1</sup> K <sup>-1</sup> ] | THR [kJ g <sup>-1</sup> ] | FGC [J g <sup>-1</sup> K <sup>-1</sup> ] |
|-----------------|--------------|-----------------------|---------------------------|---|---------------------------|--|
| But_Ac          | 0.24 ± 0.01  | 423 ± 1               | 454 ± 15                  | 454 ± 14                                  | 27.5 ± 0.1                | 392 ± 3                                  |
| But_DOB11_1.5 P | 0.27 ± 0.01  | 425 ± 1               | 428 ± 8                   | 429 ± 8                                   | 27.3 ± 0.6                | 319 ± 17                                 |
| But_RDP_0.5 P   | 0.24 ± 0.01  | 412 ± 1               | 435 ± 7                   | 436 ± 6                                   | 27.3 ± 0.1                | 397 ± 3                                  |
| But_DOPO_0.8 P  | 0.24 ± 0.01  | 424 ± 1               | 447 ± 10                  | 448 ± 11                                  | 27.4 ± 0.2                | 372 ± 8                                  |

temperature was held at 40 °C for two minutes and subsequently heated at 10 K min<sup>-1</sup> to 300 °C, where it was kept isothermal for 10 min. To analyze the products, a mass spectrometer (5977B, Agilent Technologies, US) was used with 70 eV ionization energy and a scan range of 15–550 amu. The GC injector was heated to 300 °C and the split was 1:30. The spectra were compared with the NIST14 MS library.

**Hot stage FTIR microscopy:** To analyze the condensed-phase effect of the flame retardants in the adhesive formulations, the PSAs were placed on glass cover slips and heated horizontally on a THMS600 cell from Linkam, UK. The pictures and FTIR reflection spectra were taken by a Lumos 2 IR microscope from Bruker, US. The samples were heated up from room temperature to 600 °C at a heating rate of 25 K min<sup>-1</sup> under nitrogen atmosphere.

### 2.2.3. Flammability tests

**UL 94:** The UL 94 test is the state of the art test to assess the flammability of PSA tapes and was conducted in a UL 94 chamber from Fire Testing Technology Ltd. (UK). When measuring the films as single-layer PSA tape, the films either burned to the clamp within seconds or dodged the burner flame, which was reflected in inconsistent test results. Thus, multi-layered samples were prepared to prevent shrinking and distortion of the very thin PSA tapes. The sample thickness was increased from 0.1 mm to 1 mm (125 × 13 × 1 mm) by stacking the tapes, resulting in a multilayer sample.

**Oxygen Index (OI):** The OI was measured in an oxygen index device from Fire Testing Technology Ltd. (UK). Because the sample holder frame that is described in ISO 4589–2 was not suitable, the PET carrier tapes were tested as folded samples that were prepared from a 100 mm × 80 mm piece of adhesive tape. First, the edge of the sheet was

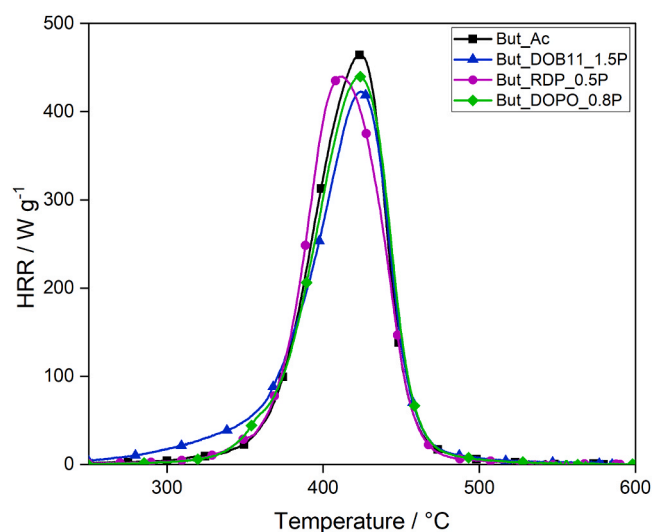


Fig. 3. PCFC measurement of the different adhesives.

folded into a length of 6 mm and subsequently folded/wrapped until the complete 100 mm were folded, resulting in an  $80 \times 7 \times 1.5$  mm specimen which was eventually cut to  $70 \times 7 \times 1.5$  mm. For the AL carrier tapes a different measurement method was performed because only the outer layer of the tape was burning, and incomparable results were obtained. To achieve better repeatability for the AL tapes, the sample holder frame that is described in ISO 4589–2 was used, and steady, reproducible burning took place, allowing tapes with the same carrier to be compared.

### 3. Results

#### 3.1. Adhesive analysis

To obtain the typical tacky behavior of pressure-sensitive adhesives, a low glass transition temperature ( $T_g$ ) is necessary, preferably below  $0^\circ\text{C}$ . If a homogenous mixture is formed, the  $T_g$  of a formulation can be estimated by the Fox Eq. (1) [26]. The  $T_g$  of the PSA ingredients and of the formulations are shown in Table 2.

$$\frac{1}{T_g} = \frac{w(1)}{T_g(1)} + \frac{w(2)}{T_g(2)} \quad (1)$$

Table 2 shows all flame retardants had a low  $T_g$  which did not differ significantly from the  $T_g$  of But\_Ac. All dispersions with flame retardant were suitable as pressure-sensitive adhesives. The DSC graphs of the PSAs are shown in Fig. S1.

Table 3 shows the test results of the peel test of all PSA tapes. It was observed that all flame retardants had a significant impact on the peel strength. All AL carrier tapes with flame retardants had a peel strength reduced by at least 57 % because both the adhesion to the carrier and the cohesive integrity of the adhesive were worsened by the adhesive. The PET carrier tapes had a weak adhesive strength between carrier and adhesive, which resulted in a low peel strength of the But\_Ac tape. This weak bond was not worsened by the flame retardants, and the peel strength was more than doubled by the addition of RDP. It is supposed that the addition of RDP as a flame retardant that is more compatible with PET due to its aromatic structure and  $\pi$  interactions helps to improve the adhesion between the carrier and the adhesive.

The SAFT test (Table 4) shows that both PSA tapes without flame retardant already lost their mechanical integrity at around  $70^\circ\text{C}$ . PSA tapes containing DOB11, or RDP even fell off at the start temperature of  $40^\circ\text{C}$ . This negative effect on the mechanical properties is a well-known problem for blended flame retardants in adhesives due to their softening impact and immiscibility with the polymer. But\_DOPO\_0.8 P, the

adhesive with a reactive flame retardant that formed covalent bonds to the polymer, had higher temperature resistance and withstood the maximum temperature of the test ( $160^\circ\text{C}$ ) when tested with a weight of 500 g. Even with a higher applied weight (1000 g), But\_DOPO\_0.8 P resisted a higher temperature ( $112^\circ\text{C}$  AL/  $79^\circ\text{C}$  PET) than the other adhesives. The covalently bonded DOPO hinders the polymer chains from sliding past each other and thus improves the temperature resistance.

#### 3.2. Thermal analysis of the adhesives

##### 3.2.1. TGA

The TGA results in Fig. 2 show a decomposition of the pressure-sensitive adhesive polymer matrix (PButAc) starting at  $344^\circ\text{C}$ . The flame retardants that were added shift the start of the decomposition to lower temperatures. As seen in Table 5, both concentrations of DOB11 shift the 5 % mass loss temperature by  $32^\circ\text{C}$  from  $340$  to  $308^\circ\text{C}$ . Using RDP as a flame retardant, in contrast, prevents this shift so that the adhesive has the same start of pyrolysis temperature in the TGA as But\_Ac. It has been shown in the literature [27,28] that the flame retardant performance of arylphosphates is stronger, and that condensed-phase effects of phosphorus flame retardants are improved if the decomposition of matrix and flame retardant overlap, which is the case for But\_Ac and RDP as seen in the DTG curve in Fig. 2. But\_DOPO\_0.8 P does not shift the decomposition start to lower temperatures even though DOPO-pentyl-methacrylate starts to decompose earlier in TGA. This can be explained by the covalent bond between the polymer and the flame retardant and implies a high share of covalent bonds of the DOPO-pentyl-methacrylate. Price et al. have already shown that flame retardants that are covalently bonded tend to remain in the condensed phase longer and volatilize at higher temperatures [29]. DOB11 and DOPO-pentyl-methacrylate resemble each other and are expected to volatilize at similar temperatures and work in a similar mode of action, but the covalent bond forces the DOPO-pentyl-methacrylate to remain in the condensed phase until the polymer decomposes. The residue of the adhesives was only slightly affected by the flame retardants.

##### 3.2.2. Pyrolysis combustion flow calorimeter

The PCFC measurements in Table 6 show that the residual and the total heat release (THR) of all samples are very similar, which indicates that the amount and the effective heat of combustion of the evolving gases are the same. As seen in Fig. 3, But\_DOB11\_1.5 P starts to volatilize earlier and causes the heat release rate (HRR) slope to start at lower temperatures. But\_RDP\_0.5 P has its peak of heat release rate (PHRR) at  $412^\circ\text{C}$ , which indicates a catalyzed polymer degradation and is the reason for the trend to a higher fire growth capacity (FGC).

##### 3.2.3. Pyrolysis GC/MS

The Py-GC/MS of But\_Ac (Fig. S2) shows the typical thermal decomposition products of PButAc. The main decomposition products are listed in Table S1 and explained by the decomposition mechanism in Fig. 4. The first and second peaks are attributed to n-butane and n-butanol, which emerge from the alkyl (butyl) residue of PButAc. The ester hydrolyzes or is thermally degraded into poly(acrylic acid) and the alkyl fragments. Polyacrylates are also known for decomposition via depolymerization, which takes place as seen in peak 3 which is attributed to the educt, butyl acrylate. The  $\beta$  scission within the polymer backbone is responsible for peak 4, forming a dimer of butyl acrylate. These results correspond with the literature, which mentions mainly side chain degradation and the depolymerization of acrylates [30–32]. The MS spectra of the peaks are shown in Fig. S3–S8.

3.2.3.1. Decomposition mechanism of DOB11. As shown in the Py-GC/MS analysis in Fig. S9, the flame retardant DOB11 is volatile but

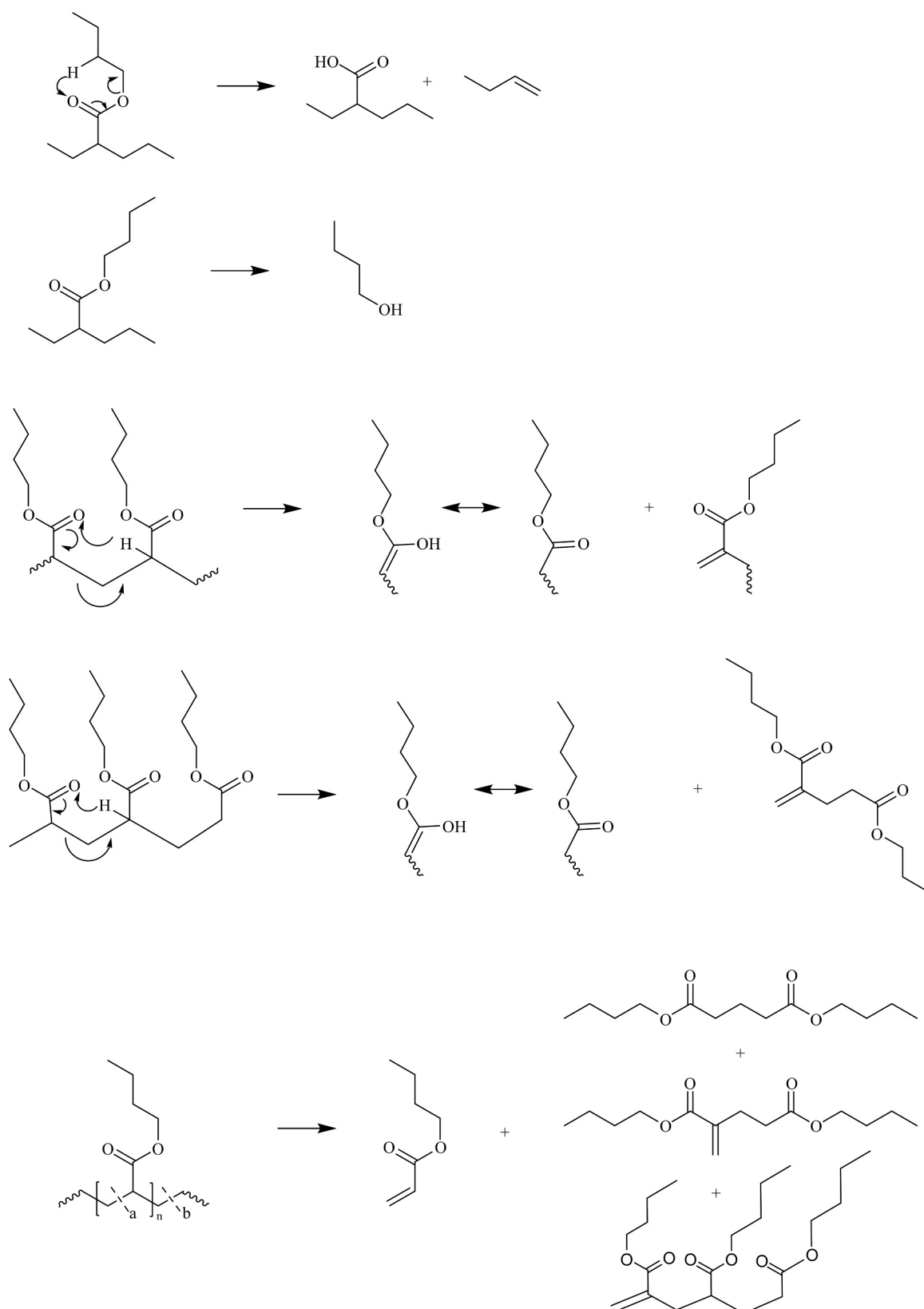


Fig. 4. Decomposition mechanism of But.Ac.

stable at high temperatures. Using a pyrolyzer temperature of 500 °C, a high amount of the complete molecule is observed in the gas phase. The single decomposition products are listed in Table S1, and the mass spectra of the main products are shown in Fig. S10-S19. Besides the main

product and the side chain decomposition products (green box), typical decomposition products for DOPO (derivates) are observed (blue box). These DOPO decomposition products and the proposed decomposition mechanism in Fig. 5 correspond with the literature [33]. Depending on

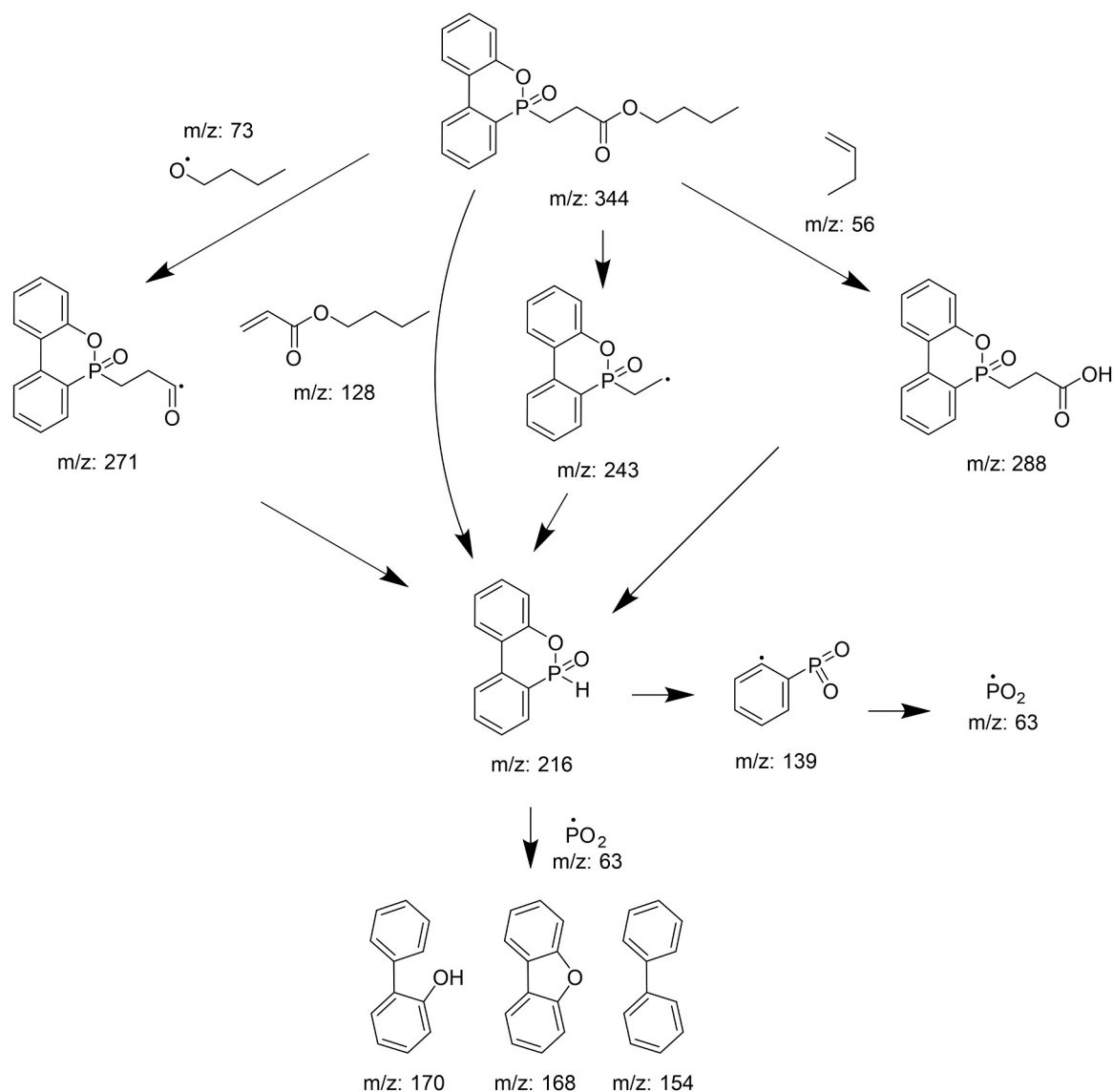


Fig. 5. Proposed decomposition mechanism of DOB 11.

the matrix polymer, chemical environment, and decomposition temperatures, DOPO derivatives can act in the condensed and gas phases depending on the matrix they are used in and how DOPO is chemically bonded. [34–37]. Considering the TGA and Py-GC/MS results, DOB11 is predominantly effective in the gas phase releasing PO<sub>2</sub> radicals.

**3.2.3.2. Decomposition mechanism of RDP.** Fig. S20 shows the Py-GC/MS spectrum of RDP. It decomposes into triphenyl phosphate, (TPP), diphenyl resorcinol phosphate, phenol, and styrene, which are found in the gas phase (Table S1). A decomposition mechanism is proposed in Fig. 6. TPP is known for its flame retardancy in the gas phase in multiple applications [38]. The amount of RDP that is transferred into the gas phase is small compared to DOB11, which is due to the products that remain in the condensed phase. The MS spectra of the single GC peaks are shown in Fig. S21–24. Liu and Yao comprehensively investigated the decomposition mechanism of RDP and found that TPP is formed as a volatile component and polyphosphoric acid as a condensed-phase active product during the thermal decomposition of RDP [39]. Fig. 9 and the Py-GC/MS products correspond with these findings. In TGA, the condensed phase action has no statistical relevance. Other research has observed different condensed-phase and gas phase mechanisms depending on the chemical surroundings of RDP [40,41]. In the

investigated pressure-sensitive adhesive, the polyphosphoric acid could act as a charring agent, and transesterification mechanisms of the PSA polymer are suspected.

**3.2.3.3. Decomposition of DOPO-pentyl-methacrylate.** Fig. S25 shows the Py-GC/MS spectrum of DOPO-pentyl-methacrylate and the decomposition products (Table S1). Besides the flame retardant itself, typical DOPO decomposition products such as dibenzofuran and o-hydroxybiphenyl are found in the gas phase which indicate a similar flame retardant mechanism as DOB 11. The mass spectra of the decomposition products are shown in Fig. S26–S34. The proposed decomposition mechanism is presented in Fig. 7 and agrees with the literature of similar DOPO-derivates [42,43]. The volatilized PO and PO<sub>2</sub> radicals act as radical scavengers and thus poison the flame.

Comparing all flame retardants, the Py-GC/MS investigations show that DOB 11 and DOPO-pentyl-methacrylate act in a similar way. The TGA shows that the main difference is the temperature they are volatilized at depending on whether they are blended or copolymerized in the adhesive matrix. Both show the typical decomposition to DOPO-derivate-specific products which release PO radicals. RDP releases less species into the gas phase (mainly TPP and phenol) and is suspected to act predominantly in the condensed phase. The pyrolysis characteristics



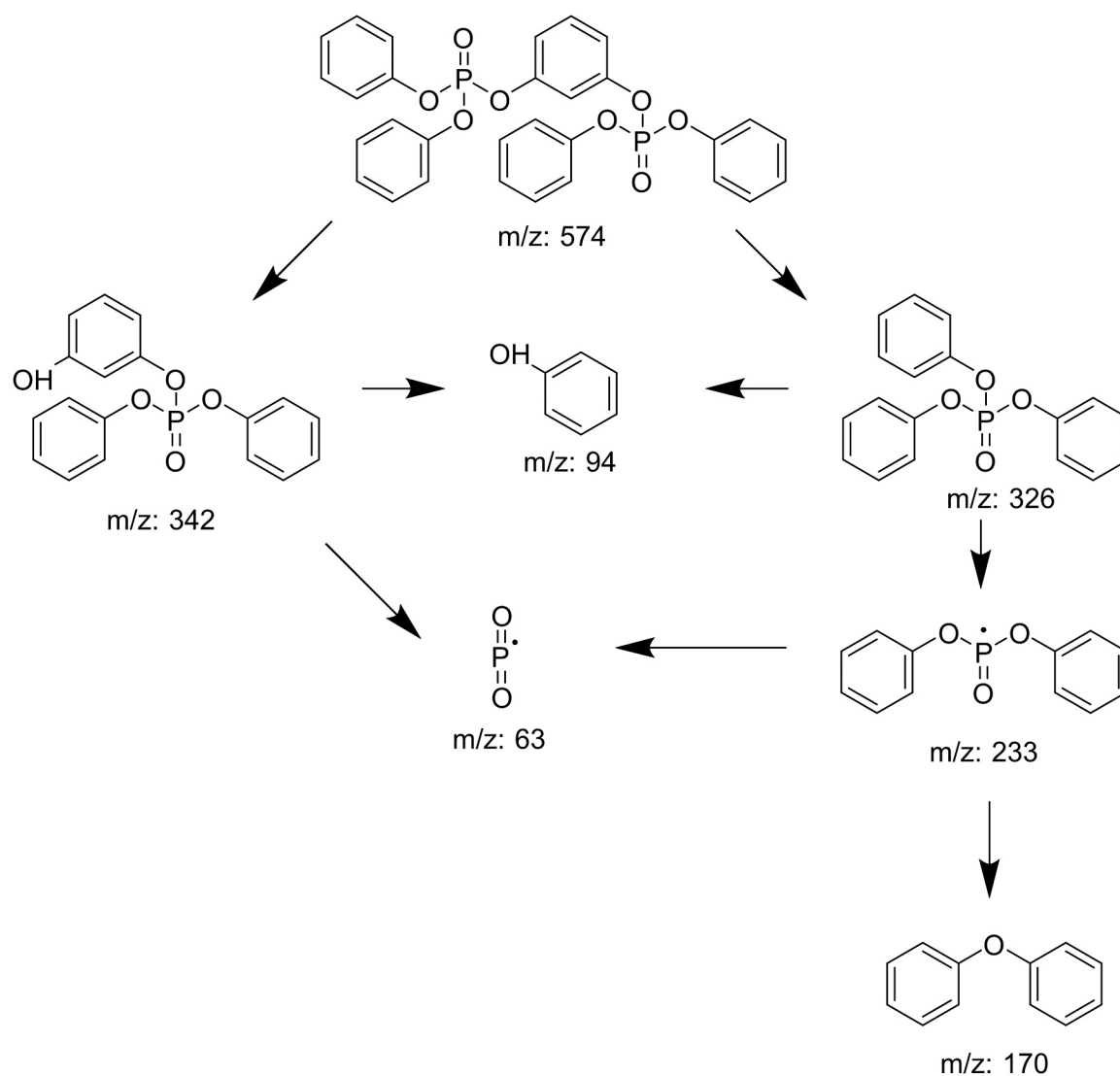


Fig. 6. Proposed decomposition mechanism of RDP.

in the Py-GC/MS of all flame retardants in combination with the PSA matrix (PButAc) is shown in Fig. 8.

**3.2.3.4. Py-GC/MS comparison between the PSAs and the effect of flame retardants.** The comparison of the Py-GC/MS spectra in Fig. 8 show that the flame retardants do not change the decomposition pathway of the But\_Ac, but But\_DOB11\_1.5 P and But\_DOPO\_0.8 P have specific peaks that are attributed to the flame retardants. For DOB11, the peak at around 28 min is the flame retardant that volatilizes as an undecomposed molecule. Also, DOPO\_Ac\_0.8 P has specific peaks that are found in the chromatogram at 25.4 and 30.1 min. These peaks are attributed to DOPO derivatives and act in the gas phase in the above described mechanisms. RDP, as a flame retardant blended into the adhesive, has only a very small extra peak compared to But\_Ac at 24.1 min which is referred to TPP and is thus assumed to act mostly in the condensed phase which agrees with literature where phosphates tend to act in the condensed phase and phosphinates are likely to be predominantly active in the gas phase [44,45].

#### 3.2.4. Hot stage FTIR

The hot stage FTIR shows significant differences in the condensed-phase structure after pyrolysis at 600 °C. Fig. 9 shows the microscope images of a) But\_Ac, b) But\_DOB11\_1.5 P, and c) But\_RDP\_0.5 P. For

But\_Ac, barely any surface charring was observed. But\_DOB11\_1.5 P and But\_RDP\_0.5 P clearly show a charred surface.

For RDP, the charred surface is suspected to be formed due to the present phosphate group, which is known to produce (poly-) phosphoric acid when thermally decomposed. Phosphoric acid catalyzes elimination reactions such as alcohol eliminations and eventually leads to charring of the surface.

The hot stage FTIR spectra in Fig. 10 show the differences between the charred surface of But\_RDP\_0.5 P and But\_DOB11\_1.5 P and the mostly smooth surface of the non-flame-retarded But\_Ac. The surface of the But\_Ac sample shows dominant peaks at 1670 and 1014  $\text{cm}^{-1}$ , which are attributed to the C=O and C-O ester vibrations. The IR spectra of both charred adhesives show aromatic peaks at 1601 and 1445  $\text{cm}^{-1}$ . Further, the 1264  $\text{cm}^{-1}$  is only observed at the charred surface and is attributed to aromatic C-O vibrations. For RDP, a flame retardant containing phosphate, the peak at 757  $\text{cm}^{-1}$  is attributed to the P-O vibrations of phosphate which are still present at 600 °C and prove the condensed-phase mode of action of the suspected phosphoric acid precursors. The vibrations around 1740  $\text{cm}^{-1}$  which are typical for acrylates are still present in the But-Ac, but almost eliminated for the flame-retarded adhesives. But\_Ac shows a strong band at 1014  $\text{cm}^{-1}$  which is attributed to the carboxylic acid which emerges when the butylalcohol rest is split from the ester as butene and water.

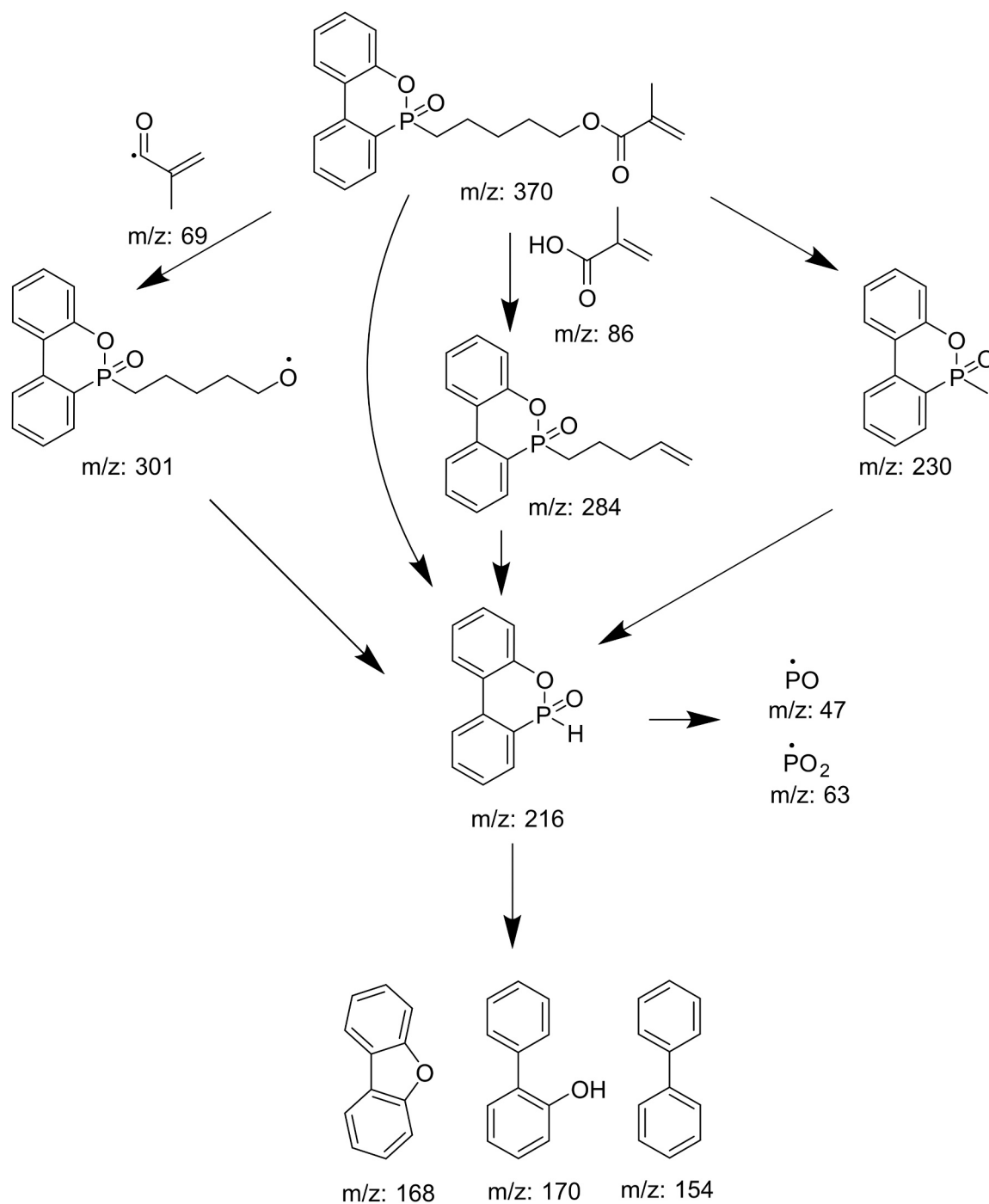


Fig. 7. Decomposition mechanism of DOPO-pentyl-methacrylate.

### 3.3. Fire testing

#### 3.3.1. UL 94

The UL 94 ratings in Table 7 show that DOB11 helps to achieve a V-2 rating. In contrast, RDP and the covalently bonded DOPO-pentyl-methacrylate achieve no rating in the vertical test. TGA shows that the adhesive with DOB11 decomposes faster, leading to earlier dripping of the sample. This improved melt dripping behavior is a common way to improve the UL 94 rating of certain materials such as thin films. RDP and DOPO-pentyl-methacrylate do not lead to lower decomposition temperatures in TGA and thus do not improve the melt dripping of the adhesive tapes.

AL as a carrier leads to increased burning speed upward through the

specimens. Dripping is entirely inhibited by the fire-resistant AL, which prevents extinguishing. Thus, all AL carrier tapes fail to achieve a UL 94 vertical rating.

#### 3.3.2. Oxygen index

The oxygen index, presented in Table 8, shows an increased value for all flame retardants. The OI of PSA containing DOB11 rises as the concentration of flame retardant increases. Normalized on the phosphorus content, the flame retardants DOPO-pentyl-methacrylate and RDP are more effective in the PET carrier system and behave like DOB11 with 1.5 % phosphorus content. Coated on AL, all flame retardants improve the OI slightly.

The flammability tests imply a connection between pyrolytic

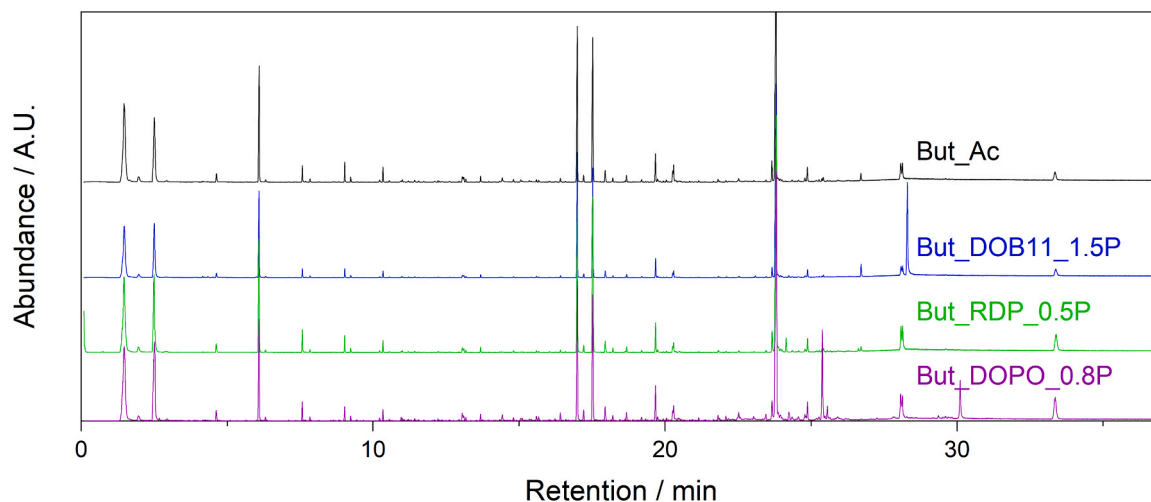


Fig. 8. Comparison of Py-GC/MS chromatograms of But\_Ac, But\_DOB11\_1.5 P and But\_RDP\_0.5 P and But\_DOPO\_0.8 P.

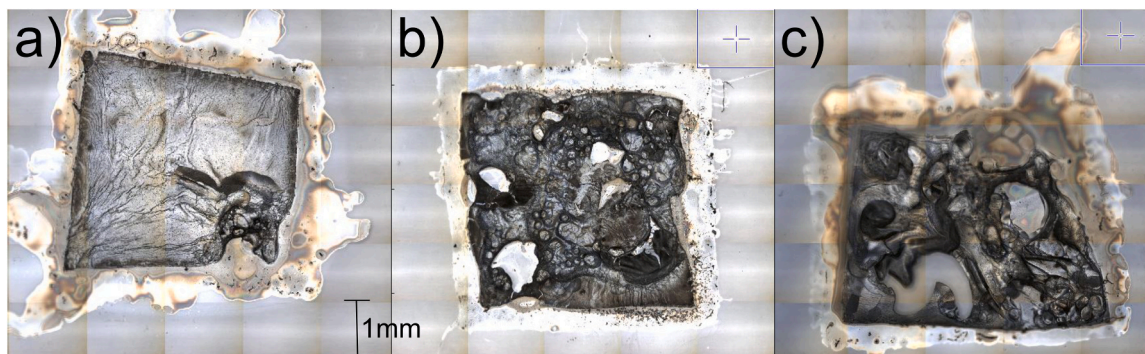


Fig. 9. Hot stage microscopy comparison of a) But\_Ac, b) But\_DOB11\_1.5 P and c) But\_RDP\_0.5 P.

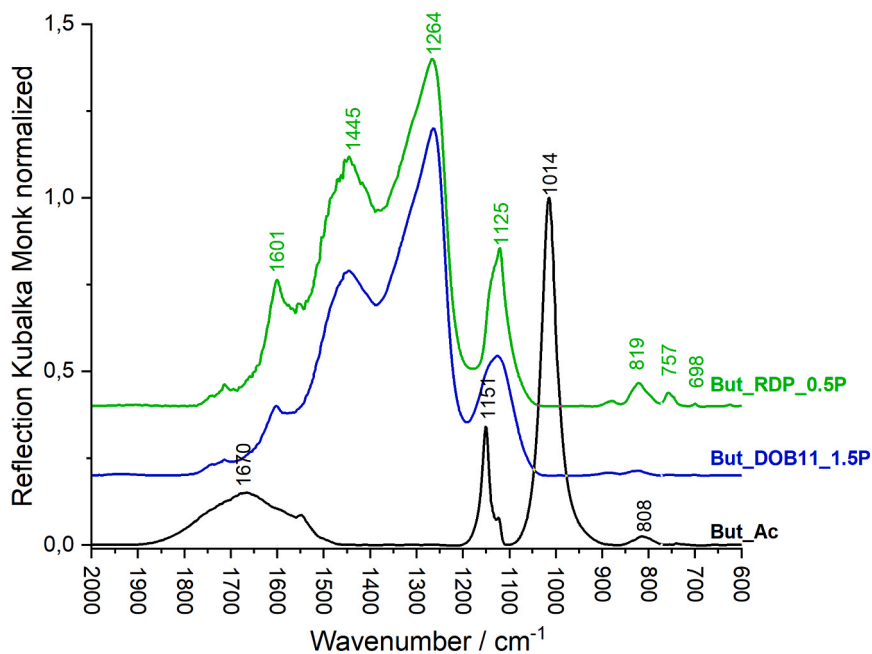


Fig. 10. Hot stage IR spectra of But\_Ac, But\_DOB11\_1.5 P and But\_RDP\_0.5 P at 600 °C.

**Table 7**  
UL 94 ratings of adhesive tapes.

| Tape               | Igniting cotton | UL 94 rating |
|--------------------|-----------------|--------------|
| But_Ac_PET         | Y               | N.R.         |
| But_DOB11_0.5p_PET | Y               | V-2          |
| But_DOB11_1.5p_PET | Y               | V-2          |
| But_RDP_0.5p_PET   | Y               | N.R.         |
| But_DOPO_0.8P_PET  | Y               | N.R.         |
| But_Ac_AL          | Y               | N.R.         |
| But_DOB11_0.5p_AL  | Y               | N.R.         |
| But_DOB11_1.5p_AL  | Y               | N.R.         |
| But_RDP_0.5p_AL    | Y               | N.R.         |
| But_DOPO_0.8P_AL   | Y               | N.R.         |

Data are partially published in [46]

**Table 8**  
Oxygen indices of adhesive tapes with different carriers.

| Tape              | Oxygen index [vol.-%] |
|-------------------|-----------------------|
| But_50_REF_PET    | 17.6 ± 0.2            |
| DOB11_0.5p_PET    | 18.5 ± 0.4            |
| DOB11_1.5p_PET    | 19.7 ± 0.2            |
| RDP_0.5p_PET      | 19.6 ± 0.2            |
| But_DOPO_0.8P_PET | 19.2 ± 0.2            |
| But_Ac_AL         | 23.2 ± 0.2            |
| But_DOB11_0.5p_AL | 24.1 ± 0.2            |
| But_DOB11_1.5p_AL | 24.2 ± 0.2            |
| But_RDP_0.5p_AL   | 23.9 ± 0.2            |
| But_DOPO_0.8P_AL  | 23.4 ± 0.2            |

Data are partially published in [46]

behavior and fire test results in different ignition scenarios. A lower decomposition temperature in TGA leads to increased dripping in UL 94 test and thus achieves a better ranking (V-2) than the adhesive tapes where an adhesive with a higher decomposition temperature is used. Also, the flame retardants active in the gas phase achieve higher rankings than those active in the condensed phase. In the OI, dripping can be neglected, and the condensed-phase-active flame retardants work as well as the gas phase active ones.

#### 4. Conclusions

This research article provides insight into the mechanism of phosphorus-based flame retardants in pressure sensitive adhesive (tapes) and how their pyrolysis characteristics and flammability are connected. Three different flame retarded (DOB11, RDP, DOPO-pentyl-methacrylate) PSA were investigated in a multi-methodical approach to investigate the flame retardants' mode of action and structure-mechanism relationship in a PSA matrix. DOB11 as a DOPO derivate volatilizes at lower temperatures (TGA) than the PSA matrix (PButAc) and acts predominantly in the gas phase. In the Py-GC/MS, it decomposes into the typical gas phase active pyrolysis products of DOPO which release PO and PO<sub>2</sub> radicals. The covalent bonded DOPO-pentyl-methacrylate volatilizes later in TGA and is held in the polymer matrix until the PSA itself decomposes and the flame retardant is released. It decomposes to similar DOPO species as the DOB11 and releases PO and PO<sub>2</sub> radicals which agrees with the literature of similar DOPO derivatives [47]. RDP as an arylphosphate releases only small amounts of gas phase active species (TPP), acts predominantly in the condensed phase, and is suspected to act as a precursor for phosphoric/polyphosphoric acid. All flame retardants release gas phase active species during pyrolysis without changing the gas phase decomposition products of the PSA matrix. The early decomposing DOPO derivatives that are gas phase active were especially effective in UL 94 while RDP as a condensed phase active flame retardant performs best in OI measurements. The copolymerization of the DOPO-pentyl-methacrylate leads to exceptional mechanical properties at elevated temperatures which is, in addition to the

immobilization, a further advantage and considered a future technology for the development of new PSA.

#### Author statement

All authors declare to be accountable for all aspects of the work and that questions related to the accuracy or integrity of any part of the work will be appropriately investigated and resolved. All authors have made substantial contributions to the following:

The conception and design of the study, or acquisition of data, or analysis and interpretation of data.

Drafting the article or revising it critically for important intellectual content.

Final approval of the version to be submitted.

#### CRediT authorship contribution statement

**Kerstin Flothmeier:** Writing – original draft, Methodology, Investigation. **Andreas Hartwig:** Writing – review & editing, Supervision, Project administration, Funding acquisition, Conceptualization. **Vitus Hupp:** Writing – original draft, Project administration, Methodology, Investigation. **Bernhard Schartel:** Writing – review & editing, Supervision, Project administration, Funding acquisition, Conceptualization.

#### Declaration of Competing Interest

The authors declare that they have no known competing financial interests or personal relationships that could have appeared to influence the work reported in this paper.

#### Data availability

Data will be made available on request.

#### Acknowledgements

The research was based on an IGF Project. The IGF Project (20762 N) of the Research Association DECHEMA (Deutsche Gesellschaft für Chemische Technik und Biotechnologie e. V., 60486 Frankfurt am Main, Germany) was supported by the AiF within the framework of the program "Förderung der Industriellen Gemeinschaftsforschung (IGF)" of the German Federal Ministry for Economic Affairs and Climate Action, based on a decision of the Deutschen Bundestag.

I'd like to thank Dr. Alexander Battig for his support and advice in Py-GC/MS measurements and evaluation. I thank Dr. Volker Wachten-dorf and Yannik Wägner for their expertise in Hot stage FTIR microscopy. Further, I'd like to thank Fernanda Romero for her UL 94 and OI measurements.

#### Appendix A. Supporting information

Supplementary data associated with this article can be found in the online version at [doi:10.1016/j.jaap.2024.106658](https://doi.org/10.1016/j.jaap.2024.106658).

#### References

- [1] Müller B., Rath W. Formulating Adhesives and Sealants. Vincentz Network; 2014.
- [2] S.L. Waaijers, D. Kong, H.S. Hendriks, C.A. de Wit, I.T. Cousins, R.H.S. Westerkink, P.E.G. Leonards, M.H.S. Kraak, W. Admiraal, P. de Voogt, J.R. Parsons, Persistence, Bioaccumulation, and Toxicity of Halogen-Free Flame Retardants, in: D. M. Whitacre (Ed.), *Reviews of Environmental Contamination and Toxicology*, Springer New York, 2013, pp. 1–71.
- [3] T.R. Hull, R.J. Law, Å. Bergman, Environmental drivers for replacement of halogenated flame retardants. In: Papaspyrides CD, Kiliaris P, eds, *Chapter 4. Polymer Green Flame Retardants*, Elsevier, 2014, pp. 119–179. Chapter 4.
- [4] X.M. Feng, G.Q. Li, UV curable, flame retardant, and pressure-sensitive adhesives with two-way shape memory effect, *Polymer* (2022) 249124835.

- [5] X.-L. Wang, L. Chen, J.-N. Wu, T. Fu, Y.-Z. Wang, Flame-retardant pressure-sensitive adhesives derived from epoxidized soybean oil and phosphorus-containing dicarboxylic acids, *ACS Sustain. Chem. Eng.* 5 (4) (2017) 3353–3361.
- [6] L.J. Zeng, L. Yang, J.B. Liu, S.K. Lu, L.H. Ai, Y. Dong, Z.B. Ye, P. Liu, Preparation and properties of flame-retardant polyurethane pressure sensitive adhesive and its application, *J. Compos. Sci.* 7 (2) (2023) 85.
- [7] Hupp V., Schartel B., Flothmeier K., Hartwig A. Fire behavior of pressure-sensitive adhesive tapes and bonded materials. *Fire and Materials*. n/a(n/a).
- [8] A.K. Antosik, M. Polka, Z. Czech, M. Piatek-Hnat, K. Mozelewska, Flammability of selected silicone pressure-sensitive adhesives, *Przemysl Chem.* 97 (7) (2018) 1151–1153.
- [9] X. Liu, J.Q. Zhao, X.D. Lin, Construction of strong non-covalent interactions for preparation of flame-retarded acrylic pressure-sensitive adhesives with improved shear and peel strengths, *J. Appl. Polym. Sci.* 139 (19) (2022) e52122.
- [10] M. Son, J. Kim, M. Oh, D. Kim, H.J. Choi, K. Lee, K. Chung, S. Lee, Phosphorus-based flame retardant acrylic pressure sensitive adhesives with superior peel strength and transfer characteristics, *Prog. Org. Coat.* 185 (2023) 107931.
- [11] X. Liu, E. Folk, Sorption and migration of organophosphate flame retardants between sources and settled dust, *Chemosphere* 278 (2021) 130415.
- [12] C. Rauer, B. Lazarov, S. Harrad, A. Covaci, M. Stranger, A review of chamber experiments for determining specific emission rates and investigating migration pathways of flame retardants, *Atmos. Environ.* 82 (2014) 44–55.
- [13] M. Tokumura, S. Ogo, K. Kume, K. Muramatsu, Q. Wang, Y. Miyake, T. Amagai, M. Makino, Comparison of rates of direct and indirect migration of phosphorus flame retardants from flame-retardant-treated polyester curtains to indoor dust, *Ecotoxicol. Environ. Saf.* 169 (2019) 464–469.
- [14] M. Liu, B. Peng, G. Su, M. Fang, Reactive flame retardants: are they safer replacements? *Environ. Sci. Technol.* 55 (21) (2021) 14477–14479.
- [15] Z.X. Zhang, J. Zhang, B.-X. Lu, Z.X. Xin, C.K. Kang, J.K. Kim, Effect of flame retardants on mechanical properties, flammability and foamability of PP/wood-fiber composites, *Compos. Part B: Eng.* 43 (2) (2012) 150–158.
- [16] B. Musić, N. Knez, J. Bernard, Flame retardant behaviour and physical-mechanical properties of polymer synergistic systems in rigid polyurethane foams, *Polymers* 14 (21) (2022) 4616.
- [17] A. Subasinghe, R. Das, D. Bhattacharyya, Study of thermal, flammability and mechanical properties of intumescent flame retardant PP/kenaf nanocomposites, *Int. J. Smart Nano Mater.* 7 (3) (2016) 202–220.
- [18] L. Yan, Y.B. Zheng, X. Liang, Q. Ma, Copolymerization of 1-oxo-2,6,7-trioxa-1-phosphabicyclo[2,2,2]oct-4-yl methyl acrylate and (10-oxo-10-hydro-9-oxa-10-phosphaphenanthrene-10-yl) methyl acrylate with styrene and their thermal degradation characteristics, *J. Appl. Polym. Sci.* 115 (2) (2010) 1032–1038.
- [19] X. Tao, H. Duan, W. Dong, X. Wang, S. Yang, Synthesis of an acrylate constructed by phosphaphenanthrene and triazine-trione and its application in intrinsic flame retardant vinyl ester resin, *Polym. Degrad. Stab.* 154 (2018) 285–294.
- [20] M. Rakotomalala, S. Wagner, M. Döring, Recent Developments in Halogen Free Flame Retardants for Epoxy Resins for Electrical and Electronic Applications, *Materials* 3 (8) (2010) 4300–4327.
- [21] J. Sag, D. Goedderz, P. Kukla, L. Greiner, F. Schönberger, M. Döring, Phosphorus-Containing Flame Retardants from Biobased Chemicals and Their Application in Polyesters and Epoxy Resins, *Molecules* 24 (20) (2019) 3746.
- [22] K.A. Salmeia, S. Gaan, An overview of some recent advances in DOPO-derivatives: chemistry and flame retardant applications, *Polym. Degrad. Stab.* 113 (2015) 119–134.
- [23] F. Bier, J.-L. Six, A. Durand, DOPO-based phosphorus-containing methacrylic (co) polymers: glass transition temperature investigation, *Macromol. Mater. Eng.* 304 (4) (2019) 1800645.
- [24] A. Battig, J.C. Markwart, F.R. Wurm, B. Schartel, Hyperbranched phosphorus flame retardants: multifunctional additives for epoxy resins, *Polym. Chem.* 10 (31) (2019) 4346–4358, <https://doi.org/10.1039/C9PY00737G>.
- [25] A. Battig, J.C. Markwart, F.R. Wurm, B. Schartel, Sulfur's role in the flame retardancy of thio-ether-linked hyperbranched polyphosphoesters in epoxy resins, *Eur. Polym. J.* 122 (2020) 109390.
- [26] T.G. Fox Jr., P.J. Flory, Second-Order Transition Temperatures and Related Properties of Polystyrene. I. Influence of Molecular Weight, *J. Appl. Phys.* 21 (6) (1950) 581–591.
- [27] B. Perret, K.H. Pawlowski, B. Schartel, Fire retardancy mechanisms of arylphosphates in polycarbonate (PC) and PC/acrylonitrile-butadiene-styrene, *J. Therm. Anal. Calorim.* 97 (3) (2009) 949–958.
- [28] B. Schartel, B. Perret, B. Dittrich, M. Ciesielski, J. Krämer, P. Müller, V. Altstädt, L. Zang, M. Döring, Flame retardancy of polymers: the role of specific reactions in the condensed phase, *Macromol. Mater. Eng.* 301 (1) (2016) 9–35.
- [29] D. Price, L.K. Cunliffe, K.J. Bullett, T.R. Hull, G.J. Milnes, J.R. Ebdon, B.J. Hunt, P. Joseph, Thermal behaviour of covalently bonded phosphate and phosphonate flame retardant polystyrene systems, *Polym. Degrad. Stab.* 92 (6) (2007) 1101–1114.
- [30] S. Özlem, J. Hacıoğlu, Thermal degradation of poly(n-butyl methacrylate), poly(n-butyl acrylate) and poly(t-butyl acrylate), *J. Anal. Appl. Pyrolysis* 104 (2013) 161–169.
- [31] S. Duquesne, J. Lefebvre, R. Delobel, G. Camino, M. LeBras, G. Seeley, Vinyl acetate/butyl acrylate copolymers—part 1: mechanism of degradation, *Polym. Degrad. Stab.* 83 (1) (2004) 19–28.
- [32] S. Ozlem, E. Aslan-Gürel, R.M. Rossi, J. Hacıoğlu, Thermal degradation of poly(isobornyl acrylate) and its copolymer with poly(methyl methacrylate) via pyrolysis mass spectrometry, *J. Anal. Appl. Pyrolysis* 100 (2013) 17–25.
- [33] X. Wang, Y. Hu, L. Song, W. Xing, H. Lu, P. Lv, G. Jie, Flame retardancy and thermal degradation mechanism of epoxy resin composites based on a DOPO substituted organophosphorus oligomer, *Polymer* 51 (11) (2010) 2435–2445.
- [34] A. Bifulco, C.D. Varganici, L. Rosu, F. Mustata, D. Rosu, S. Gaan, Recent advances in flame retardant epoxy systems containing non-reactive DOPO based phosphorus additives, *Polym. Degrad. Stab.* 200 (2022) 109962.
- [35] C.K. Kundu, X. Wang, M.Z. Rahman, L. Song, Y. Hu, Application of Chitosan and DOPO derivatives in fire protection of polyamide 66 textiles: towards a combined gas phase and condensed phase activity, *Polym. Degrad. Stab.* 176 (2020) 109158.
- [36] B. Schartel, A.I. Balabanovich, U. Braun, U. Knoll, J. Artner, M. Ciesielski, M. Döring, R. Perez, J.K.W. Sandler, V. Altstädt, T. Hoffmann, D. Pospiech, Pyrolysis of epoxy resins and fire behavior of epoxy resin composites flame-retarded with 9,10-dihydro-9-oxa-10-phosphaphenanthrene-10-oxide additives, *J. Appl. Polym. Sci.* 104 (4) (2007) 2260–2269.
- [37] S. Brehme, B. Schartel, J. Goebbels, O. Fischer, D. Pospiech, Y. Bykov, M. Döring, Phosphorus polyester versus aluminium phosphinate in poly(butylene terephthalate) (PBT): Flame retardancy performance and mechanisms, *Polym. Degrad. Stab.* 96 (5) (2011) 875–884.
- [38] K.H. Pawlowski, B. Schartel, Flame retardancy mechanisms of triphenyl phosphate, resorcinol bis(diphenyl phosphate) and bisphenol A bis(diphenyl phosphate) in polycarbonate/acrylonitrile-butadiene-styrene blends, *Polym. Int.* 56 (11) (2007) 1404–1414.
- [39] C. Liu, Q. Yao, Mechanism of thermal degradation of aryl bisphosphates and the formation of polyphosphates, *J. Anal. Appl. Pyrolysis* 133 (2018) 216–224.
- [40] E.A. Murashko, G.F. Levchik, S.V. Levchik, D.A. Bright, S. Dashevsky, Fire-retardant action of resorcinol bis(diphenyl phosphate) in PC-ABS blend. II. Reactions in the condensed phase, *J. Appl. Polym. Sci.* 71 (11) (1999) 1863–1872.
- [41] Z. Jiang, S. Liu, J. Zhao, X. Chen, Flame-retarded mechanism of SEBS/PPO composites modified with mica and resorcinol bis(diphenyl phosphate), *Polym. Degrad. Stab.* 98 (12) (2013) 2765–2773.
- [42] L. Qian, Y. Qiu, N. Sun, M. Xu, G. Xu, F. Xin, Y. Chen, Pyrolysis route of a novel flame retardant constructed by phosphaphenanthrene and triazine-trione groups and its flame-retardant effect on epoxy resin, *Polym. Degrad. Stab.* 107 (2014) 98–105.
- [43] S. Huo, J. Wang, S. Yang, X. Chen, B. Zhang, Q. Wu, B. Zhang, Flame-retardant performance and mechanism of epoxy thermosets modified with a novel reactive flame retardant containing phosphorus, nitrogen, and sulfur, *Polym. Adv. Technol.* 29 (1) (2018) 497–506.
- [44] U. Braun, A.I. Balabanovich, B. Schartel, U. Knoll, J. Artner, M. Ciesielski, M. Döring, R. Perez, J.K.W. Sandler, V. Altstädt, T. Hoffmann, D. Pospiech, Influence of the oxidation state of phosphorus on the decomposition and fire behaviour of flame-retarded epoxy resin composites, *Polymer* 47 (26) (2006) 8495–8508.
- [45] B. Schartel, Phosphorus-based Flame Retardancy Mechanisms—Old Hat or a Starting Point for Future Development? *Materials* 3 (10) (2010) 4710–4745.
- [46] V. Hupp, B. Schartel, K. Flothmeier, A. Hartwig, Flame Retarded Adhesive Tapes and Their Influence on the Fire Behavior of Bonded Parts, *Fire Technol.* (2024).
- [47] A. Schäfer, S. Seibold, W. Lohstroh, O. Walter, M. Döring, Synthesis and properties of flame-retardant epoxy resins based on DOPO and one of its analog DPPO, *J. Appl. Polym. Sci.* 105 (2) (2007) 685–696.

# Pyrolysis and flammability of phosphorus based flame retardant pressure sensitive adhesives and adhesive tapes

Vitus Hupp,<sup>a</sup> Bernhard Schartel,<sup>a\*</sup> Kerstin Flothmeier,<sup>b</sup> Andreas Hartwig<sup>b,c</sup>

<sup>a</sup> Bundesanstalt für Materialforschung und -prüfung (BAM), Unter den Eichen 87, 12205 Berlin, Germany; bernhard.schartel@bam.de

<sup>b</sup> Fraunhofer Institute for Manufacturing Technology and Advanced Materials, Wiener Straße 12, 28359 Bremen, Germany

<sup>c</sup> University of Bremen, Department 2 Biology/Chemistry, Leobener Straße 3, 28359 Bremen, Germany

\*Corresponding author

## Supporting Information

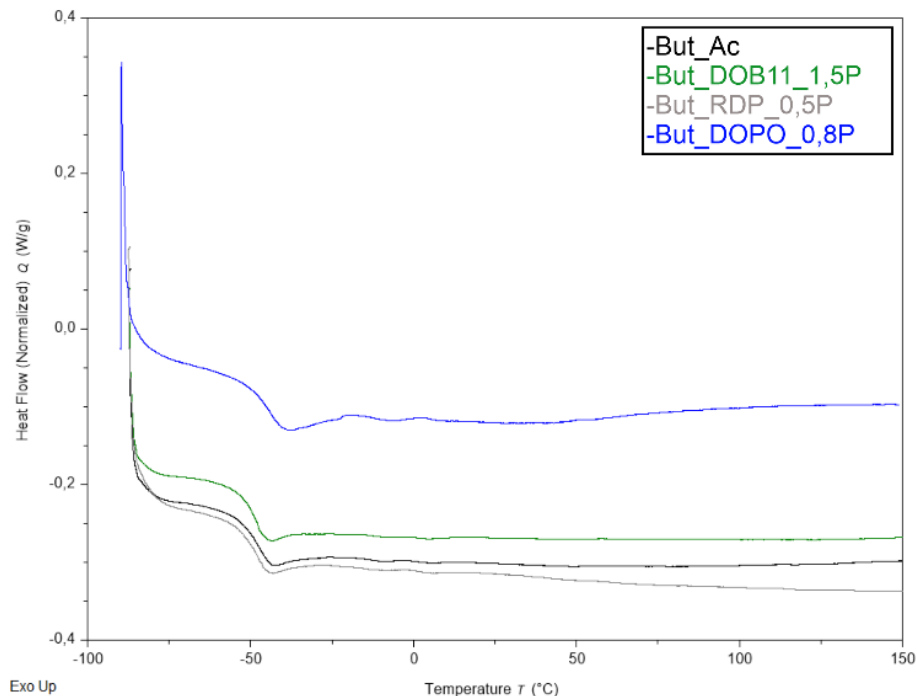
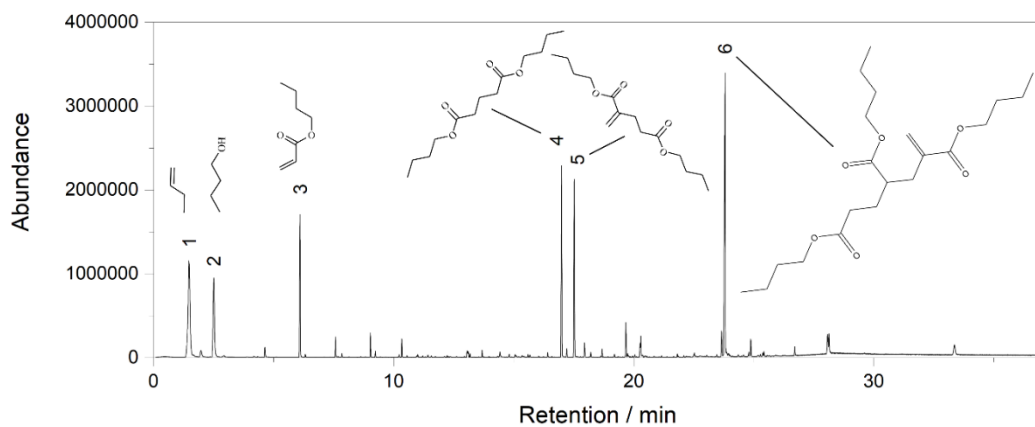
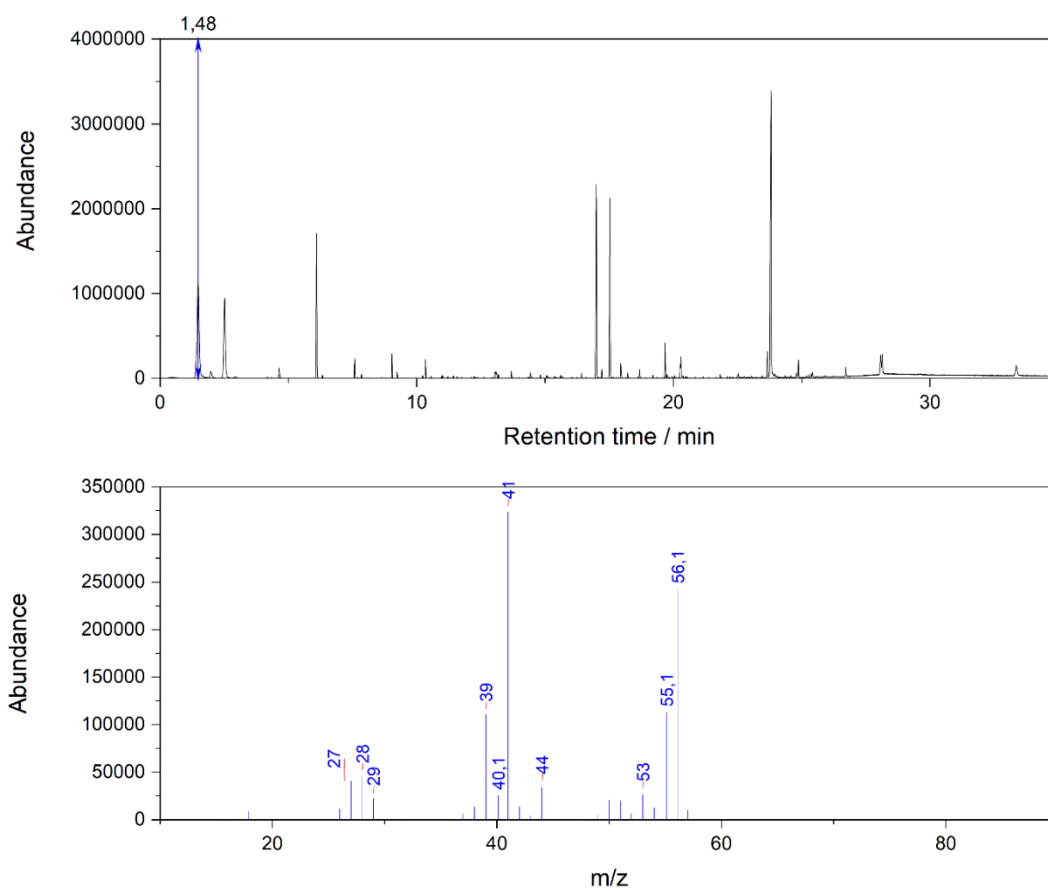


Fig. S1 DSC graphs of the pressure sensitive adhesives.



**Fig. S2** But\_Ac Py-GC/MS spectrum.



**Fig. S3** Peak 1 of the But\_Ac mass spectrum (butene).

**Table S1**

Decomposition products and their CAS numbers of But\_Ac and all flame retardants

| Peak                            | Retention [min] | Chemical name   | CAS No.     |
|---------------------------------|-----------------|---|-------------|
| <b>But_Ac</b>                   |                 |   |             |
| 1                               | 1.48            | 1-Butene  | 106-98-9    |
| 2                               | 2.52            | 1-Butanol   | 71-36-3     |
| 3                               | 6.07            | Butyl acrylate (Monomer)  | 141-32-2    |
| 4                               | 16.99           | Dibutyl glutarate (Dimer)   | 6624-57-3   |
| 5                               | 17.52           | Pentanedioic acid, 2-methylene-dibutyl ester (dimer)                              | 23720-21-0  |
| 6                               | 23.79           | Tributyl hex-5-ene-1,3,5-tricarboxylate   |             |
| <b>DOB11</b>                    |                 |   |             |
| 1                               | 1.40            | 2-Butene  | 106-98-9    |
| 2                               | 2.50            | 1-Butanol   | 71-36-3     |
| 3                               | 6.00            | Styrene   | 100-42-5    |
| 4                               | 6.10            | 2-Propenoic acid, butyl ester   | 141-32-2    |
| 5                               | 13.70           | Biphenyl  | 92-52-4     |
| 6                               | 15.40           | o-Hydroxybiphenyl   | 90-43-7     |
| 7                               | 15.40           | Dibenzofuran  | 132-64-9    |
| 8                               | 18.40           | 9H-Fluorene, 9-methylene-   | 4425-82-5   |
| 9                               | 22.10           | DOPO  | 35948-25-5  |
| 10                              | 23.10           | 6-Thenylbenzo [c][2,1]benzoxaphosphinine 6-oxide                                  |             |
| 11                              | 26.30           | 9,10-Dihydro-9-oxa-10-phosphaphenanthrene-10-propanoic acid methyl ester 10-oxide | 63562-42-5  |
| 12                              | 28.40           | DOB11   | 848820-98-4 |
| <b>RDP</b>                      |                 |   |             |
| 1                               | 6.00            | Styrene   | 100-42-5    |
| 2                               | 7.60            | Phenol  | 108-95-2    |
| 3                               | 24.10           | TPP   | 115-86-6    |
| 4                               | 26.65           | Diphenyl-resorcinol phosphate   |             |
| <b>DOPO-pentyl-methacrylate</b> |                 |   |             |
| 1                               | 4.59            | Methacrylic acid  | 79-41-4     |
| 2                               | 13.65           | Biphenyl  | 92-52-4     |
| 3                               | 15.37           | o-Hydroxybiphenyl   | 90-43-7     |
| 4                               | 15.42           | Dibenzofuran  | 132-64-9    |
| 5                               | 22.55           | DOPO-methyl   |             |
| 6                               | 25.39           | DOPO-4-pentenyl   |             |
| 7                               | 27.91           | DOPO-5-pentanol   |             |
| 8                               | 29.72           | DOPO-pentyl-(2-methyl-propanoate)   |             |
| 9                               | 30.29           | DOPO-pentyl-methacrylate  |             |



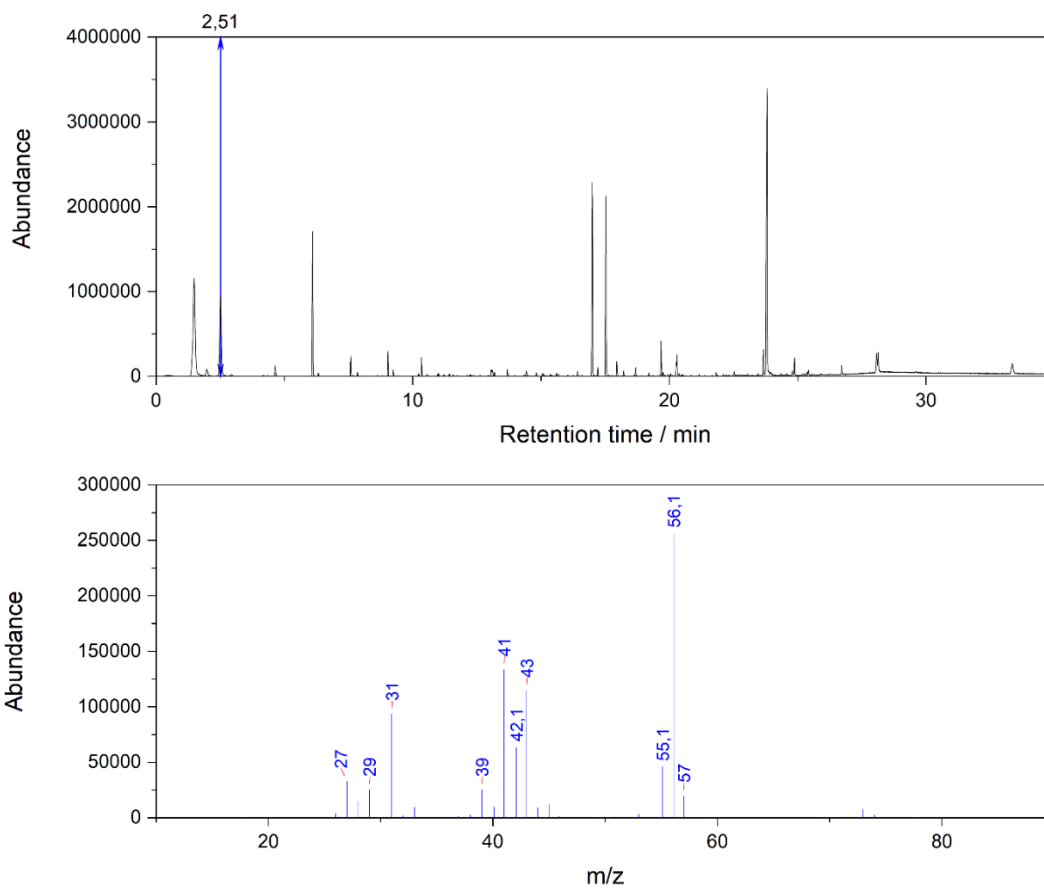


**Fig. S4** Peak 2 of the But\_Ac mass spectrum (butanol).

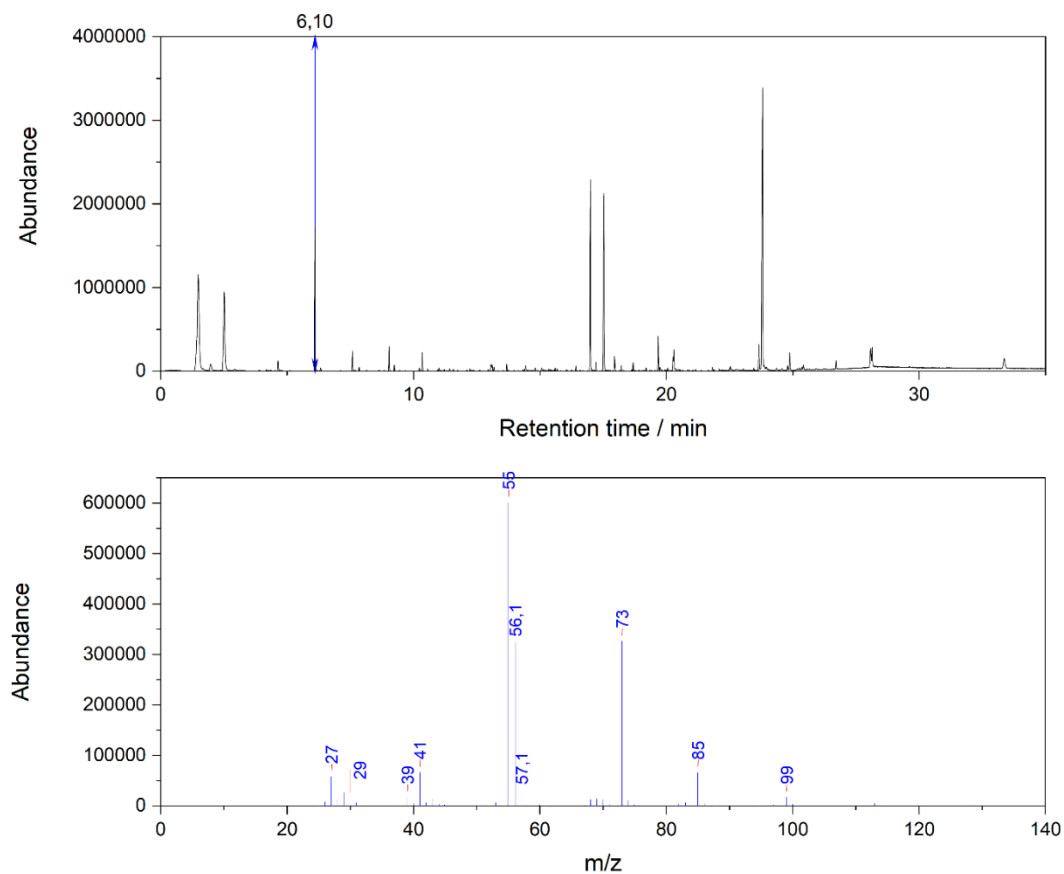


**Fig. S5** Peak 3 of the But\_Ac mass spectrum (butyl acrylate (monomer)).

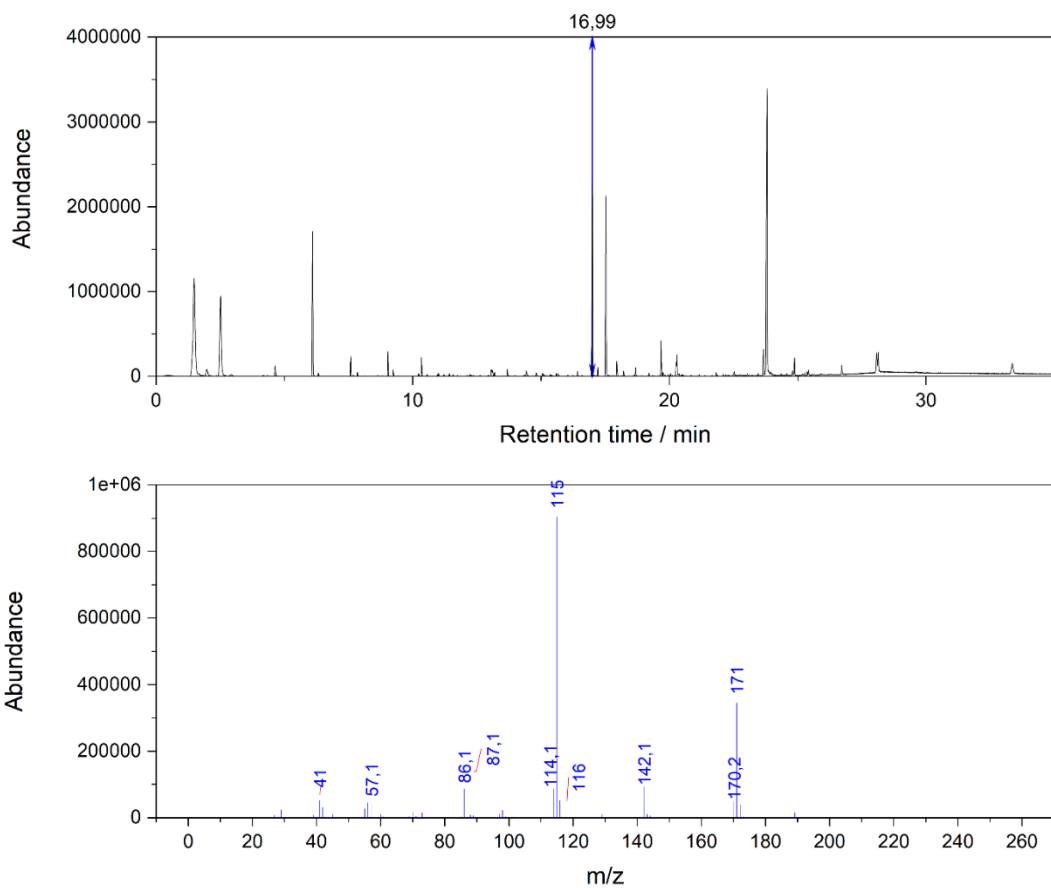


**Fig. S6** Peak 4 of the But\_Ac mass spectrum (dibutyl glutarate (dimer)).

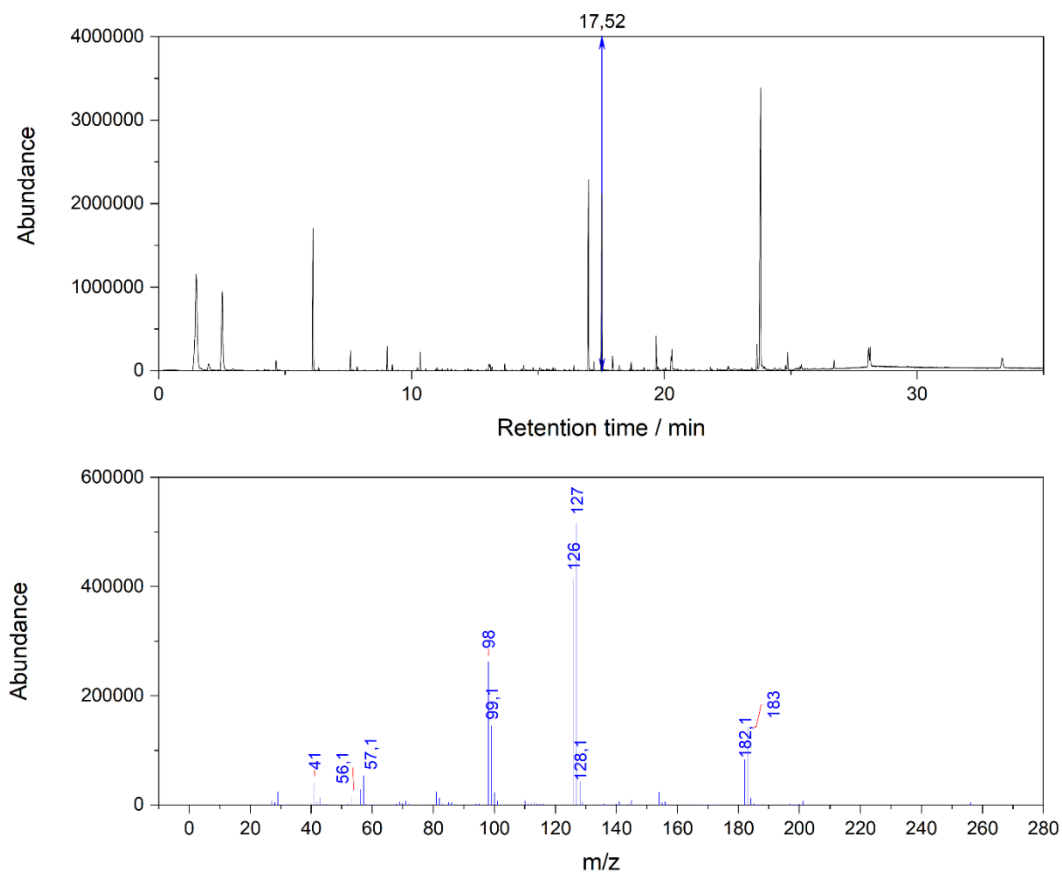


**Fig. S7** Peak 5 of the But\_Ac mass spectrum (pentanedioic acid, 2-methylene-dibutyl ester (dimer)).

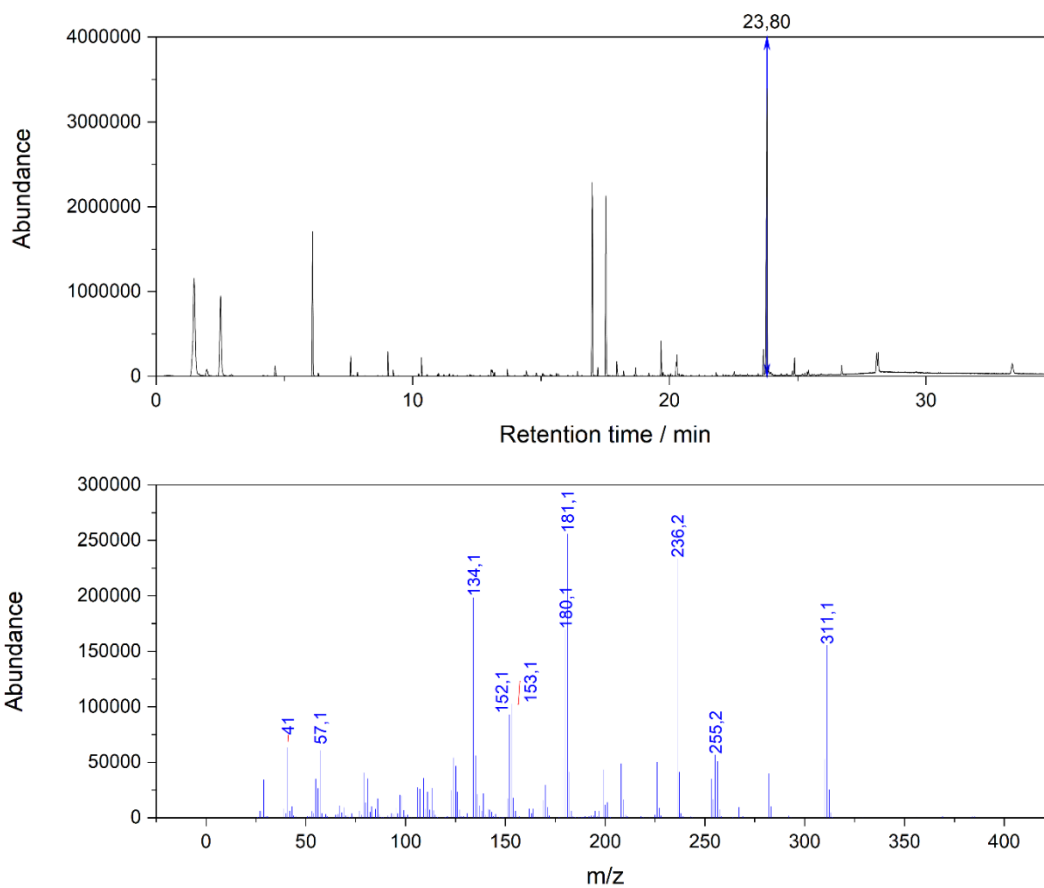


**Fig. S8** Peak 6 of the But\_Ac mass spectrum (tributyl hex-5-ene-1,3,5-tricarboxylate).

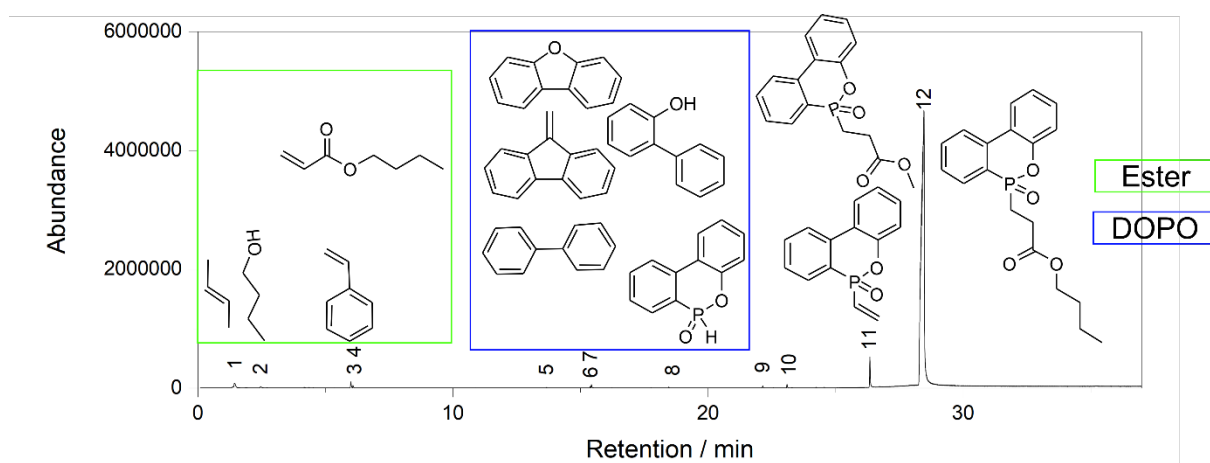


**Fig. S9** Py-GC/MS spectrum of DOB11 and structure of the decomposition products.

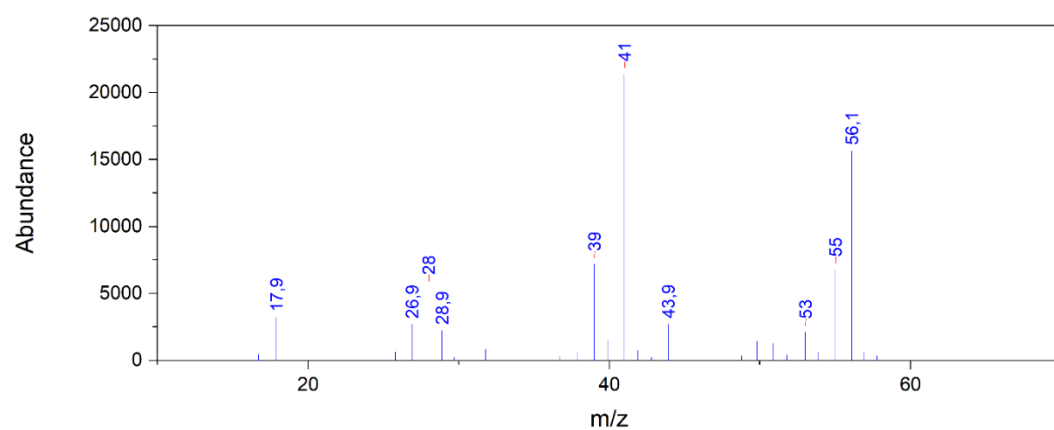
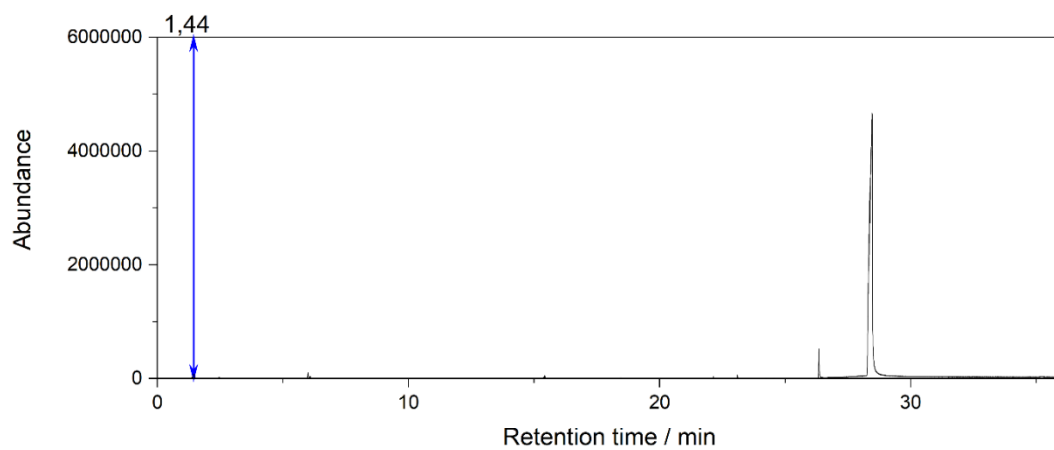


**Fig. S10:** DOB11 Py-GC/MS Peak 1 (2-butene)

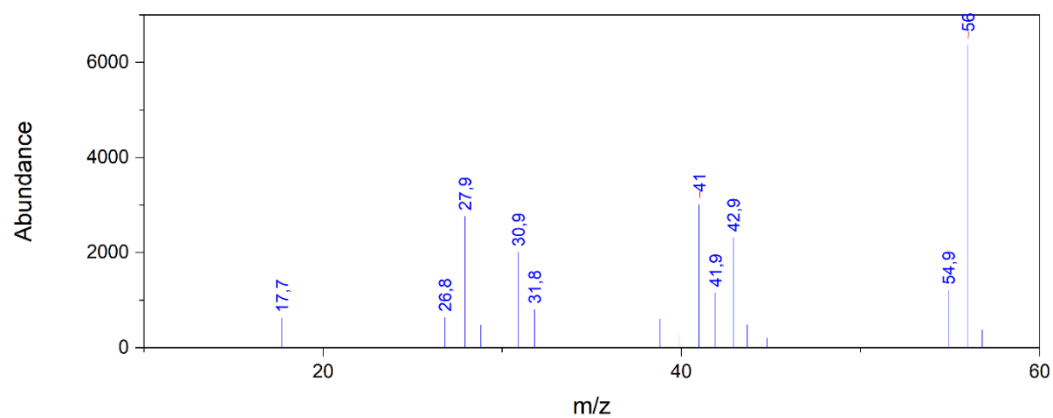
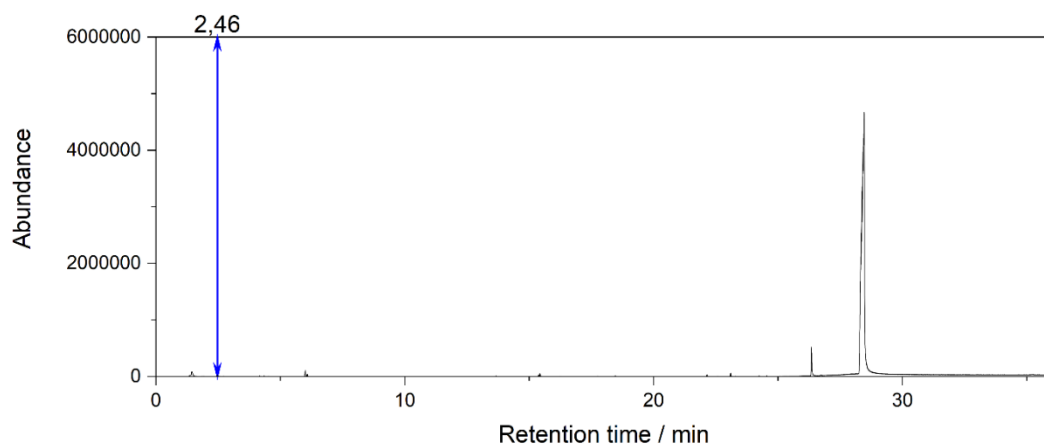


**Fig. S11:** DOB11 Py-GC/MS Peak 2 (1-butanol)

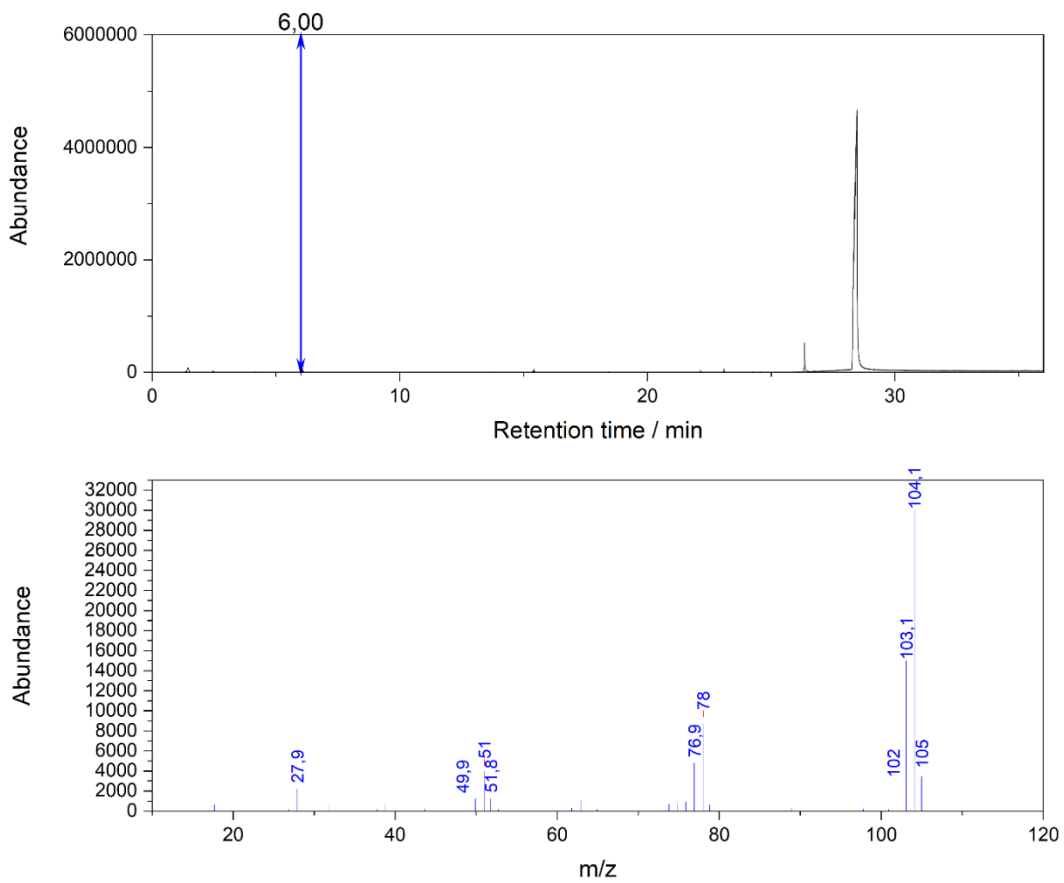


**Fig. S12:** DOB11 Py-GC/MS Peak 3 (styrene)

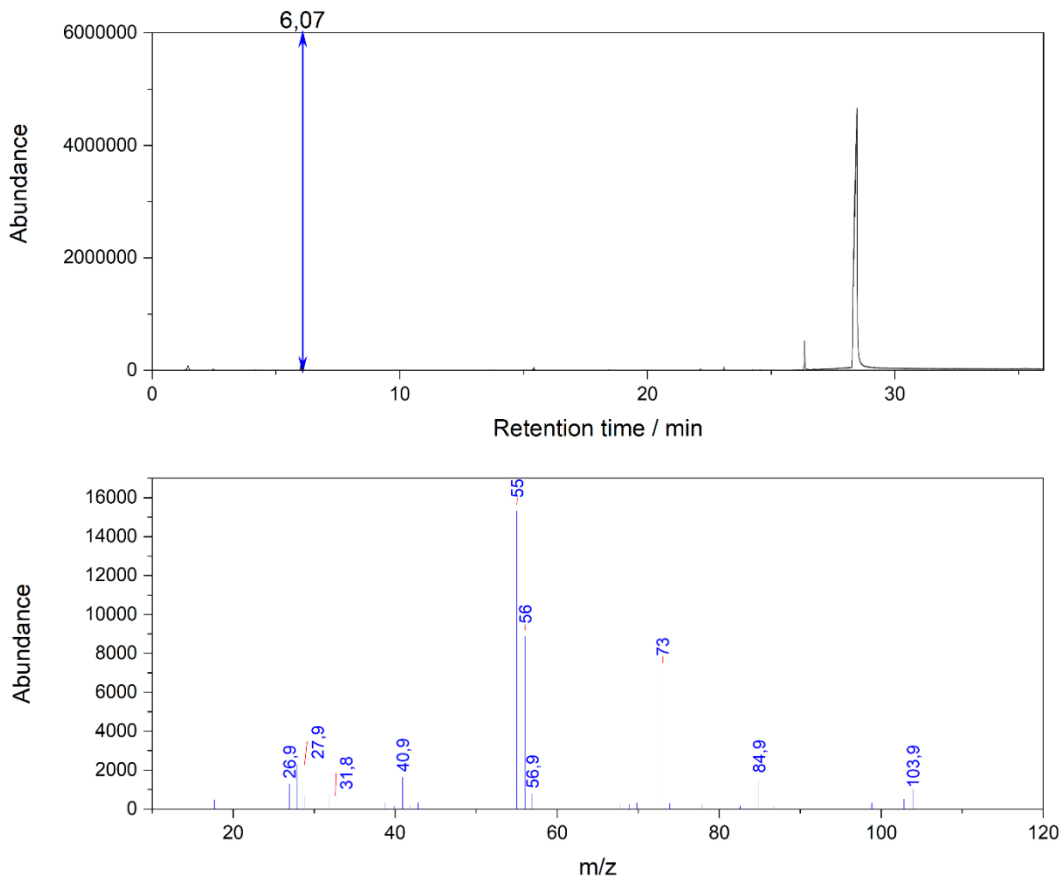


**Fig. S13:** DOB11 Py-GC/MS Peak 4 (butyl acrylate)

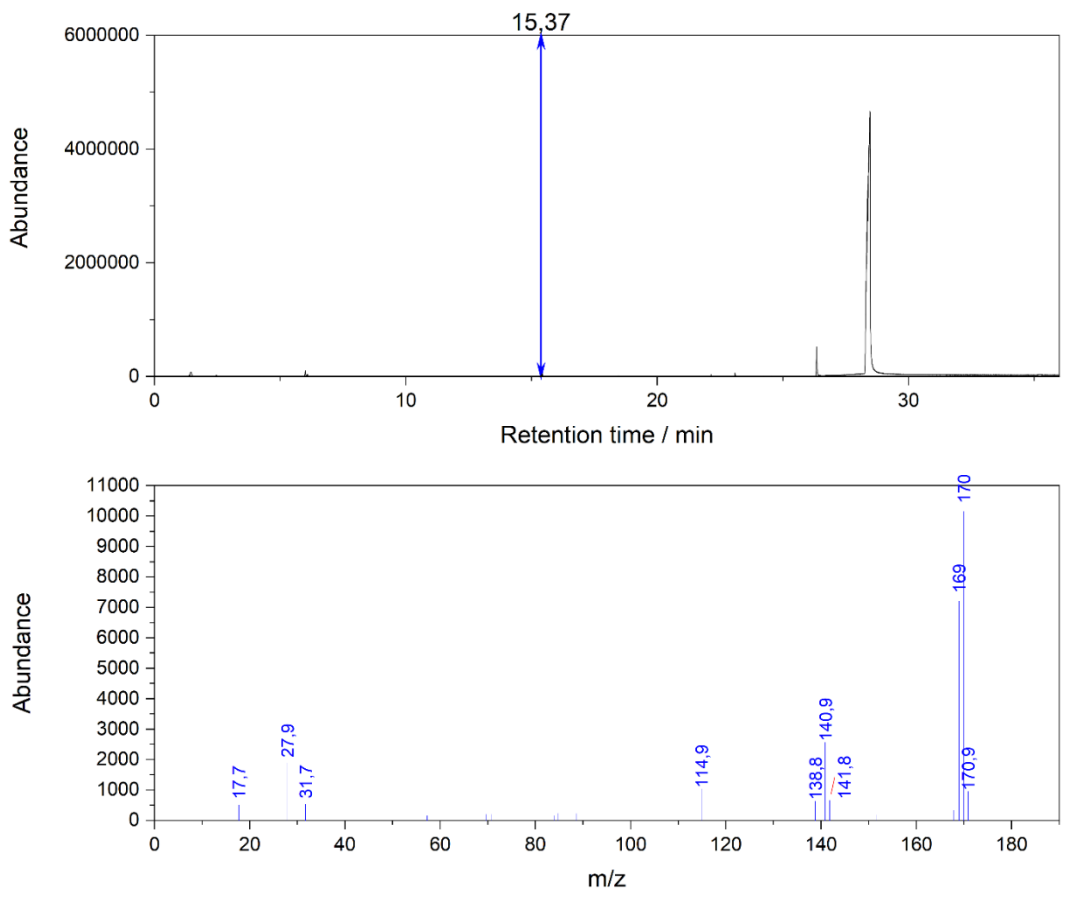


**Fig. S14:** DOB11 Py-GC/MS Peak 6 (2-hydroxybiphenyl)

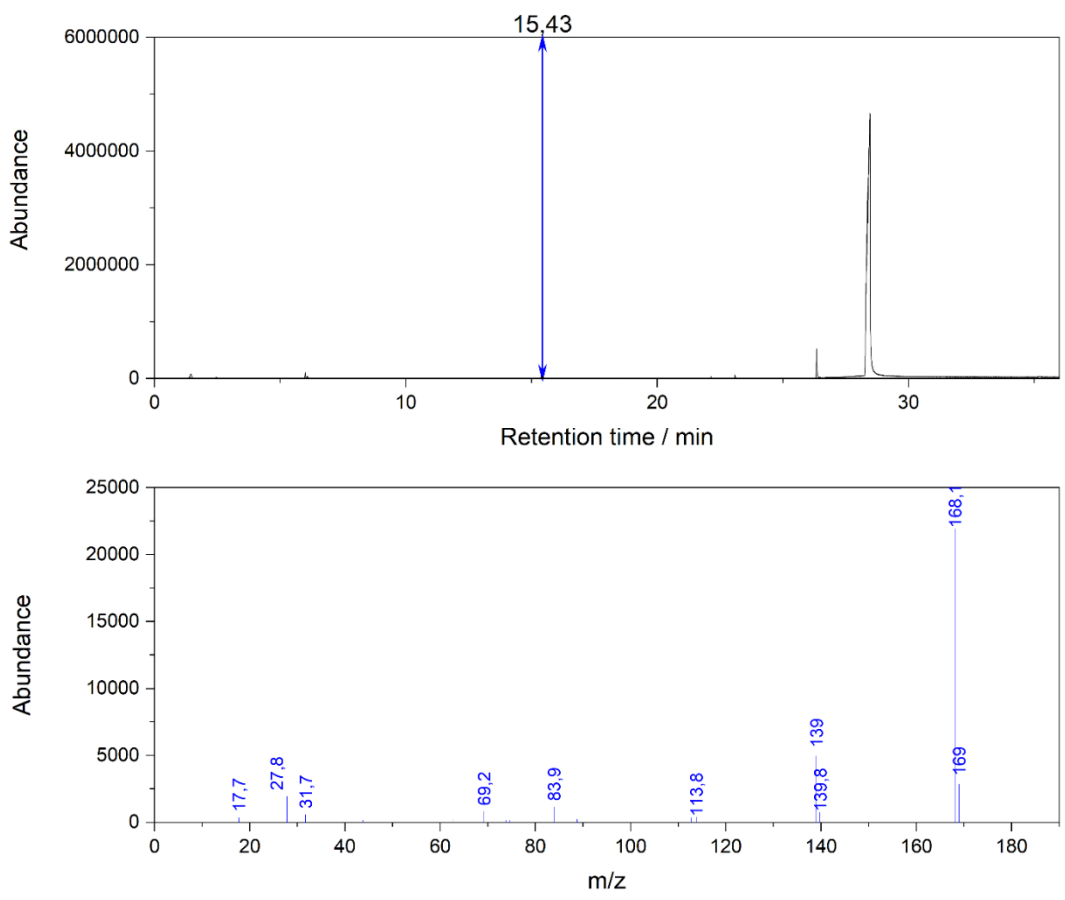


**Fig. S15:** DOB11 Py-GC/MS Peak 7 (dibenzofuran)

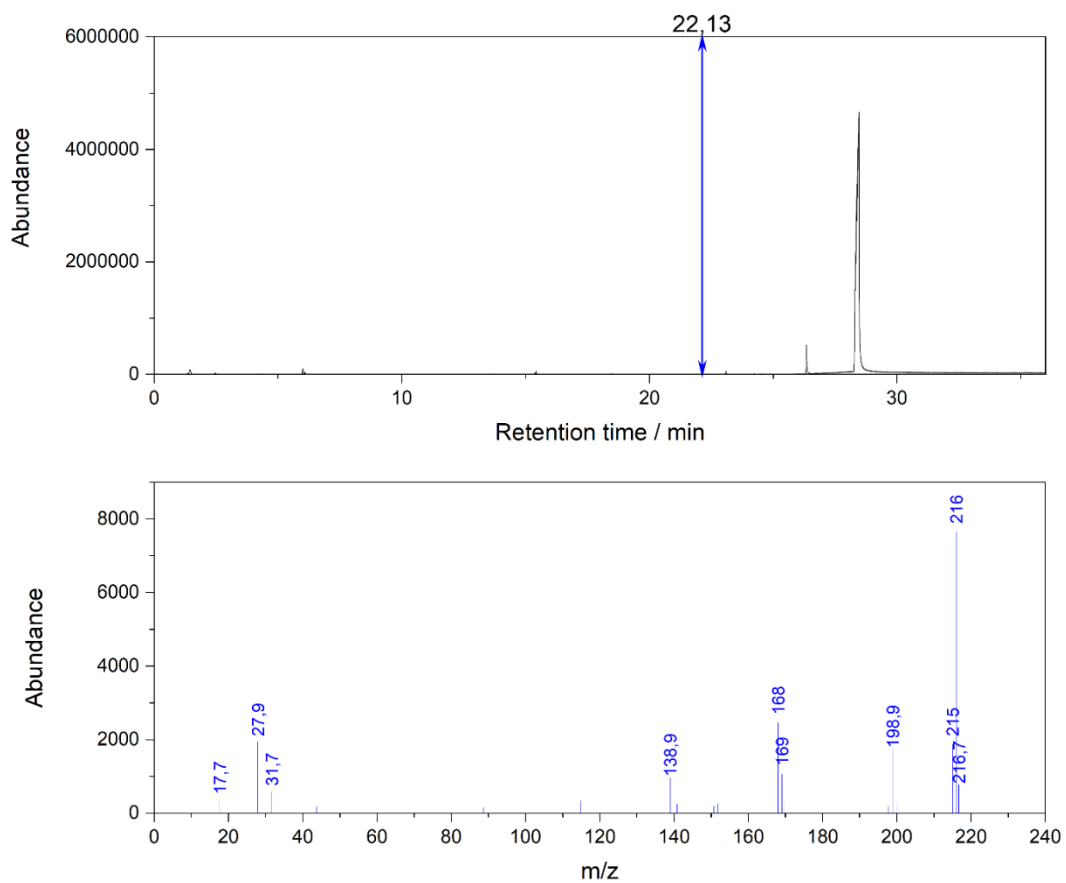


**Fig. S16:** DOB11 Py-GC/MS Peak 9 (DOPO)

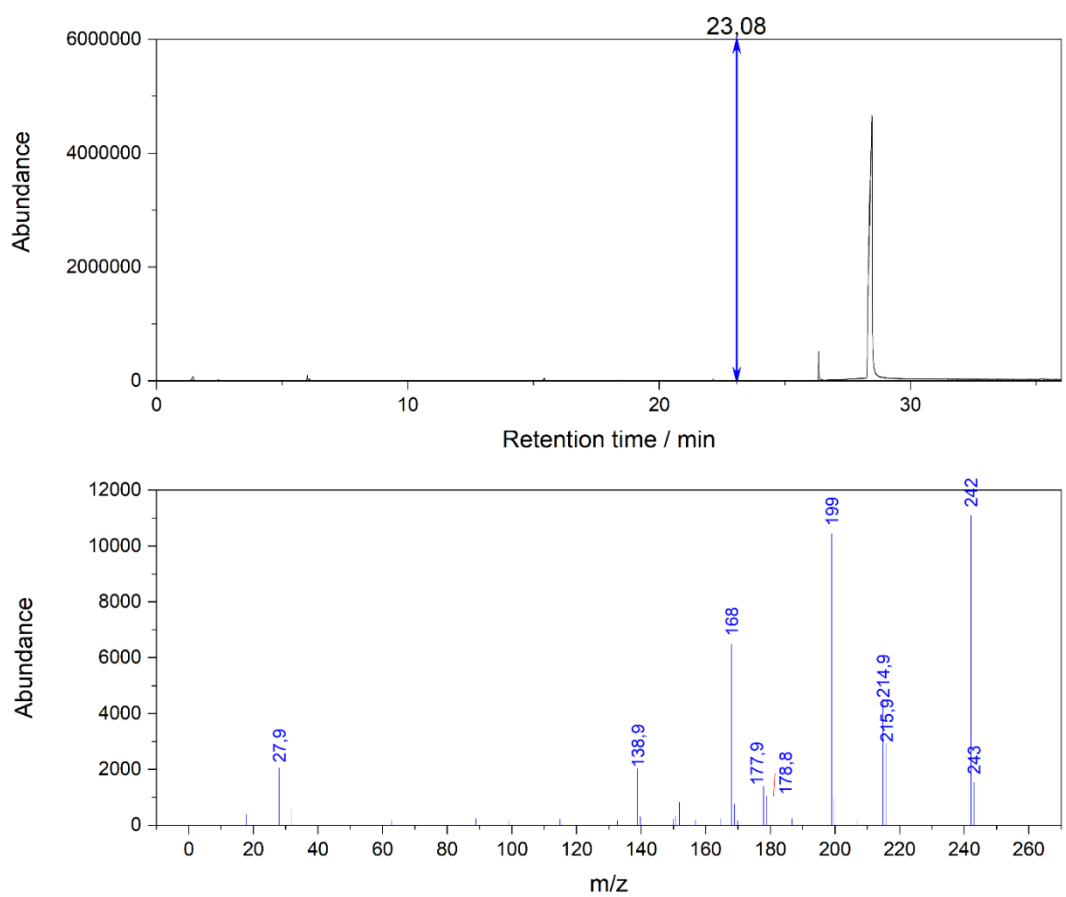


**Fig. S17:** DOB11 Py-GC/MS Peak 10 (DOPO-vinyl)

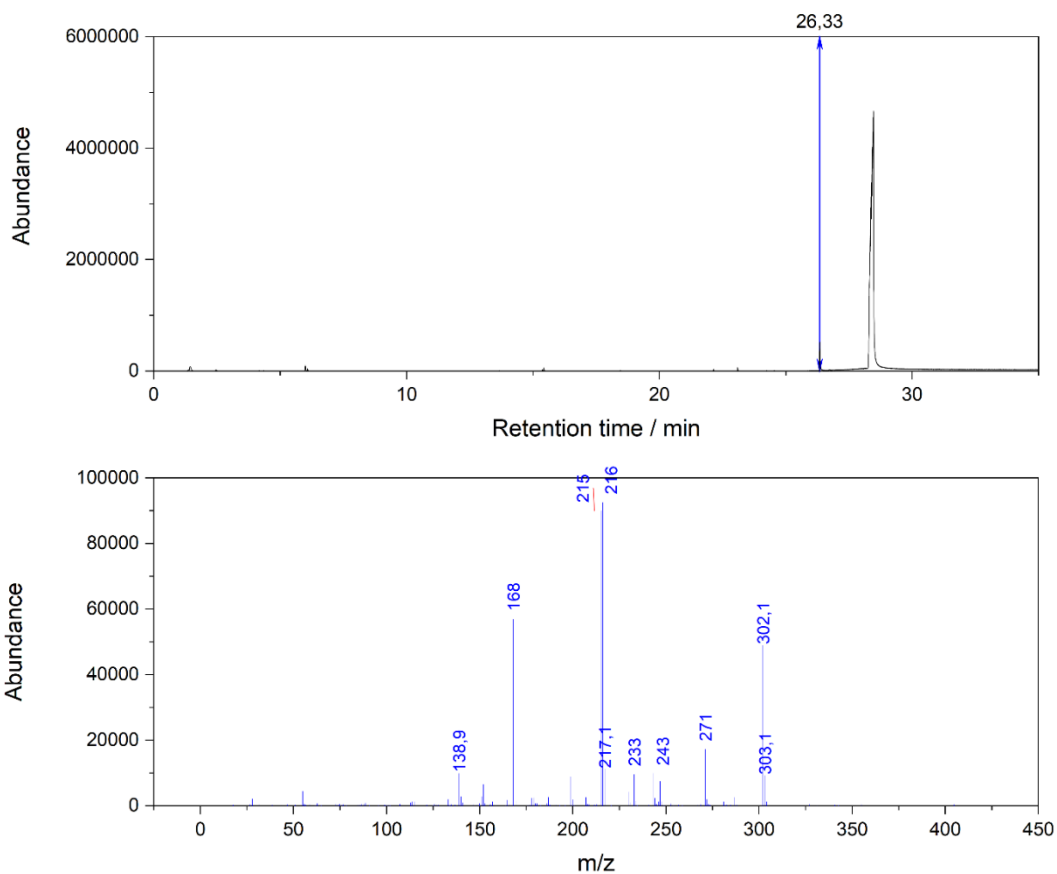


**Fig. S18:** DOB11 Py-GC/MS Peak 11 (DOPO-methyl propanoate)

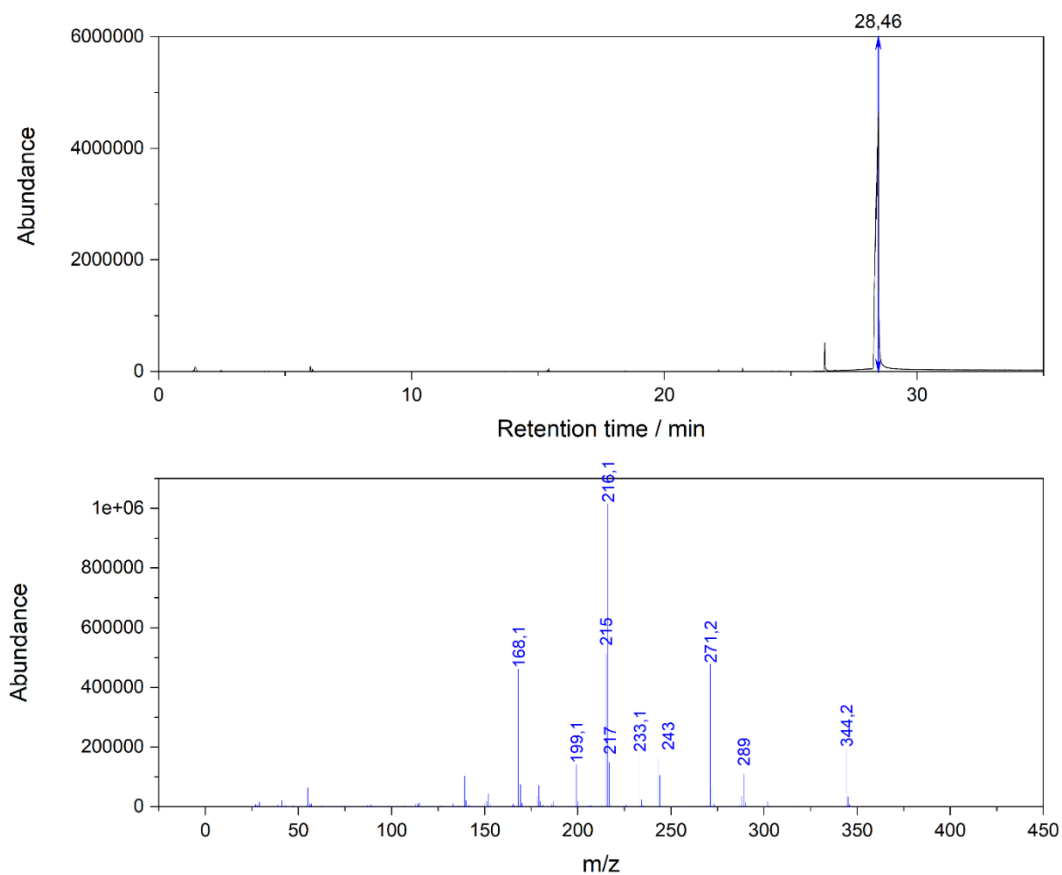


**Fig. S19** Mass spectrum of the second main product peak of the Py-GC/MS spectrum of DOB11 (DOB 11 molecule).



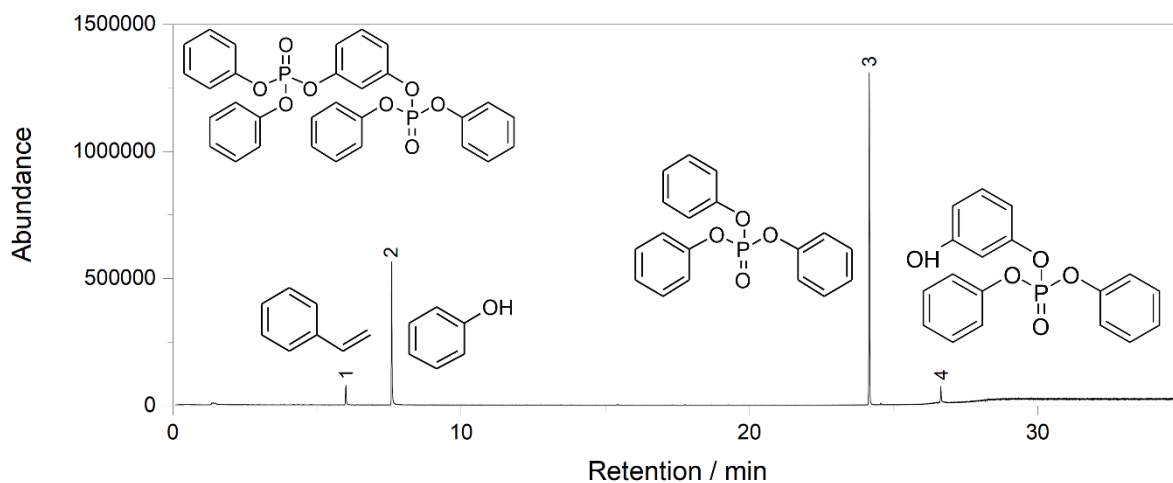


**Fig. S20:** Py-GC/MS spectrum of RDP

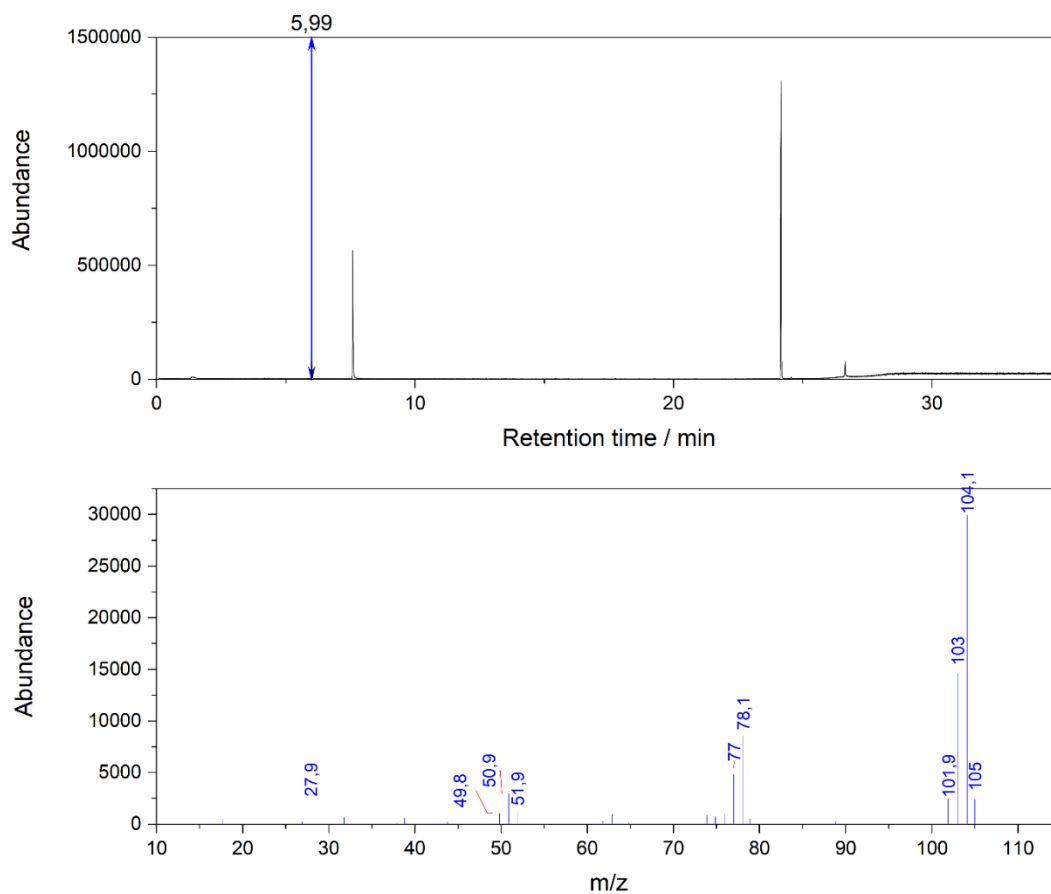


**Fig. S21** Mass spectrum of the first main product peak of the Py-GC/MS spectrum of RDP (styrene).

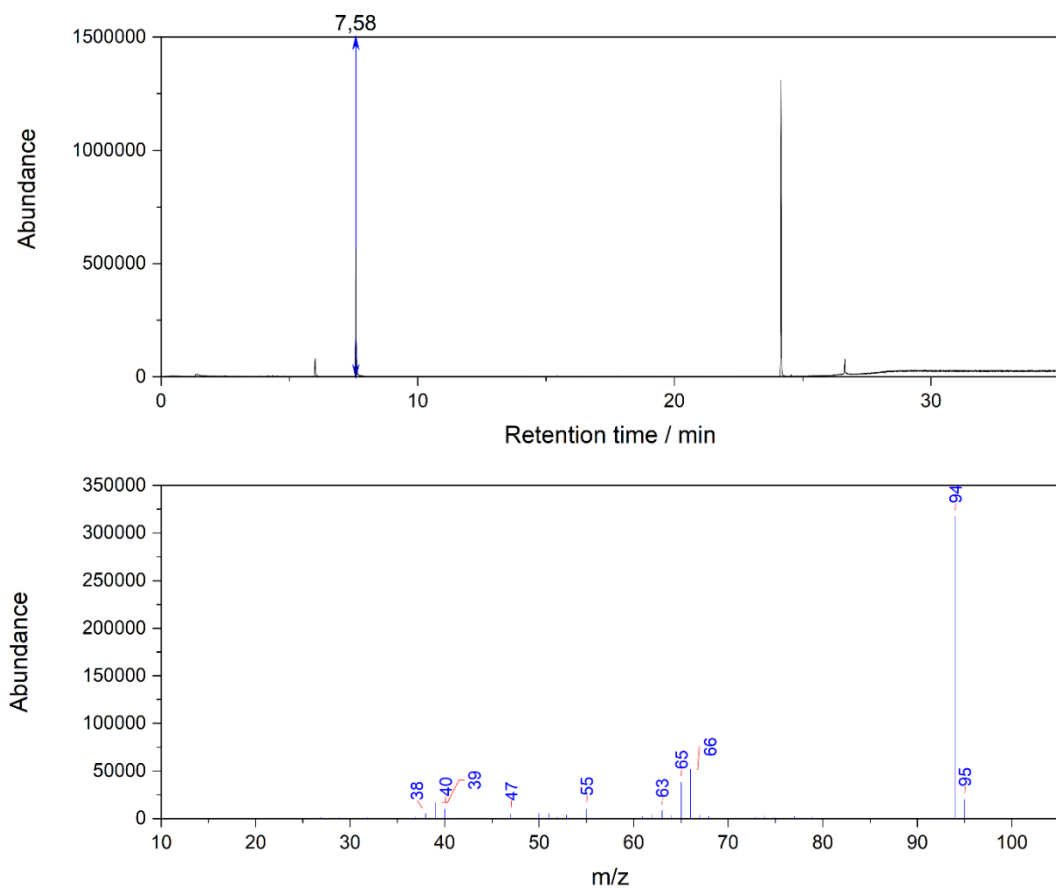


**Fig. S22** Mass spectrum of the second main product peak of the Py-GC/MS spectrum of RDP (phenol).

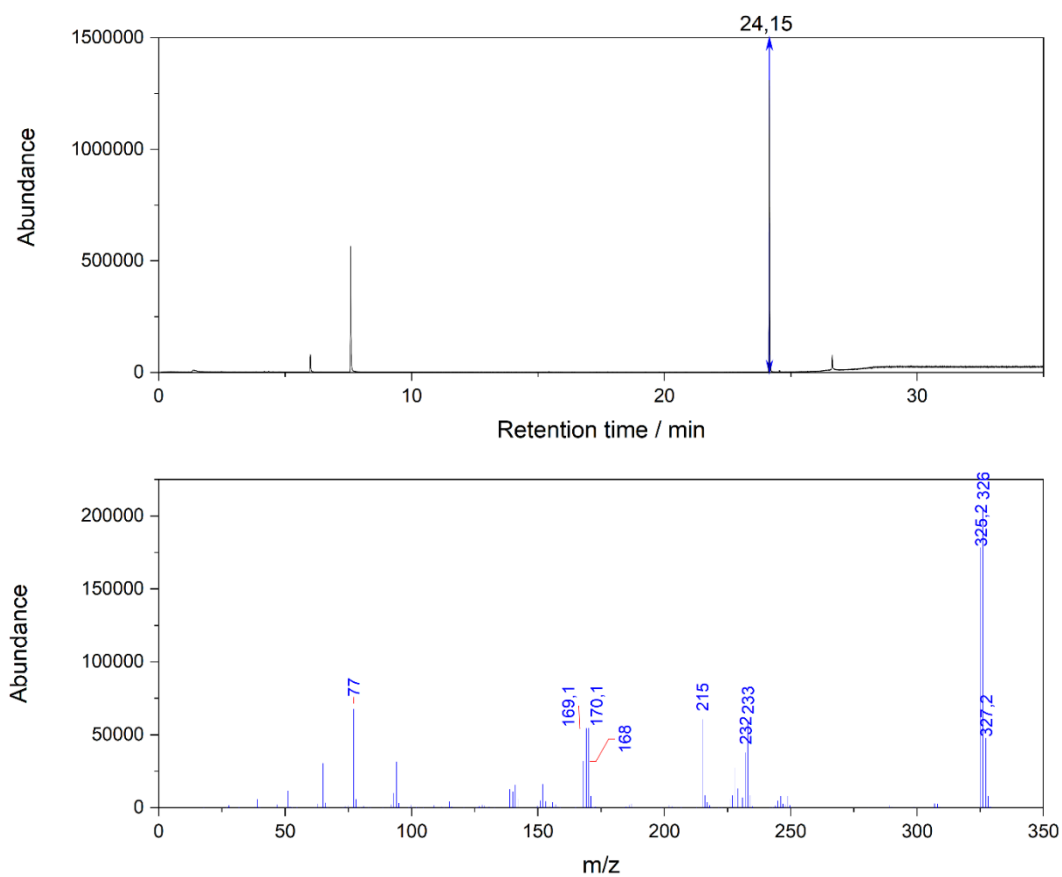


**Fig. S23** Mass spectrum of the third main product peak of the Py-GC/MS spectrum of RDP (TPP).

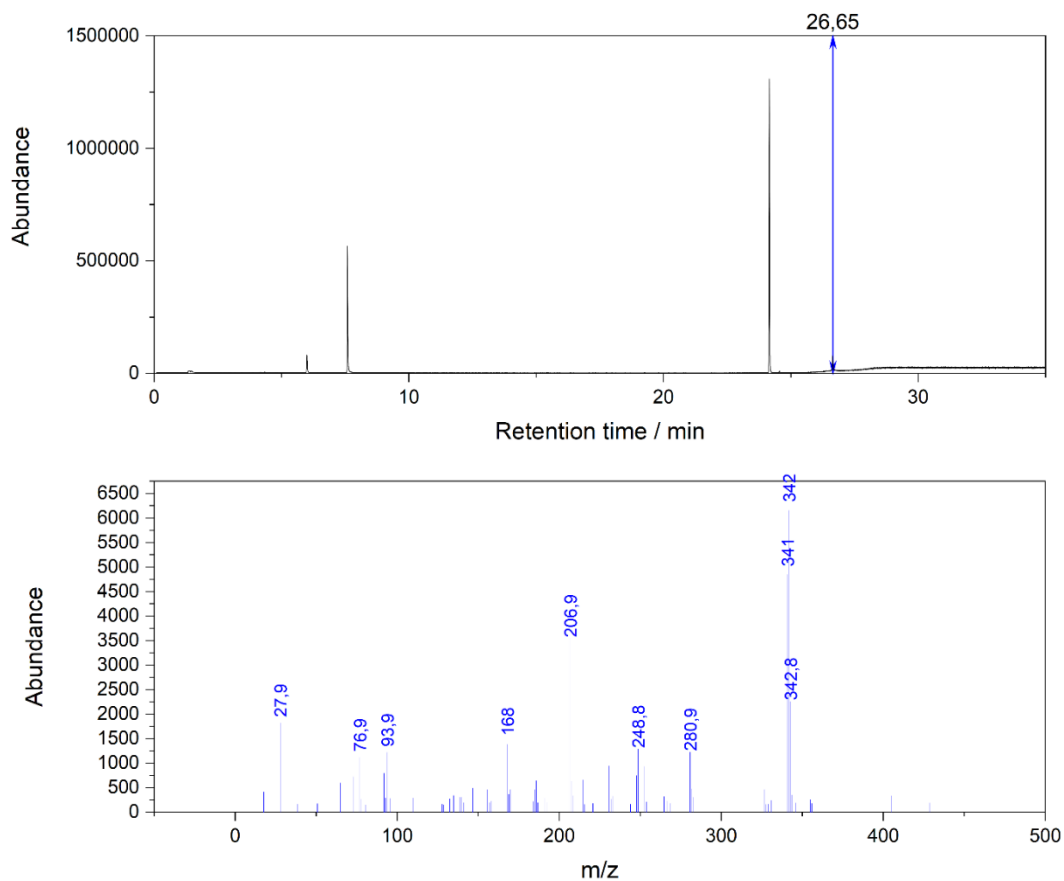


**Fig. S24** Peak 4 of the Py-GC/MS spectrum of RDP (diphenyl resorcinol phosphate)

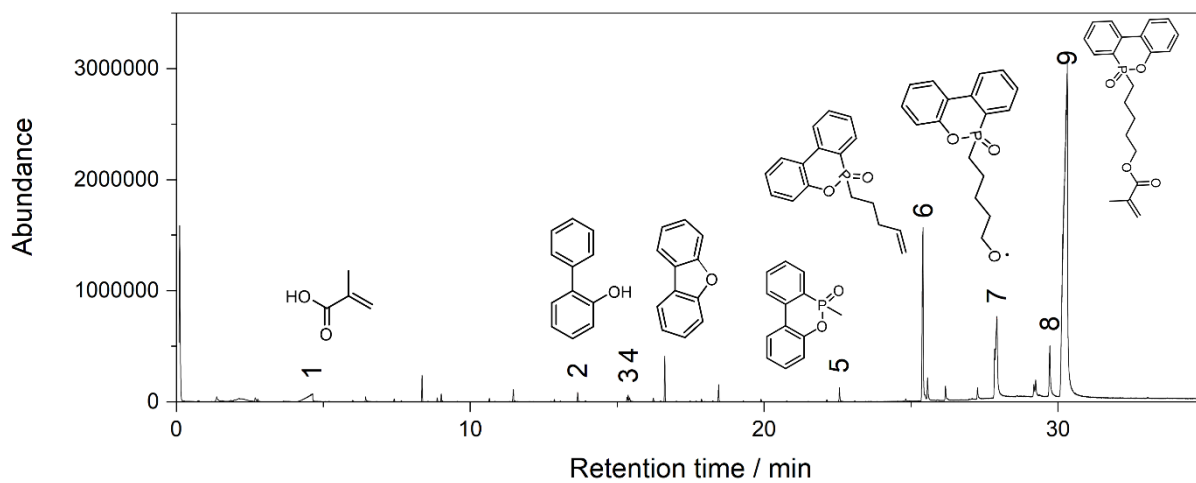


**Fig. S25** Py-GC/MS of DOPO-pentyl-methacrylate

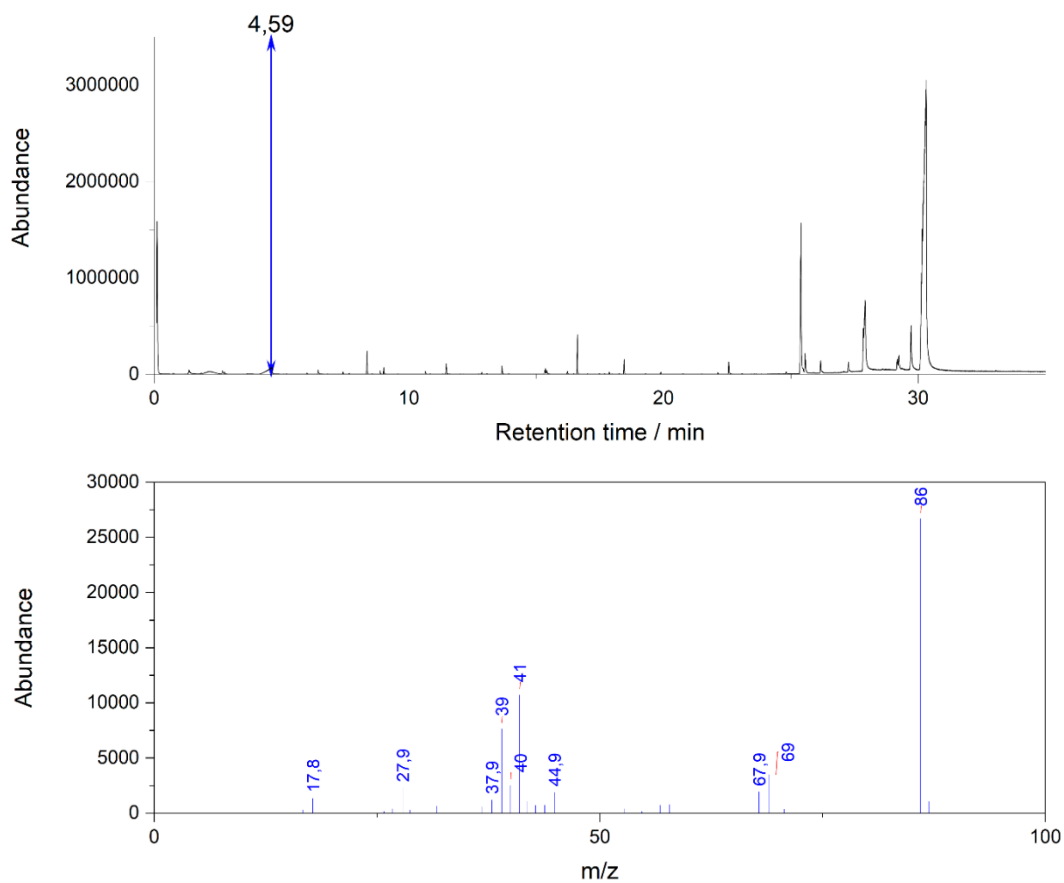


**Fig. S26** Mass spectrum of Peak 1 of DOPO-pentyl-methacrylate (methacrylic acid)

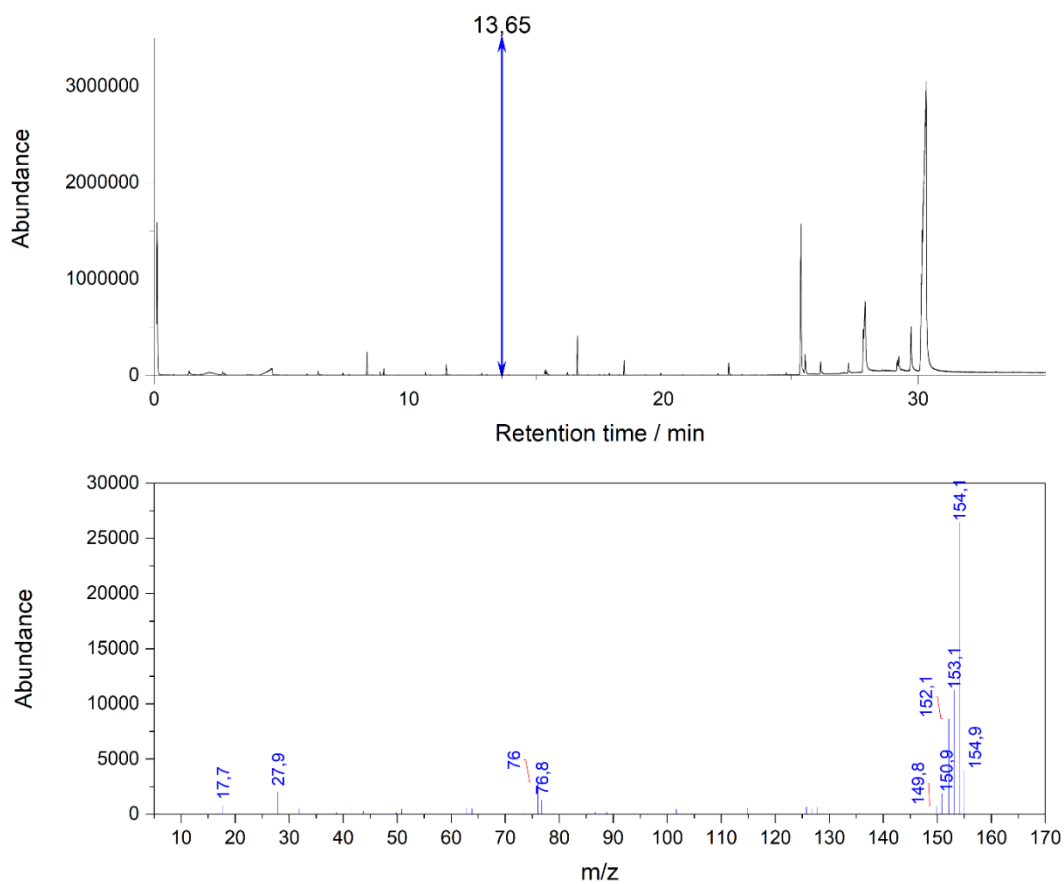


**Fig. S27** Mass spectrum of peak 2 of DOPO-pentyl-methacrylate (biphenyl)

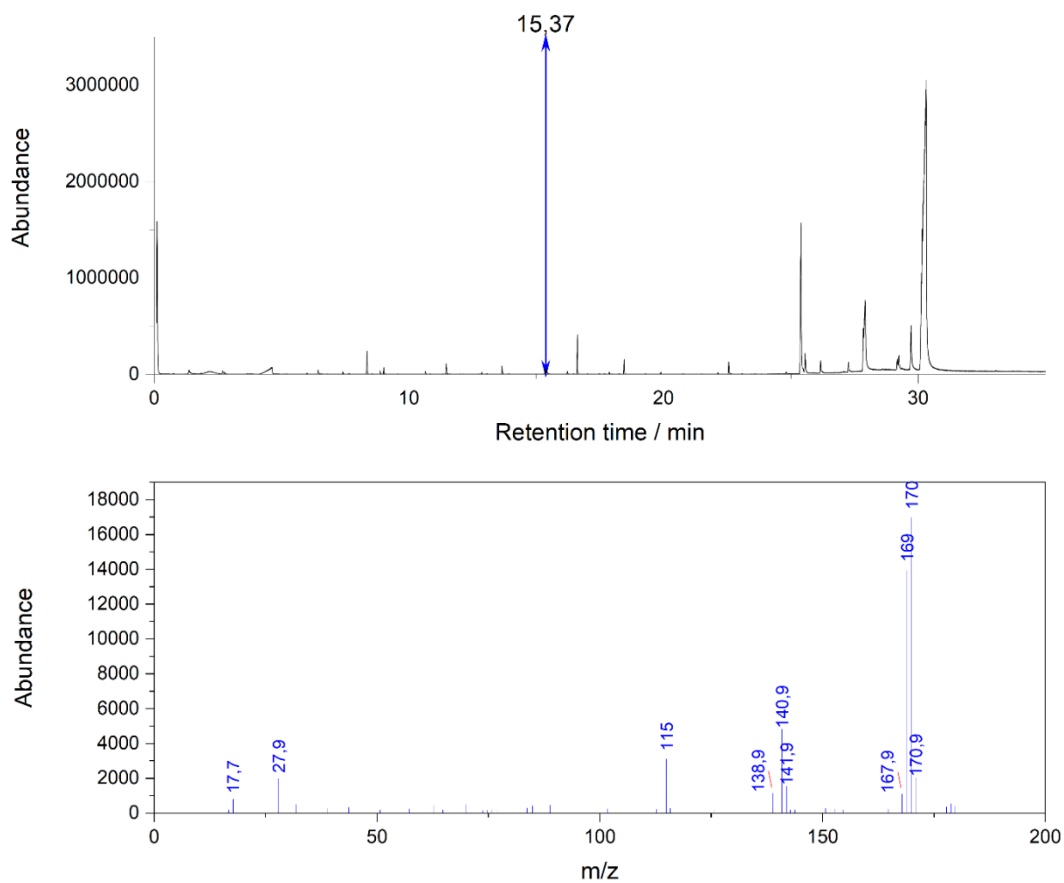


**Fig. S28** Mass spectrum of Peak 3 of DOPO-pentyl-methacrylate (o-hydroxybiphenyl)

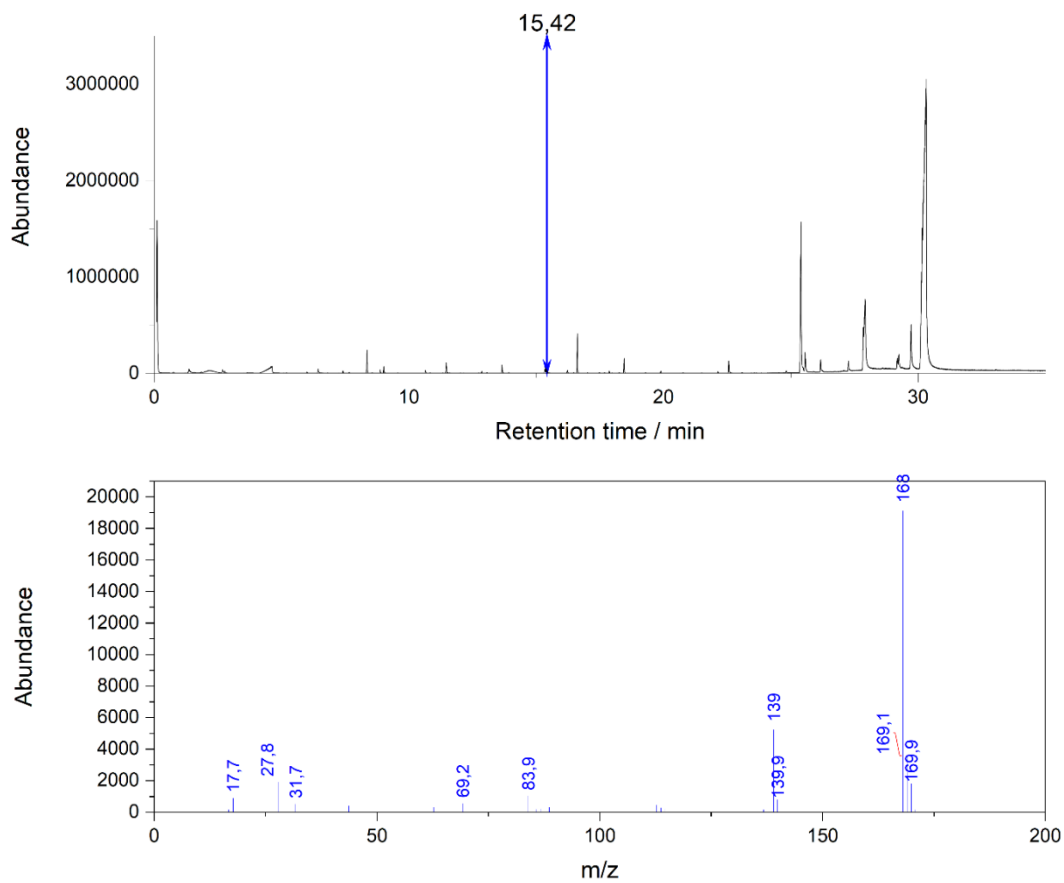


**Fig. S29** Mass spectrum of peak 4 of DOPO-pentyl-methacrylate (dibenzofuran)

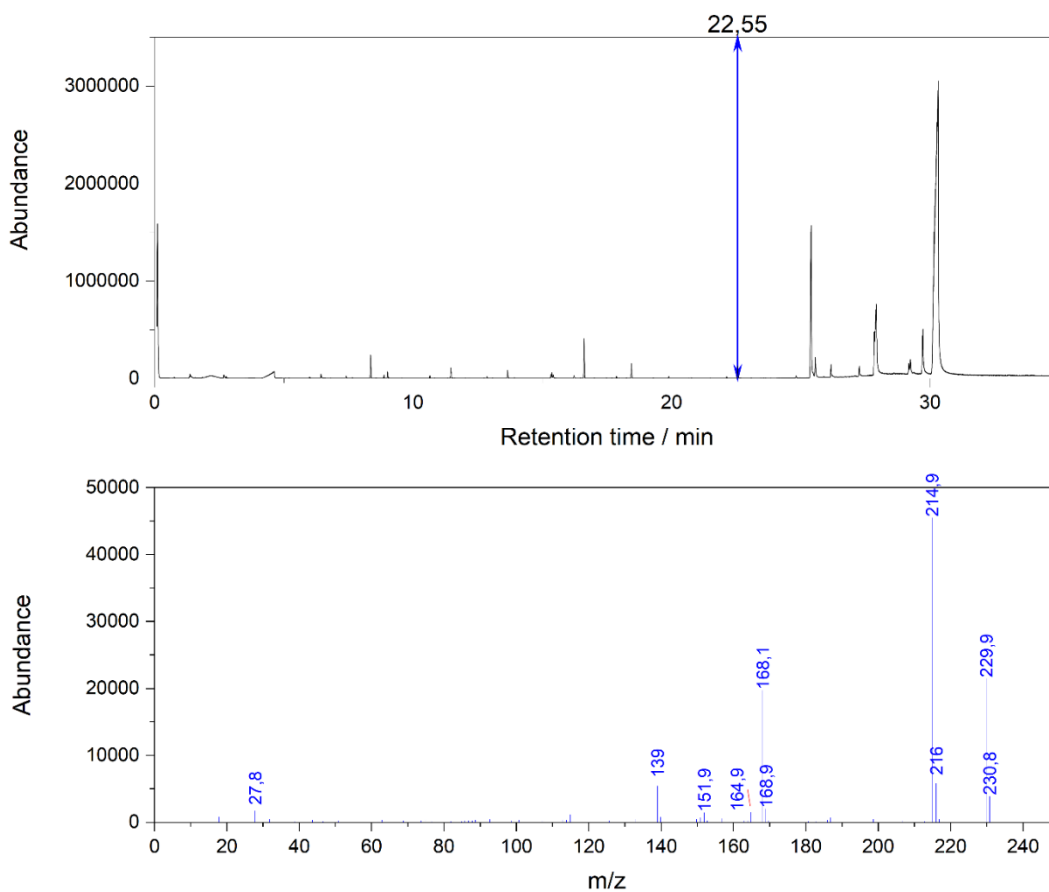


**Fig. S30** Mass spectrum of peak 5 of DOPO-pentyl-methacrylate (DOPO-methyl)

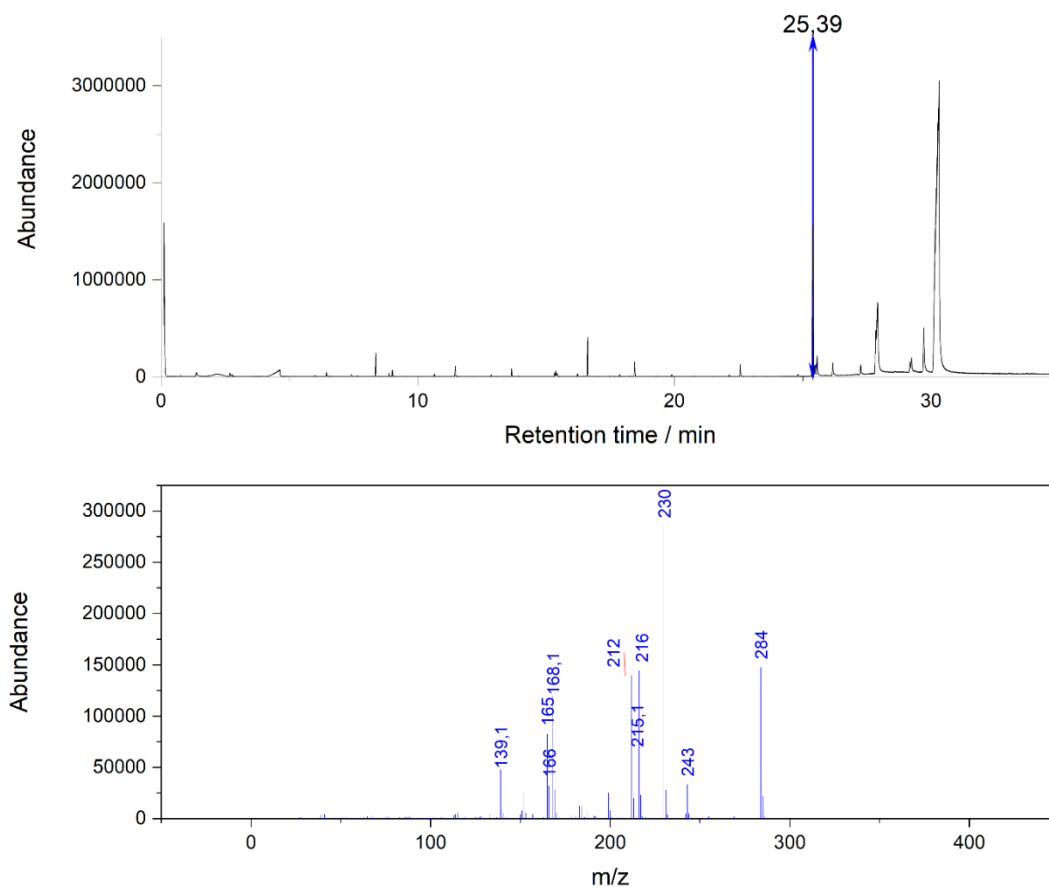


**Fig. S31** Mass spectrum of peak 6 of DOPO-pentyl-methacrylate (DOPO-pentyl)

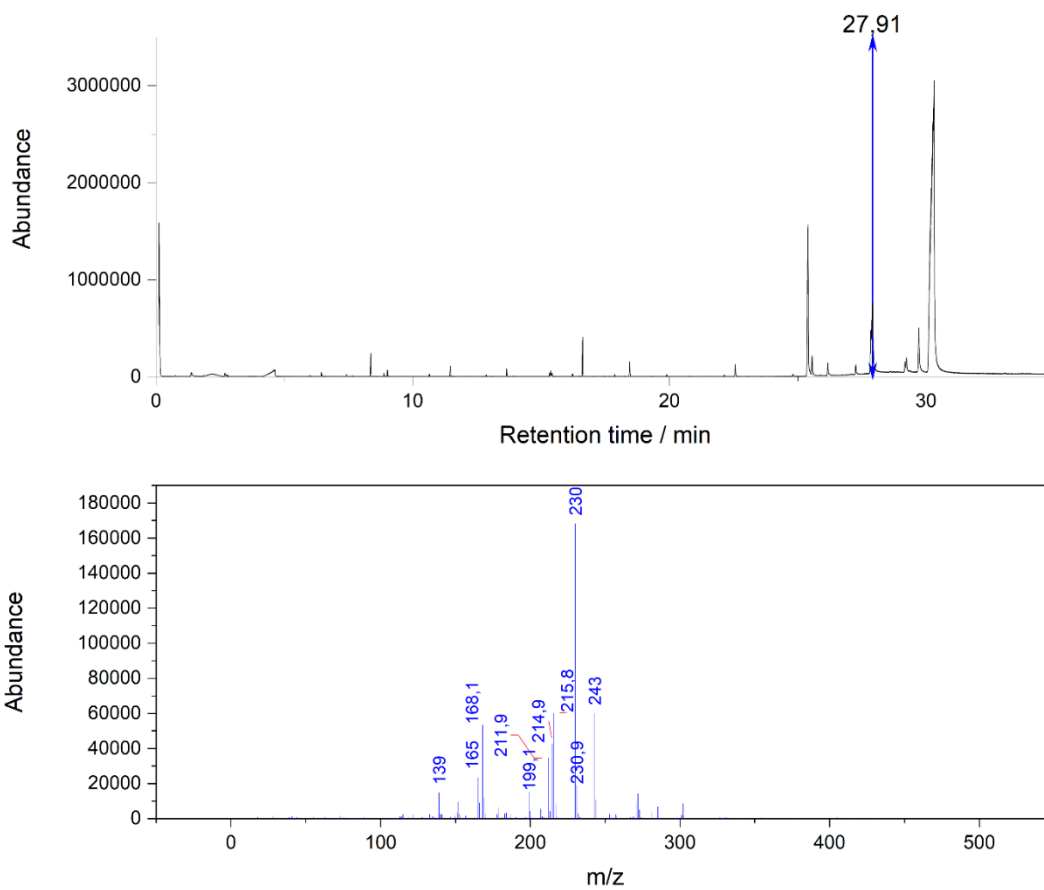


**Fig. S32** Mass spectrum of Peak 7 of DOPO-pentyl-methacrylate (DOPO-pentanol)

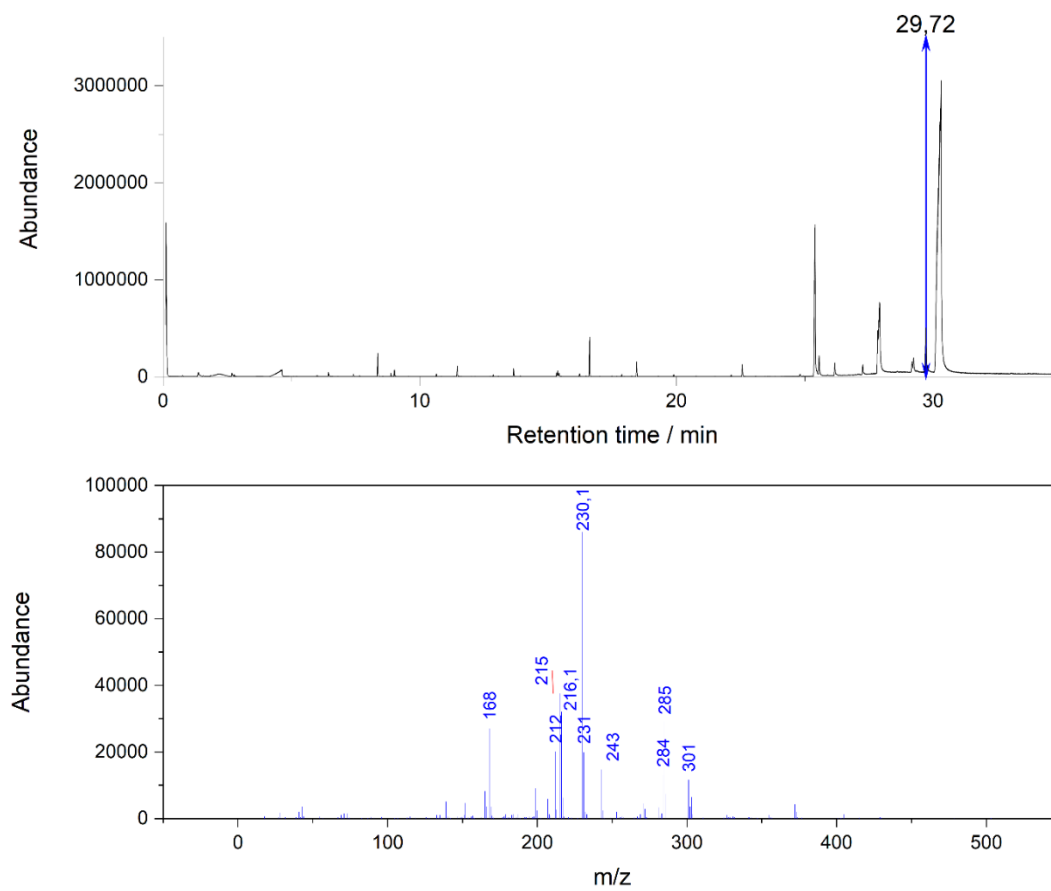


**Fig. S33** Mass spectrum of peak 8 of DOPO-pentyl-methacrylate (DOPO-pentyl-(2-methylpropanoate))

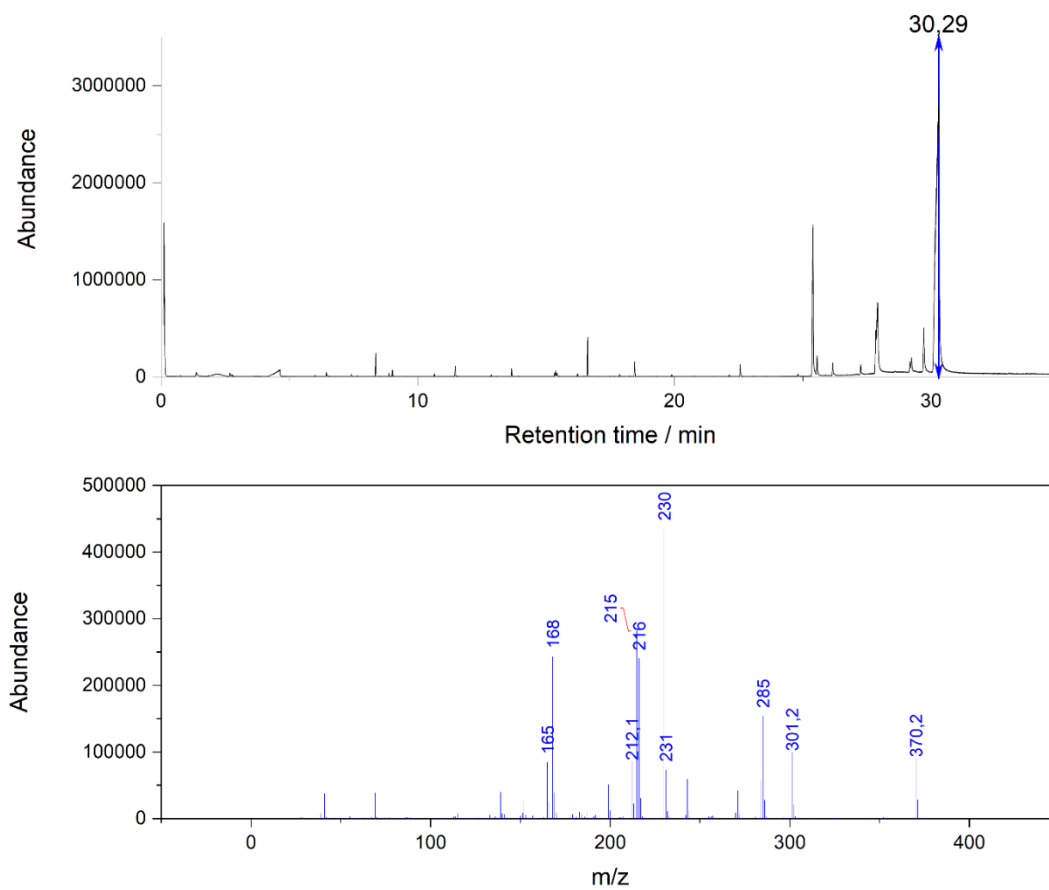


**Fig. S34** Mass spectrum of Peak 9 of DOPO-pentyl-methacrylate (DOPO-pentyl-methacrylate, educt)



### **5.3. Flame Retarded Adhesive Tapes and Their Influence on the Fire Behavior of Bonded Parts**

Vitus Hupp, Bernhard Schartel, Kerstin Flothmeier, Andreas Hartwig

Fire Technology, **2024**

<https://doi.org/10.1007/s10694-024-01637-2>

Published under a Creative Commons license:

<https://creativecommons.org/licenses/by/4.0/>

This article is accepted and published (no issue yet)

Author contribution:


- Conceptual work for paper and experiments
- Sample preparation
- Fire testing
  - Flammability tests
  - Cone Calorimeter tests
  - Development of the Fire resistance test
  - Fire resistance tests
- Data evaluation
- Figure ideas and design throughout the article
- Scientific discussion and writing the article
- Correction, spell-checking all versions

## **Abstract**

Pressure-sensitive adhesive tapes are used in automobiles, railway vehicles and construction, where flame retardancy is of major importance. This is why industrial applicants often buy, and industrial tape manufacturers often produce, flame-retardant adhesive tapes, advertised for their good flammability characteristics. Yet, how flame retardant tapes influence the fire behavior of bonded materials is a rather open question. To investigate this issue, three different substrates were bonded, using eight double-sided adhesive tapes containing two different carriers and two different flame retardants. The bonded substrates were compared to their monolithic counterparts in terms of flammability, fire behavior and fire stability. The fire behavior of adhesive tape-bonded materials differed significantly from the monolithic substrates. The usage of different adhesive tapes led to different burning behavior of the bonded materials mainly due to different carrier systems. In contrast, the implementation of flame retardant into the adhesive had rather minor or no effect on the burning behavior of the bonded substrates despite their positive effect on the flammability of the free-standing tape. The carrier changed the HRR curve in the cone calorimeter and was able to both, reduce and increase fire hazards. Using the carrier with the better fire performance can lower the fire growth rate by 20%, the peak of heat release rate by 27%, and the maximum average rate of heat emission by 30% in cone calorimeter tests. Overall, the fire behavior of bonded materials is a complex interaction between substrate, adhesive, and carrier, and depends on the fire scenario the materials are exposed to.



# Flame Retarded Adhesive Tapes and Their Influence on the Fire Behavior of Bonded Parts

*Vitus Hupp and Bernhard Schartel \*, Bundesanstalt für Materialforschung und -prüfung (BAM), Unter den Eichen 87, 12205 Berlin, Germany*  
*Kerstin Flothmeier, Fraunhofer Institute for Manufacturing Technology and Advanced Materials, Wiener Straße 12, 28359 Bremen, Germany*  
*Andreas Hartwig, Fraunhofer Institute for Manufacturing Technology and Advanced Materials, Wiener Straße 12, 28359 Bremen, Germany and Department 2 Biology/Chemistry, University of Bremen, Leobener Straße 3, 28359 Bremen, Germany*

**Received:** 17 January 2024/**Accepted:** 16 August 2024

**Abstract.** Pressure-sensitive adhesive tapes are used in automotives, railway vehicles and construction, where flame retardancy is of major importance. This is why industrial applicants often buy, and industrial tape manufacturers often produce, flame-retardant adhesive tapes, advertised for their good flammability characteristics. Yet, how flame-retardant tapes influence the fire behavior of bonded materials is a rather open question. To investigate this issue, three different substrates were bonded, using eight double-sided adhesive tapes containing two different carriers and two different flame retardants. The bonded substrates were compared to their monolithic counterparts in terms of flammability, fire behavior and fire stability. The fire behavior of adhesive tape bonded materials differed significantly from the monolithic substrates. The usage of different adhesive tapes led to different burning behavior of the bonded materials mainly due to different carrier systems. In contrast, the implementation of flame retardant into the adhesive had rather minor or no effect on the burning behavior of the bonded substrates despite their positive effect on the flammability of the free-standing tape. The carrier changed the HRR curve in the cone calorimeter and was able to both, reduce and increase fire hazards. Using the carrier with the better fire performance can lower the fire growth rate by 20%, the peak of heat release rate by 27%, and the maximum average rate of heat emission by 30% in cone calorimeter tests. Overall, the fire behavior of bonded materials is a complex interaction between substrate, adhesive, and carrier, and depends on the fire scenario the materials are exposed to.

**Keywords:** Pressure-sensitive adhesive tapes, Bonded materials, Fire behaviour, Fire resistance, Flame retardant, Cone calorimeter

---

\*Correspondence should be addressed to: Bernhard Schartel, E-mail: [bernhard.schartel@bam.de](mailto:bernhard.schartel@bam.de)



## 1. Introduction

The use of adhesive joints increased strongly in automobiles, railway vehicles and construction over recent decades due to advances in lightweight technology, and electric mobility and the use of bonded materials such as cross laminated timber in buildings. In these applications, the fire behavior of the bonds and adhesives is of major importance and needs to be understood and optimized to prevent danger to life and property. It is well known that blends and combinations of materials such as laminate structures have a fire behavior different from the sum of their single components [1–4]. This leads to the assumption that bonds, as a combination of several materials including substrate, adhesive and optional interlayers, also behave differently from the individual materials that they consist of. In the literature, many articles on flame-retardant adhesives [5–8] have already shown that adhesives and incorporated flame retardants can change the fire behavior of bonded materials with a high adhesive content such as plywood [9], wood particle boards [10] or flame-retardant expanded polystyrene [11]. In the glued material cross-laminated timber as well, adhesive bonds change the fire behavior drastically [12]. For laminates like structural insulated panels, adhesives between the layers can change the fire behavior, while flame retardants in the adhesives can improve the flame retardancy of the bonded material [13]. A special case of adhesives are pressure-sensitive adhesives (PSA) and PSA tapes. They are widely used in several applications due to their easy application and durability. Due to their low glass transition temperature ( $T_g$ ), they are permanently sticky and adhere to a vast spectrum of surfaces. PSA consist mainly of rubber-like polymers that are intrinsically flammable with the exception of silicone-based PSA. The popular use of intrinsically flammable PSA suggests the enhancement of the fire behavior by flame retardants would be beneficial. Flame retardants can improve the burning behavior of PSA tapes [14] but there is a lack of knowledge of how these tapes act in their application in bonds. Especially in industrial applications, flame-retarded adhesive tapes are sold and advertised with UL 94 ratings, and other flame-retardant properties of the tapes are tested as free-standing material that is not bonded to any substrate. The approach to protecting an adhesive tape resembles the method of protecting thin foils to improve their UL 94 rating (V-2 or V-0) even though the end application is an entirely different one. The question of whether using flame retardants in adhesive tapes improves the burning behavior of bonded materials has not yet been answered and is of great interest to adhesive tape manufacturers and customers. In this research paper, the burning behavior of different PSA tapes and PSA-bonded materials is investigated, namely wood, polymethyl methacrylate (PMMA) and bisphenol-A polycarbonate (PC). Substrates with a wide spectrum of burning characteristics (charring or melting behavior) were chosen to examine the specific interactions between substrate and adhesive. Wood represents non-melting, charring materials; PMMA represents melting, non-charring materials, and PC represents melting, charring materials. As flame retardants, a dihydro-9-oxa-10-phosphaphenanthrene-10-oxide (DOPO)-derivate and resorcinol bis (diphenyl phosphate) (RDP) were used to protect the poly(*n*-butyl acrylate) polymer matrix of the PSA. DOPO(-derivates) [15–18] and RDP [19–22] are

known for their good flame retardancy effects in the gas and condensed phases. Since recent research [23] has proven that flame retardants and carriers behave differently depending on the material combination and matrix, poly(ethylene terephthalate) (PET) and aluminum foil are used as carriers in different substrate configurations. The PSA tape bonded materials were investigated during ignition, developing fire and in a fully developed fire scenario.

## **2. Materials**

**Chemicals:** 6H-dibenz[c,e][1,2]oxaphosphorin-6-propanoic acid, butyl ester, 6-oxide (DOB 11) was provided by Metadynea (Krems, Austria) and resorcinol bis(diphenyl phosphate) (RDP) by ICL Industrial Products (Tel Aviv, Israel). Disponil FES 32 and Disponil A1080 were provided by BASF (Ludwigshafen, Germany). Sodium peroxodisulphate, *n*-dodecyl mercaptan, acrylic acid and *n*-butyl acrylate were purchased from Merck (Taufkirchen, Germany).

**Carriers:** PET foil was provided by TESA (Hamburg, Germany) and aluminum (AL) foil in a thickness of 30  $\mu\text{m}$  was purchased from VWR International GmbH (Darmstadt, Germany).

**Substrates:** Beech wood was purchased as planks from Kula Holz-GmbH & Co. KG, (Berlin, Germany). Extruded colorless PMMA (Plexiglas® XT) from Evonik Industries AG (Germany) and PC from Covestro AG (Germany) (Makrolon® GP) were purchased from Thyssenkrupp Plastics GmbH (Germany) in the dimensions 1000  $\times$  2000  $\times$  2 mm<sup>3</sup>.

## **3. Methods**

### ***3.1. Preparation of Adhesive Tapes and Bonded Specimen***

**Pressure-sensitive adhesives:** The PSA was prepared by emulsion polymerization. To prepare a homogenous PSA dispersion it is necessary to prepare a pre-emulsion and an initiator solution.

**Polymerization procedure:** For the pre-emulsion, water (57 g), Disponil FES 32 (4.77 g), Disponil A1080 (0.94 g) and acrylic acid (0.72 g) were placed in a 500 ml beaker and stirred magnetically. Afterward, *n*-butyl acrylate (149.25 g), the flame retardant, and *n*-dodecyl mercaptan (0.15 g) were added and stirred continuously. To prepare the initiator solution, sodium peroxodisulphate (0.48 g) was dissolved in water (12.3 g) in a 50 ml beaker. Polymerization took place in a 500 ml reaction vessel in which water (82 g) and Disponil FES 32 (0.67 g) were placed and heated to 85 °C while stirring under argon atmosphere. In one shot 0.8 g initiator was added, and 4.5 g pre-emulsion were added after 15 min. Subsequently, the rest of the initiator solution was added to the pre-emulsion and this mixture was added dropwise to the reaction vessel over a period of one hour. The reaction was stirred for an additional 2 h at 85 °C. Finally, the dispersion was filtered through a 50  $\mu\text{m}$  sieve. For better processability, the pH of all dispersions was adjusted to

pH 8 by adding 25% ammonia solution. To achieve a good rheology for coating, Rheovis AS 1125 (1 wt.%) was added.

**Coating:** All double-sided PSA tapes were prepared in the following way. The dispersions were coated onto the PET or AL foil with a Zehnter automatic film applicator ZAA 2300 at a speed of 25 mm/s. The wet film thickness was adjusted to 110  $\mu\text{m}$ . After 5 min drying in air at ambient conditions, the films were heated for 10 min in an oven at 110  $^{\circ}\text{C}$ . The back was coated in the same way after applying a release paper on the already coated side. Eight different double-sided adhesive tapes were prepared to obtain products with different flame retardants and carriers (Table 1).

**Adhesive bonding:** To prepare bonded samples, the release liner of the adhesive tapes was removed, and the PSA tapes were placed onto one side of the substrates. Air bubbles were removed by a rubber hand-pressure roll. Subsequently, the second release liner was removed, and the other substrate was adhered to the tape. Again, the rubber roll was applied at the surface of the bonded material to remove potentially incorporated air bubbles. These sandwich-like laminates were prepared in different dimensions according to the demands of the following fire behavior investigations. The adhesive properties are not relevant and therefore not mentioned.

### 3.2. Flammability Tests

**UL 94:** The UL 94 test was performed according to the current UL 94 standard. The test was performed in an UL 94 Test chamber from Fire Testing Technology (UK).

To rate the flammability of the tapes that are not bonded to any object, the tapes were measured as a multilayer specimen to avoid shrinkage and distortion. Eight layers of the PSA tapes were stacked to obtain specimens 125 mm  $\times$  13 mm  $\times$  1 mm in size. Each adhesive tape layer was 120  $\mu\text{m}$  thick.

The bonded materials (substrate/tape/substrate) were measured in the dimensions of 125 mm  $\times$  13 mm  $\times$  4.1 mm. The bonds were manufactured as a sandwich-like connection between Substrate and adhesive tape (substrate

**Table 1**  
**Specimen Names and Descriptions of the Adhesive Tapes**

| Name                | Description  |
|---------------------|--|
| Butac_50_REF_PET    | Poly ( <i>n</i> -butyl acrylate) (PSA) coated on PET           |
| Butac_DOB11_0.5_PET | PSA with DOB 11 and a phosphorus content of 0.5% coated on PET |
| Butac_DOB11_1.5_PET | PSA with DOB 11 and a phosphorus content of 1.5% coated on PET |
| Butac_RDP_0.5_PET   | PSA with RDP and a phosphorus content of 0.5% coated on PET    |
| Butac_50_REF_AL     | Poly ( <i>n</i> -butyl acrylate) (PSA) coated on AL            |
| Butac_DOB11_0.5_AL  | PSA with DOB 11 and a phosphorus content of 0.5% coated on AL  |
| Butac_DOB11_1.5_AL  | PSA with DOB 11 and a phosphorus content of 1.5% coated on AL  |
| Butac_RDP_0.5_AL    | PSA with RDP and a phosphorus content of 0.5% coated on AL     |

plate/tape/substrate plate) where both, substrate plates, consisted of the same material.

**Oxygen index:** The oxygen index was measured according to ISO 4589–2. The oxygen index of the PET carrier tapes was measured from samples that were prepared by folding the adhesive tape, resulting in a 70 mm × 7 mm × 1.5 mm specimen. A 100 mm × 80 mm piece of tape was cut from a DIN A4 sheet of double-sided tape and subsequently folded to the demanded size. The AL tapes were measured in the frame holder that is described in EN 4589–2 and normally used for thin foils or plastics that do not distort while burning. The bonded materials (substrate/tape/sample) were measured in the dimensions of 100 mm × 10 mm × 4 mm.

### ***3.3. Burning Behavior***

**Cone Calorimeter:** The Cone Calorimeter tests were performed in a cone calorimeter from Fire Testing Technology (UK) according to ISO 5660. The distance between the cone heater coil and sample surface was adjusted to 35 mm to leave more space for the sample to expand while still ensuring a homogenous heat flux of 50 kW m<sup>-2</sup> over the entire irradiated area (less than 10% deviation) [24]. PC, for example, is known for its expansion in cone calorimeter tests [25], making it advisable to increase the distance over the standard 25 mm. A heat flux of 50 kW m<sup>-2</sup> was chosen to simulate a developing fire, while simultaneously considering the heat flux required by EN 45545–2 for application in railway vehicles. The bonded wood samples were measured in an aluminum tray with four wires preventing the bending of the specimen. All samples were measured in an aluminum tray using the standard stainless steel specimen holder without the retainer frame.

### ***3.4. Fire Stability***

The fire stability was measured in a small-scale test which was developed to determine the stability of the adhesive bond against a flame, simulating a fully developed fire. Thus the necessity of the time-consuming, expensive, large-scale tests that are normally performed [26] to measure the fire stability was eliminated [27]. This test is designed to generate a ranking of the effects of different flame retardants on the fire stability of the adhesive joint. Therefore, two substrates of the same material were bonded together by the tapes and a weight of 3 kg was mounted to the lower half of the substrate as shown in Fig. 1. The substrate thickness was 4 mm for wood and 1 mm for zinc plated steel. The two substrates were chosen due to their different behavior during fire exposure. Steel as an incombustible material is expected to stay unharmed during the test whereas wood is suspected to be ignited and deform during the test. Thus, for steel, only the thermal stability of the adhesive joint is relevant for the failure. For wood in contrast, the interaction between deforming, decomposing wood and the adhesive gap plays a role. The loaded sample was fixed in a clamp in a stand and exposed to a defined burner flame. The heat flux and temperature of the flame was calibrated for a certain distance between burner and the specimen surface and was kept the same for all

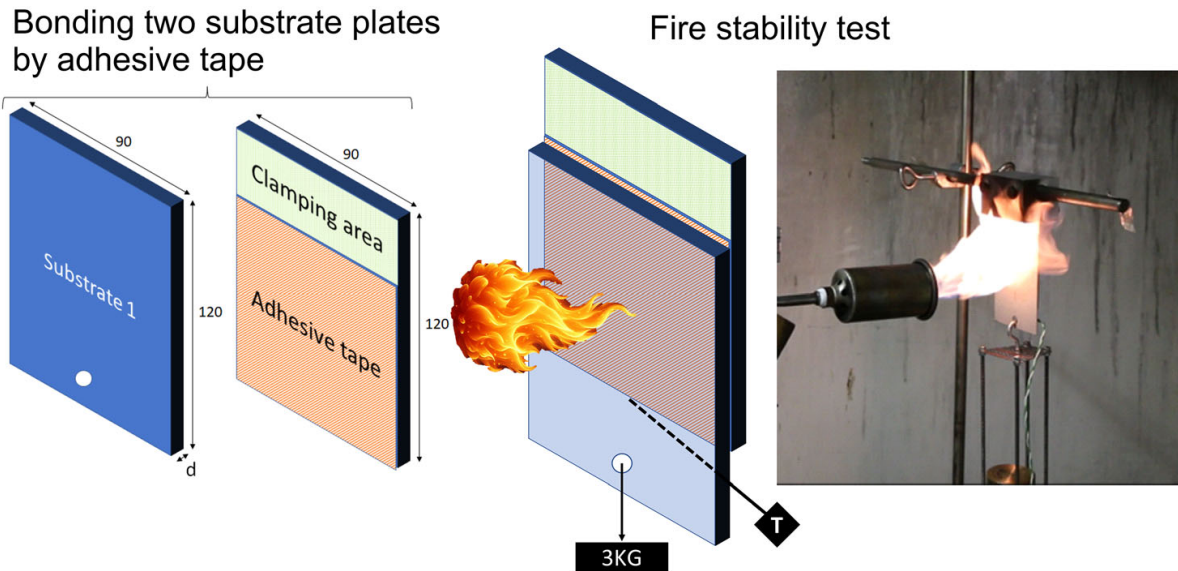


**Figure 1. Fire stability test for adhesive bonds in a full developed fire scenario; T = Thermocouple; d = thickness of the substrate (4 mm for wood, 1 mm for zinc plated steel).**

measurements. The calibration was performed with a heat flux meter which was installed in the recess of a calcium silicate plate with a direct exposure to the burner flame. An irradiance of  $75 \text{ kW m}^{-2}$ , as a full developed fire heat flux [28], was chosen as the irradiance level at the specimen surface. The distance was fixed at 12.5 cm and the gas flow of the burner (propane) was kept constant at  $3 \text{ L min}^{-1}$ . The time to failure of the adhesive bond and the temperature of the back surface of the substrate plate that is exposed to the burner flame was measured to obtain information about how the single components of the adhesive tape and the substrates influence the adhesive's stability in a fully developed fire. The back temperature of the first layer represents the temperature impact that the adhesive is exposed to.

## 4. Results and Discussion

### 4.1. Flammability Tests

*4.1.1. Adhesive Tapes With Different Carrier Systems* Table 2 shows the flammability test results that were obtained in the vertical UL 94 and OI. In UL 94, the DOB 11 flame retardant had the greatest effect, and the tapes containing DOB 11 were rated V-2, extinguished by dripping and igniting the cotton wool. Dripping is an effective mechanism to achieve a V-2 rating in the UL 94 test due to the loss of material from the pyrolyzing zone and thus a pronounced cooling effect [29, 30]. All tapes that failed to achieve a UL 94 V rating burned until the flame reached the clamp. The OI was improved slightly by every flame retardant compared to the non-protected PSA. As for the carriers, AL led to a rapid burning of the outer adhesive layer on the non-combustible metal carrier. Thus, dripping was prevented, and none of the AL tapes achieved a UL 94 vertical rating.



4.1.2. *Adhesive Tape Bonded Materials* Table 3 shows the flammability test results of the bonded substrates and the monolithic (consisting of one homogenous material) materials in comparison. In the UL 94 test, the adhesive tapes had no negative impact on the burning process of the specimens. All investigated samples achieved the same rating and behaved like the monolithic substrate. In UL 94, the ignition scenario is from the bottom of the specimen, climbing fast up the sides of the sample. Thus, the inner adhesive tape layer plays a negligible role in this testing method.

The OI results show that the tapes had different impacts on the flammability of the substrates. In wood, all tapes with different flame retardants had no impact beyond the standard deviation, except for the RDP flame-retarded tape. It increased the OI by about 1.5 vol % compared to the other tapes. This increase by the flame retardant active in the condensed phase is explained by improved

**Table 2**  
**Results for the Free-Standing Adhesive Tapes in Flammability Tests**

| Sample              | UL 94 | OI [vol %] ± 0.2 |
|---------------------|-------|------------------|
| Butac_PET           | N.R   | 17.6             |
| Butac_DOB11_0.5_PET | V-2   | 18.5             |
| Butac_DOB11_1.5_PET | V-2   | 19.7             |
| Butac_RDP_0.5_PET   | N.R   | 19.7             |
| Butac_50_REF_AL     | N.R   | 23.3             |
| Butac_DOB11_0.5_AL  | N.R   | 24.1             |
| Butac_DOB11_1.5_AL  | N.R   | 24.2             |
| Butac_RDP_0.5_AL    | N.R   | 23.9             |

*N.R.* No vertical rating

**Table 3**  
**UL 94 Vertical Test Results of the Adhesive Tape Bonded Substrates as Compared to the Monolithic Material**

| Sample name         | Wood       |                     | PMMA       |                     | PC         |                     |
|---------------------|------------|---------------------|------------|---------------------|------------|---------------------|
|                     | UL 94<br>V | OI (vol<br>%) ± 0.3 | UL 94<br>V | OI (vol<br>%) ± 0.3 | UL 94<br>V | OI (vol<br>%) ± 0.3 |
| Monolithic          | N.R        | 27.7                | N.R        | 17.7                | V-2        | 27.1                |
| Butac_PET           | N.R        | 27.5                | N.R        | 19.5                | V-2        | 27.3                |
| Butac_DOB11_0.5_PET | N.R        | 27.5                | N.R        | 18.9                | V-2        | 26.3                |
| Butac_DOB11_1.5_PET | N.R        | 27.6                | N.R        | 18.8                | V-2        | 26.9                |
| Butac_RDP_0.5_PET   | N.R        | 29.3                | N.R        | 20.0                | V-2        | 27.2                |
| Butac_50_REF_AL     | N.R        | 27.7                | N.R        | 18.6                | V-2        | 28.7                |
| Butac_DOB11_0.5_AL  | N.R        | 28.3                | N.R        | 18.8                | V-2        | 28.5                |
| Butac_DOB11_1.5_AL  | N.R        | 28.3                | N.R        | 18.4                | V-2        | 28.9                |
| Butac_RDP_0.5_AL    | N.R        | 27.3                | N.R        | 18.3                | V-2        | 28.1                |

charring, which is relevant in the OI. The high OI values are typically for untreated bonded beech wood [31] and other wood species (pine) [32] due to their charring properties. In PMMA, there is a trend toward an increased OI for the bonded materials. Comparing the OI of the tape materials and the OI of PMMA, the OI of PET and aluminum (non-flammable) are higher than that of PMMA. This leads to a small increase. In PC, the flammability of the PET-taped samples resembled the flammability of the monolithic material. When the AL carrier tapes were used, a trend toward increased OI was observed.

## 4.2. Cone Calorimeter Measurements

### 1. Wood

Figure 2 shows the HRR curve of the different wood samples. Monolithic wood is compared with the tape bonded wood. The same adhesives are compared with different carriers (PET and aluminum). The burning behavior differs between these three samples. For monolithic wood, there are two local maxima of heat release rate, whereas for the bonded wood there are three local maxima at different positions. The local maxima can either be interpreted as a peak due to the following decrease in HRR. Here, the local maxima are described as PHRR. Monolithic wood has the typical shape of two PHRR described in the literature [33, 34] where the peak heights and forms depend on the wood species and material dimension. First, the surface heats up, ignites, and builds up the first PHRR. Then a char layer is built up, which causes a plateau with a HRR minimum (after ignition)

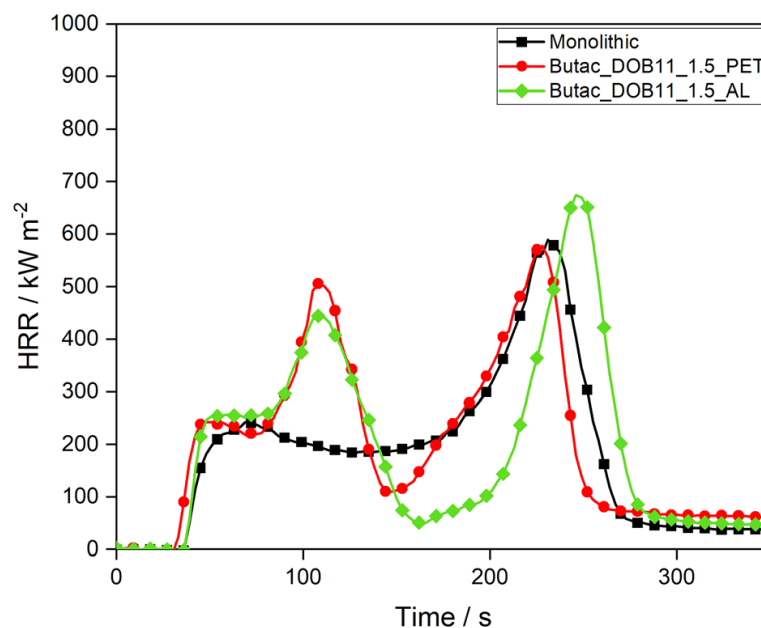


**Figure 2. Cone calorimeter HRR curve of monolithic wood compared with different adhesive tape bonded woods. Butac\_DOB11 coated on different carriers as a representative sample.**

due to its insulating effect [35]. After the char layer cracks, pyrolysis progresses and the wood beneath the char layer burns so that the second PHRR emerges. After the fire load is exhausted, the HRR drops to the afterglow level.

For the bonded wood, the first layer of wood ignited and subsequently the char layer built up (first peak/shoulder); then, after a small minimum at around 75 s, the char layer cracked and the second PHRR emerged. After the first layer of wood was burned, the HRR decreased, and the all-time minimum after ignition appeared. This minimum is caused by the char layer of the first wood layer, the insulation by the adhesive layer, and the char layer of the second wood layer, which prevent heat conduction within the substrate. Furthermore, the adhesive joint displayed a weak spot within the sample for mechanical impact. The wood samples deformed and shrank heterogeneously due to fiber orientation and natural inhomogeneities within the material. The first layer shrank and created small gaps between the first and second substrate layers, which act as an insulation layer in the cone calorimeter measurement. The HRR reached its all-time maximum after ignition at around 250 s as soon as the adhesive gap breached and the char layer of the second wood layer cracked. The typical shoulder or separation into two PHRR of the second layer was missing, which led to the assumption that the char layer of the second wood layer already built up during burning of the first layer.

The carriers, PET, and AL, differ in their ability to insulate the second wood layer from the impact of the flame. The aluminum, as a metal foil, blocked the irradiation and the pyrolysis for a longer time than the burnable PET carrier. The non-combustible AL foil protected the surface of the second wood layer over the entire time of the measurement whereas there was no protection for the second wood layer in the PET tape-bonded specimens after the PET tape was consumed. This result already agrees with the literature, which shows that AL interlayers delay the burning of the second layer of material [36]. This led to an earlier PHRR (third peak) of the PET-carrier bonded wood, which automatically led to a higher maximum average rate of heat emission (MARHE)<sub>3</sub>, as can be seen in Table 4. The subscript numbers describe the chronology of events in the burning process. The PHRR<sub>3</sub> of the aluminum carrier tapes were higher, but later than for the PET-carrier taped samples. The cone calorimeter measurements of the glued wood samples were similar to those of bonded multilayer arrangements such as plywood [37] or wood foam core sandwich panels [2] where the insulating effect of the adhesive layer(s) leads to a decrease in HRR and changes the curve compared to a monolithic material.

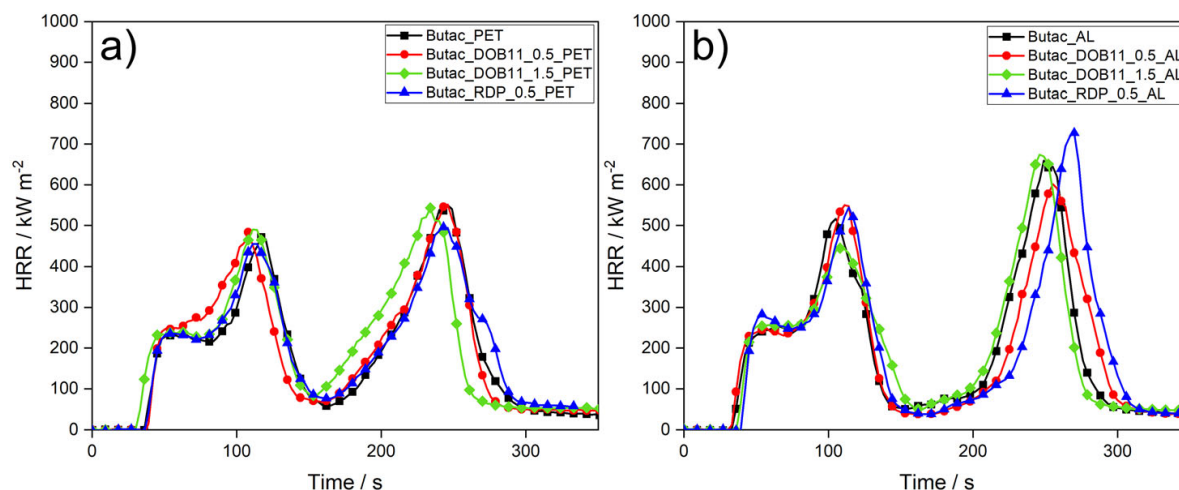
Figure 3a shows a comparison of all PET carrier tapes. The same tapes that differ in UL 94 rating and OI have the same burning behavior in cone calorimeter evaluations. Figure 3b shows the AL carrier tapes where no flame retardant had a significant impact on the burning behavior. All deviations are within the range of error.

Table 4 shows the characteristic values of the different wood samples in the cone calorimeter. The time to ignition ( $t_{ig}$ ) tended to lower ignition times for the bonded materials due to the reduced thermal thickness of the first layer compared to the monolithic material (the dimensions of the specimen are the same). For thermally thin materials, the ignition time reduces with the thickness of the material [28].

**Table 4**  
**Characteristic Values of the Cone Calorimeter Wood Measurement of Monolithic and Bonded Wood**

| Sample              | $t_{ig}$ (s) $\pm$ 3 | FIGRA<br>(kW m <sup>-2</sup> s <sup>-1</sup> ) $\pm$ 0.3 | PHRR<br>(kW m <sup>-2</sup> ) $\pm$ 50 | THE<br>(MJ m <sup>-2</sup> ) $\pm$ 2 | MARHE <sub>1</sub><br>(kW m <sup>-2</sup> ) $\pm$ 10 | MARHE <sub>2</sub><br>(kW m <sup>-2</sup> ) $\pm$ 10 | MARHE <sub>3</sub><br>(kW m <sup>-2</sup> ) $\pm$ 10 |
|---------------------|----------------------|--|--|--------------------------------------|--|--|--|
| Monolithic          | 37                   | 4.0  | 589                                    | 66                                   | 99   | 229  |  |
| Butac_PET           | 35                   | 4.9  | 493                                    | 70                                   | 106  | 206  | 237  |
| Butac_DOB11_0.5_PET | 35                   | 5.1  | 567                                    | 69                                   | 111  | 223  | 244  |
| Butac_DOB11_1.5_PET | 29                   | 5.2  | 560                                    | 70                                   | 119  | 221  | 252  |
| Butac_RDP_0.5_PET   | 37                   | 4.3  | 494                                    | 66                                   | 96   | 199  | 217  |
| Butac_50_REF_AL     | 34                   | 5.2  | 634                                    | 69                                   | 107  | 221  | 207  |
| Butac_DOB11_0.5_AL  | 30                   | 5.1  | 651                                    | 68                                   | 118  | 230  | 226  |
| Butac_DOB11_1.5_AL  | 35                   | 4.8  | 618                                    | 69                                   | 108  | 220  | 220  |
| Butac_RDP_0.5_AL    | 36                   | 5.1  | 637                                    | 70                                   | 106  | 218  | 218  |

$t_{ig}$  Time to ignition, FIGRA fire growth rate, THE total heat evolved



**Figure 3. Cone calorimeter HRR curves of wood, bonded with (a) all PET carrier tapes in comparison, (b) all AL carrier tapes in comparison.**

The PHRR for the monolithic wood is determined by the peak in the final, gradual decay phase. This peak was higher than in PET-taped samples. Aluminum samples, in contrast, had a more pronounced PHRR once the aluminum barrier was overcome. The all-time MARHE is determined by the last peak (peak 3) for most of the samples. Comparing bonded and monolithic material, the MARHE was similar for all samples, even though the determining HRR peaks were at different times and different heights. Comparing the THE, all samples released the same level of heat over the entire test period, which amounts to the same level of combustion at flameout. Discussing  $MARHE_1$ ,  $MARHE_2$ , and  $MARHE_3$ , Table 5 shows that the  $MARHE_1$ , which is determined by the first peak/shoulder of HRR, was higher for the bonded samples. The first layer of material tended to ignite earlier and had a steeper slope in HRR, which leads to an earlier peak and thus a higher  $MARHE$ .  $MARHE_3$  existed only for the bonded specimen and was similar for AL- and PET-bonded materials.  $MARHE_3$  is determined by the last peak for almost all the samples. Monolithic samples had a higher PHRR than the PET samples, but the peak appeared later, so that the  $MARHE_2$  was lower than the  $MARHE_3$  of the bonded samples. AL-bonded samples had the highest peak 3, but the AL insulation shifted it to a significantly later time so that the  $MARHE_3$  is reduced, and they had the lowest  $MARHE_3$ .

## 2. PMMA

Figure 4 shows the comparison between monolithic PMMA and the Butac\_DOB11\_1.5 taped samples with PET and AL carriers. The monolithic PMMA behaved as expected with the typical shape of the HRR curve described in the literature [38, 39]. The differences are due to the carriers interrupting the heat transfer by conduction and convection within the sample. After ignition, the HRR of the taped samples tended to rise more rapidly than the HRR of the monolithic

**Table 5**  
**Characteristic Values of the Cone Calorimeter Measurement of**  
**Monolithic and Bonded PMMA**

| Sample              | $t_{ig}$<br>(s) $\pm 2$ | FIGRA ( $\text{kW m}^{-2}$<br>$\text{s}^{-1}$ ) $\pm 0.2$ | PHRR ( $\text{kW m}^{-2}$ ) $\pm 90$ | MARHE ( $\text{kW m}^{-2}$ ) $\pm 20$ | THE ( $\text{MJ m}^{-2}$ ) $\pm 2$ |
|---------------------|-------------------------|---|--------------------------------------|---------------------------------------|------------------------------------|
| Monolithic          | 38                      | 8.1   | 1181                                 | 590                                   | 116                                |
| Butac_PET           | 39                      | 7.9   | 1150                                 | 594                                   | 119                                |
| Butac_DOB11_0.5_PET | 37                      | 7.6   | 1109                                 | 594                                   | 121                                |
| Butac_DOB11_1.5_PET | 42                      | 7.6   | 1140                                 | 577                                   | 120                                |
| Butac_RDP_0.5_PET   | 37                      | 8.4   | 1139                                 | 608                                   | 122                                |
| Butac_AL            | 39                      | 8.3   | 870                                  | 413                                   | 120                                |
| Butac_DOB11_0.5_AL  | 36                      | 9.0   | 846                                  | 430                                   | 118                                |
| Butac_DOB11_1.5_AL  | 38                      | 8.9   | 854                                  | 423                                   | 117                                |
| Butac_RDP_0.5_AL    | 37                      | 10.1  | 920                                  | 425                                   | 116                                |

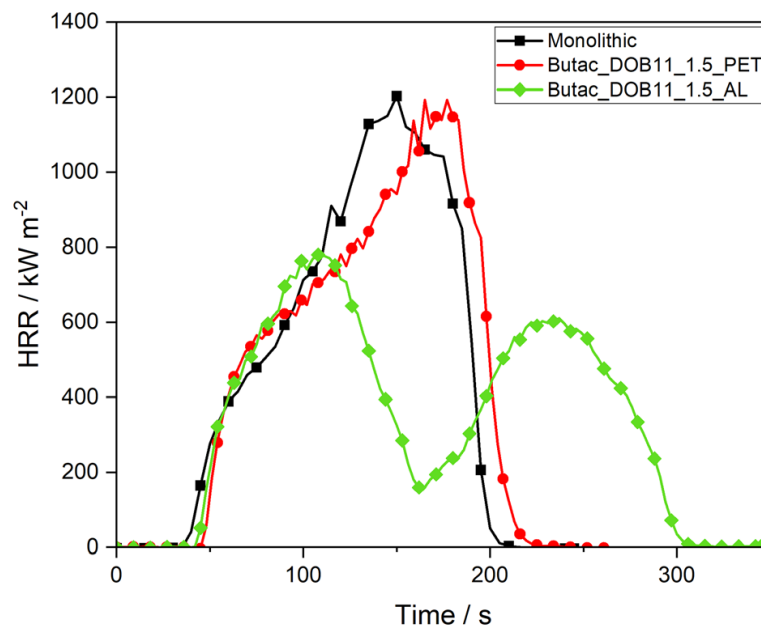


**Figure 4. Cone calorimeter HRR curve of monolithic PMMA compared with different adhesive tape bonded PMMA. Butac\_DOB11 coated on different carriers as a representative sample.**

PMMA. The interrupted heat conduction led to a reduced sample thickness and thus to a faster heating up of the first layer. After 100 s, the first layer of PMMA was consumed; in the PET-taped material, the adhesive gap was eliminated by melting the adhesive and the carrier. The PET tape, with its higher melting point, delayed the burning process, which led to a reduced slope of the HRR compared to the monolithic PMMA. Monolithic PMMA and the taped sample with PET carrier tape behaved very similarly after the first layer of PMMA and the PET tape were burned. The AL-carrier taped samples behaved quite differently: After the first layer of PMMA was consumed, Butac\_DOB11\_1.5\_AL showed a strong

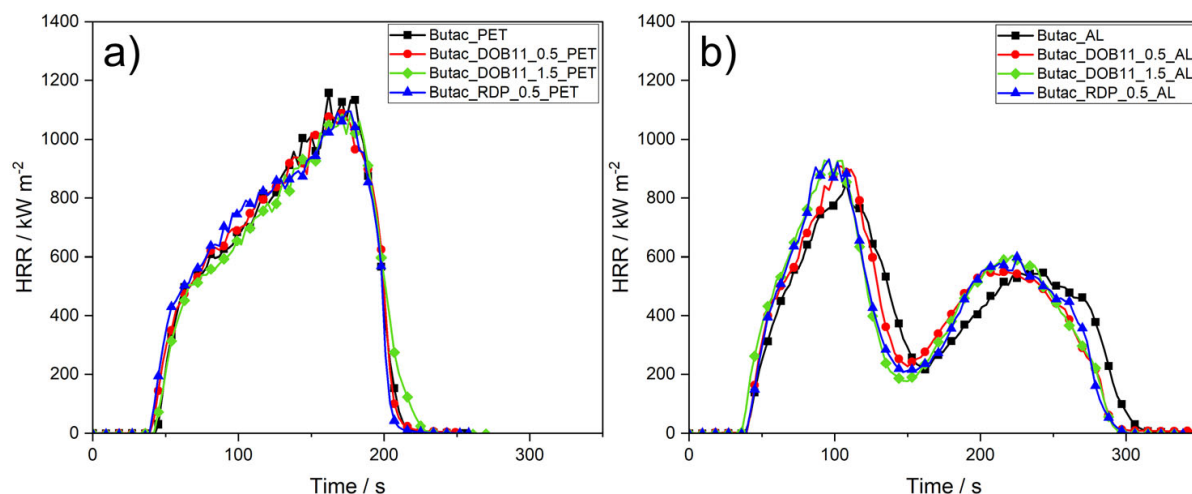


**Figure 5. Cone calorimeter HRR curves of PMMA, bonded with (a) all PET carrier tapes in comparison, (b) all AL carrier tapes in comparison.**

decrease in HRR, which was caused by the AL as a non-combustible material protecting the second layer from irradiation and preventing heat transfer by convection from the first layer. A HRR minimum was observed at 160 s. After this minimum was overcome, the second layer started to burn with a lower PHRR than the first layer due to the remaining incombustible AL layer.

Figure 5 shows the comparison between the different adhesives used to bond PMMA with a) PET carriers and b) AL carriers. As in wood, the amount of flame retardant and adhesive is too small to make a difference in burning behavior. All adhesives behave the same considering the uncertainties of the samples. The carriers, in contrast, have a remarkable effect on the burning behavior and completely transform the HRR curve. As shown in Table 5, PHRR, FIGRA and MARHE changed significantly, and the fire risk was clearly reduced when an aluminum carrier tape was used for the bond. The FIGRA was higher for the aluminum tapes due to the early peak of heat release rate. For the PET tapes and the monolithic PMMA, the PHRR took place at the end of the burning process. In the AL-taped samples, the PHRR shifted to the front and happened shortly after ignition. The PHRR of AL tapes was reduced by around 25% compared to the PET tapes, which can be explained by the heat conduction into the second sample layer by the AL tape. In the PET tape, the PHRR took place at the end of the burning process as the samples got thinner and thinner and heated up faster because no more heat was conducted away from the sample surface. The sample became thermally thinner, so that more material was volatilized at once and the PHRR was reached. In the AL sample, the first layer of PMMA was responsible for the PHRR, and the same effect happened as in the monolithic sample/PET samples. The first layer got thinner and heated up faster, creating the PHRR. The difference is that in this case, the heat was conducted into the remaining layer of PMMA, which prevented the first layer from heating up as fast and subsequently prevented it from forming the same PHRR as the monolithic sample. Due to the

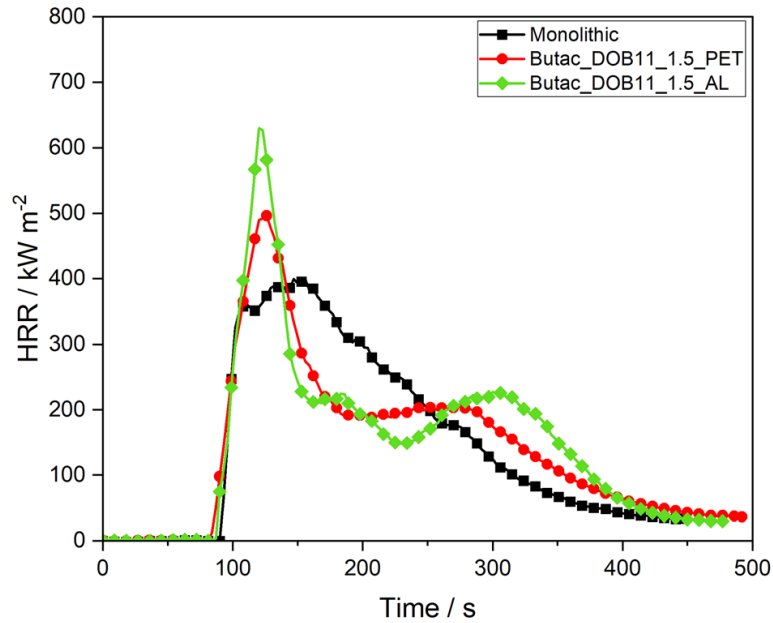


**Figure 6. Cone calorimeter HRR curve of monolithic PC compared with different adhesive tapes bonded PC. Butac\_DOB11 coated on different carriers as representative PSA.**

shift of the PHRR, also the MARHE is smaller. In all samples, the complete PMMA is consumed and only the AL layer remains which leads to the same THE values.

### 3. PC

Figure 6 shows the comparison between monolithic PC and the taped samples. There are significant discrepancies between the HRR curves and characteristic values. After ignition at the same time, the HRR rises to its peak as it is common for PC and other charring plastics. The PHRR differs between the monolithic, PET-carrier taped, and the AL-carrier taped samples. The increase of the PHRR is due to the reduced layer thickness and the stronger separation: In monolithic PC, there is just one block of polymer that can melt and burn, and no disturbance of heat conductivity and char formation takes place. The typical HRR with a high heat release rate after ignition the PHRR shortly afterwards and the subsequent decrease in HRR with a strong afterglow is typical for PC [40–42]. In the bonded materials, the first layer of polymer can deform and create gaps that hinder the heat transfer into the underlying layer. This leads to a faster heating of the first layer and thus a higher PHRR. The influence of PET and AL tapes is significant. The separating effect of aluminum is even stronger pronounced and leads to an even higher PHRR. After the PHRR, all samples build up a char layer that is typical for PC. The char layer differs from taped to monolithic samples. The first layer is rapidly consumed, forming a char layer which afterwards protects the second layer as a barrier. The whole second layer tends to burn with a plateau-like HRR curve shape for PET. For AL-carrier tapes, a tendency toward a valley of



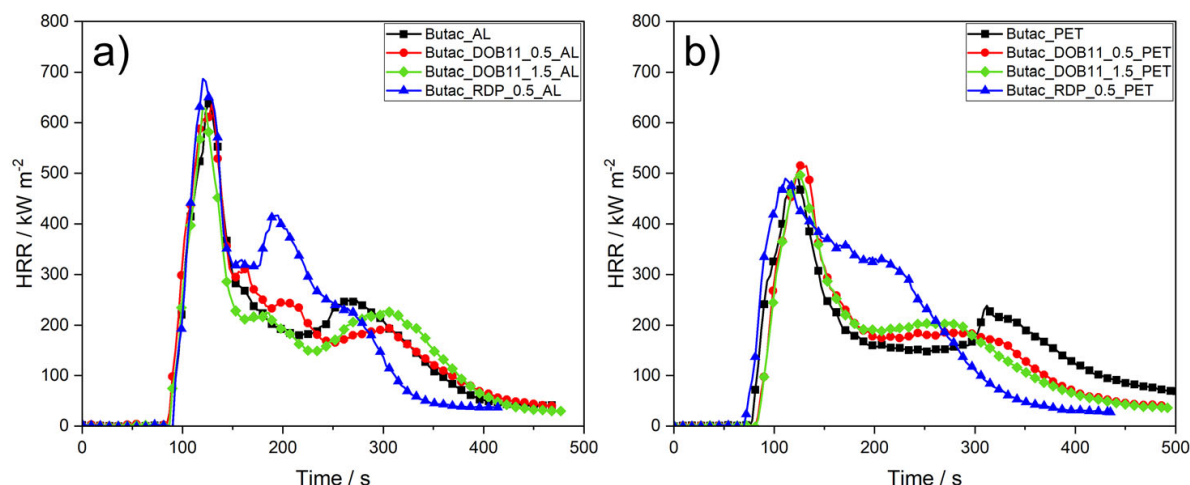


**Figure 7. Cone calorimeter HRR curves of PMMA, bonded with a) all AL carrier tapes in comparison and b) all PET carrier tapes in comparison.**

HRR is observed due to its strong barrier effect and because it is not consumed during the burning process as the PET carrier tapes. The monolithic PC doesn't have that fast consumption of the first layer and chars continuously over the whole burning process leading to a fading HRR.

Figure 7 shows the HRR curve of different tape bonded PC specimens. The key results (Table 6) of the cone calorimeter measurements resemble each other and for AL-tapes as well as for PET-tapes, there are only slight differences depending on which adhesive and flame retardant is used. The discrepancies are mainly due to a high variation of char formation after the PHRR which is typical for PC. Reviewing the comparison over all materials investigated, the cone calorimeter measurements show that rather the carrier than the adhesive or flame retardant in the adhesive makes the difference contemplating the fire behavior of these bonded substrates.

### 4.3. Fire Stability Test

The test, developed and built by us, serves as a qualitative measurement method which can be used to investigate the influence of flame retardants or other changes in adhesive formulations on the fire stability of the adhesive joint. The fire stability test shows that different flame retardants influence the thermal stability of the adhesive.

RDP, as a more condensed phase active flame retardant, improved the fire performance of the adhesive bond with different carrier and substrate materials. Table 7 shows the time to failure and the back-surface temperature of the bonded substrate at that time. Comparing zinc-plated steel and wood, of course, zinc-plated steel had the lower time to failure, because it has higher thermal conductivity, and the adhesive temperature rises faster. The temperatures on the back surface at which the adhesive joints failed were similar. Comparing the adhesives, those with RDP as a flame retardant that is predominantly active in the condensed phase, showed the longest time to failure in beech wood (47 s PET and 51 s AL carrier)

**Table 6**  
**Characteristic Values of the Cone Calorimeter PC Measurement of Monolithic and Bonded PC**

| Sample              | $t_{ig}$<br>(s) $\pm 2$ | FIGRA (kW m <sup>-2</sup> )<br>s <sup>-1</sup> ) $\pm 0.2$ | PHRR (kW m <sup>-2</sup> ) $\pm 90$ | MARHE (kW m <sup>-2</sup> ) $\pm 20$ | THE (MJ m <sup>-2</sup> ) $\pm 2$ |
|---------------------|-------------------------|--|-------------------------------------|--------------------------------------|-----------------------------------|
| Monolithic          | 79                      | 3.5  | 420                                 | 207                                  | 66                                |
| Butac_PET           | 72                      | 4.5  | 538                                 | 188                                  | 76                                |
| Butac_DOB11_0.5_PET | 83                      | 3.9  | 504                                 | 178                                  | 69                                |
| Butac_DOB11_1.5_PET | 87                      | 3.9  | 498                                 | 179                                  | 68                                |
| Butac_RDP_0.5_PET   | 76                      | 4.5  | 475                                 | 237                                  | 76                                |
| Butac_AL            | 88                      | 5.3  | 654                                 | 200                                  | 74                                |
| Butac_DOB11_0.5_AL  | 79                      | 5.2  | 634                                 | 209                                  | 75                                |
| Butac_DOB11_1.5_AL  | 85                      | 5.4  | 669                                 | 189                                  | 72                                |
| Butac_RDP_0.5_AL    | 86                      | 6.2  | 735                                 | 244                                  | 76                                |

**Table 7**  
**Fire Stability of Different Substrates Bonded by PSA Tapes**

| Adhesive tape       | Wood        |                  | Zinc-plated steel |                  |
|---------------------|-------------|------------------|-------------------|------------------|
|                     | Time (s)    | Temperature (°C) | Time (s)          | Temperature (°C) |
| Butac_PET           | 26 $\pm$ 8  | 81 $\pm$ 17      | 20 $\pm$ 3        | 86 $\pm$ 24      |
| Butac_DOB11_0.5_PET | 34 $\pm$ 5  | 79 $\pm$ 4       | 18 $\pm$ 2        | 97 $\pm$ 16      |
| Butac_DOB11_1.5_PET | 24 $\pm$ 8  | 68 $\pm$ 16      | 14 $\pm$ 4        | 69 $\pm$ 9       |
| Butac_RDP_0.5_PET   | 51 $\pm$ 6  | 84 $\pm$ 11      | 26 $\pm$ 3        | 117 $\pm$ 18     |
| Butac_AL            | 27 $\pm$ 2  | 75 $\pm$ 20      | 17 $\pm$ 1        | 75 $\pm$ 5       |
| Butac_DOB11_0.5_AL  | 16 $\pm$ 7  | 57 $\pm$ 17      | 14 $\pm$ 5        | 78 $\pm$ 16      |
| Butac_DOB11_1.5_AL  | 25 $\pm$ 6  | 65 $\pm$ 15      | 18 $\pm$ 2        | 81 $\pm$ 8       |
| Butac_RDP_0.5_AL    | 47 $\pm$ 10 | 87 $\pm$ 9       | 23 $\pm$ 1        | 108 $\pm$ 17     |

and in zinc-plated steel (23 s PET and 26 s AL carrier). It withstood the highest back-surface temperatures in beech wood (87 °C and 84 °C) and in zinc-plated steel (108 °C and 117 °C). While this fire stability test doesn't replace large scale testing, it provides insight into certain material combinations and helps ranking the tapes. If the results can be transferred to real applications and large scale (must be investigated), the test save resources that would be otherwise spent on testing unpromising PSA-bonded materials.

## 5. Conclusions

The influence of different flame retarded PSA tapes on the flammability, fire behavior and fire stability of bonded materials was investigated. The flame retardants DOB 11 as well as RDP showed improvement in the flammability of the free-standing adhesive tapes. Using DOB 11 in PET carrier adhesive tapes led to a

V-2 rating, in contrast to the non-flame-retarded tape and the RDP tape, which failed the vertical UL 94 test. No AL carrier tape passed the UL 94 test with a rating because extinguishing via dripping was not possible due to the non-combustible AL carrier. In OI investigations, both flame retardants increased the OI slightly, from 17.6 vol % to 19.7 vol % for the PET carrier tapes, and from 23.3 vol % to 24.2 vol % for the AL tapes. These improvements were not measured in the flammability of bonded materials which showed the same OI as their corresponding monolithic materials. In the fire scenario of a developing fire, depicted by the cone calorimeter, the behavior of bonded materials was significantly different from the monolithic materials. The adhesive tapes influenced the way heat was transported within the sample. They created gaps between the individual layers and thus hindered heat transfer by conduction or affected the convective heat transport within the melt due to barrier effects. These barrier effects are dominated by the choice of carrier in the adhesive tape, which leads to individual changes in the HRR curves of all substrates. PET carrier tapes, as a thermoplastic material, can melt and lose their barrier effects as soon as the pyrolysis/melt front approaches and overcomes the first substrate layer, as was the case for bonded PMMA. AL carriers, in contrast, did not lose their barrier effect over the whole burning process and remained until the end of the test. This is why AL carriers reduce MARHE and PHRR in PMMA by 25 and 30% compared to the monolithic material and the PET-carrier taped PMMA. In PC as a charring material, the usage of an AL carrier tape created an insulating barrier that generated a gap between the layers during burning. This resulted in a PHRR after ignition 30% higher, and a FIGRA 30% higher than for the monolithic material. For wood, the HRR shape observed was entirely different between that of the monolithic and taped materials. As for PC, the adhesive joint displayed a weak spot in the sample, such that the first layer loosened and deformed due to the impact of the cone heater. This generated an additional peak in the HRR curve and led to a 20% increase in the FIGRA.

The performed cone calorimeter investigations are not only academic investigations but serve as release relevant tests for the interior of railway vehicles (EN 45545, 2020). Also, the UL 94 tests are applied in industry as release relevant test for electric applications.

Considering the burning behavior of the different bonded substrates, the influence of adhesive tapes leads to burning behavior significantly different than that of the monolithic material and yields new fire hazards. But in contrast to the current state of the art, the solution is not to protect the adhesive tape so that it can pass certain tests like UL 94. Instead, it is advisable to adapt the adhesive tape and tailor the carrier to the application and substrate it is used in.

## **Acknowledgements**

The research was based on an IGF Project. The IGF Project (20762 N) of the Research Association DECHEMA (Deutsche Gesellschaft für Chemische Technik und Biotechnologie e. V., 60486 Frankfurt am Main, Germany) was supported by

the AiF within the framework of the program “Förderung der Industriellen Gemeinschaftsforschung (IGF)” of the German Federal Ministry for Economic Affairs and Climate Action, based on a decision of the Deutschen Bundestag. I would like to thank Fernanda Romero who supported the UL 94 and OI measurements, Yin Yam Chan for the support in fire stability measurements and Michael Schneider and Detlev Rättsch for the sample manufacturing.

## **Funding**

Open Access funding enabled and organized by Projekt DEAL.

## **Data Availability**

Derived data supporting the findings of this study are available from the corresponding authors on request. Some materials and discussion were supplied by industrial partners within the IGF project as their contribution to the pre-competitive and independent research, following the strict rules of IGF framework to ensure compliance.

## **Declarations**

**Conflict of interests** The authors declare no conflict of interests.

**Ethical approval** Some materials and discussion were supplied by industrial partners within the IGF project as their contribution to the pre-competitive and independent research, following the strict rules of IGF framework to ensure compliance.

## **Open Access**

This article is licensed under a Creative Commons Attribution 4.0 International License, which permits use, sharing, adaptation, distribution and reproduction in any medium or format, as long as you give appropriate credit to the original author(s) and the source, provide a link to the Creative Commons licence, and indicate if changes were made. The images or other third party material in this article are included in the article's Creative Commons licence, unless indicated otherwise in a credit line to the material. If material is not included in the article's Creative Commons licence and your intended use is not permitted by statutory regulation or exceeds the permitted use, you will need to obtain permission directly from the copyright holder. To view a copy of this licence, visit <http://creativecommons.org/licenses/by/4.0/>.

## References

1. Bethke C, Weber L, Goedderz D, Standau T, Doring M, Altstadt V (2020) Fire behavior of flame retarded sandwich structures containing PET foam cores and epoxy face sheets. *Polym Compos* 41(12):5195–5208. <https://doi.org/10.1002/pc.25786>
2. Dietenberger MA, Shalbafan A, Welling J (2018) Cone calorimeter testing of foam core sandwich panels treated with intumescent paper underneath the veneer (FRV). *Fire Mater* 42(3):296–305. <https://doi.org/10.1002/fam.2492>
3. Gallo E, Schartel B, Acierno D, Cimino F, Russo P (2013) Tailoring the flame retardant and mechanical performances of natural fiber-reinforced biopolymer by multi-component laminate. *Compos Part B-Eng* 44(1):112–119. <https://doi.org/10.1016/j.compositesb.2012.07.005>
4. Yu Z, Liu J, Zhang Y, Luo J, Lu C, Pan B (2015) Thermo-oxidative degradation behavior and fire performance of high impact polystyrene/magnesium hydroxide/microencapsulated red phosphorus composite with an alternating layered structure. *Polym Degrad Stab* 115:54–62. <https://doi.org/10.1016/j.polymdegradstab.2015.02.015>
5. Wang Z-H, Liu B-W, Zeng F-R, Lin X-C, Zhang J-Y, Wang X-L, Wang Y-Z, Zhao H-B. (2022) Fully recyclable multifunctional adhesive with high durability, transparency, flame retardancy, and harsh-environment resistance. *Sci Adv* 8(50):eadd8527. <https://doi.org/10.1126/sciadv.add8527>
6. Zeng Y, Yang W, Xu P, Cai X, Dong W, Chen M, Du M, Liu T, Jan Lemstra P, Ma P (2022) The bonding strength, water resistance and flame retardancy of soy protein-based adhesive by incorporating tailor-made core-shell nanohybrid compounds. *Chem Eng J* 428:132390. <https://doi.org/10.1016/j.cej.2021.132390>
7. Pang H, Ma C, Shen Y, Sun Y, Li J, Zhang S, Cai L, Huang Z (2021) Novel bionic soy protein-based adhesive with excellent prepressing adhesion, flame retardancy, and mildew resistance. *ACS Appl Mater Interfaces* 13(32):38732–38744. <https://doi.org/10.1021/acsami.1c11004>
8. Tirri T, Aubert M, Wilén C-E, Pfaendner R, Hoppe H (2012) Novel tetrapotassium azo diphosphonate (INAZO) as flame retardant for polyurethane adhesives. *Polym Degrad Stab* 97(3):375–382. <https://doi.org/10.1016/j.polymdegradstab.2011.12.005>
9. Wu MT, Song W, Wu YZ, Qu W (2020) Preparation and characterization of the flame retardant decorated plywood based on the intumescent flame retardant adhesive. *Materials* 13(3):676. <https://doi.org/10.3390/ma13030676>
10. Tang Y, Wang D-Y, Jing X-K, Ge X-G, Yang B, Wang Y-Z (2008) A formaldehyde-free flame retardant wood particleboard system based on two-component polyurethane adhesive. *J Appl Polym Sci* 108(2):1216–1222. <https://doi.org/10.1002/app.27662>
11. Zhu Z-M, Xu Y-J, Liao W, Xu S, Wang Y-Z (2017) Highly flame retardant expanded polystyrene foams from phosphorus–nitrogen–silicon synergistic adhesives. *Ind Eng Chem Res* 56(16):4649–4658. <https://doi.org/10.1021/acs.iecr.6b05065>
12. Frangi A, Fontana M, Hugi E, Jobstl R (2009) Experimental analysis of cross-laminated timber panels in fire. *Fire Saf J* 44(8):1078–1087. <https://doi.org/10.1016/j.fire-saf.2009.07.007>
13. Li KY, Li YJ, Zou YY, Yuan BH, Walsh A, Carradine D (2023) Improving the fire performance of structural insulated panel core materials with intumescent flame-retardant epoxy resin adhesive. *Fire Technol* 59(1):29–51. <https://doi.org/10.1007/s10694-021-01203-0>
14. Son M, Kim J, Oh M, Kim D, Choi HJ, Lee K, Chung K, Lee S (2023) Phosphorus-based flame retardant acrylic pressure sensitive adhesives with superior peel strength

- and transfer characteristics. *Prog Org Coat* 185:107931. <https://doi.org/10.1016/j.porg-coat.2023.107931>
15. Bifulco A, Varganici CD, Rosu L, Mustata F, Rosu D, Gaan S. (2022) Recent advances in flame retardant epoxy systems containing non-reactive DOPO based phosphorus additives. *Polym Degrad Stab*, 200109962. <https://doi.org/10.1016/j.polymdegradstab.2022.109962>
  16. Wang H, Li S, Zhu ZM, Yin XZ, Wang LX, Weng YX, Wang XY (2021) A novel DOPO-based flame retardant containing benzimidazolone structure with high charring ability towards low flammability and smoke epoxy resins. *Polym Degrad Stab* 183:109426. <https://doi.org/10.1016/j.polymdegradstab.2020.109426>
  17. Artner J, Ciesielski M, Ahlmann M, Walter O, Doring M, Perez RM, Altstadt V, Sandler JKW, Schartel B (2007) A novel and effective synthetic approach to 9,10-dihydro-9-oxa-10-phosphaphenanthrene-10-oxide (DOPO) derivatives. *Phosphorus Sulfur Silicon Relat Elem* 182(9):2131–2148. <https://doi.org/10.1080/10426500701407417>
  18. Perret B, Schartel B, Stoss K, Ciesielski M, Diederichs J, Doring M, Kramer J, Altstadt V (2011) Novel DOPO-based flame retardants in high-performance carbon fibre epoxy composites for aviation. *Eur Polymer J* 47(5):1081–1089. <https://doi.org/10.1016/j.eurpolymj.2011.02.008>
  19. Pawlowski KH, Schartel B (2007) Flame retardancy mechanisms of triphenyl phosphate, resorcinol bis(diphenyl phosphate) and bisphenol bis(diphenyl phosphate) in polycarbonate/acrylonitrile-butadiene-styrene blends. *Polym Int* 56(11):1404–1414. <https://doi.org/10.1002/pi.2290>
  20. Liu SM, Jiang L, Jiang ZJ, Zhao JQ, Fu Y (2011) The impact of resorcinol bis(diphenyl phosphate) and poly(phenylene ether) on flame retardancy of PC/PBT blends. *Polym Adv Technol* 22(12):2392–2402. <https://doi.org/10.1002/pat.1775>
  21. Jang Y-M, Yu C-J, Choe K-S, Choe C-H, Kim C-H (2021) Preparation and flame retardant properties of cotton fabrics treated with resorcinol bis(diphenyl phosphate). *Cellulose* 28(7):4455–4467. <https://doi.org/10.1007/s10570-021-03780-3>
  22. Dukarski W, Krzyzanowski P, Gonsior M, Rykowska I (2021) Flame retardancy properties and physicochemical characteristics of polyurea-based coatings containing flame retardants based on aluminum hydroxide, resorcinol bis(diphenyl phosphate), and tris chloropropyl phosphate. *Materials* 14(18):5168
  23. Hupp V, Schartel B, Flothmeier K, Hartwig A (2024) Fire behavior of pressure-sensitive adhesive tapes and bonded materials. *Fire Mater* 48(1):114–127. <https://doi.org/10.1002/fam.3171>
  24. Schartel B, Bartholmai M, Knoll U (2005) Some comments on the use of cone calorimeter data. *Polym Degrad Stab* 88(3):540–547. <https://doi.org/10.1016/j.polymdegradstab.2004.12.016>
  25. Zhang J, Koubaa A, Xing D, Godard F, Li P, Tao Y, Wang X-M, Wang H (2021) Fire retardancy, water absorption, and viscoelasticity of borated wood—polycarbonate biocomposites. *Polymers* 13(14):2234
  26. Xu Q, Hofmeyer H, Maljaars J, van Herpen RAP (2023) Full-scale fire resistance testing and two-scale simulations of sandwich panels with connections. *Fire Technol* . <https://doi.org/10.1007/s10694-023-01463-y>
  27. Hull TR (2008) 11—Challenges in fire testing: reaction to fire tests and assessment of fire toxicity. In: Horrocks AR, Price D (eds) *Advances in Fire Retardant Materials* Woodhead Publishing, , pp 255–290
  28. Schartel B, Hull TR (2007) Development of fire-retarded materials—Interpretation of cone calorimeter data. *Fire Mater* 31(5):327–354. <https://doi.org/10.1002/fam.949>

29. Seah DGJ, Dasari A (2023) Understanding the influence of melt dripping on UL94 test response in a PA11 system. *Polym Testing* 118:107893. <https://doi.org/10.1016/j.polymeresting.2022.107893>
30. Turski Silva Diniz A, Huth C, Schartel B. (2020) Dripping and decomposition under fire: Melamine cyanurate vs. glass fibres in polyamide 6. *Polym Degrad Stab* 171:109048. <https://doi.org/10.1016/j.polymdegradstab.2019.109048>
31. Borysiuk P, Jaskolowski W, Boruszewski P, Jencyk-Tolleczo I, Jablonski M, Bylinski D (2011) Ignitability of wood impregnated with fireproof agent based on diammonium hydrogen phosphate, citric acid and sodium benzoate. *Forest Wood Technol* 73:181–185
32. Lin C-F, Karlsson O, Mantanis G, Sandberg D. (2020) Fire performance and leach resistance of pine wood impregnated with guanyl-urea phosphate/boric acid and a melamine-formaldehyde resin. *Euro J Wood Wood Prod* 78. <https://doi.org/10.1007/s00107-019-01483-y>
33. Batiot B, Luche J, Rogaume T (2014) Thermal and chemical analysis of flammability and combustibility of fir wood in cone calorimeter coupled to FTIR apparatus. *Fire Mater* 38(3):418–431. <https://doi.org/10.1002/fam.2192>
34. Paál M, Rychlý J, Vykydalová A, Šurina I, Lisý A, Brezová V, Nemčková K, Labuda J (2023) Burning and thermal degradation of wood under defined conditions: a route of preparation of carbonaceous char and its characterization for potential applicability in evaluation of real fire. *Fire Technol* 59(5):2733–2749. <https://doi.org/10.1007/s10694-023-01422-7>
35. Maraveas C, Miamis K, Matthaïou CE (2015) Performance of timber connections exposed to fire: a review. *Fire Technol* 51(6):1401–1432. <https://doi.org/10.1007/s10694-013-0369-y>
36. Hou J, Cai Z, Lu K (2017) Cone calorimeter evaluation of reinforced hybrid wood–aluminum composites. *J Fire Sci* 35(2):118–131. <https://doi.org/10.1177/0734904116683717>
37. Wang W, Zammarano M, Shields JR, Knowlton ED, Kim I, Gales JA, Hoehler MS, Li J (2018) A novel application of silicone-based flame-retardant adhesive in plywood. *Constr Build Mater* 189:448–459. <https://doi.org/10.1016/j.conbuildmat.2018.08.214>
38. Luche J, Rogaume T, Richard F, Guillaume E (2011) Characterization of thermal properties and analysis of combustion behavior of PMMA in a cone calorimeter. *Fire Saf J* 46(7):451–461. <https://doi.org/10.1016/j.firesaf.2011.07.005>
39. Babrauskas V (2002) Chpt. 3-1. Heat release rates. In: Walton D (eds) *The SFPE handbook of fire protection engineering*. 3rd ed. National FireProtection Association Inc., USA
40. Schartel B, Braun U, Knoll U, Bartholmai M, Goering H, Neubert D, Pötschke P (2008) Mechanical, thermal, and fire behavior of bisphenol a polycarbonate/multiwall carbon nanotube nanocomposites. *Polym Eng Sci* 48(1):149–158. <https://doi.org/10.1002/pen.20932>
41. Vahabi H, Etteradossi O, Ferry L, Longuet C, Sonnier R, Lopez-Cuesta JM (2013) Polycarbonate nanocomposite with improved fire behavior, physical and psychophysical transparency. *Eur Polymer J* 49(2):319–327. <https://doi.org/10.1016/j.eurpolymj.2012.10.031>
42. Hu Z, Chen L, Zhao B, Luo Y, Wang D-Y, Wang Y-Z (2011) A novel efficient halogen-free flame retardant system for polycarbonate. *Polym Degrad Stab* 96(3):320–327. <https://doi.org/10.1016/j.polymdegradstab.2010.03.005>

## 6. Further investigations

Since PSA tapes are a very specific type of adhesive, the question rose, whether the new findings about the fire behavior of PSA tape-bonded materials are transferrable to other types of adhesives such as liquid adhesives and their bonds. To answer this question, beech wood cone calorimeter samples were prepared in the same manner as the adhesive tape bonds except for using a 1K PU adhesive instead of adhesive tapes. In the cone calorimeter measurements, the PU adhesive gap had similar effects on the burning behavior of the wood as the PET carrier adhesive tapes, resulting in an additional peak in the HRR curve followed by a local HRR minimum. This additional peak is caused by the separate burning of the bonded layers as it is described in section 5.1 and 5.3 for adhesive tape bonds. The similar results for 1K PU adhesive and PET tape imply that not only in wood, but also in other materials, the fire behavior of liquid adhesive bonded materials is similar to that of adhesive tape-bonded materials and this dissertation serves not only as a basis for the development of new adhesive tapes and their bonds, but for bonded materials in general.

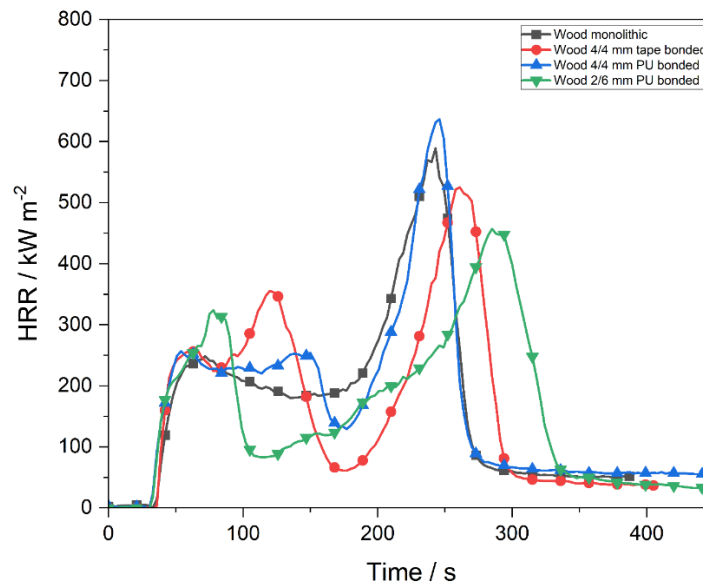


Figure 15: Comparison between monolithic, tape-bonded and 1K PU adhesive-bonded beech wood in the cone calorimeter.



## 7. Summary

PSA (tapes) are permanently sticky adhesives that can be applied by slight pressure to a large variety of surfaces. This easy application has led to the widespread use of PSA not only in the DIY sector but also in the construction, railway vehicle, and automotive industries, where the fire behavior of the materials is of crucial importance. The fire behavior of PSA-bonded materials is therefore a research topic of high interest to industry and academia. Due to the viscoelastic state of PSA, it is a challenge to develop well compatible flame retardants that do not bloom out or migrate to the adhesive surface and degrade the adhesion between the substrate and the adhesive. To overcome this problem, phosphorus flame retardants, as a very versatile class of flame retardants that can be modified to meet the specific demands of the polymer matrix, are a good choice for a PSA matrix. A further advantage of phosphorus-based flame retardants is that they are effective at low concentrations, allowing the PSA tapes to keep their mechanical properties. They act in several modes of protection, depending on the chemical environment of phosphorus within the flame retardant and the polymer matrix in which they are used.

The state of art is to develop phosphorus-based flame retardant PSA tapes that perform well in flammability tests and expect them to have beneficial influence in the bonded product, without this relationship being proven. The questions of how different flame retardants work in PSA and PSA tapes and how these flame retardant adhesives influence the burning behavior of bonded materials is elaborated on in this doctoral dissertation.

In the first step of this dissertation, the fire behavior and pyrolysis of commercially available phosphorus-based flame retardant adhesives (tapes) were analyzed and compared to adhesive tapes without flame retardant to gain a basic understanding of how adhesive tapes behave in fire and how flame retardants affect this behavior. Fire behavior analysis was performed in different fire scenarios and bond designs established in a multi-methodical approach. The reaction of the adhesive tape to a small flame was investigated as a free standing object, bonded one-sided onto different substrates, and as sandwich like bonds (substrate/tape/substrate). The interaction between flame retardant, adhesive matrix, carrier, and substrate was explained by systematically examining the pyrolysis of the adhesive, the flammability of the tapes, and the fire behavior of bonded materials in an ignition and a developing fire scenario. Py-GC/MS, TGA FTIR, PCFC and hot-stage FTIR measurements were used to identify the mode of action of the flame retardant and its interaction with the PSA matrix. The flammability tests, UL 94, OI, and the single-flame source test identified the effect of the flame retardant on the flammability of the tape and the effect on the

flammability of bonded materials. Measuring and comparing the fire behavior of the bonded and monolithic materials in the cone calorimeter led to an understanding of how PSA tapes influence the fire behavior of bonded substrates. The fire behavior of different monolithic and bonded substrates with a wide spectrum of burning characteristics was investigated to gain information on the substrate specificity of the tape influence.

The second step of the dissertation consisted in preparing differently phosphorus-based flame retardant PSA and PSA tapes. One predominantly gas phase active, one condensed phase active and one covalently bonded phosphorus flame retardant were used in a PSA matrix which mainly consisted of poly(n-butyl acrylate). Determining the adhesion and cohesion properties of the PSA tapes guaranteed the possible application as PSA tape. Their flame retardant mechanism and decomposition and combustion behavior were analyzed thoroughly in Py-GC/MS, TGA FTIR, hot-stage FTIR and PCFC to gain precise insights into the chemical and physical mechanisms that govern the pyrolysis process. The different modes of actions and mechanisms were subsequently connected to the flammability of adhesive tapes which were prepared from the synthesized flame retardant PSA and assessed in UL 94 and OI.

In the last step of this systematic doctoral dissertation, the self-prepared adhesive tapes were used to bond different substrates whose fire behaviors were then investigated in different fire scenarios simulating ignition, developing and fully developed fire. This made it possible to connect the pyrolysis mechanism, mode of action, and fire behavior of the free standing adhesive tapes with the fire behavior of bonded materials. Different carriers (AL and PET) were used in different substrates (wood, bisphenol-A polycarbonate, polymethyl methacrylate) to yield in an understanding of the influence of the adhesive tape carrier on the burning behavior of the individual substrates.

The first step shows that phosphorus flame retardants significantly improve the flammability of the commercially available adhesive tapes. The gas phase active flame retardant resulted in a UL 94 V-2 rating and a large increase (5.3 vol.-%) in OI, and significantly changed the burning behavior in the single-flame source test. Tape-bonded materials behaved substantially different from their monolithic counterparts in cone calorimeter measurements, where the adhesive tape mostly acted as an insulating barrier separating the bonded substrate layers. This separation led to new fire risks in PC and increased the FIGRA up to 20% and the PHRR up to 26%. Cone calorimeter measurements also showed that phosphorus flame retardants and carriers must be tailored to each other because they can react and degrade the protective properties of the carrier, as it was the case for the AL carrier in combination with a

commercial phosphorus flame retardant. The strong enhancing effect of the flame retardant on the flammability of the non-bonded adhesive tapes was not present in adhesive tape-bonded materials where the fire behavior was determined by the substrates.

During the second step of this dissertation, the individual decomposition of the PSA matrix and the flame retardants were analyzed in Py-GC/MS, TGA FTIR and PCFC and detailed decomposition and flame retardant mechanisms were postulated. The gas phase active DOB 11 released PO and PO<sub>2</sub> radicals at low temperatures resulting in a V-2 UL 94 rating at small concentrations. The condensed phase active flame retardant, RDP, improved the charring of the PSA tape surface, as it is suspected to be a precursor of phosphoric/ polyphosphoric acid. These acids lead to elimination reactions which result in unsaturated structures and finally enhanced char formation. The small amount of RDP had, normalized on the p-concentration and compared to the other flame retardants, the biggest positive effect on the OI of the adhesive tape. DOPO-pentyl-methacrylate alone has a low decomposition temperature (starting at 300 °C) but was covalently bonded to the polymer backbone and therefore decomposed together with the polymer (starting at 350° C). It released PO and PO<sub>2</sub> radicals that improved the flammability in all fire tests. In addition to its beneficial influence on the fire behavior, the covalently bonded flame retardant also increased the mechanical properties at elevated temperatures, which is an important parameter for PSA tapes. The pyrolysis and flammability of these different flame retardant types for PSA show that the phosphorus flame retardants have individual advantages and need to be tailored to the matrix and the application.

The third and final step of this doctoral dissertation focusses on the fire behavior of self-prepared adhesive tapes with different flame retardant PSA and different carriers used to bond substrates representative of automotive, railway vehicle, and construction applications. Cone calorimeter measurements showed that it is not the adhesives and the flame retardants in the PSA matrix that result in changes in the fire behavior, but rather the choice of carrier. In the case of PMMA, for example, an AL carrier can improve the fire behavior by acting as a barrier to protect the underlying material, leading to a 25% reduction in MARHE and a 30% reduction in PHRR compared to a PET carrier. The same AL carrier used in PC substrates resulted in a 30% increase of MARHE and FIGRA, indicating higher fire hazards and poorer performance in the cone calorimeter test.

To determine the transferability of the results obtained for adhesive tapes to other adhesives, the fire behavior of adhesive tape-bonded materials was compared to materials bonded by liquid thin-layer adhesives. Similar effects of the liquid adhesives

were obtained in the cone calorimeter, suggesting that the findings for the burning behavior of adhesive tape bonds are likely to be generalizable to materials that are bonded by other adhesives.

Overall, a fundamental understanding of the fire behavior of adhesive tapes and bonded materials was generated and the individual effect of different flame retardants for PSA tapes was investigated thoroughly. Based on the new findings, the state of the art PSA development is questioned and new, more end application focused research is suggested. The strong impact of adhesive gaps in several tape-bonded materials provides a promising outlook for future research into the fire behavior of materials bonded by other adhesives and using different substrates and applications.

## 8. Zusammenfassung

Haftklebstoffe bzw. Haftklebebänder sind permanent klebrige Klebstoffe, die durch leichten Druck auf eine Vielzahl von Oberflächen appliziert werden können. Diese einfache Handhabung führte zu einem weit verbreiteten Einsatz von PSA nicht nur im DIY Bereich, sondern auch im Bauwesen, Schienenfahrzeugen und Automobilen, wo dem Brandverhalten der geklebten Materialien eine entscheidende Bedeutung zukommt. Das Brandverhalten von PSA-verklebten Materialien ist daher ein bedeutendes, jedoch bisher kaum verstandenes Forschungsthema für Industrie und Wissenschaft. Der viskoelastische Zustand von PSA vor und nach der Applikation stellt bei der Entwicklung geeigneter Flammenschutzmittel eine zusätzliche Herausforderung dar, da diese leichter ausblühen oder an die Klebstoffoberfläche migrieren und so die Adhäsion zwischen Substrat und Klebstoff verschlechtern können. Um diese Probleme zu überwinden, stellen phosphorbasierte Flammenschutzmittel, die vielseitig modifiziert und immobilisiert werden können, eine geeignete Wahl dar. Ein weiterer Vorteil von Flammenschutzmitteln auf Phosphorbasis ist, dass sie bereits in geringen Konzentrationen wirksam sind, so dass die mechanischen Eigenschaften der PSA Tapes weitgehend erhalten bleiben. Phosphor kann je nach chemischer Umgebung im Flammenschutzmittel und der Polymermatrix auf verschiedene Arten wirken, welche sich auf den Anwendungszweck abstimmen lässt.

Der Stand der Technik bei der Entwicklung von phosphorbasierendem flammgeschützten PSA Tapes ist es, Klebebänder zu entwickeln, die in UL 94-Tests gut abschneiden und daraus einen positiven Beitrag zum Brandverhalten geklebter Materialien abzuleiten, ohne dass dieser Zusammenhang nachgewiesen ist. Dieser Zusammenhang wird in dieser Dissertation hinterfragt und das Brandverhalten von flammgeschützten Haftklebebändern sowie deren Klebverbunde umfassend untersucht. In drei Schritten werden die Einflüsse von Haftklebstoff, Träger, Flammenschutzmittel und Substrat auf das Brandverhalten von Haftklebverbunden analysiert und zuletzt eine Übertragbarkeit auf andere Klebstoffsysteme diskutiert.

Im ersten Schritt dieser Dissertation wurde das Brandverhalten und die Pyrolyse von kommerziell verfügbaren phosphorbasierendem flammgeschützten Haftklebstoffen bzw. Haftklebebändern analysiert und mit entsprechenden Klebebändern ohne Flammenschutzmittel verglichen, um ein grundlegendes Verständnis dafür zu erlangen, wie sich Klebebänder im Brandfall verhalten und wie Flammenschutzmittel dieses Verhalten beeinflussen. Die Analyse des Brandverhaltens wurde in verschiedenen Brandszenarien und Klebdesigns in einem multimethodischen Ansatz durchgeführt. Das Brandverhalten der PSA Tapes im Szenario des Brandbeginns bzw. die Entflammbarkeit wurde als freistehendes Objekt, einseitig auf verschiedene Substrate geklebt und als

sandwichartige Verklebung (Substrat/Klebeband/Substrat) untersucht. Die Wechselwirkung zwischen Flammschutzmittel, Polymer, Träger und Substrat wurden durch die systematische Untersuchung der Pyrolyse des Klebstoffs, der Entflammbarkeit der Klebebänder und des Brandverhaltens der geklebten Materialien analysiert. Py-GC/MS-, TGA FTIR-, PCFC- und hot-stage FTIR Messungen wurden eingesetzt, um die Wirkungsweise des Flammschutzmittels und seine Interaktion mit der PSA Matrix zu ermitteln. In den Entflammbarkeitstests, UL 94, OI und Einzelflammtest (ISO 11925-2) wurden die Reaktionen der Klebebänder und geklebten Materialien auf die Einwirkung eine Kleinbrennerflamme analysiert.

Im Cone Calorimeter wurde das Brandverhalten von Klebverbunden und diversen monolithischen Substraten untersucht und so gezielt der substratspezifische Einfluss der Klebfuge auf das Brandverhalten bestimmt.

Im zweiten Schritt der Dissertation wurden verschieden phosphorbasiert flammgeschützte PSA und PSA Tapes hergestellt, um deren pyrolytischen Eigenschaften sowie deren Zusammenhang mit der Entflammbarkeit zu untersuchen. Ein überwiegend gasphasen-aktives, ein in der kondensierten Phase aktives und ein kovalent gebundenes Phosphor-Flammschutzmittel wurden in eine Poly(n-butyl acrylat) PSA-Matrix implementiert. Die Bestimmung von  $T_g$  sowie Adhäsions- und Kohäsionseigenschaften stellten eine Verwendbarkeit der hergestellten Klebstoffe als PSA sicher und zeigten den Einfluss von Flammschutzmitteln auf die klebtechnischen Eigenschaften. Flammschutzmechanismen sowie ihr Zersetzungs- und Verbrennungsverhalten wurden ausführlich in Py-GC/MS, TGA FTIR, hot-stage FTIR und PCFC analysiert, um einen genauen Einblick in die chemischen und physikalischen Mechanismen zu erhalten, die den Pyrolyseprozess steuern. Im Anschluss wurden Zusammenhänge zwischen den verschiedenen Wirkungsweisen und Mechanismen der Flammschutzmittel und der Entflammbarkeit der Klebebänder in UL 94 und OI untersucht.

Im letzten Schritt dieser Doktorarbeit wurden verschiedene Substrate durch die selbst hergestellten Klebebänder verklebt, und deren Brandverhalten anschließend in verschiedenen Brandszenarien untersucht. Die Analyse im Szenario des Brandbeginns, des sich entwickelnden Brandes und des Vollbrandes ermöglichte es, die Pyrolysemechanismen, die Wirkungsweisen der Flammschutzmittel und die Brandverhalten der freistehenden Klebebänder mit den Brandverhalten der verklebten Materialien zu verknüpfen. Verschiedene Träger (Aluminium und Polyethylenterephthalat) wurden in verschiedenen Substraten (Holz, Bisphenol-A-Polycarbonat, Polymethylmethacrylat) verwendet, um den Einfluss des Klebebandträgers auf das Brandverhalten der einzelnen Substrate zu verstehen.

Der erste Schritt zeigt die deutliche Verbesserung des Brandverhaltens der PSA Tapes durch kommerzielle Flammschutzmittel. Das gasphasenaktive Flammschutzmittel erzielte im UL 94 Test ein V-2 Rating (ohne Flammschutz kein V-Rating), steigerte den OI um 5,3 Vol.-% und führte zu einem deutlich verbesserten Brandverhalten im Einzelflammtest. Die PSA Tape Klebverbunde zeigten ein deutlich anderes Brandverhalten im Cone Calorimeter als ihre monolithischen Gegenstücke, bei denen das Klebeband hauptsächlich als isolierende Barriere wirkte. Diese thermische Separation der Schichten führte zu neuen Brandrisiken bei PC und erhöht die FIGRA um bis zu 20% und die PHRR um bis zu 26%. Cone Calorimeter Messungen zeigten außerdem die potenzielle Reaktion zwischen Carrier und Flammschutzmittel, welche im Fall von AL als Carrier zu verschlechterten Schutzeigenschaften des Trägers führte. Die erhebliche Reduktion der Entflammbarkeit der Klebebänder durch das Flammschutzmittel ist bei den PSA Klebeverbunden vernachlässigbar, da hier das Brandverhalten durch die Substrate diktiert wird.

Im zweiten Schritt dieser Dissertation wurde die individuelle Pyrolyse der PSA-Matrix und der Flammschutzmittel mittels Py-GC/MS, TGA FTIR, PCFC und hot-stage FTIR analysiert und detaillierte Mechanismen postuliert. Das gasphasenaktive DOB 11 setzte bei niedrigen Temperaturen PO- und PO<sub>2</sub>-Radikale frei, die bereits in geringen Konzentrationen das V-Rating im UL 94 Test von keinem auf ein V-2 verbesserten. RDP, als festphasenaktives Flammschutzmittel, induzierte die Verkohlung der PSA Tape Oberfläche, da es vermutlich Phosphorsäure/Polyphosphorsäure freisetzt, welche bekanntermaßen die Charbildung induziert bzw. verstärkt. RDP hatte, normalisiert auf die p-Konzentration, den größten positiven Effekt auf den OI der Klebebänder. DOPO-pentyl-methacrylat wies als ungebundenes Flammschutzmittel eine niedrige Zersetzungstemperatur (ab 300 °C) auf, zersetzt sich jedoch bei kovalenter Bindung an das Polymer erst zusammen mit der Matrix (Poly(n-butyl acrylat)) ab 350 °C. DOPO-pentyl-methacrylat setzt PO- und PO<sub>2</sub>-Radikale frei, was die Brandeigenschaften im Szenario der Brandentstehung in verschiedenen Tests verbessert. Zusätzlich wurden die mechanischen Eigenschaften bei erhöhten Temperaturen durch DOPO-pentyl-methacrylat erheblich verbessert, was einen wichtigen Parameter für viele PSA Anwendungen darstellt. Die Pyrolyse und die Entflammbarkeit dieser verschiedenen Flammschutzmitteltypen für PSA zeigen, dass die Phosphor-Flammschutzmittel individuelle Vorteile haben und auf die Matrix und die Anwendung im Verbund zugeschnitten werden müssen.

Der dritte und letzte Schritt zeigte das Brandverhalten von Klebebändern mit verschiedenen flammgeschützten PSA und verschiedenen Trägern, die zum Verkleben von Substraten verwendet werden, die für den Einsatz in Autos, Schienenfahrzeugen und

im Bauwesen repräsentativ sind. Cone Calorimeter Messungen veranschaulichten, dass nicht die Klebstoffe und Flammschutzmittel in der PSA-Matrix zu Veränderungen im Brandverhalten führten, sondern vielmehr die Wahl des Trägers. Bei PMMA beispielsweise, kann ein AL-Träger das Brandverhalten verbessern, indem er als Barriere das darunter liegende Material schützt. Dies führt zu einem um 25 % verringerten MARHE-Wert und einer um 30% verringerten PHRR-Wert im Vergleich zu einem PET-Träger. Der gleiche AL-Träger führte bei der Untersuchung von PC Klebverbunden zu einer 30%igen Erhöhung von MARHE und FIGRA, was eine erhöhte Brandgefahr und neue Risiken im Brandfall bedeutet.

Um die Übertragbarkeit der für Klebebänder erzielten Ergebnisse auf andere Klebstoffe zu ermitteln, wurde das Brandverhalten von mit Klebebändern verklebten Materialien mit dem von Materialien, die durch flüssige Dünnschichtklebstoffe verklebt wurden, verglichen. Es wurden ähnliche Auswirkungen des Flüssigklebstoffs auf das Brandverhalten der Substrate im Cone Calorimeter festgestellt, was darauf hindeutet, dass die Erkenntnisse über das Brandverhalten von Haftklebverbunden wahrscheinlich auf andere Klebverbunde übertragbar sind, die mit flüssigen Dünnschichtklebstoffen verklebt wurden.

Alles in allem wurde ein fundamentales Verständnis des Brandverhaltens von Klebebändern und verklebten Materialien geschaffen und der Einfluss verschiedener Flammschutzmittel für PSA-Bänder umfassend untersucht. Aufgrund der neuen Erkenntnisse wird der aktuelle Stand der PSA-Entwicklung in Frage gestellt und neue, auf die Endanwendung fokussierte Forschungsarbeiten vorgeschlagen. Der starke Einfluss von Klebfugen in PSA Klebverbunden und die Indizien der Übertragbarkeit auf andere Klebverbunde geben einen vielversprechenden Ausblick auf zukünftige Forschungsarbeiten zum Brandverhalten von verklebten Materialien.



## 9. References

- [1] Mordor Intelligence. *Adhesives Market SIZE & SHARE ANALYSIS - GROWTH TRENDS & FORECASTS UP TO 2028*. **2024**. Accessed 29.07.2024. <https://www.mordorintelligence.com/industry-reports/global-adhesives-market#keysellingpoints>.
- [2] US Census Bureau. *Industry revenue of “adhesive manufacturing” in the U.S. from 2012 to 2024 (in billion U.S. Dollars)*. **2020**. Accessed 29.07.2024. <https://www.statista.com/forecasts/409491/adhesive-manufacturing-revenue-in-the-us>.
- [3] Bishopp J. Adhesives for Aerospace Structures. In: *Handbook of Adhesives and Surface Preparation*. Ebnesajjad S ed., William Andrew Publishing; **2011**: 301-344. <https://doi.org/10.1016/B978-1-4377-4461-3.10013-6>.
- [4] Chakraborty BC. Naval Applications of Structural Adhesives. In: *Structural Adhesives: Properties, Characterization and Applications*. Mittal KL, Panigrahi SK ed., Scrivener Publishing LLC; **2023**: 397-444. <https://doi.org/10.1002/9781394175604.ch9>.
- [5] Wang W, Zammarano M, Shields JR, Knowlton ED, Kim I, Gales JA, Hoehler MS, Li J. **2018** A novel application of silicone-based flame-retardant adhesive in plywood. *Construction and Building Materials*. 189: 448-459. <https://doi.org/10.1016/j.conbuildmat.2018.08.214>.
- [6] Wen M-Y, Zhu J-Z, Zhu M, Sun Y-X, Park H-J, Shi J. **2020** Research on Flame Retardant Formaldehyde-Free Plywood Glued by Aqueous Polymer Isocyanate Adhesive. *Journal of the Korean Wood Science and Technology*. 48(5):755-764. <https://doi.org/10.5658/WOOD.2020.48.5.755>.
- [7] Zelinka SL, Sullivan K, Pei S, Ottum N, Bechle NJ, Rammer DR, Hasburgh LE. **2019** Small scale tests on the performance of adhesives used in cross laminated timber (CLT) at elevated temperatures. *International Journal of Adhesion and Adhesives*. 95:102436. <https://doi.org/10.1016/j.ijadhadh.2019.102436>.
- [8] Ronquillo G, Hopkin D, Spearpoint M. **2021** Review of large-scale fire tests on cross-laminated timber. *Journal of Fire Sciences*. 39(5):327-369. <https://doi.org/10.1177/073490412111034460>.
- [9] Li K, Li Y, Zou Y, Yuan B, Walsh A, Carradine D. **2023** Improving the Fire Performance of Structural Insulated Panel Core Materials with Intumescent Flame-Retardant Epoxy Resin Adhesive. *Fire Technology*. 59(1):29-51. <https://doi.org/10.1007/s10694-021-01203-0>.
- [10] Feldstein MM, Moscalets AP. *Innovations in Pressure-sensitive Adhesive Products*. Smithers Rapra Technology Ltd.; **2016**.

- [11] Müller B, Rath W. *Formulating Adhesives and Sealants*. Vincentz Network; **2014**; pp. 214.
- [12] Zhou W, Hubbard MJ, Carr J, inventors; Holcim Technology Ltd, assignee. Pressure-sensitive adhesives including expandable graphite. US patent US10336887B2. **2015**.
- [13] Yusuke MD, Yoshio N, Furuta TG, inventors; Flame-retardant thermally-conductive pressure-sensitive adhesive sheet. Korea patent KR101896730B1. **2011**.
- [14] Son M, Kim J, Oh M, Kim D, Choi HJ, Lee K, Chung K, Lee S. **2023** Phosphorus-based flame retardant acrylic pressure sensitive adhesives with superior peel strength and transfer characteristics. *Progress in Organic Coatings*. 185:107931. <https://doi.org/10.1016/j.porgcoat.2023.107931>.
- [15] Feng X, Li G. **2022** UV curable, flame retardant, and pressure-sensitive adhesives with two-way shape memory effect. *Polymer*. 249: 124835. <https://doi.org/10.1016/j.polymer.2022.124835>.
- [16] Wang X-L, Chen L, Wu J-N, Fu T, Wang Y-Z. **2017** Flame-Retardant Pressure-Sensitive Adhesives Derived from Epoxidized Soybean Oil and Phosphorus-Containing Dicarboxylic Acids. *ACS Sustainable Chemistry & Engineering*. 5(4):3353-3361. <https://dx.doi.org/10.1021/acssuschemeng.6b03201>.
- [17] Everaerts AI, Clemens LM. Pressure sensitive adhesives. In: *Adhesion Science and Engineering*. Dillard DA, Pocius AV, Chaudhury M ed., Elsevier Science B.V.; **2002**: 465-534:chap 11. <https://doi.org/10.1016/B978-044451140-9/50011-1>.
- [18] Czech Z, Kowalczyk A. Pressure-sensitive adhesives. In: *Adhesives: Types, Mechanics and Applications*. 1, Nova Science Publishers, Incorporated; **2011**: 47-69:chap 2.
- [19] Grand View Research. Pressure Sensitive Adhesives Market Size, Share & Trends Analysis Report By Product (Graphic Films, Tapes), By Technology, By Adhesive Chemistry (Acrylic, Rubber), By End-use (Automotive, Packaging), And Segment Forecasts, 2023 - 2030. **2022**. Accessed 17.01.2024. <https://www.grandviewresearch.com/industry-analysis/pressure-sensitive-adhesives-market>.
- [20] He X, Wu J, Huang G, Wang X. **2010** Effect of Alkyl Side Chain Length on Relaxation Behaviors in Poly(n-alkyl Acrylates) and Poly(n-alkyl Methacrylates). *Journal of Macromolecular Science, Part B*. 50(1):188-200. <https://doi.org/10.1080/00222341003648870>.

- [21] Fleischhaker F, Haehnel AP, Misske AM, Blanchot M, Haremza S, Barner-Kowollik C. **2014** Glass-Transition-, Melting-, and Decomposition Temperatures of Tailored Polyacrylates and Polymethacrylates: General Trends and Structure–Property Relationships. *Macromolecular Chemistry and Physics*. 215(12):1192-1200. <https://doi.org/10.1002/macp.201400062>.
- [22] Fox TG. **1956** Influence of Diluent and of Copolymer Composition on the Glass Temperature of a Polymer System. *Bulletin of the American Physical Society*. 1:123.
- [23] Markets and Markets. Water-based Adhesive Market by Resin Type (PAE, PVA Emulsion, VAE Emulsion, SB Latex, and PUD), Application (Tapes & Labels, Paper & Packaging, Woodworking, Building & Construction, and Automotive & Transportation), and Region - Global Forecast to 2023. **2018**. Accessed 14.06.2024. <https://www.marketsandmarkets.com/Market-Reports/water-based-adhesive-market-267560071.html>.
- [24] Chaudhury MK. **1996** Interfacial interaction between low-energy surfaces. *Materials Science and Engineering*. 16(3):97-159. [https://doi.org/10.1016/0927-796X\(95\)00185-9](https://doi.org/10.1016/0927-796X(95)00185-9).
- [25] **2019** DIN EN ISO 29862:2019-09. Klebebänder - Bestimmung der Klebkraft.
- [26] **2019** ASTM D3654. Standard Test Methods for Shear Adhesion of Pressure-Sensitive Tapes.
- [27] **2015** ASTM D4498. Standard Test Method for Heat-Fail Temperature in Shear of Hot Melt Adhesives.
- [28] **2019** ASTM D6195. Standard Test Methods for Loop Tack.
- [29] Schartel B, Hull TR. **2007** Development of fire-retarded materials— Interpretation of cone calorimeter data. *Fire and Materials*. 31(5):327-354. <https://doi.org/10.1002/fam.949>.
- [30] Weil ED, Levchik SV. 1 - Introduction. In: *Flame Retardants (Second Edition)*. Weil ED, Levchik SV ed., Hanser; **2016**: 1-4. <https://doi.org/10.3139/9781569905791.001>.
- [31] Levchik SV, Levchik GF, Balabanovich AI, Weil ED, Klatt M. **1999** Phosphorus oxynitride: a thermally stable fire retardant additive for polyamide 6 and poly(butylene terephthalate). *Die Angewandte Makromolekulare Chemie*. 264(1): 48-55. [https://doi.org/10.1002/\(SICI\)1522-9505\(19990201\)264:1<48::AID-APMC48>3.0.CO;2-W](https://doi.org/10.1002/(SICI)1522-9505(19990201)264:1<48::AID-APMC48>3.0.CO;2-W).
- [32] Bourbigot S, Le Bras M, Duquesne S, Rochery M. **2004** Recent Advances for Intumescent Polymers. *Macromolecular Materials and Engineering*. 289(6): 499-511. <https://doi.org/10.1002/mame.200400007>.

- [33] Turski Silva Diniz A, Huth C, Schartel B. **2020** Dripping and decomposition under fire: Melamine cyanurate vs. glass fibres in polyamide 6. *Polymer Degradation and Stability*. 171: 109048. <https://doi.org/10.1016/j.polymdegradstab.2019.109048>.
- [34] Schartel B. 2 - The Burning of Plastics. In: *Plastics Flammability Handbook (Fourth Edition)*. Troitzsch J, Antonatus E ed., Hanser Verlag; **2021**: 23-52. <https://doi.org/10.3139/9781569907634.002>.
- [35] Schartel B, Beck U, Bahr H, Hertwig A, Knoll U, Weise M. **2012** Sub-micrometre coatings as an infrared mirror: A new route to flame retardancy. *Fire and Materials*. 36(8):671-677. <https://doi.org/10.1002/fam.1122>.
- [36] Antosik AK, Bartoszewski A, Półka M, Wilpiszewska K, Bartkowiak M. **2024** Effect of vermiculite on the fire retarding properties of silicone pressure-sensitive adhesives. *International Journal of Adhesion and Adhesives*. 132: 103733. <https://doi.org/10.1016/j.ijadhadh.2024.103733>.
- [37] Antosik AK, Grajczyk A, Półka M, Zdanowicz M, Halpin J, Bartkowiak M. **2024** Influence of Talc on the Properties of Silicone Pressure-Sensitive Adhesives. *Materials*. 17(3): 708. <https://doi.org/doi:10.3390/ma17030708>.
- [38] Park GH, Kim KT, Ahn YT, Lee H-i, Jeong HM. **2014** The effects of graphene on the properties of acrylic pressure-sensitive adhesive. *Journal of Industrial and Engineering Chemistry*. 20(6):4108-4111. <https://doi.org/10.1016/j.jiec.2014.01.008>.
- [39] Hashim R, Sulaiman O, Kumar RN, Tamyez PF, Murphy RJ, Ali Z. **2009** Physical and mechanical properties of flame retardant urea formaldehyde medium density fiberboard. *Journal of Materials Processing Technology*. 209(2): 635-640. <https://doi.org/10.1016/j.jmatprotec.2008.02.036>.
- [40] Li S, Wang X, Chen T, Xu M, Liu L, Gao S, Wei Y, Li B. **2022** Effects of a composite flame retardant system on the flame retardancy and mechanical performance of epoxy resin adhesive. *Journal of Vinyl and Additive Technology*. 28(4): 775-787. <https://doi.org/10.1002/vnl.21921>.
- [41] Torregrosa-Coque R, Álvarez-García S, Martín-Martínez JM. **2011** Effect of temperature on the extent of migration of low molecular weight moieties to rubber surface. *International Journal of Adhesion and Adhesives*. 31(1): 20-28. <https://doi.org/10.1016/j.ijadhadh.2010.09.002>.
- [42] van der Veen I, de Boer J. **2012** Phosphorus flame retardants: Properties, production, environmental occurrence, toxicity and analysis. *Chemosphere*. 88(10):1119-1153. <https://doi.org/10.1016/j.chemosphere.2012.03.067>.

- [43] Velencoso MM, Battig A, Markwart JC, Schartel B, Wurm FR. **2018** Molecular Firefighting—How Modern Phosphorus Chemistry Can Help Solve the Challenge of Flame Retardancy. *Angewandte Chemie International Edition*. 57(33): 10450-10467. <https://doi.org/10.1002/anie.201711735>.
- [44] Liang S, Hemberger P, Neisius NM, Bodi A, Grützmacher H, Levalois-Grützmacher J, Gaan S. **2015** Elucidating the Thermal Decomposition of Dimethyl Methylphosphonate by Vacuum Ultraviolet (VUV) Photoionization: Pathways to the PO Radical, a Key Species in Flame-Retardant Mechanisms. *Chemistry – A European Journal*. 21(3): 1073-1080. <https://doi.org/10.1002/chem.201404271>.
- [45] Liang S, Hemberger P, Steglich M, Simonetti P, Levalois-Grützmacher J, Grützmacher H, Gaan S. **2020** The Underlying Chemistry to the Formation of PO<sub>2</sub> Radicals from Organophosphorus Compounds: A Missing Puzzle Piece in Flame Chemistry. *Chemistry – A European Journal*. 26(47): 10795-10800. <https://doi.org/10.1002/chem.202001388>.
- [46] Brehme S, Schartel B, Goebbels J, Fischer O, Pospiech D, Bykov Y, Döring M. **2011** Phosphorus polyester versus aluminium phosphinate in poly(butylene terephthalate) (PBT): Flame retardancy performance and mechanisms. *Polymer Degradation and Stability*. 96(5): 875-884. <https://doi.org/10.1016/j.polyimdegradstab.2011.01.035>.
- [47] Shmakov AG, Korobeinichev OP, Mebel AM, Porfiriev DP, Ghildina AR, Osipova KN, Knyazkov DA, Gerasimov IE, Liu Z, Yang B. **2023** High-temperature thermal decomposition of triphenyl phosphate vapor in an inert medium: Flow reactor pyrolysis, quantum chemical calculations, and kinetic modeling. *Combustion and Flame*. 249: 112614. <https://doi.org/10.1016/j.combustflame.2022.112614>.
- [48] König A, Kroke E. **2012** Flame retardancy working mechanism of methyl-DOPO and MPPP in flexible polyurethane foam. *Fire and Materials*. 36(1): 1-15. <https://doi.org/10.1002/fam.1077>.
- [49] Levchik S. Phosphorus-Based Flame Retardants. In: *Non-Halogenated Flame Retardant Handbook*. **2021**: 23-99. <https://doi.org/10.1002/9781119752240.ch2>
- [50] Liu C, Yao Q. **2018** Mechanism of thermal degradation of aryl bisphosphates and the formation of polyphosphates. *Journal of Analytical and Applied Pyrolysis*. 133: 216-224. <https://doi.org/10.1016/j.jaap.2018.03.022>.
- [51] Myers RE, Licursi E. **1985** Inorganic Glass Forming Systems as Intumescent Flame Retardants for Organic Polymers. *Journal of Fire Sciences*. 3(6): 415-431. <https://doi.org/10.1177/073490418500300603>.

- [52] Braun U, Balabanovich AI, ScharTEL B, Knoll U, Artner J, Ciesielski M, Döring M, Perez R, Sandler JKW, Altstädt V, Hoffmann T, Pospiech D. **2006** Influence of the oxidation state of phosphorus on the decomposition and fire behaviour of flame-retarded epoxy resin composites. *Polymer*. 47(26): 8495-8508. <https://doi.org/10.1016/j.polymer.2006.10.022>.
- [53] Pawlowski KH, ScharTEL B. **2007** Flame retardancy mechanisms of triphenyl phosphate, resorcinol bis(diphenyl phosphate) and bisphenol A bis(diphenyl phosphate) in polycarbonate/acrylonitrile–butadiene–styrene blends. *Polymer International*. 56(11): 1404-1414. <https://doi.org/10.1002/pi.2290>.
- [54] Salmeia KA, Gaan S. **2015** An overview of some recent advances in DOPO-derivatives: Chemistry and flame retardant applications. *Polymer Degradation and Stability*. 113: 119-134. <https://doi.org/10.1016/j.polymdegradstab.2014.12.014>.
- [55] Özer MS, Gaan S. **2022** Recent developments in phosphorus based flame retardant coatings for textiles: Synthesis, applications and performance. *Progress in Organic Coatings*. 171: 107027. <https://doi.org/10.1016/j.porgcoat.2022.107027>.
- [56] Bifulco A, Varganici CD, Rosu L, Mustata F, Rosu D, Gaan S. **2022** Recent advances in flame retardant epoxy systems containing non-reactive DOPO based phosphorus additives. *Polymer Degradation and Stability*. 200: 109962. <https://doi.org/10.1016/j.polymdegradstab.2022.109962>.
- [57] Sag J, Goedderz D, Kukla P, Greiner L, Schönberger F, Döring M. **2019** Phosphorus-Containing Flame Retardants from Biobased Chemicals and Their Application in Polyesters and Epoxy Resins. *Molecules*. 24(20): 3746. <https://doi.org/doi:10.3390/molecules24203746>.
- [58] Garth K, Döring M, Kraemer R, Roth M, Thomas C. **2019** Novel phosphinate-containing zinc polyacrylate and its utilization as flame retardant for polyamides. *Journal of Applied Polymer Science*. 136(22): 47586. <https://doi.org/10.1002/app.47586>.
- [59] Varganici C-D, Rosu L, Bifulco A, Rosu D, Mustata F, Gaan S. **2022** Recent advances in flame retardant epoxy systems from reactive DOPO–based phosphorus additives. *Polymer Degradation and Stability*. 202: 110020. <https://doi.org/10.1016/j.polymdegradstab.2022.110020>.
- [60] Troitzsch J, Antonatus E. 3 - Flame Retardants and Flame-Retarded Plastics. In: *Plastics Flammability Handbook (Fourth Edition)*. Troitzsch J, Antonatus E ed., Hanser; **2021**: 53-128. <https://doi.org/10.3139/9781569907634.003>.

- [61] Bier F, Six J-l, Durand A. **2019** DOPO-Based Phosphorus-Containing Methacrylic (Co)Polymers: Glass Transition Temperature Investigation. *Macromolecular Materials and Engineering*. 304: 1800645. <https://doi.org/10.1002/mame.201800645>.
- [62] Grexa O, Lübke H. **2001** Flammability parameters of wood tested on a cone calorimeter. *Polymer Degradation and Stability*. 74(3): 427-432. [https://doi.org/10.1016/S0141-3910\(01\)00181-1](https://doi.org/10.1016/S0141-3910(01)00181-1).
- [63] Quintiere JG. *Combustion in Natural Fires*. 2 ed. Principles of Fire Behavior. CRC Press; **2017**; pp. 39.
- [64] Technical InfoPyrolysis-GC/MS. Frontier Lab. Accessed: 31.07.2024, 2024. <https://www.frontier-lab.com/technical-information/methodology/part3/>.
- [65] Huggett C. **1980** Estimation of rate of heat release by means of oxygen consumption measurements. *Fire and materials*. 4(2): 61-65. <https://doi.org/10.1002/fam.810040202>.
- [66] Schartel B, Pawlowski KH, Lyon RE. **2007** Pyrolysis combustion flow calorimeter: A tool to assess flame retarded PC/ABS materials? *Thermochimica Acta*. 462(1): 1-14. <https://doi.org/10.1016/j.tca.2007.05.021>.
- [67] FAA Micro Calorimeter. Accessed: 31.07.2024, <https://www.fire-testing.com/faa-micro-calorimeter/>.
- [68] Sonnier R. Chapter 3 - Microscale forced combustion: Pyrolysis-combustion flow calorimetry (PCFC). In: *Analysis of Flame Retardancy in Polymer Science*. Vahabi H, Saeb MR, Malucelli G ed., Elsevier; **2022**: 91-116. <https://doi.org/10.1016/B978-0-12-824045-8.00003-4>.
- [69] Babrauskas V. **1982** Development of the Cone Calorimeter—A Bench-Scale Heat Release Rate Apparatus Based on Oxygen Consumption. *NBSIR 82-2611*.
- [70] Schartel B, Bartholmai M, Knoll U. **2005** Some comments on the use of cone calorimeter data. *Polymer Degradation and Stability*. 88(3): 540-547. <https://doi.org/10.1016/j.polymdegradstab.2004.12.016>.
- [71] Efectis. Cone Calorimeter. Accessed: 10.06.2024, [https://efectis.com/app/uploads/2017/08/Leaflet\\_ConeCalori.pdf](https://efectis.com/app/uploads/2017/08/Leaflet_ConeCalori.pdf).